

Functional characterisation of EGFR mutations in cancer

Peter Harrison

A thesis submitted for the degree of Doctor of
Philosophy

The Institute of Cancer Research
University of London

Declaration

The work presented in this thesis was completed under the supervision of Dr Paul Huang in the Molecular and Systems Oncology Team at The Institute of Cancer Research, London

I, Peter Harrison, confirm that the work presented in this thesis is my own. Where information has been derived from other sources, I confirm that this has been clearly indicated in the thesis.

Abstract

Large-scale pan-cancer sequencing of tumour samples has identified a plethora of epidermal growth factor receptor (*EGFR*) mutations along the full length of the gene. However, clinical studies have demonstrated that distinct mutations have different responses to anti-EGFR therapy, leading to a disparity in outcomes for patients. This thesis sought to study *EGFR* mutations from across all cancer types in order to establish the optimal kinase inhibitors for distinct EGFR mutants. Expression vectors encoding 18 distinct *EGFR* mutants were generated and expressed in the Ba/F3 model cell line. The sensitivity of these mutants to 9 EGFR inhibitors (EGFRi) and 53 other small molecule inhibitors was examined, confirming previous observations and providing novel insight into the sensitivities of distinct EGFR mutants to different inhibitors. Notably, TAS6417 and poziotinib, which are currently under clinical investigation in non-small cell lung cancer (NSCLC) harbouring exon 20 insertion (Ex20Ins) mutant EGFR, were shown to be active against 6 extracellular domain EGFR mutants (L62R, R108G, A289D/T/V, G598V) for which there are currently no approved anti-EGFR therapies. Furthermore, 6 broad-spectrum kinase inhibitors (dasatinib, saracatinib, bosutinib, cediranib, vandetanib, and ponatinib) were found to selectively inhibit a subset of kinase domain mutants (746_750del, 747_751del, and L858R). This thesis also used N-ethyl-N-nitrosourea (ENU) mutagenesis to investigate resistance mechanisms to poziotinib and TAS6417 in Ba/F3 cells expressing 3 distinct Ex20Ins mutants (A767_769dupASV, S768_dupSVD, and N771_H773dupNPH). T790M and C797S mutations were identified in cells with acquired poziotinib resistance, with T790M occurring more frequently than C797S. Interestingly, the overall frequency of T790M or C797S in poziotinib-resistant cells varied between the distinct Ex20Ins mutants. Only additional C797S mutations were identified in cells with acquired TAS6417 resistance. T790M and C797S mutations were shown to prevent EGFR inhibition following poziotinib treatment and C797S was shown to prevent EGFR inhibition following TAS6417 treatment. Both T790M and C797S mutations conferred similar levels of resistance to poziotinib, but C797S conferred greater resistance to TAS6417 compared to T790M. Finally, the heat shock protein 90 (Hsp90) inhibitor luminespib was shown to overcome T790M- or C797S-mediated resistance to poziotinib or TAS6417.

COVID19 Impact Statement

ICR labs closed on 23/03/20. At this time, my wife was 9 weeks pregnant and therefore was considered “clinically vulnerable”. Following government advice regarding pregnant women on the evening of 16/03/20, I met with my primary supervisor (Paul Huang) on 17/03/20 and planned to immediately stop experiments. On 19/03/20 my wife received a text from her GP instructing her to self-isolate and stay at home, meaning that I had to do all tasks outside our home (e.g. grocery shopping, collecting prescriptions, etc.).

At the time of lab closure, I had 2 large ongoing experiments that had be stopped:

ENU mutagenesis experiments using CUTO17 cells:

These experiments were anticipated to validate the results described in chapter 5 from ENU mutagenesis screens using Ba/F3 cells. Screens were set up on 09/03/20.

CRISPR tiling mutagenesis experiments using CUTO17 cells:

These experiments were planned as an orthogonal approach to the ENU mutagenesis screens described above. Cell lines expressing a guide-RNA library for *EGFR* at MOI 0.3 had already been prepared. Transfection conditions for Cas9-construct transfection had already been optimised. Screens were set up on 16/03/20.

ICR labs reopened on 08/06/20. When the labs reopened, our main lab capacity was reduced from 15 to 5 to comply with social distancing measures. Our tissue culture lab capacity was also reduced from 4 to 1 for June and July. Rearrangement of the tissue culture lab increased capacity from 1 to 2 from August onwards. Both main lab and tissue culture lab access was controlled via a rota system. These restrictions significantly impacted productivity.

Due to the lab closure and my personal circumstances, I was granted a deadline extension from 03/10/20 to 16/01/21. This extension meant that my wife gave birth


before my new deadline (07/10/20) and I therefore took 2 weeks paternity leave (07/10/20 – 21/10/20).

Additionally, I was alerted by the NHS COVID19 app that I had been in contact with someone with coronavirus and must self-isolate for 10 days from 13/12/20 until midnight 23/12/20. This prevented me from running additional replicates for the experiments presented in Figure 5.10 and Figure 5.11.

Peter Harrison

A handwritten signature in black ink, appearing to read 'P. Harrison', with a long horizontal flourish extending to the right.

Paul Huang

A handwritten signature in black ink, appearing to read 'Paul Huang', with a horizontal line underneath.

Acknowledgments

First, I would like to thank my supervisor, Dr Paul Huang, for giving me the opportunity to work in his lab and for his continual support and guidance throughout my PhD.

I would also like to thank all members of the Molecular and Systems Oncology Team, both past and present, for their invaluable advice and making the lab such a fun place to work. In particular I would like to thank Maya Nolan and Katie Flight, two hard-working and talented master's students I was fortunate enough to supervise.

Outside the lab, I would like to thank my friends and family for the joy they bring to my life.

Most importantly, I would like to thank my remarkable wife Joanna, who took on infinitely more than her fair share of my stress during my PhD.

Finally, I would like to thank my little boy, Arlo, who always makes me laugh (even when he's kept me up all night).

Table of contents

Abstract.....	3
COVID19 Impact Statement.....	4
Acknowledgments.....	6
Table of contents.....	7
List of tables.....	14
List of Abbreviations.....	15
1.1 Overview of receptor tyrosine kinases.....	20
1.1.1 Receptor tyrosine kinases in cancer biology.....	23
1.1.2 Receptor tyrosine kinases as therapeutic targets.....	25
1.2 EGFR structure and signalling.....	26
1.2.1 Mitogen-activated protein kinase.....	30
1.2.2 SRC.....	31
1.2.3 Signal transducers and activators of transcription.....	32
1.2.4 Phosphatidylinositol 3-kinase.....	33
1.2.5 Phospholipase C γ	34
1.3 <i>EGFR</i> aberrations in cancer.....	34
1.3.1 Common <i>EGFR</i> mutations in NSCLC.....	36
1.3.1.1 L858R.....	36
1.3.1.2 Exon 19 deletions.....	37
1.3.2 EGFR inhibitors as first-line therapy in NSCLC.....	38
1.3.2.1 First-generation EGFR inhibitors.....	39
1.3.2.2 Second generation EGFR inhibitors.....	41
1.3.2.3 Acquired resistance to EGFR inhibitors in the first-line setting.....	44
1.3.3 Third-generation EGFR inhibitors as salvage therapy in NSCLC.....	48
1.3.3.1 Acquired resistance to third-generation EGFRi.....	52
1.3.3.2 EGFR-independent mechanisms of resistance.....	59
1.3.4 Clinical characteristics of common <i>EGFR</i> mutations in NSCLC.....	61
1.3.5 Rare EGFR mutations in NSCLC.....	62
1.3.5.1 Exon 20 insertions.....	62
1.3.5.2 G719X.....	67
1.3.5.3 L861X.....	69
1.3.5.4 S768X.....	70

1.3.5.5	E709X	71
1.3.5.6	Exon 19 insertions.....	72
1.3.5.7	Compound mutations	74
1.3.6	EGFR mutations in GBM	75
1.3.6.1	EGFR-vIII	76
1.3.6.2	A289X	79
1.3.6.3	Rare <i>EGFR</i> mutations in GBM.....	80
1.4	Conclusions and aims	81
2.1	Mammalian cell culture.....	85
2.1.1	Cell lines and maintenance.....	85
2.1.2	Cell counting	87
2.1.3	Storage of cell lines	87
2.1.4	Generation of stable cell lines using retrovirus	87
2.1.4.1	Generation of retrovirus to infect murine cell lines	87
2.1.4.2	Generation of retrovirus to infect human cell lines	88
2.1.4.3	Infection of target cell lines.....	88
2.2	Molecular biology techniques	89
2.2.1	Bacterial transformation	89
2.2.2	Plasmid preparation.....	89
2.2.3	Glycerol stock	91
2.2.4	Agarose gel electrophoresis	91
2.2.5	Sanger sequencing.....	91
2.2.6	Generation of mutant EGFR expression constructs.....	92
2.2.6.1	Cloning.....	92
2.2.6.2	Site-directed mutagenesis.....	94
2.2.7	Generation of mutant SRC expression constructs	97
2.2.8	Genomic DNA extraction from Ba/F3 clones isolated from ENU screens to identify acquired <i>EGFR</i> mutations	97
2.2.9	Polymerase chain reaction of <i>EGFR</i> extracted from Ba/F3 clones isolated from ENU screens to identify acquired <i>EGFR</i> mutations.....	97
2.2.10	Droplet digital polymerase chain reaction (ddPCR) to confirm presence of <i>EGFR</i> T790M mutation in gefitinib-resistant PC9 cells	98
2.3	Protein analysis techniques.....	99
2.3.1	Protein extraction and quantification.....	99

2.3.2	Sodium dodecyl sulphate-polyacrylamide gel electrophoresis.....	99
2.3.3	Western blotting.....	99
2.4	Phenotypic assays	101
2.4.1	Chemical inhibitor preparation and storage	101
2.4.2	Cell viability assays.....	103
2.4.3	Growth curve by confluency.....	103
2.4.4	Colony formation assay	103
2.4.5	Spheroid growth assay	104
2.4.6	IL-3 independent growth curve	104
2.5	Screening techniques.....	105
2.5.1	EGFR inhibitor screen	105
2.5.2	Small molecule inhibitor screen	105
2.5.3	N-ethyl-N-nitrosourea mutagenesis screen.....	106
3.1	Introduction	108
3.2	Selection of cancer-associated <i>EGFR</i> mutations for inclusion in the study 111	
3.3	Generation of expression vectors encoding <i>EGFR</i> mutations.....	113
3.4	Identification of an optimal model cell line to study cancer-associated <i>EGFR</i> mutations	114
3.4.1	NIH-3T3	114
3.4.2	H3122	123
3.4.3	MCF10A.....	126
3.4.4	Ba/F3	129
3.5	Generation of a Ba/F3 panel expressing <i>EGFR</i> mutations.....	131
3.6	Growth properties of <i>EGFR</i> -mutant expressing Ba/F3 cells under IL-3 deprivation.....	135
3.7	Discussion.....	137
4.1	Introduction	146
4.2	<i>EGFR</i> i and small molecule inhibitor screen set-up.....	149
4.3	Assessment of the sensitivity of <i>EGFR</i> mutants to a panel of <i>EGFR</i> inhibitors.....	151
4.4	A small molecule inhibitor screen reveals mutant-specific sensitivities	156
4.5	Analysis of small molecule inhibitor screen hits determines putative shared targets	161

4.6	Generation of SRC and EGFR gatekeeper mutant cell lines.....	163
4.7	SRC-gatekeeper mutant does not confer resistance to broad-spectrum TKIs identified in small molecule inhibitor screen	167
4.8	EGFR-gatekeeper mutation confers resistance to broad-spectrum TKIs identified in small molecule inhibitor screen	169
4.9	SRC can act as a dasatinib “sink”	172
4.10	EGFR-T790M prevents EGFR inhibition by broad-spectrum TKIs identified in small molecule inhibitor screen	175
4.11	A289V is inhibited at lower doses of dasatinib compared to L858R.....	176
4.12	Increased sensitivity to small molecule inhibitor screen hits is also observed in a human NSCLC cell line.....	179
4.13	Discussion.....	183
5.1	Introduction	192
5.2	Ba/F3 cells expressing Ex20Ins mutants are resistant to gefitinib but sensitive to poziotinib and TAS6417	194
5.3	An ENU mutagenesis screen identifies potential resistance mechanisms to poziotinib and TAS6417 treatment.....	197
5.4	T790M and C797S confer a similar level of resistance to poziotinib but C797S confers greater resistance to TAS6417 compared to T790M.....	203
5.5	Ba/F3 cells expressing dup771 with an additional T790M or C797S mutation are sensitive to a Hsp90 inhibitor	211
5.6	Discussion.....	213
6.1	Introduction	223
6.2	Outstanding challenges for studying EGFR-mutant cancers.....	223
6.2.1	Overreliance on model systems.....	223
6.2.2	Tumour heterogeneity and residual disease	226
6.2.3	Targeting EGFR mutations in GBM	227
6.3	Emerging opportunities for the treatment of EGFR-mutant cancers.....	231
6.3.1	Adaptive therapies and polypharmacology	231
6.3.2	Immunotherapy.....	236
6.3.3	PROTAC degraders.....	239
6.4	Concluding remarks	241

List of figures

Figure 1.1 – Crystal structure of the EGFR kinase domain.	22
Figure 1.2 – Activation of EGFR.....	27
Figure 1.3 – Simplified overview of signalling downstream of EGFR.	30
Figure 1.4 – Key residues and common mutations in the EGFR kinase domain...35	
Figure 1.5 – Pie chart showing the frequencies of EGFR mutations in NSCLC. ...36	
Figure 1.6 – Acquired resistance to first-line EGFRi.	46
Figure 1.7 – Acquired resistance to third-generation EGFRi.....	52
Figure 1.8 – Current clinical options for patients harbouring EGFR mutations.....	83
Figure 3.1 – Outline of proposed experimental pipeline to characterise EGFR mutations from across cancer types.....	110
Figure 3.2 - The frequency of <i>EGFR</i> mutations selected for study in this project.	113
Figure 3.3 – Effect of expression of EGFR mutants on gefitinib sensitivity and proliferation in NIH-3T3 cells.	117
Figure 3.4 – Effect of expression of EGFR mutations on gefitinib sensitivity and proliferation in NIH-3T3 cells in the presence of EGF.	119
Figure 3.5 – Effect of altering cell culture conditions to increase EGFR-dependence in NIH-3T3 cells expressing EGFR mutants.	122
Figure 3.6 – H3122 cells assessed as a model for studying EGFR mutations. ...	125
Figure 3.7 - MCF10A cells assessed as a model for studying EGFR mutations.	128
Figure 3.8 – Ba/F3 cells assessed as a model for studying EGFR mutations.	131
Figure 3.9 – Workflow for generating an expanded panel of mutant EGFR-expressing Ba/F3 cells.	133
Figure 3.10 – Optimisation of EGFR expression levels in Ba/F3 cells prior to IL-3 depletion.	134
Figure 3.11 – A panel of 18 EGFR mutants confer IL-3 independent growth in Ba/F3 cells.	136
Figure 4.1 – Aims of EGFRi and small molecule inhibitor screen.....	148
Figure 4.2 – An EGFRi screen reveals the sensitivity of EGFR mutants to a panel of EGFRi.	154
Figure 4.3 – IC ₅₀ analysis of the EGFRi screen.	155
Figure 4.4 - Small molecule inhibitor screen reveals mutant-specific sensitivities to 6 broad-spectrum TKIs.....	157
Figure 4.5 - Pearson’s correlation analysis of drug screen replicates.	158
Figure 4.6 – Specific EGFR mutants show increased sensitivity to 6 broad-spectrum TKIs compared to other mutants.	159
Figure 4.7 – Shared targets of hits from the small molecule inhibitor screen.	162

Figure 4.8 – All 6 hits from the small molecule inhibitor screen reduce EGFR phosphorylation and 3 reduce SRC phosphorylation.	163
Figure 4.9 – Generation of SRC gatekeeper cell lines.	164
Figure 4.10 – Generation of EGFR gatekeeper cell lines.	166
Figure 4.11 - Expression of SRC-T338I does not rescue sensitivity to dasatinib, saracatinib, bosutinib, cediranib, vandetanib, or ponatinib in Ba/F3 cells expressing del746, del747, or L858R.	168
Figure 4.12 – IC ₅₀ analysis shows that expression of SRC-T338I does not rescue sensitivity to dasatinib, saracatinib, bosutinib, cediranib, vandetanib, or ponatinib in Ba/F3 cells expressing del746, del747, or L858R.	169
Figure 4.13 – Expression of EGFR-T790M rescues the sensitivity of Ba/F3 cells harbouring del746, del747, or L858R to dasatinib, saracatinib, bosutinib, cediranib, and vandetanib.	171
Figure 4.14 – IC ₅₀ analysis shows that expression of EGFR-T790M in Ba/F3 cells harbouring del746, del747, or L858R rescues sensitivity to dasatinib, saracatinib, bosutinib, cediranib, and vandetanib.	172
Figure 4.15 – SRC can act as a dasatinib “sink”.	174
Figure 4.16 - Expression of EGFR-T790M prevents EGFR inhibition following treatment with kinase inhibitors.	176
Figure 4.17 – Dasatinib treatment causes loss of SRC phosphorylation in sensitive and resistant EGFR mutants and loss of EGFR phosphorylation at lower doses in a sensitive mutants compared to a resistant mutants.	178
Figure 4.18 – Generation of derivative PC9 cell lines expressing SRC-WT, SRC-T338I, or harbouring a secondary T790M mutation in EGFR.	180
Figure 4.19 – EGFR-T790M rescues kinase inhibitor sensitivity in human PC9 NSCLC cells with endogenous del746.	182
Figure 5.1 – Ex20Ins mutants are more sensitive to poziotinib and TAS6417 compared with gefitinib.	195
Figure 5.2 – Phosphorylation of Ex20Ins mutant EGFR is reduced by poziotinib and TAS6417 but not by gefitinib.	196
Figure 5.3 – Schematic of the ENU mutagenesis screens.	198
Figure 5.4 – IC ₉₉ of Ex20Ins mutants to poziotinib and TAS6417.	199
Figure 5.5 – Amplification of the <i>EGFR</i> kinase domain is confirmed by agarose gel.	201
Figure 5.6 – Secondary mutations identified in resistant subpopulations isolated from ENU mutagenesis screens.	202
Figure 5.7 – Amplification of the whole <i>EGFR</i> gene is confirmed by agarose gel.	204
Figure 5.8 – Resistant subpopulations isolated from the ENU mutagenesis screens are resistant to poziotinib and TAS6417 compared with parental cells.	207
Figure 5.9 – Resistant subpopulations sustain EGFR phosphorylation following treatment with poziotinib or TAS6417.	209

Figure 5.10 – C797S-harboured clone sustains EGFR phosphorylation at 10-fold higher TAS6417 doses compared to T790M-harboured clone.	210
Figure 5.11 – Small molecule inhibitor screen reveals resistant subpopulations are sensitive to luminespib.	212
Figure 7.1 – Sanger sequencing of <i>EGFR</i> mutants.....	246

List of tables

Table 1.1 – Inhibitors that have been clinically investigated in <i>EGFR</i> -mutant NSCLC.....	38
Table 1.2 - Summary of the sensitivities of EGFR mutations found in NSCLC to EGFRi.....	62
Table 1.3 - Summary of the sensitivities of EGFR mutations found in GBM to EGFRi.....	76
Table 2.1 – Cell lines and growth conditions.....	86
Table 2.2 – Plasmids and selectable markers.....	90
Table 2.3 – Primer sequences for sequencing, PCR amplification, and cloning. ..	93
Table 2.4 – Primer sequences for QuikChange Lightning Site-directed Mutagenesis kit.....	95
Table 2.5 – Primer sequences for Q5 Site-directed Mutagenesis kit.....	96
Table 2.6 – Primary and secondary antibodies.....	101
Table 2.7 – Chemical compounds.....	102
Table 3.1 – Mutations included in this study and their associated cancer types.	112
Table 4.1– Inhibitors used in the small molecule inhibitor screen.	150
Table 5.1 – Details of resistant subpopulations selected for further investigation.	203
Table 6.1 – Current clinical use or clinical investigation of polypharmacology.	235

List of Abbreviations

ABL1	Abelson murine leukaemia viral oncogene homologue 1
AKT	Akt serine/threonine kinase
ALK	Anaplastic lymphoma kinase
ALKi	ALK inhibitor
ALL	Acute lymphoblastic leukaemia
ATP	Adenosine triphosphate
BAD	BCL-2-associated agonist of cell death
Bax	Bcl-2-associated X protein
BCA	Bicinchoninic acid
BCL-XL	B-cell lymphoma-extra large
BCR-ABL	Breakpoint cluster region-Abelson murine leukaemia viral oncogene homologue 1
BET	Bromodomain and extraterminal
BRAF	B-Raf proto-oncogene, serine/threonine kinase
BSA	Bovine serum albumin
Cbl	Casitas B-lineage lymphoma proto- oncogene
CD20	B-lymphocyte antigen CD20
cfDNA	Cell-free DNA
C-lobe	Carboxy-terminus
CNS	Central nervous system
CRC	Colorectal cancer
CRISPR	Clustered regularly interspaced short palindromic repeats
ctDNA	Circulating tumour DNA
C-terminus	Carboxy-terminus
CTG	Cell-Titre Glo
DAG	Diacyl glycerol
ddPCR	Digital droplet polymerase chain reaction
DDR2	Discoidin domain receptor 2
DFG	Aspartic acid-phenylalanine-glutamine
DMSO	Dimethyl sulphoxide
EDTA	Ethylenediaminetetraacetic acid
EGF	Epidermal growth factor
EGFR	Epidermal growth factor receptor

EGFRi	Epidermal growth factor receptor inhibitor
EGFR-KDD	Epidermal growth factor receptor-Kinase domain duplication
EML4-ALK	Echinoderm microtubule-associated protein-like4-anaplastic lymphoma kinase
EMT	Epidermal-to-mesenchymal transition
ENM	Elastic network modelling
ENU	N-ethyl-N-nitrosourea
ER	Oestrogen receptor
ErbB2 - 4	Erb-B2 receptor tyrosine kinase 2 - 4
ERK	Extracellular signal-regulated kinase
EV	Empty vector
Ex19Del	Exon 19 deletion
Ex19Ins	Exon 19 insertion
Ex20Ins	Exon 20 insertion
FBS	Foetal bovine serum
FDA	Food and Drug Administration
FGFR 1 - 3	Fibroblast growth factor receptor 1 - 3
GAB1	Grb2-associated-binding protein 1
GBM	Glioblastoma multiforme
GDP	Guanosine diphosphate
GRB2	Growth factor receptor-bound protein 2
GSK3 β	Glycogen synthase kinase-3 β
GTP	Guanosine triphosphate
HER1 - 4	Human epidermal growth factor receptor 1 - 4
HGF	Hepatocyte growth factor
HR	Hazard ratio
HRD	Histidine-arginine-aspartic acid
HS	Horse serum
Hsp90	Heat shock protein 90
IGF1R	Insulin-like growth factor 1 receptor
IgG1	Immunoglobulin G1
IL-3	Interleukin 3
IP3	Inositol triphosphate
IRS	Insulin receptor substrate
JAK	Janus kinase

KIT	KIT proto-oncogene, receptor tyrosine kinase
KRAS	KRAS proto-oncogene, GTPase
mAb	Monoclonal antibody
MAF	Mutant allele frequency
MAPK	Mitogen-activates protein kinase
MD	Molecular dynamics
MDM2	Mouse double minute 2 homolog
MEK	Mitogen-activated protein kinase kinase
MET	MET proto-oncogene, receptor tyrosine kinase
MMAF	Monomethyl auristatin F
MOI	Multiplicity of infection
NF-1	Neurofibromin 1
NGF	Nerve growth factor
NGS	Next-generation sequencing
NICE	The National Institute for Health and Care Excellence
N-lobe	Amino-terminus
NRAS	NRAS proto-oncogene, GTPase
NSCLC	Non-small-cell lung cancer
N-terminus	Amino-terminus
ORR	Objective response rate
OS	Overall survival
P27KIP1	p27 Kinase inhibitory protein 1
PBS	Phosphate buffered saline
PCR	Polymerase chain reaction
PDGFR	Platelet-derived growth factor receptor
PDK1	Phosphoinositide-dependent kinase-1
PDK2	Phosphoinositide-dependent kinase-2
PDX	Patient-derived xenograft
PEI	Polyethylenimine
PFS	Progression-free survival
PI3K	Phosphatidylinositol 3-kinase
PIK3CA	Phosphatidylinositol 4,5-bisphosphate 3-kinase catalytic subunit
PIP2	Phosphatidylinositol 4,5-bisphosphate
PKC	Protein kinase C
PLC γ	Phospholipase C γ

PLK1	Polo-like kinase 1
P-loop	Phosphate-binding loop
PR	Partial response
PROTAC	Proteolysis targeting chimeras
PTB	Phosphotyrosine-binding domain
PTEN	Phosphatase and tensin homolog
PTK6	Protein-tyrosine kinase 6
RAF	RAF proto-oncogene, serine/threonine kinase
RAS	RAS proto-oncogene, GTPase
RECIST	Response Evaluation Criteria in Solid Tumours
RR	Response rate
RRAS	RAS-related protein
RT	Room temperature
RTK	Receptor tyrosine kinase
SCCHN	Squamous cell carcinoma of the head and neck
SCLC	Small-cell lung cancer
SD	Stable disease
SDM	Site-directed mutagenesis
SDS-PAGE	Sodium dodecyl sulphate-polyacrylamide gel electrophoresis
SFK	SRC family kinase
SH1 - 4	SRC homology 1 – 4 domain
SHC	SRC homology 2 domain containing transforming protein 1
SOS	Son of sevenless
SRC	SRC proto-oncogene, non-receptor tyrosine kinase
STAT	Signal transducers and activators of transcription
TACC3	Transforming acidic coiled-coil-containing protein 3
TALEN	Transcription activator-like effector nuclease
TBS	Tris-buffered saline
TKI	Tyrosine kinase inhibitor
TTF	Time-to-treatment failure
UPS	Ubiquitin-proteasome system
VEGF	Vascular endothelial growth factor
VEGFR	Vascular endothelial growth factor receptor
VHL	Von Hippel-Lindau
WT	Wild type

Chapter 1

Introduction

1.1 Overview of receptor tyrosine kinases

Receptor tyrosine kinases (RTKs) are transmembrane glycoproteins that catalyse the transfer of phosphate groups from adenosine triphosphate (ATP) onto tyrosine residues of protein substrates (Hubbard, 1999). Through this, RTKs are able to control a wide range of cellular processes, such as cell growth, metabolism, differentiation, and motility. There are 58 RTKs in the human genome, which can be categorised into 20 subfamilies based on the sequence of the kinase domain (Robinson *et al.*, 2000). In addition to these RTKs, there are also 32 non-receptor tyrosine kinases. The majority of RTKs are single polypeptide chains with a similar molecular structure comprised of a glycosylated extracellular domain, a single-pass transmembrane domain, and intracellular domains including the juxtamembrane region, kinase domain, and C-terminal region. Although the extracellular regions of RTKs are highly variable, the kinase domains are conserved and show similarities to the kinase domains of serine/threonine and dual-specificity kinases, although with distinguishing subdomain motifs (Robinson *et al.*, 2000).

With the exception of the insulin receptor (IR) family, RTKs generally exist as inactive monomers in the membrane and form active dimers following stimulation with extracellular ligands (Heldin, 1995; Hubbard, 1999; Ward *et al.*, 2007). Ligands induce receptor dimerisation through binding to the extracellular domain of RTKs. The majority of RTK ligands are dimeric and induce dimerisation by binding simultaneously to two monomeric receptors, acting as a bridge to cross-link two monomers into a dimer with a 1:2 ligand:receptor ratio (Lemmon and Schlessinger, 2010). Dimerisation of the extracellular domains brings the intracellular kinase domains into close proximity with one another, which facilitates the destabilisation of autoinhibitory interactions and leads to kinase domain activation. Destabilisation of autoinhibitory interactions most commonly occurs through phosphorylation of key tyrosine residues in either the activation loop, juxtamembrane region, or C-terminal region (Nolen *et al.*, 2004; Du and Lovly, 2018). Active kinase domains then phosphorylate tyrosine residues on the receptor that act as binding sites for downstream signalling proteins containing phosphotyrosine-binding (PTB) or SRC homology 2 (SH2) domains that specifically bind to phosphotyrosine (Schlessinger and Lemmon, 2003). These phosphorylated tyrosine residues can also recruit

docking proteins that are then phosphorylated by the RTK and in turn recruit downstream signalling proteins (Schlessinger, 2000). Most RTKs have multiple phosphorylated tyrosine residues and recruit numerous docking proteins, enabling them to effect a large number of signalling proteins (Lemmon and Schlessinger, 2010). Through this, RTKs can act as nodes in transmitting information from the exterior to the interior of the cell.

Although the inactive conformation of kinase domains are distinct between different RTKs, the active conformations show a high degree of similarity (Noble *et al.*, 2004). Kinase domains are divided into two lobes, the N-lobe and the C-lobe, which are separated by the ATP-binding site (Figure 1.1). The binding of both ATP and the substrate protein is mediated by a loop within the C-lobe called the activation loop (Jura *et al.*, 2011). The N-terminal region of the activation loop harbours the highly conserved DFG motif. The side chain of the aspartate in the DFG motif coordinates a magnesium ion that is required for binding ATP. The C-terminal portion of the activation loop serves as a docking platform for substrate proteins. Immediately preceding the activation loop is the catalytic loop, which contains the HRD motif that accepts the proton from the hydroxyl group of the substrate during the phosphorylation reaction. In the N-lobe of the kinase domain, the α C-helix and the glycine-rich P-loop play important roles in facilitating kinase activity. In the active conformation, the α C-helix packs tightly against the rest of the N-lobe enabling interactions between conserved glutamate and lysine residues located in the α C-helix and the β 3 sheet of the N-lobe respectively (Figure 1.1). Together, these residues coordinate the α - and β -phosphate groups of ATP. Similarly, the P-loop coordinates the binding of ATP, forming interactions with the β - and γ -phosphate groups.

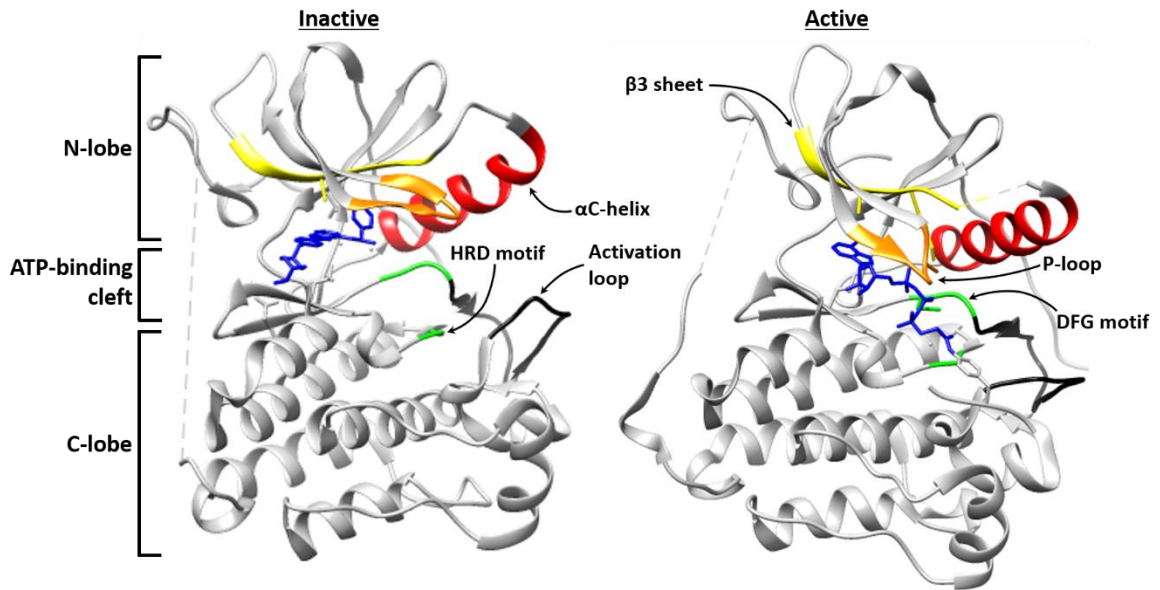


Figure 1.1 – Crystal structure of the EGFR kinase domain. The structure of kinase domains is highly conserved among RTKs. It is divided into two lobes, the N-lobe and the C-lobe, that are separated by the ATP-binding cleft. There are several key regions that have important roles in catalysis. The DFG motif (labelled in green) coordinates a magnesium ion that is required for binding ATP. The activation loop (labelled in black) serves as a docking platform for ATP and substrate proteins. The HRD motif (labelled in green) accepts the proton from the hydroxyl group of the substrate during the phosphorylation reaction. In the active conformation, interactions between the α C-helix (labelled in red) and the β 3 sheet (labelled in yellow) play important roles in coordinating the α - and β -phosphate groups of ATP, whilst the P-loop (labelled in orange) coordinates the binding of the β - and γ -phosphate groups of ATP. Active [PDB:2GS6], inactive [PDB:2J6M]. Figures were produced using UCSF Chimera and Microsoft Powerpoint.

RTKs all activate downstream signalling through a similar set of signalling proteins, raising the question of how different RTKs are able to exert specific responses through shared pathways (Schlessinger, 2004). The dynamics of signalling activation play an important role in the consequences of signalling pathway activation. This is exemplified by the differing responses of the rat pheochromocytoma cell line PC12 to epidermal growth factor (EGF) and nerve growth factor (NGF) (Marshall, 1995; Murphy *et al.*, 2002). Both EGF and NGF activate mitogen-activated protein kinase (MAPK) signalling. However, EGF stimulation causes transient MAPK activation while NGF induces sustained MAPK activation. This difference in signalling dynamics causes PC12 cells to either proliferate or differentiate when stimulated with either EGF or NGF respectively. There is also significant cross-talk between signalling pathways. This can occur at

the receptor level or further down the signalling pathway. For example, cross-talk at the receptor level is observed between epidermal growth factor receptor (EGFR) and MET, where inhibition of either receptor causes decreased activation of the other (Guo *et al.*, 2008). Cross-talk downstream of RTKs is observed between insulin and EGF signalling networks, where insulin stimulation has been shown to amplify the effects of EGF through the adaptor proteins GRB2-associated-binding protein 1 (GAB1) and insulin receptor substrate (IRS) (Borisov *et al.*, 2009). Signalling pathways can also involve feedback loops that either amplify or dampen signalling in response to activation, including inactivation of RTKs (Buday *et al.*, 1995; Gu and Neel, 2003). In addition to regulation by feedback loops, activation of RTKs is controlled by tyrosine phosphatases that maintain low levels of RTK activation in the absence of ligand stimulation and dephosphorylate receptors following activation (Jallal *et al.*, 1992; Sörby and Östman, 1996). Endocytosis and degradation of RTKs following ligand stimulation also plays an important role in the attenuation of RTK mediated signalling (von Zastrow and Sorkin, 2007; Sorkin and Goh, 2009; Zwang and Yarden, 2009).

1.1.1 Receptor tyrosine kinases in cancer biology

Genetic aberrations in RTKs are common in many diseases, including cancer. These aberrations can be categorised into four mechanisms: gain-of-function mutations, genomic amplification, chromosomal rearrangement, and autocrine activation (Lemmon and Schlessinger, 2010).

Gain-of-function mutations most commonly occur within the DFG motif and activation loop of the kinase domain (Du and Lovly, 2018). In non-small cell lung cancer (NSCLC), the L858R point mutation within the activation loop of EGFR causes a 50-fold increase in kinase activity compared to WT-EGFR (Yun *et al.*, 2007). However, mutations in RTKs outside of the kinase domain have also been reported. Extracellular domain mutations in fibroblast growth factor receptor-3 (FGFR3) have been reported in carcinomas of the uterine cervix (Wu *et al.*, 2000). The S249C FGFR3 mutation causes constitutive FGFR3 signalling through abnormal dimerisation due to the formation of intermolecular disulphide bonds

(Robertson *et al.*, 1998). Transmembrane domain mutations in human epidermal growth factor receptor 2 (HER2) have been described that impair protein turnover (Yamamoto *et al.*, 2014), and mutations in the juxtamembrane region have been identified that release autoinhibitory interactions, resulting in hyperactivation of the RTKs (Heinrich *et al.*, 2003)

Genomic amplification leads to an increased concentration of RTKs at the cell membrane. This promotes constitutive dimerisation of the receptors, causing hyperactivity (Carraway and Sweeney, 2002). Furthermore, increased RTK concentrations can overwhelm negative regulatory mechanisms. RTK amplification has been identified in a number of different cancers: amplification of *EGFR* (Selvaggi *et al.*, 2004) and *MET* (Xu *et al.*, 2010) has been reported in lung cancer; amplification of fibroblast growth factor receptor-1 (*FGFR1*), fibroblast growth factor receptor-2 (*FGFR2*) (Pearson *et al.*, 2016) and *HER2* (Yaziji *et al.*, 2004) has been identified in breast cancer; and platelet-derived growth factor receptor- α (*PDGFR α*) amplification has been identified in high-grade astrocytomas (Carraway and Sweeney, 2002).

Chromosomal rearrangements lead to the formation of fusion proteins. The first fusion protein identified was breakpoint cluster region-Abelson murine leukaemia viral oncogene homologue 1 (BCR-ABL), which is a product of a fusion between chromosomes 9 and 22. This fusion results in an unusually short chromosome, named the Philadelphia chromosome, that was initially identified in chronic myeloid leukaemia (Tough *et al.*, 1961). The fusion protein product of the Philadelphia chromosome is a constitutively active kinase owing to the substitution of a regulatory region of the ABL1 non-receptor tyrosine kinase with a truncated portion of the BCR protein (Nagar *et al.*, 2003). Since the identification of BCR-ABL, many other fusion proteins have been identified in cancer, including fusions involving RTKs such as EGFR-RAD51 and echinoderm microtubule-associated protein-like4-anaplastic lymphoma kinase (EML4-ALK) in NSCLC (Soda *et al.*, 2007; Konduri *et al.*, 2016). Interestingly, the location of the fusion determines whether the fusion protein is membrane-bound or cytoplasmic. If the fusion occurs at the C-terminus of the RTK (i.e.: downstream of the kinase domain), as is the case with EGFR-RAD51, then the fusion protein will be membrane bound (Konduri *et al.*, 2016). However, if the fusion

occurs at the N-terminus of the RTK, as is the case with EML4-ALK, then the fusion protein will be cytoplasmic (Soda *et al.*, 2007).

Finally, autocrine activation of RTKs has been reported in cancer. Autocrine activation occurs when a cancer cell secretes a ligand to activate an RTK on its own membrane. This has been identified in acute myeloid leukaemia, where aberrant expression of hepatocyte growth factor (HGF) has been shown to lead to autocrine activation of the RTK MET, which drives oncogenesis (Kentsis *et al.*, 2012).

1.1.2 Receptor tyrosine kinases as therapeutic targets

The central role that RTKs play in cancer biology has made them important drug targets. Drugs that target RTKs can be divided into two categories: monoclonal antibodies that target the extracellular portion of the receptor, and small molecule inhibitors that bind to the intracellular portion of the receptor.

There are several different mechanisms by which monoclonal antibodies can kill cells: antibodies can be conjugated to radioactive isotopes or toxins to deliver this material to the target cell; antibodies can initiate an immune response; and antibodies can block receptors and sequester secreted growth factors (Reichert and Valge-Archer, 2007). Ibritumomab tiuxetan is a monoclonal antibody used in the treatment of non-Hodgkin's lymphoma (Milenic *et al.*, 2004). It is comprised an immunoglobulin G1 (IgG1) antibody that targets B-cells via the CD20 antigen and a metal chelator which is labelled with the radioactive isotope yttrium-90 (Zinzani and Broccoli, 2017). Rituximab is another antibody used to treat non-Hodgkin lymphoma that also targets B-cells via the CD20 antigen (Weiner, 2010). Rituximab initiates an immune response whereby target cells are killed by antibody-dependent cellular cytotoxicity and complement-dependent cytotoxicity. Cetuximab is a chimeric monoclonal antibody that competes with EGF to bind to EGFR, preventing phosphorylation of EGFR and promoting internalisation and degradation of the receptor (Sato *et al.*, 1983; Fans *et al.*, 1994; Goldstein *et al.*, 1995). Binding of cetuximab to EGFR causes cell cycle arrest in G1 through upregulation of the cyclin-dependent kinase inhibitor p27KIP1 (Wu *et al.*, 1996), and induces apoptosis

through induction of pro-apoptotic proteins such as Bcl-2-associated X protein (Bax) (Mandal *et al.*, 1998).

The first small molecule tyrosine kinase inhibitor (TKI) approved for the treatment of cancer was imatinib, which received U.S. Food and Drug administration (FDA) approval for the treatment of chronic myeloid leukaemia in 2001. Imatinib was designed to selectively inhibit BCR-ABL (Druker *et al.*, 1996). Investigators used the structure of ATP-binding sites to design and screen a series of compounds, leading to the identification of imatinib. Although designed to be selective for BCR-ABL, imatinib has been shown to inhibit other RTKs and has subsequently been approved for KIT mutated gastrointestinal stromal tumours and PDGFR rearranged chronic myeloproliferative diseases (Apperley *et al.*, 2002; Demetri *et al.*, 2002). This highlights a key feature of small molecule inhibitors: some are “broad-spectrum”, capable of inhibiting many RTKs, while others are highly selective. Dasatinib is an example of a “broad-spectrum” inhibitor. Originally developed as a second-generation BCR-ABL inhibitor, dasatinib was designed to target the active conformation of ABL1 (Kantarjian *et al.*, 2006). This confers a very broad selectivity upon dasatinib as the active conformation of kinase domains is much more highly conserved between kinases compared with the inactive conformation. By contrast, the EGFR inhibitors (EGFRi) gefitinib and erlotinib show high levels of selectivity for EGFR, and are able to inhibit EGFR without inhibiting the closely related HER2 (Shawver *et al.*, 2002).

1.2 EGFR structure and signalling

EGFR is a member of the ErbB family of RTKs, which also includes HER2 (ErbB2), HER3 (ErbB3), and HER4 (ErbB4). EGFR is a single-chain glycoprotein with a prototypical RTK structure, comprised of an extracellular ligand binding domain, a single transmembrane domain, and an intracellular region containing a juxtamembrane region, a tyrosine kinase domain, and a C-terminal regulatory region (Burgess *et al.*, 2003).

The extracellular region of EGFR has four domains (I – IV, also known as L1, S1, L2, and S2 domains) (Bajaj *et al.*, 1987). Domains I and III share 37% sequence

identity, whereas domains II and IV are homologous Cys-rich domains (Ward *et al.*, 1995). The dimerisation mechanism of EGFR is distinct from other RTKs, which generally form dimers with only one ligand present where the ligand acts as a bridge that cross-links two monomers together to form a dimer (Figure 1.2) (Wlesmann *et al.*, 1999; Wehrman *et al.*, 2007). During EGFR dimerisation, each monomer binds to a single EGF ligand through domains I and III. This draws these domains together, requiring the receptor to adopt an “extended” configuration (Garrett *et al.*, 2002; Ogiso *et al.*, 2002). This rearrangement breaks an intramolecular “tether” between domains II and IV, exposing the “dimerisation arm” (Figure 1.2). This dimerisation arm is then able to form intermolecular interactions with other “extended” EGFR monomers to form a dimer with a 2:2 ligand:receptor ratio. Seven ligands have been identified that can bind to EGFR (Schneider and Wolf, 2009).

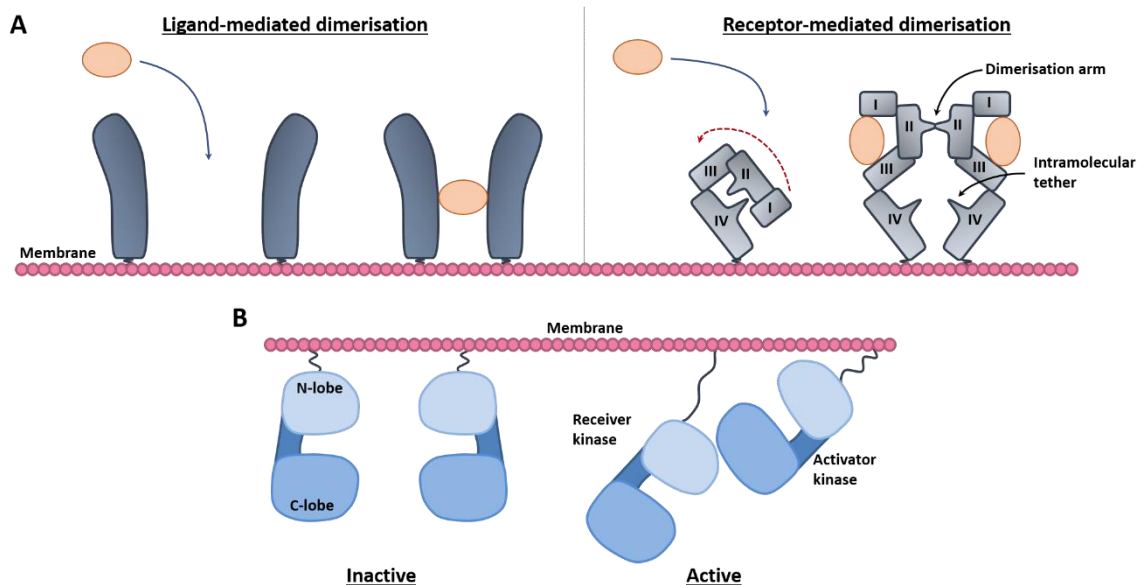


Figure 1.2 – Activation of EGFR. (A) The majority of RTKs undergo “ligand-mediated” dimerisation (left). This is where a bivalent ligand interacts with two monomers, acting as a bridge to cross-link the two receptors together to form a dimer with a 1:2 ligand:receptor configuration. EGFR undergoes “receptor-mediated” dimerisation (right). Here, each monomer binds to one ligand. Ligand binding induces a conformational change that exposes a dimerisation arm that is buried in the non-ligand bound state. This dimerisation arm strongly associates with the dimerisation arm of other monomers, leading to the formation of dimers in a 2:2 ligand:receptor configuration. (B) Activation of the EGFR kinase domain occurs through the formation of asymmetric kinase dimers. This is where the C-lobe of the “activator” kinase interacts with the N-lobe of the “receiver” kinase, forming

allosteric interactions that stabilise an active conformation. (A, B) Figures produced using Microsoft Powerpoint.

The intracellular kinase domain of EGFR is also prototypical of RTKs, formed of two lobes, the N-lobe and the C-lobe, separated by an ATP-binding pocket (Figure 1.1). The α C-helix, located within the N-lobe, contains the E762 residue, which forms a catalytically important salt-bridge interaction with K745 when the kinase is in the active conformation (Figure 1.4) (Jura *et al.*, 2009). Together, K762 and E745 bind and orientate ATP by forming interactions with the α - and β - phosphate of ATP respectively. In the inactive conformation of the kinase domain the α C-helix is rotated outwards, which prevents the formation of the E762-K745 salt bridge. This inactive conformation is stabilised by a helical turn within the N-terminal portion of the activation loop, which is located in the C-lobe (Yun *et al.*, 2007). The inactive conformation of the EGFR kinase domain bears a striking resemblance to the inactive conformations of SRC and CDK2, and so is often referred to as the “SRC/CDK2-like inactive” conformation (Shan *et al.*, 2012). Activation of the kinase domain also differs from the majority of RTKs, which utilise phosphorylation to relieve autoinhibitory interactions (Nolen *et al.*, 2004; Du and Lovly, 2018). Rather, activation of the EGFR kinase domain relies on allosteric interactions. Following dimerisation, the kinase domains form an asymmetric dimer where one kinase domain (the “activator”) stabilises the other kinase domain (the “receiver”) in an active conformation (Figure 1.2) (Zhang *et al.*, 2006b). The juxtamembrane section near the N-lobe of the activator kinase domain engages with the C-lobe of the receiver kinase domain, stabilising the receiver kinase domain in an α C-helix “in” conformation, allowing the formation of the E762-K745 salt bridge and subsequent binding of ATP (Jura *et al.*, 2009).

Activation of the kinase domain leads to phosphorylation of tyrosine residues on the C-terminal tail of EGFR, which act as docking sites for downstream signalling proteins (Yarden and Sliwkowski, 2001). Tyrosine residues on the C-terminal tail undergo both autophosphorylation and phosphorylation by other kinases (Sato, 2013). Different phosphorylated tyrosine residues recruit different downstream signalling proteins. For example, STAT3 (signal transducer and activator of transcription-3) has been shown to bind to Y1068 (Zhang *et al.*, 2006a) and the adapter protein SHC (SRC homology 2 domain containing transforming protein 1)

has been shown to bind to Y1173 (Batzer *et al.*, 1994; Prigent *et al.*, 1996). However, there is redundancy in the C-terminal tyrosines that signalling proteins are recruited to (Schulze *et al.*, 2005; Huang *et al.*, 2010). For example, SHC has been shown to bind to Y974, Y1086, Y1114, and Y1148 in addition to Y1173. Interestingly, stimulation of EGFR with different ligands can result in the phosphorylation of distinct patterns of tyrosine residues on the C-terminal tail (Guo *et al.*, 2003). The combination of the different binding affinities of downstream signalling proteins to specific tyrosine residues on the C-terminal tail of EGFR and the distinct patterns of C-terminal phosphorylation following stimulation with different ligands facilitates the recruitment of a wide range of effector molecules to the receptor. Recruitment of these proteins leads to the formation of signalling complexes and initiation of downstream signalling cascades (Figure 1.3). Additionally, phosphorylation of tyrosine residues on the C-terminal tail leads to the recruitment of the E3 ubiquitin ligase Cbl which induces internalisation and degradation of EGFR, attenuating signalling (Avraham and Yarden, 2011).

In the following sections I describe in detail the major signalling pathways activated by EGFR (Figure 1.3).

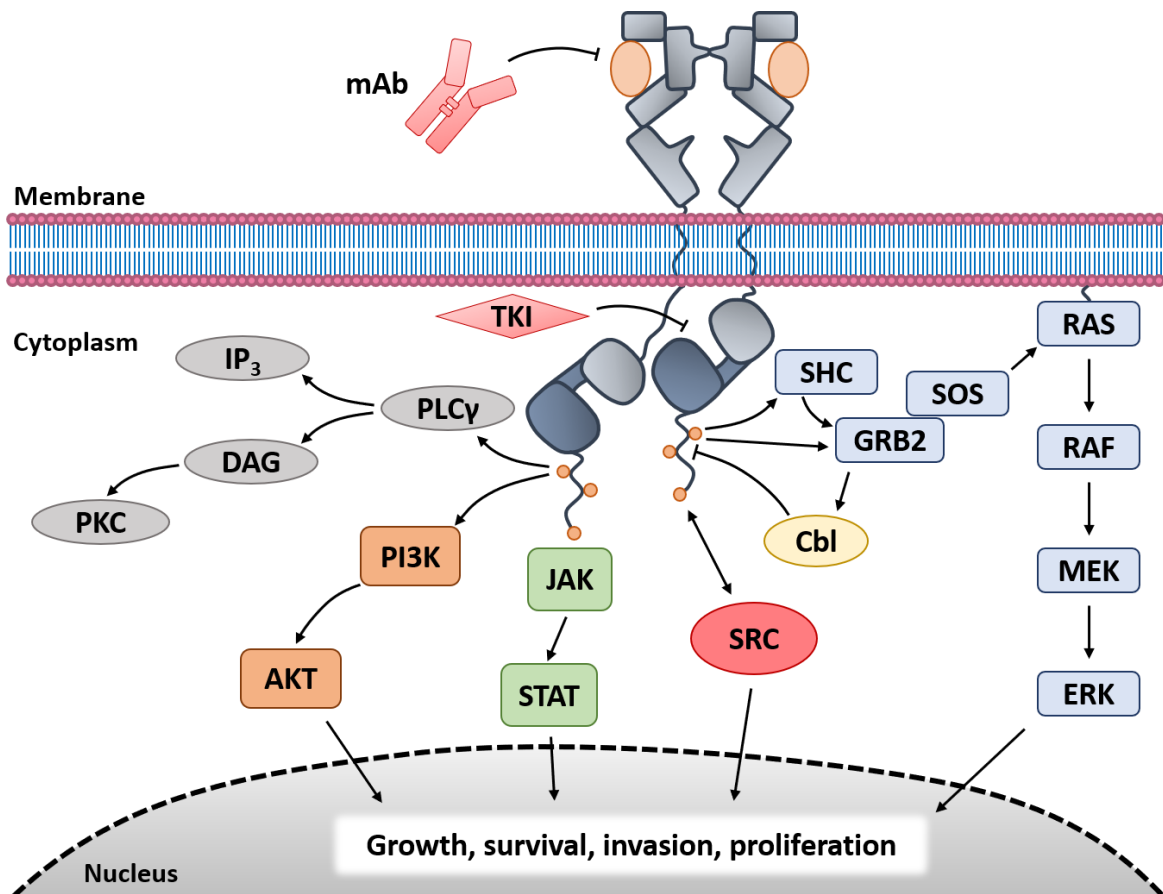


Figure 1.3 – Simplified overview of signalling downstream of EGFR. Monoclonal antibodies (mAb) bind to the extracellular region of EGFR to either prevent ligand binding, deliver a toxin, or initiate an immune response. Tyrosine kinase inhibitors (TKI) bind to the intracellular kinase domain of EGFR to inhibit kinase activity. Phosphorylated tyrosine residues on the C-terminal tail of EGFR can bind to adapter proteins (e.g. SHC and GRB2) or directly recruit downstream signalling proteins to activate signalling networks that are associated with oncogenic phenotypes. Figure produced using Microsoft Powerpoint.

1.2.1 Mitogen-activated protein kinase

The MAPK (mitogen-activated protein kinase) or ERK signalling pathway is aberrantly activated in many cancers (Bos, 1989; Davies *et al.*, 2002). Following EGFR activation, a complex of growth factor receptor-bound protein 2 and son of sevenless (GRB2-SOS) bind to phosphotyrosine residues on the C-terminal tail of EGFR either directly or via the adapter protein SHC (Lowenstein *et al.*, 1992; Batzer *et al.*, 1994). This induces a conformational change in SOS which enables it to recruit and activate RAS. RAS is a membrane bound GTPase that cycles between an active guanine triphosphate (GTP) bound form and an inactive guanine

diphosphate (GDP) bound form (Molina and Adjei, 2006). Active RAS then recruits and activates RAF, which in turn activates MEK which finally activates ERK. Phosphorylated ERK translocates to the nucleus where it activates numerous transcription factors to promote cell survival, cell motility, and cell division (Roskoski, 2012). A key result of ERK activation is entry to the cell cycle via induction of cyclin D1 expression. ERK activation causes cyclin D1 expression through the phosphorylation of the transcription factor Myc (Seth *et al.*, 1991), which directly participates in the transcription of cyclin D1 (Daksis *et al.*, 1994), and the transcription of immediate early response genes (IEGs) via the activation of ternary complex factors such as Elk-1 and SAP-1 (Whitmarsh *et al.*, 1995). IEGs, such as *c-fos*, cause the transcription of late response genes such as *Fra-1* which in turn lead to the expression of cyclin D1 (Burch *et al.*, 2004; Murphy and Blenis, 2006; Chambard *et al.*, 2007). Importantly, *c-fos* is very unstable and will only accumulate if it is phosphorylated by ERK under conditions of sustained ERK activation, highlighting the important role of signalling dynamics discussed earlier (Marshall, 1995; Murphy *et al.*, 2002).

1.2.2 SRC

SRC is one of nine non-receptor tyrosine kinases referred to as SRC-family kinases (SFK). The other kinases are FYN, YES, BLK, YRK, FGR, HCK, LCK, and LYN (Yeatman, 2004). Of these, SRC is the most commonly implicated in cancer. Structurally, SRC is composed of four SRC homology domains (SH1, SH2, SH3, and SH4) and a C-terminal tail (Brown and Cooper, 1996). The SH4 domain contains an important myristylation site that anchors SRC to the plasma membrane, the SH1 domain is the catalytic domain and harbours the autophosphorylation site Y419, and the C-terminus harbours Y530 which is central to SRC kinase regulation. When Y530 is phosphorylated it interacts with the SH2 domain, while the SH3 domain interacts with the SH1 catalytic domain (Yamaguchi and Hendrickson, 1996; Yeatman, 2004). These interactions stabilise a closed, inactive conformation of SRC which buries the kinase domain, reducing its ability to bind substrates. Dephosphorylation of Y530 releases these interactions and allows the kinase domain to adopt an open, active conformation.

Interestingly, EGFR and SRC appear to be able to activate one another in a bi-directional fashion. Stimulation of EGFR with EGF has been shown to lead to increased SRC activation (Oude Weernink *et al.*, 1994; Weernink and Rijksen, 1995). Similarly, active SRC is able to phosphorylate EGFR on Y845, leading to activation of EGFR without ligand stimulation (Maa *et al.*, 1995; Sato *et al.*, 1995). SRC can also potentiate EGFR signalling by inducing the degradation of Cbl, thus impairing the degradation of EGFR (Bao *et al.*, 2003).

In addition to activating EGFR, SRC plays a central role in the regulation of adhesion, migration, invasion, and proliferation (Thomas and Brugge, 1997; Yeatman, 2004). SRC promotes adhesion, migration, and invasion through disrupting focal adhesions and adherens junctions (Carragher and Frame, 2002; Carragher *et al.*, 2003). Focal adhesions are sites at which the actin cytoskeleton of a cell interact with extracellular matrix proteins via integrins (Sastry and Burrige, 2000), and adherens junctions are sites where neighbouring cells form interactions via E-cadherin molecules (Yap *et al.*, 1997; Jamora and Fuchs, 2002). SRC plays (Zou *et al.*, 2002) a key role in the disassembly of focal adhesions by inhibiting RAS-related protein (RRAS), which maintains the integrity of focal adhesions MENDELEY CITATION PLACEHOLDER 86, and activating focal adhesion kinase (FAK), which promotes this disassembly of focal adhesions (Ren *et al.*, 2000). SRC also regulates the disassembly of adherens junctions by inducing the phosphorylation and ubiquitylation of the E-cadherin complex, resulting in the endocytosis of E-cadherin (Fujita *et al.*, 2002). Additionally, SRC promotes cell cycle progression by inducing Myc expression (Barone and Courtneidge, 1995).

1.2.3 Signal transducers and activators of transcription

Signal transducers and activators of transcription (STATs) are a family of seven proteins that share a highly conserved structure; STATs have an SH2 domain, a DNA-binding domain, and an N-terminal domain involved in protein-protein interactions (Kisseleva *et al.*, 2002). STATs can be activated by cytokine receptors and by growth factor receptors. In cytokine signalling, STATs become activated through the phosphorylation of a C-terminal tyrosine residue by Janus kinases

(JAKs) (Silva, 2004). Phosphorylation of this tyrosine residue enables STAT monomers to dimerise through interactions between the phosphotyrosine residue of one monomer and the SH2 domain of another. EGFR can activate STAT signalling independently of JAK (David *et al.*, 1996), however JAK may help recruitment of STAT to a complex of EGFR and SRC to enhance activation (Zhang *et al.*, 2000). Once activated, STAT dimers translocate to the nucleus where they regulate genes associated with proliferation, differentiation, and angiogenesis. In particular, STAT3 and STAT5 are associated with oncogenesis as they are involved in promoting cell-cycle progression, cellular transformation, and preventing apoptosis (Calò *et al.*, 2003).

1.2.4 Phosphatidylinositol 3-kinase

Phosphatidylinositol 3-kinase (PI3K) is a heterodimeric lipid kinase comprised of a regulatory subunit (p85) and a catalytic subunit (p110, also referred to as PIK3CA) (Vivanco and Sawyers, 2002). p85 is constitutively bound to the p110 subunit via an inter-SH2 domain. In response to EGFR activation, the PI3K heterodimer is recruited from the cytoplasm to the cell membrane by interactions between phosphorylated tyrosine residues on the C-terminal tail of EGFR and an SH2 domain on the p85 subunit of PI3K. When localised to the membrane the p110 subunit is able to phosphorylate an inositol-containing lipid in the membrane, phosphatidylinositol bisphosphate (PIP₂), leading to the formation of phosphatidylinositol triphosphate (PIP₃). PIP₃ recruits AKT, a serine/threonine kinase, to the cell membrane. This occurs through interactions between PIP₃ and the pleckstrin homology domain of AKT. Following recruitment to the membrane, AKT is activated by phosphorylation on T308 and S473 by phosphoinositide-dependent kinase-1 (PDK1) and PDK2 respectively (Alessi *et al.*, 1997; Vanhaesebroeck and Alessi, 2000). Recruitment of AKT to the membrane is attenuated by phosphatase and tensin homolog (PTEN), which dephosphorylates PIP₃ to form PIP₂ (Chalhoub and Baker, 2009). Once activated, AKT plays crucial roles in promoting cell survival, growth, and proliferation (Vivanco and Sawyers, 2002). AKT promotes cell survival through phosphorylating several proteins, including BCL-2-associated agonist of cell death (BAD), which prevents the

formation of pro-apoptotic BAD-BCL-XL (B-cell lymphoma-extra large) heterodimers (Datta *et al.*, 1997), mouse double minute 2 homolog (MDM2), which allows MDM2 to promote the degradation of the pro-apoptotic protein p53 (Mayo and Donner, 2001; Zhou *et al.*, 2001), and the protease caspase-9, which inhibits the pro-death catalytic activity of caspase-9 (Cardone *et al.*, 1998). AKT also promotes cell growth by phosphorylating the mammalian target of rapamycin (mTOR), a serine/threonine kinase that regulates protein synthesis (Navé *et al.*, 1999). Finally, AKT promotes cell proliferation by preventing the degradation of cyclin D1 through the regulation of glycogen synthase kinase-3 β (GSK3 β) activity (Diehl *et al.*, 1998). Phosphorylation of cyclin D1 by GSK3 β targets cyclin D1 for degradation by the proteasome. AKT inhibits this activity by phosphorylating GSK3 β , thus allowing cyclin D1 to accumulate.

1.2.5 Phospholipase C γ

Phospholipase C γ (PLC γ) is recruited to phosphotyrosine residues on the C-terminal tail of EGFR through interactions with its SH2 domains (Chattopadhyay *et al.*, 1999). At the membrane, PLC γ hydrolyses PIP₂ into inositol 1,3,5-trisphosphate (IP₃), which is involved in calcium signalling, and diacyl glycerol (DAG), which recruits protein kinase C (PKC) to the membrane (Schönwasser *et al.*, 1998). PKC is activated at the membrane and subsequently activates the MAPK pathway, leading to cell proliferation and survival (McClellan *et al.*, 1999).

1.3 *EGFR* aberrations in cancer

Given that EGFR activates signalling networks associated with promoting cell survival, growth, invasion, and proliferation it is unsurprising that aberrations that result in hyperactivation of EGFR are common in many cancers. This has led to the extensive investigation of EGFR as a therapeutic target. Oncogenic *EGFR* aberrations include point mutations, in-frame deletions, in-frame insertions, gene rearrangement, and genomic amplification. Although common *EGFR* mutations, such as the L858R point mutation that is commonly found in NSCLC and the EGFR-

vIII deletion variant commonly found in glioblastoma multiforme (GBM), have been well studied many of the rare *EGFR* mutations identified in cancer remain poorly characterised. In the following sections, I discuss the different *EGFR* mutations that occur in cancer, focusing on the mechanism by which mutations alter the activity of EGFR and our ability to target these mutations therapeutically. Mutations in *EGFR* most commonly occur in NSCLC and GBM, and so my discussion focusses on mutations identified in these cancers.

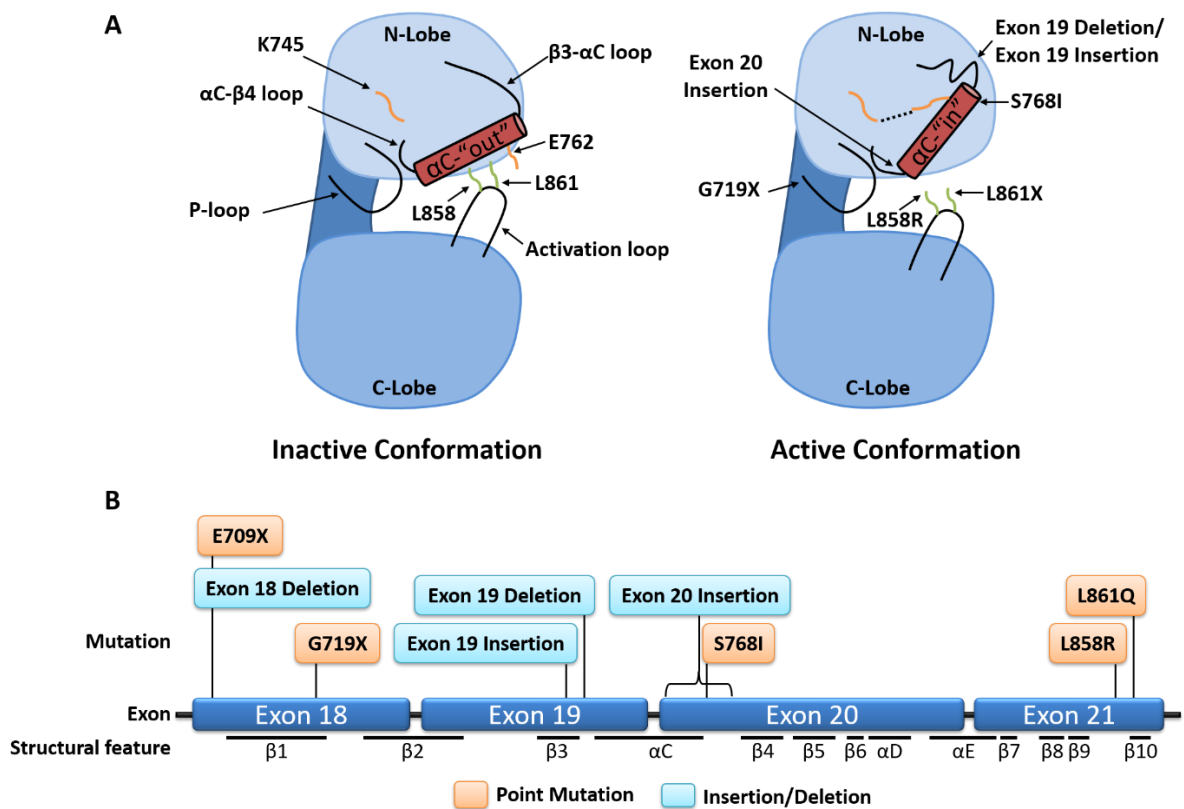


Figure 1.4 – Key residues and common mutations in the EGFR kinase domain. (A) Cartoons depicting the EGFR kinase domain. In the inactive conformation (left) the α C-helix is in an “out” conformation and the catalytically important salt-bridge interaction between K745 and E762 is broken. In the active conformation (right) the α C-helix is in an “in” conformation and K745 and E762 can interact (indicated by a dashed blue line). On the left, important regions of the kinase domain are labelled. On the right, kinase domain mutations are labelled. (B) Linear domain map of the EGFR kinase domain showing the position of structural features and cancer-associated mutations within the kinase domain. (A, B) Figure produced using Microsoft Powerpoint. Adapted from (Harrison *et al.*, 2019).

1.3.1 Common *EGFR* mutations in NSCLC

Activating mutations in *EGFR* occur in 10-20% of Caucasian and at least 50% of Asian NSCLC patients (Rosell et al., 2009; D'Angelo et al., 2011; Collisson et al., 2014; Shi et al., 2014). Two mutations account for ~85% of *EGFR* mutations in NSCLC; the L858R point mutation in exon 21 and deletion mutations in exon 19 (Figure 1.5) (Gazdar, 2009).

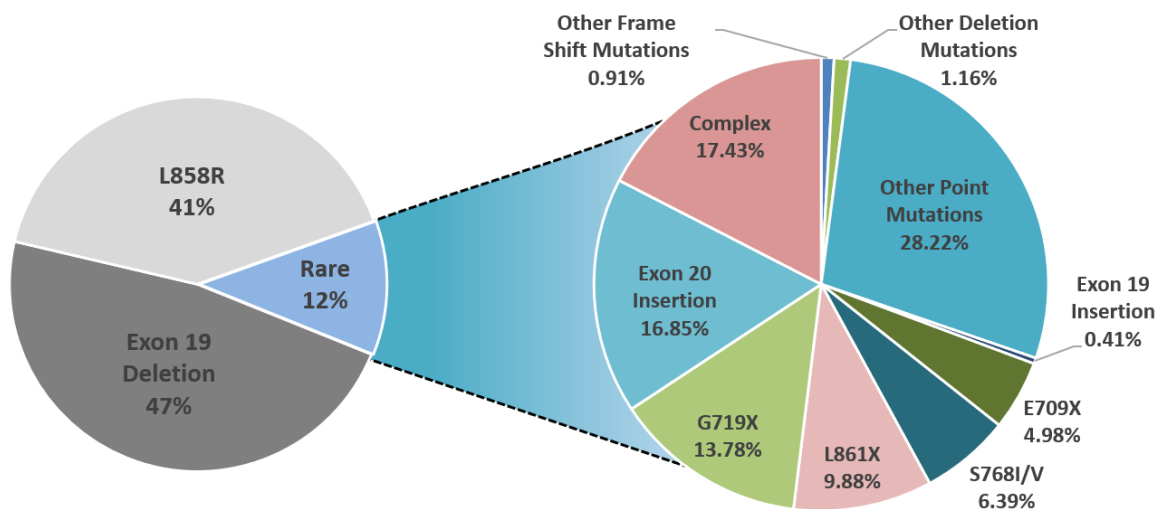


Figure 1.5 – Pie chart showing the frequencies of *EGFR* mutations in NSCLC. Data was acquired from COSMIC database. Data was filtered to contain only mutations from adenocarcinoma. The common resistance mutations T790M and C797S were filtered out. Figures were produced using Microsoft Powerpoint and Microsoft Excel. Adapted from (Harrison *et al.*, 2019).

1.3.1.1 L858R

L858R accounts for ~40% of all *EGFR* mutations in NSCLC and is the single most common *EGFR* mutation in NSCLC (Kobayashi and Mitsudomi, 2016). L858 is located within the helical turn of the activation loop and forms crucial hydrophobic interactions with residues in the N-lobe that “locks” the α C-helix in the outwardly rotated inactive conformation (Figure 1.4 A). Substitution of leucine for arginine at position 858 cannot be accommodated in this inactive conformation, owing to the

much larger side chain of arginine compared to leucine. By contrast, L858R is readily accommodated in the active conformation, which is further stabilised by interactions between the positively charged R858 and a surrounding cluster of negatively charged residues (E758, D855, and D837) (Yun *et al.*, 2007; Shan *et al.*, 2012). Importantly, molecular dynamics (MD) simulations have shown that L858R suppresses local intrinsic disorder at the dimerisation interface around the α C-helix within the N-lobe of the kinase domain (Shan *et al.*, 2012). This increases the mutant receptor's propensity for dimerisation. In particular, L858R mutant receptors show a greatly enhanced capacity to act as "receivers" in an asymmetric dimer, whilst retaining "activator" activity similar to wild-type (WT)-EGFR (Brewer *et al.*, 2013). This leads to an increase in dimerisation-dependent kinase activity in L858R compared to WT-EGFR that can occur in the absence of ligand. *In vitro* kinase assays have shown that L858R is approximately 50 times more active than WT-EGFR, and experiments using cell lines expressing L858R showed increased EGFR phosphorylation following stimulation with EGF compared to cells expressing WT-EGFR (Lynch *et al.*, 2004; Yun *et al.*, 2007).

1.3.1.2 Exon 19 deletions

Exon 19 deletions (Ex19Del) account for ~45% of all *EGFR* mutations in NSCLC (Kobayashi and Mitsudomi, 2016). Although a 5 amino acid deletion between E746 and A750 (746_750del) is the most common Ex19Del (~67%), at least 30 variants have been reported with differences in the exact position and size of the deletion (Chung *et al.*, 2012; Kobayashi and Mitsudomi, 2016). Deletions are also occasionally accompanied by a substitution or insertion mutation. These deletions occur in the loop preceding the α C-helix (Figure 1.4). Loss of residues from this loop "pulls" the α C-helix inward into the active conformation, stabilising the E762-K745 salt bridge (Eck and Yun, 2010; Shan *et al.*, 2012; Tamirat *et al.*, 2019). In contrast to L858R mutations, Ex19Del promote dimerisation-independent kinase activity (Cho *et al.*, 2013). *In vitro* experiments have shown that Ex19Del have increased kinase activity compared to WT (de Gunst *et al.*, 2007).

1.3.2 EGFR inhibitors as first-line therapy in NSCLC

Targeting EGFR in NSCLC using EGFR inhibitors has been extensively investigated in both the preclinical and clinical setting. In the following sections, I discuss the use of EGFRi in NSCLC and resistance mechanisms to these inhibitors. Inhibitors that have been clinically investigated in the treatment of *EGFR*-mutant NSCLC are summarised in Table 1.1.

Inhibitor (Trade name)	EGFRi generation	FDA Approved	Indication	Key studies
Gefitinib (Iressa)	First	Y	First-line NSCLC with L858R or Ex19Del	IPASS (Mok et al. 2009), WJTOG3405 (Maemondo et al., 201), NEJ002 (Mitsudomi et al., 2010)
Erlotinib (Tarceva)	First	Y	First-line NSCLC with L858R or Ex19Del	EURTAC (Rossel et al., 2012)
Afatinib (Giotrif)	Second	Y	First-line NSCLC with L858R, Ex19Del, G719X, S768I, or L861R	LUX-Lung 3 (Sequist et al., 2013), LUC-Lung 6 (Wu et al., 2014)
Dacomitinib (Vizimpro)	Second	Y	First-line NSCLC with L858R or Ex19Del	ARCHER 1050 (Mok et al., 2018)
Neratinib (Nerlynx)	Second	N	N/A	NCT00266877 (Sequist et al., 2010b)
Rociletinib (Xegafri)	Third	N	N/A	TIGER-X (Sequist et al., 2015b), TIGER-2 (Sequist et al., 2016)
Osimertinib (Tagrisso)	Third	Y	Second-line NSCLC with T790M mutation following first-line EGFRi therapy. First-line NSCLC with L858R or Ex19Del.	AURA extension (Goss et al., 2016), AURA2 (Yang et al., 2017), AURA3 (Mok et al., 2017a), FLAURA (Soria et al., 2017, Ramalingam et al., 2020)
Pozotinib	Ex20Ins-targeting	N	N/A	NCT03066206 (Robichaux et al., 2018), ZENITH20 (NCT03066206)
TAK-788 (Mobocertinib)	Ex20Ins-targeting	N	N/A	EXCLAIM (NCT02716116, Doebele et al., 2018), EXCLAIM 2 (NCT04129502)
TAS6417	Ex20Ins-targeting	N	N/A	NCT04036682

Table 1.1 – Inhibitors that have been clinically investigated in *EGFR*-mutant NSCLC.

1.3.2.1 First-generation EGFR inhibitors

Gefitinib is a small molecule inhibitor that inhibits EGFR signalling in cell line models and reduces the growth of EGFR-expressing human tumour xenografts in mice (Wakeling *et al.*, 2002). Based on these data, the clinical efficacy of gefitinib was assessed in cancer types where EGFR was typically highly expressed, such as glioma and NSCLC (Frederick *et al.*, 2000; Arteaga, 2003). In glioma, despite frequent amplification and rearrangements of EGFR, there was no significant clinical benefit to gefitinib treatment (Rich *et al.*, 2004). Similarly in NSCLC, despite overexpression of EGFR in 40-80% of NSCLC, addition of gefitinib to chemotherapy provided no benefit (Giaccone *et al.*, 2004; Herbst *et al.*, 2004).

Despite these disappointing results, significant variability in the response to gefitinib revealed a subset of patients who showed an exceptional response to gefitinib treatment. A multi-institutional phase II trial found that Japanese patients showed a higher ORR compared to non-Japanese patients (27.5% vs. 10.4%; odds ratio = 3.27; $p = 0.0023$) (Fukuoka *et al.*, 2003). Multiple studies have since found that gefitinib treatment is associated with longer survival in female patients compared to male patients, non-smokers compared with smokers, and in patients with adenocarcinomas (Kris *et al.*, 2003; Jänne *et al.*, 2004; Miller *et al.*, 2004). Two groups analysed patient tumour samples to determine the mechanism of exceptional response to gefitinib (Lynch *et al.*, 2004; Paez *et al.*, 2004). Sequencing analysis revealed mutations around the ATP-binding pocket of the tyrosine kinase domain of EGFR, including deletions in exon 19 and the substitutions G719C/S, L858R, and L861Q. Lynch *et al.* showed that these mutations were not found in matched normal tissue, suggesting that they were acquired somatically during tumour formation. Paez *et al.* noted that *EGFR* mutation status correlates with patient characteristics: mutations were more frequent in Japanese patients compared to patients from the US (26% vs. 2%); mutations were more frequent in women compared to men (20% vs. 9%); and mutations were more frequent in adenocarcinomas compared to other histological subtypes (21% vs. 2%). By expressing EGFR constructs harbouring L858R and a deletion in exon 19 between L757 and P752 with concomitant insertion of a serine residue at this position

(delL747_P752insS) in the African green monkey fibroblast cell line Cos-7, Lynch *et al.* showed that the cells expressing the mutant receptors were more sensitive to gefitinib compared to Cos-7 cells expressing WT-EGFR (Lynch *et al.*, 2004). Western blot analysis revealed that the mutant receptors showed a higher level of phosphorylation following EGF stimulation compared to WT-EGFR and remained phosphorylated for longer. They also found that receptor phosphorylation was reduced by a lower dose of gefitinib in the mutant receptors compared to WT-EGFR. Similarly, Paez *et al.* showed that H3255 cells, a human NSCLC cell line that harbours an L858R mutation, are more sensitive to gefitinib both in terms of EGFR phosphorylation and cell growth compared to other NSCLC cell lines harbouring WT-EGFR (Paez *et al.*, 2004). These observations are supported by subgroup analysis of the phase III Iressa Pan-Asia Study (IPASS) clinical trial which found that NSCLC patients harbouring mutations in *EGFR* had prolonged progression-free survival (PFS) when treated with gefitinib compared to those treated with carboplatin-paclitaxel (hazard ratio (HR) 0.48, $p < 0.001$), whereas patients with WT-EGFR had shorter median PFS when treated with gefitinib (HR 2.85, $p < 0.001$) (Mok *et al.*, 2009). Following this, two phase III trials (WJTOG3405 and NEJ002) enrolled only patients with EGFR mutations and found that gefitinib treatment significantly improved median PFS in this patient population compared to chemotherapy (Maemondo *et al.*, 2010; Mitsudomi *et al.*, 2010).

Erlotinib is another first-generation EGFRi that was undergoing clinical investigation at a similar time to gefitinib. Initially erlotinib received FDA approval for NSCLC in patients without EGFR mutation status determination, showing an improvement in median OS and RR compared to placebo (6.7 vs. 4.7 months and 9% vs. <1% respectively) (Shepherd *et al.*, 2005). Subsequent studies focused on the use of erlotinib in EGFR mutation positive patients in the first-line setting compared to chemotherapy and reported results very similar to gefitinib (Rosell *et al.*, 2012). Studies comparing gefitinib and erlotinib as first-line therapy for EGFR mutation positive NSCLC have found no significant difference in RR, PFS, or OS (Lim *et al.*, 2014; Urata *et al.*, 2016; Yang *et al.*, 2017b). In the UK, both drugs are recommended for first-line use in patients with EGFR mutation positive NSCLC (Brown *et al.*, 2010)

Gefitinib and erlotinib are structurally similar, and both inhibit EGFR via the same reversible binding mechanism (Yun *et al.*, 2007). Yun *et al.* report that gefitinib forms a single hydrogen bond with M793, which lies at the “hinge” region of the kinase in the back of the ATP binding pocket that links the N- and C-lobes. This binding mode is highly similar to that reported for erlotinib (Stamos *et al.*, 2002). Strikingly, despite evidence that L858R is more sensitive to gefitinib compared to WT-EGFR, Yun *et al.* report no differences in the structure of L858R and WT-EGFR when bound to gefitinib. Instead, the authors note a marked increase in gefitinib affinity in L858R ($K_d = 2.6$ nM) compared to WT ($K_d = 53.5$ nM). Similar data was reported for erlotinib, with Carey *et al.* reporting lower K_i for L858R (6.25 nmol/L) and 746_750del (3.3 nmol/L) compared with WT (17.5 nmol/L). Furthermore, L858R and 746_750del are associated with a reduced affinity for ATP, which the inhibitors compete with for binding (Carey *et al.*, 2006; Yun *et al.*, 2007). This combination of increased inhibitor affinity and decreased ATP affinity leads to the potent sensitivity of L858R and Ex19Del mutations to first-generation EGFRi.

1.3.2.2 Second generation EGFR inhibitors

Unlike first-generation EGFRi, second-generation EGFRi bind irreversibly to EGFR through covalent adduct formation at C797. Additionally, many second-generation EGFRi also bind to other members of the HER family or structurally similar receptors, such as vascular endothelial growth factor receptor (VEGFR) (Yu and Riely, 2013). Three second-generation EGFRi have been clinically assessed: neratinib, dacomitinib, and afatinib.

1.3.2.2.1 Afatinib

Afatinib is an irreversible inhibitor of all HER family members (Solca *et al.*, 2012). Unlike gefitinib and erlotinib, afatinib potently inhibits both WT and mutant forms of EGFR (Li *et al.*, 2008). Li *et al.* showed that afatinib is less selective for L858R over WT-EGFR compared with gefitinib (IC₅₀ values for L858R vs WT-EGFR are 0.8 nM vs 3 nM respectively for gefitinib, but 0.4 nM vs 0.5 nM respectively for afatinib).

Preclinical studies also suggest an increased inhibitory potency against EGFR mutants harbouring the gatekeeper mutation T790M, which is a common acquired resistance mechanism to first-generation EGFRi. Afatinib was shown to have a 10-fold lower IC₅₀ against L858R+T790M compared to gefitinib (1013 vs. 10 nM) and caused >50% reduction in tumour size in xenograft models of L858R+T790M (Li *et al.*, 2008). The increased inhibitory potency of afatinib against mutant EGFR, combined with preclinical evidence of efficacy against EGFR harbouring secondary T790M mutations, led to hopes that afatinib would improve treatment for patients currently receiving first-generation EGFRi. The LUX-Lung series of clinical trials assessed the clinical efficacy of afatinib.

Phase I trials confirmed the efficacy and safety of afatinib in *EGFR* mutant NSCLC patients (Yap *et al.*, 2010; Murakami *et al.*, 2012). Following this, LUX-Lung 2, a single arm, phase II study, reported a median PFS of 12 months in treatment naïve patients (Yang *et al.*, 2012). Afatinib was then compared with platinum-based chemotherapy in the phase III trials LUX-Lung 3 and LUX-Lung 6. Both trials found a significant increase in median PFS in the afatinib group compared to the chemotherapy group, with LUX-Lung 3 reporting 11.1 vs. 6.9 months and LUX-Lung 6 reporting 11.0 vs 5.6 months median PFS for the afatinib and chemotherapy groups respectively (Sequist *et al.*, 2013; Wu *et al.*, 2014). These trials led to the approval of afatinib as a first-line therapy for *EGFR* mutant NSCLC in the US and Europe. Despite demonstrating that afatinib improves median PFS compared to chemotherapy, neither LUX-Lung 3 or LUX-Lung 6 show an improvement in OS. However, a pooled analysis of mature OS data from both trials showed an increase in median OS in the afatinib group compared with the chemotherapy group (27.3 vs. 24.3 months) (Yang *et al.*, 2015b). Efficacy of afatinib as first-line therapy was compared against gefitinib in LUX-Lung 7, which showed that afatinib treatment increased median PFS to a statistically significant, but clinically negligible degree compared to gefitinib (11.0 vs. 10.9 months) (Park *et al.*, 2016). The authors highlight that PFS curves separate more significantly at later timepoints, commencing after median PFS. They suggest that the combination of afatinib's irreversible binding mode and preclinical evidence of its efficacy against EGFR harbouring the T790M gatekeeper mutation may contribute to more durable responses to afatinib compared with gefitinib. Supporting this hypothesis, time-to-

treatment failure (TTF) showed a more appreciable improvement in patients treated with afatinib compared to those treated with gefitinib (13.7 vs. 11.5 months). TTF is defined as the time between randomisation and treatment discontinuation (for any reason, including disease progression, treatment toxicity, and death), and was selected as a coprimary end-point as in normal clinical practice many patients continue to receive TKI treatment beyond disease progression. Despite this improvement in TTF, afatinib treatment did not improve median OS compared to gefitinib (Paz-Ares *et al.*, 2017). Currently, afatinib is approved for use as first-line therapy in EGFR-mutation positive NSCLC patients (Deeks and Keating, 2018).

1.3.2.2.2 Dacomitinib

Dacomitinib is an irreversible inhibitor with activity against EGFR, HER2, and HER4 (Engelman *et al.*, 2007b). A single-arm phase II clinical trial of dacomitinib in NSCLC patients reported a median PFS of 18.2 months (Jänne *et al.*, 2014). The phase III ARCHER 1050 trial compared dacomitinib with gefitinib as first-line therapy in NSCLC patients with EGFR mutations (Wu *et al.*, 2017). This study found an increased median PFS and median OS in the dacomitinib group compared to the gefitinib group (14.7 vs. 9.2 months and 34.1 vs. 26.8 months respectively) (Mok *et al.*, 2018). Despite these promising improvements in PFS, concerns have been raised about the ARCHER 1050 trial and its implications for the clinical utility of dacomitinib (Addeo, 2018). Crucially, ARCHER 1050 excluded patients with brain metastases, which affects almost a third of NSCLC patients with EGFR mutations during the course of their disease (Iuchi *et al.*, 2015). Although the authors highlight fewer brain metastases in the dacomitinib group compared to the gefitinib group (1/227 vs. 11/225), this is an important caveat when evaluating the conclusions of this study. However, despite this omission dacomitinib received FDA approval for the first-line treatment of NSCLC with EGFR mutations (FDA, 2018a).

1.3.2.2.3 Neratinib

Neratinib is an irreversible inhibitor of EGFR and HER2 (Kwak *et al.*, 2005). A multicentre phase II trial reported an extremely low RR of 2% in NSCLC, with no response observed in patients who did not have a sensitising *EGFR* mutation (Sequist *et al.*, 2010b). These disappointing results may be accounted for by the dose reduction from 320 mg/day to 240 mg/day due to the development of grade 3 diarrhoea in >50% of patients. Diarrhoea is an adverse event associated with inhibition of WT-EGFR, indicating that this toxicity is due to the inability of neratinib to target mutant EGFR over WT-EGFR. The authors indicate that this dose reduction may have brought drug bioavailability to subtherapeutic levels. As of March 2020 there are no ongoing studies of neratinib in NSCLC.

1.3.2.3 Acquired resistance to EGFR inhibitors in the first-line setting

1.3.2.3.1 EGFR-dependent mechanisms of resistance

Although first-generation EGFRi have led to a median PFS benefit of ~12 months compared to chemotherapy, the majority of patients develop resistant disease within 16 months (Mok *et al.*, 2009; Zhou *et al.*, 2011). Resistance occurs most frequently through “on-target” alterations to EGFR itself. The most frequent on-target alteration (~60%) is the T790M point mutation, often referred to as a “gatekeeper” mutation owing to its location at the entrance to a hydrophobic pocket at the back of the ATP-binding site (Figure 1.6) (Yu *et al.*, 2013). This hydrophobic pocket is an important determinant of kinase inhibitor specificity, and the substitution of threonine with a bulky methionine may impair binding of first-generation inhibitors to the ATP-binding site (Kobayashi *et al.*, 2005; Kwak *et al.*, 2005; Pao *et al.*, 2005). Additionally, *in vitro* kinase assays have shown that T790M prevents gefitinib from binding to EGFR by restoring the ATP affinity of L858R mutant receptors to a level comparable to WT-EGFR ($K_{m[ATP]} = 5.2 \mu\text{M}$ for WT-EGFR, $K_{m[ATP]} = 148 \mu\text{M}$ for L858R, and $K_{m[ATP]} = 8.4 \mu\text{M}$ for L858R+T790M) (Yun *et al.*, 2008). As first-generation EGFRi compete with ATP for binding to EGFR, restoration of the receptors affinity for ATP prevents

first-generation EGFRi from outcompeting ATP and thus causes resistance to these inhibitors. In addition to T790M, case reports have identified other less common secondary mutations that also confer resistance to first-generation EGFRi.

Balak *et al.* reported a patient who developed a D761Y mutation at progression on gefitinib. D761Y is located adjacent to E762 in the α C-helix which, in combination with K745, forms a catalytically important salt bridge with ATP (Balak *et al.*, 2006). *In vitro* experiments comparing the gefitinib sensitivity of cells expressing L858R, L858R+D761Y, and L858R+T790M revealed that D761Y conferred modest resistance to gefitinib compared to T790M in terms of cell viability and EGFR phosphorylation (Balak *et al.*, 2006).

Costa *et al.* reported a patient with L858R positive NSCLC who developed a L747S mutation after a 40-month response to gefitinib (Costa *et al.*, 2007). L747S is at the start of the loop between the β 3 strand and the α C-helix, towards the rear of the catalytic cleft. Analogous mutations have been detected in ABL1 (L273M) in imatinib-resistant chronic myelogenous leukaemia (Talpaç *et al.*, 2006). Expression of L858R+L747S constructs in Ba/F3 cells revealed an increase in IC₅₀ from 7 nM to ~400 nM compared to L858R alone (Costa *et al.*, 2007).

Bean *et al.* reported a patient who developed a T854A mutation after long-term treatment including gefitinib and erlotinib (Bean *et al.*, 2008). 14 months after initial resection, the patient received gefitinib for >2 years until treatment was discontinued following an episode of pneumonia. After a further 2 years, the patient received erlotinib for 2 months until treatment was discontinued due to severe thrombocytopenia. 5 months later, erlotinib treatment was restarted with palliative radiation and a pleural catheter was placed. Sequencing of DNA extracted from pleural fluid cells identified an L858R mutation and a T854A mutation in *EGFR*. T854 is located at the base of the ATP-binding site on the C-lobe, and the side chain is within contact distance of gefitinib or erlotinib. The authors suggest that T854A could cause loss of contacts with the inhibitor that would reduce binding affinity. Western blot analysis of 293T cells expressing T854A showed that EGFR phosphorylation was retained at higher erlotinib concentrations in the presence of the T854A mutation in both WT and L858R settings (Bean *et al.*, 2008).

These less common secondary mutations were examined by Chiba *et al.*, who expressed L858R+L747S, L858R+D761Y, and L858R+T854A in Ba/F3 cells (Chiba *et al.*, 2017). The authors showed that L747S and D761Y conferred a 5-fold increase in IC₅₀ compared to L858R and T854A conferred a 50-fold increase in IC₅₀ when treated with gefitinib or erlotinib. Importantly, the authors find that all three mutations are sensitive to afatinib and the third-generation EGFRi osimertinib highlighting these inhibitors as potential salvage therapies for patients who acquire these mutations.

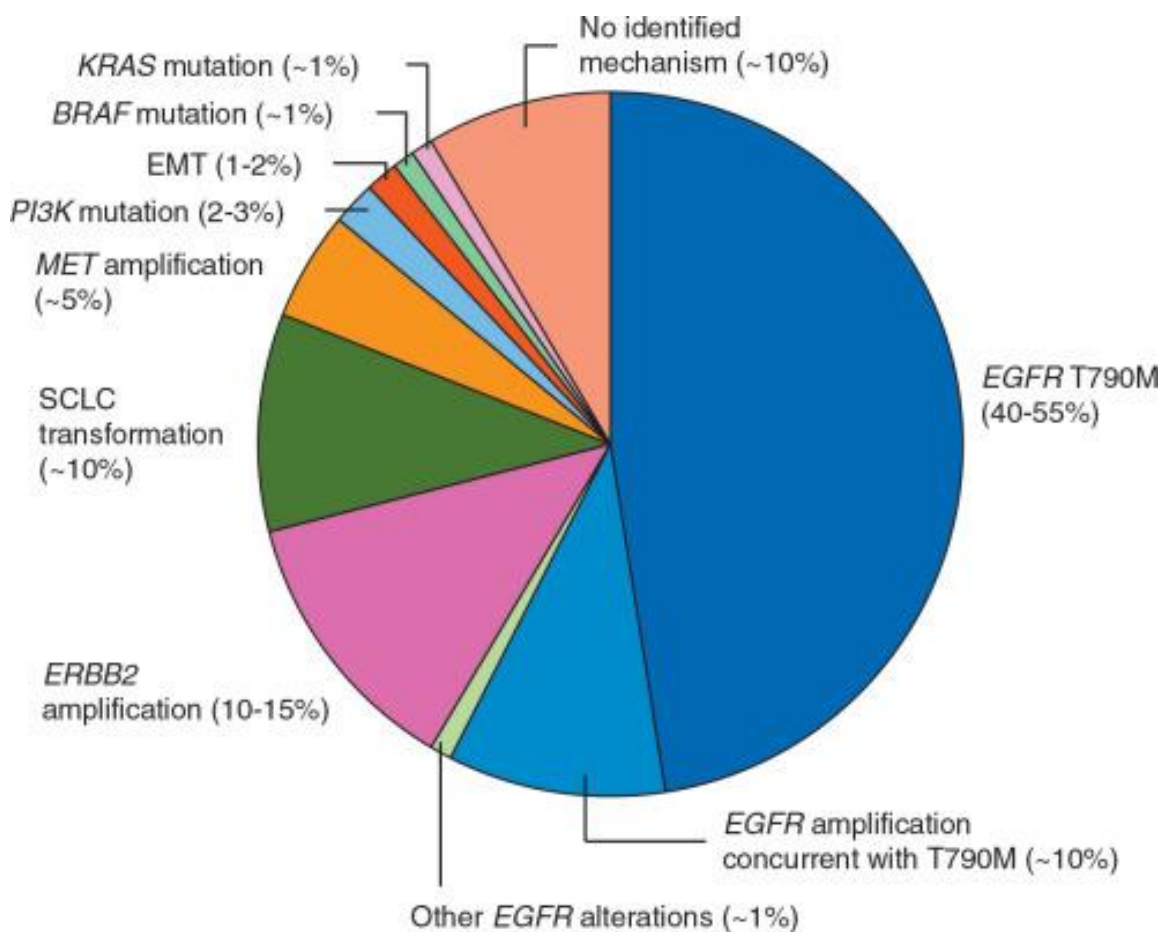


Figure 1.6 – Acquired resistance to first-line EGFRi. The frequency of resistance mechanisms to first- and second-generation EGFRi as first-line therapies. T790M with or without concurrent EGFR amplification is the most common mechanism of resistance (~60%). Amplification of HER2 is the most common EGFR-independent mechanism of resistance (10-15%). SCLC, small-cell lung cancer; EMT, epidermal-to-mesenchymal transition. Adapted with permission from Elsevier (Westover *et al.*, 2018).

1.3.2.3.2 EGFR-independent mechanisms of resistance

In addition to on-target mutations that prevent EGFRi from binding to EGFR, alterations that occur “off-target” can also drive resistance to EGFRi. These alterations are often classified as “bypass” resistance mechanisms, as they utilise alternative signalling networks to bypass EGFR and activate the same key oncogenic signalling nodes.

The most common mechanism of EGFR-independent resistance is *HER2* amplification, which occurs in around 10-15% of EGFRi resistant patients (Figure 1.6) (Takezawa *et al.*, 2012). *HER2* is also a member of the HER family of RTKs and is most well studied in breast cancer where *HER2* amplification occurs in 15-20% of cases (Burstain, 2005). In EGFRi resistant NSCLC patients, *HER2* amplification occurs mutually exclusively with T790M (Takezawa *et al.*, 2012). Cell line models of EGFRi resistance driven by *HER2* amplification have shown sustained phosphorylation of *HER3*, *AKT*, and *ERK* following erlotinib treatment compared to EGFRi sensitive cells, indicating that *HER2* amplification bypasses EGFR activation to maintain oncogenic signalling despite continued EGFRi treatment (Takezawa *et al.*, 2012). Although there is currently no approved anti-*HER2* therapy approved for EGFRi resistant NSCLC, afatinib treatment has been shown to inhibit *HER2* in cell line models of *HER2*-mediated EGFRi resistance, resulting in inhibition of *HER3*, *AKT*, and *ERK* signalling. This indicates afatinib may be a useful salvage therapy in this setting, however no clinical studies have assessed this in patients.

Amplification of *MET* is another common EGFR-independent resistance mechanism, occurring in around 5% of EGFRi resistant patients (Figure 1.6) (Sequist *et al.*, 2011; Yu *et al.*, 2013). *MET* is stimulated by HGF, and activates the downstream signalling pathways of *MAPK*, *PI3K*, and *SRC* (Abounader and Laterra, 2005). *In vitro* models revealed that *MET* amplification conferred gefitinib resistance by *HER3*-dependent activation of the *PI3K* pathway (Engelman *et al.*, 2007a). Although *MET* inhibitors are not currently clinically approved for NSCLC patients with *MET*-driven EGFRi resistance, evidence from case reports indicates that combination of EGFRi with a *MET* inhibitor benefits patients with *MET*-driven EGFRi

resistance (Gainor *et al.*, 2016a; York *et al.*, 2017). A phase IB/II clinical trial (NCT01610336) assessing the use of the MET inhibitor INC280 in combination gefitinib in this patient population is ongoing.

Other genetic alterations have also been reported as conferring EGFRi resistance but at lower frequencies (Figure 1.6). These include mutations in *KRAS* (Chabon *et al.*, 2016), *BRAF* (Ohashi *et al.*, 2012), and *PIK3CA* (Sequist *et al.*, 2011), as well as loss of phosphatase and tensin homolog (*PTEN*) (Sos *et al.*, 2009) and neurofibromin-1 (*NF-1*) (de Bruin *et al.*, 2014). Non-genetic mechanisms of resistance have also been described. Upregulation of HGF, the ligand that activates MET, has been reported (Yano *et al.*, 2011), as has upregulation of the RTKs insulin-like growth factor 1 receptor (IGF1R) (Cortot *et al.*, 2013) and FGFR1 (Ware *et al.*, 2013a). Histological transformation from NSCLC to small-cell lung cancer (SCLC) morphology and epidermal-to-mesenchymal transition (EMT) is also reported in 3-10% and 1-2% of EGFRi resistant patients respectively (Sequist *et al.*, 2011; Marcoux *et al.*, 2019). Tumours that transform to a SCLC morphology show substantially reduced expression of EGFR, rendering them unresponsive to EGFRi (Niederst *et al.*, 2015). EMT is characterised by a change in cell morphology from epithelial to a more spindle-like mesenchymal morphology and a more invasive phenotype. This is often associated with the loss of epithelial markers, such as E-cadherin, and the gain of mesenchymal markers, such as vimentin (Tsoukalas *et al.*, 2017). Although EMT is associated with EGFRi resistance, the specific mechanistic role it plays in EGFRi resistance is unclear.

1.3.3 Third-generation EGFR inhibitors as salvage therapy in NSCLC

As the most common resistance mechanism to first-generation EGFRi therapy, the T790M mutation, causes resistance by preventing reversible inhibitors from out-competing ATP, it was initially thought that irreversible second-generation EGFRi might overcome T790M-mediated resistance. Preclinical evidence showed that dacomitinib and afatinib had lower IC₅₀ values against EGFR with secondary T790M mutations and were significantly more effective at reducing growth of tumours harbouring secondary T790M mutations compared to gefitinib (Engelman *et al.*,

2007b; Li *et al.*, 2008). Despite these promising preclinical data, responses in clinical trials were disappointing, with RR of ~10% and median PFS of 4.5 months in patients with T790M mutations reported for both inhibitors (Miller *et al.*, 2012; Katakami *et al.*, 2013; Ellis *et al.*, 2014). These poor clinical responses are likely due to an inability of dacomitinib and afatinib to inhibit T790M at clinically achievable doses owing to intolerable adverse events. Dacomitinib and afatinib lack mutant EGFR selectivity, resulting in potent inhibition of WT-EGFR that is associated with adverse skin and gastrointestinal events (Yap *et al.*, 2010; Jänne *et al.*, 2011). Greater responses have been observed in patients treated with a regimen of daily afatinib combined with fortnightly cetuximab, which has shown a RR of 30% and median PFS of 4.7 months (Janjigian *et al.*, 2014). However, this combination is also associated with substantial skin and gastrointestinal adverse events. Notably, none of these treatment strategies significantly improve median PFS compared to cytotoxic chemotherapy in patients who have acquired resistance to gefitinib or erlotinib (Goldberg *et al.*, 2013; Mok *et al.*, 2017b).

Two EGFRi that are capable of inhibiting T790M with minimal effect on WT-EGFR have been developed and assessed in clinical trials. Preclinical studies have shown that rociletinib and osimertinib bind irreversibly to EGFR by covalent adduct formation at C797 and are highly potent against L858R+T790M, whilst having minimal activity against WT-EGFR (Walter *et al.*, 2013; Cross *et al.*, 2014). *In vivo* experiments showed that rociletinib and osimertinib were able to induce increased reduction of tumours harbouring L858R+T790M compared to afatinib. Interestingly, in a xenograft model of a tumour driven by WT-EGFR rociletinib had significantly reduced antitumour activity compared to afatinib (Walter *et al.*, 2013). Furthermore, tumours harvested from rociletinib treated mice had no detectable reduction in WT-EGFR phosphorylation, highlighting the mutation selectivity of rociletinib. Notably, rociletinib was shown to have activity against the rare EGFR mutations G719S, L861Q, and exon 19 insertions (Ex19Ins) but not against any Ex20Ins (Walter *et al.*, 2013).

A single-arm phase I/II trial assessed the efficacy of rociletinib in *EGFR* mutant NSCLC patients who had disease progression during previous treatment with an existing EGFRi. This trial comprised of a dose-escalation phase I component that was not restricted to T790M-positive patients and a subsequent phase II component

exclusively enrolling patients positive for T790M (Sequist *et al.*, 2015b). This trial found a 59% RR and median PFS of 13.1 months among T790M-positive patients ($n = 46$) and a 29% RR and median PFS of 5.6 months for patients without T790M ($n = 84$), indicating that rociletinib has activity in T790M-positive patients. The most significant adverse event was hyperglycaemia, with grade 3-4 hyperglycaemia observed in >24% of patients. This was caused by a metabolite of rociletinib that inhibits IGF1R/IR and was subsequently managed with antidiabetic medications, reducing grade 3-4 hyperglycaemia to 8% (Sequist *et al.*, 2015a; Simmons *et al.*, 2015; van der Steen *et al.*, 2016). Based on the promising data reported by Sequist *et al.*, the FDA granted rociletinib priority review under the Breakthrough Therapy Designation Program. However, data presented at the JP Morgan Healthcare Conference the following year showed a drastically reduced RR of 34% and 28% for patients treated with 625 mg and 500 mg twice-daily doses respectively. These new data had been updated to include “confirmed” RR, and it transpired that the initial results included both “confirmed” and “unconfirmed” RR. RECIST 1.1, the criteria for assessing response used in the trial, states that confirmation of response is required by repeat assessments no less than 4 weeks after the criteria for response was originally met (Dhingra, 2016; van der Steen *et al.*, 2016). The authors explained that at time of publication at least half the patients had undergone only one response-evaluation scan, and therefore many reported responses were actually unconfirmed PR (Sequist *et al.*, 2016). Furthermore, there is evidence to suggest rociletinib has limited central nervous system (CNS) activity (Varga *et al.*, 2015). Following these revelations the FDA decided not to approve rociletinib on the available data, leading Clovis Oncology to discontinue the development of rociletinib and terminate enrolment in all clinical trials with rociletinib (van der Steen *et al.*, 2016).

Osimertinib treatment in EGFRi resistant NSCLC was examined in two single-arm phase II clinical trials (AURA extension (NCT01802632) and AURA2 (NCT02094261)) (Goss *et al.*, 2016; Yang *et al.*, 2017a). These trials enrolled patients who experienced disease progression following previous EGFRi therapy and confirmed T790M mutations. Pooled analysis of these trials revealed a median PFS of 9.9 months and a median OS of 26.8 months, and the FDA approved osimertinib for the second-line treatment of T790M-positive NSCLC patients under

the Breakthrough Therapy Designation Program (FDA, 2017; Ahn *et al.*, 2019). In contrast to rociletinib, these studies showed the efficacy of osimertinib in patients with CNS metastases. A phase III trial (AURA3, NCT02151981) built on these trials, comparing osimertinib treatment with platinum-pemetrexed in *EGFR* mutant NSCLC patients with progressive disease following previous EGFRi therapy and confirmed T790M mutations. AURA3 reported a dramatic increase in median PFS for patients receiving osimertinib compared to those receiving platinum-pemetrexed (10.1 vs. 4.4 months) (Mok *et al.*, 2017a). Notably, each of the AURA trials reported low rates of grade 3 or higher adverse events.

In addition to potently inhibiting L858R+T790M, preclinical studies showed osimertinib was active against cell lines harbouring single L858R and Ex19Del mutations (Cross *et al.*, 2014). Furthermore, a phase I study indicated that osimertinib may be effective in treatment-naïve NSCLC patients with EGFR mutations (Ramalingam *et al.*, 2018b). These studies prompted the phase III FLAURA clinical trial (NCT02296125), which examined osimertinib as a first-line therapy for EGFR mutant NSCLC patients compared with gefitinib or erlotinib (Soria *et al.*, 2018). The FLAURA trial reported a significant improvement in median PFS for the osimertinib treatment group compared with the group receiving gefitinib or erlotinib (18.9 vs. 10.2 months). This led to the FDA approving osimertinib as a first-line therapy for EGFR mutant NSCLC (FDA, 2018b). Recently published OS data shows a significant median OS benefit in the osimertinib treatment group compared to the group treated with gefitinib or erlotinib (38.6 vs. 31.8 months) (Ramalingam *et al.*, 2020). Despite these data, in the UK osimertinib is not recommended for use as a first-line therapy by NICE (NICE, 2020). Despite noting that data from FLAURA is compelling and that use of osimertinib would remove the need for invasive biopsies to confirm T790M mutations, NICE state that a head-to-head comparison with afatinib would be required to change current guidelines, citing LUX-Lung 7 as evidence that afatinib is superior to gefitinib. Additionally, NICE state that osimertinib is not currently cost-effective at the price offered.

1.3.3.1 Acquired resistance to third-generation EGFRi

Despite the success of osimertinib in both the first-line and second-line settings, the emergence of resistant disease remains an urgent clinical problem. Just as with first-generation EGFRi, a number of EGFR-dependent and EGFR-independent mechanisms of osimertinib resistance have been reported. However, osimertinib resistance is complicated by the fact that it is used in both first- and second-line settings, with differences in resistance mechanisms reported for each setting (Figure 1.7). In the first-line setting, resistance mechanisms co-occur with primary sensitising mutations in EGFR (e.g. Ex19Del or L858R). In the second-line setting, where osimertinib is used to treat NSCLC with T790M-mediated resistance to first- or second-generation EGFRi, resistance mechanisms co-occur with both the primary EGFRi-sensitising mutation and a secondary T790M mutation.

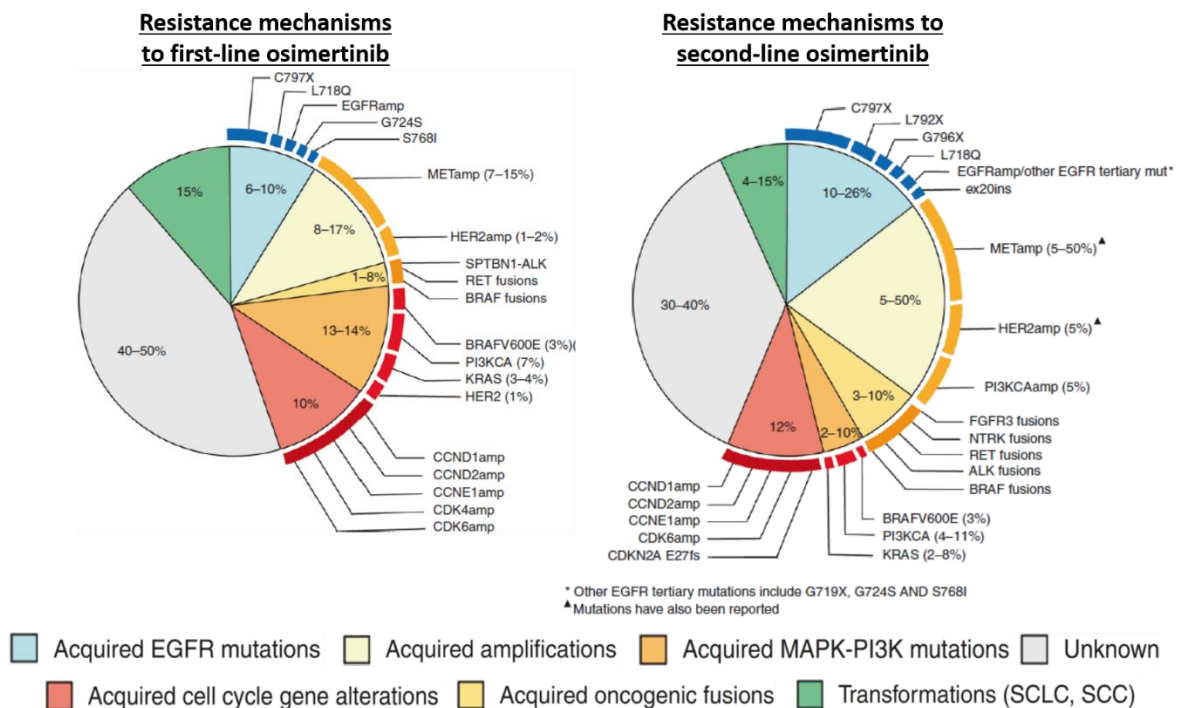


Figure 1.7 – Acquired resistance to third-generation EGFRi. The frequency of resistance mechanisms to osimertinib in the first-line (left) and second-line (right) settings. CCND, Cyclin; CDK, Cyclin-dependent kinase; SPTBN1-ALK, Spectrin-beta chain, brain 1-ALK; NTRK, Neurotrophic Tyrosine Kinase; SCC, squamous cell carcinoma. Adapted with permission from Springer Nature (Leonetti *et al.*, 2019a).

1.3.3.1.1 EGFR-dependent mechanisms of resistance

1.3.3.1.2 C797S

C797S has emerged as the major EGFR-dependent driver of resistance to osimertinib in both the first- and second-line settings, accounting for 7% and 10-26% of cases of resistance respectively (Figure 1.7) (Thress *et al.*, 2015; Papadimitrakopoulou *et al.*, 2018; Leonetti *et al.*, 2019b). Following first-line osimertinib treatment, C797S occurs as a secondary mutation in addition to a primary EGFRi-sensitising mutation (e.g. Ex19Del or L858R). When osimertinib is used in the second-line setting following T790M-mediated resistance to other EGFRi, C797S occurs as a tertiary mutation in addition to the primary EGFRi-sensitising mutation and the secondary T790M mutation. Thress *et al.* identified C797S by performing next-generation sequencing (NGS) on cell-free plasma DNA (cfDNA) collected during the phase I AURA study. C797S had previously been shown in preclinical studies to confer resistance to other irreversible inhibitors, by impairing covalent binding of these inhibitors to EGFR (Zhou *et al.*, 2009). To confirm that C797S confers resistance to osimertinib, Thress *et al.* expressed L858R+C797S and Ex19Del+C797S in Ba/F3 cells and found that cells harbouring C797S mutations were significantly less sensitive to osimertinib both in terms of cell growth and EGFR phosphorylation. Computational modelling suggests that osimertinib binds to EGFR at C797 through a direct addition mechanism in which the nucleophilic thiolate group of C797 attacks the electrophilic β -carbon of the acrylamide group of osimertinib (Paasche *et al.*, 2010; Capoferri *et al.*, 2015). As serine is less nucleophilic than cysteine, it is thought that the C797S substitution prevents the nucleophilic attack of the β -carbon of the acrylamide group of osimertinib thus preventing covalent bond formation.

Several approaches to overcome C797S mediated resistant disease are currently under investigation. EAI045 is a fourth-generation EGFRi that has been developed to be highly selective for L858R over WT-EGFR (Jia *et al.*, 2016). EAI045 binds to an allosteric site away from the ATP-binding site and is therefore not affected by C797S. However, this allosteric site is disrupted by the formation of asymmetric dimers between mutant and WT-EGFR, which causes a drastic reduction in EAI045

binding. To address this, Jai *et al.* combined EAI045 with cetuximab, an anti-EGFR antibody which prevents EGFR dimer formation. They found that the combination therapy induced significant tumour regression in mice harbouring L858R+T790M, whereas mice treated with EAI045 monotherapy did not respond. More recently, the same group described another allosteric inhibitor, JBJ-04-125-02, which has single-agent activity against *in vitro* and *in vivo* models of L858R+T790M (To *et al.*, 2019). However, JBJ-04-125-02 was not effective in all cell line models of L858R+T790M, likely due to high levels of EGFR expression causing increased dimer formation which antagonises binding of JBJ-04-125-02. Combination of JBJ-04-125-02 with osimertinib increased JBJ-04-125-02 binding to EGFR and showed increased antitumour activity compared to either single agent alone. Interestingly, as both EAI045 and JBJ-04-125-02 bind to an allosteric site that is uniquely formed in L858R mutant receptors, neither has any effect on Ex19Del. Neither inhibitor is currently under clinical investigation.

Brigatinib, a novel dual-target EGFR-ALK inhibitor has also been investigated as an approach to overcome C797S mediated resistance (Uchibori *et al.*, 2017). Computational modelling has shown that brigatinib can fit into the ATP-binding site of triple-mutant EGFR with primary L858R, secondary T790M, and tertiary C797S mutations. Furthermore, *in vitro* experiments showed that brigatinib bound to EGFR mutations with additional T790M and C797S mutations in an ATP-competitive manner. Experiments using Ba/F3 cells and the human NSCLC cell lines PC9 and MGH121 found that brigatinib was able to inhibit EGFR signalling in cells with triple-mutant EGFR harbouring primary Ex19Del, secondary T790M, and tertiary C797S mutations at significantly lower doses compared to osimertinib. *In vivo* experiments using PC9 cells harbouring triple-mutant EGFR showed that brigatinib treatment significantly reduced tumour volume compared to osimertinib, with phosphorylation of EGFR inhibited in brigatinib treated tumours. Interestingly, combination of brigatinib with cetuximab or panitumumab caused reduced expression of EGFR compared to either single agent and provided significant additional antitumour effect. Brigatinib was used to treat an *EGFR*-mutant NSCLC patient who experienced disease progression following treatment with osimertinib as a single agent and subsequently in combination with the anti-vascular endothelial growth factor (VEGF) antibody bevacizumab (Zhao *et al.*, 2018). Following disease

progression on these regimens T790M and *cis*-C797S were detected in circulating tumour DNA (ctDNA) and the patient was treated with a combination of osimertinib, bevacizumab, and brigatinib. Addition of brigatinib to the treatment strategy resulted in partial remission and a reduced abundance of C797S in ctDNA. Despite these promising data, a phase I/II trial (NCT01449461) reported disappointing responses to brigatinib, with only two of 42 patients achieving PR despite plasma concentrations of brigatinib surpassing the IC₅₀ values for triple-mutant EGFR observed by Uchibori *et al.* (Gettinger *et al.*, 2016). However, this trial was conducted in an unselected cohort of patients using brigatinib as a single agent. Further clinical investigation of brigatinib in a cohort of patients with C797S mutations and in combination with agents suggested by preclinical data is therefore warranted.

1.3.3.1.3 L718Q

L718Q was identified as a resistance mechanism to osimertinib by using an N-ethyl-N-nitrosourea (ENU) mutagenesis screen (Ercan *et al.*, 2015). This screening approach utilises the mutagen ENU to generate a large number of mutant variants within an osimertinib-sensitive population of cells. Mutagenised cells are subsequently exposed to osimertinib to isolate clones that have acquired mutations that confer resistance to osimertinib. *In vitro* experiments showed that Ba/F3 cells expressing Ex19Del+T790M+L718Q had ~10-fold increase in IC₅₀ compared to Ex19Del+T790M when treated with osimertinib. Bersanelli *et al.* identified L718Q in a patient whose disease progressed following osimertinib treatment (Bersanelli *et al.*, 2016). The patient was initially diagnosed with a primary L858R mutation in *EGFR* and developed secondary T790M mutation following gefitinib treatment. The patient then received 13 months osimertinib treatment before further disease progression. Following progression on osimertinib, sequencing of DNA extracted from a biopsy sample identified a tertiary L718Q mutation in *EGFR* in addition to the pre-existing L858R and T790M mutations, with no evidence of C797S or EGFR-independent osimertinib resistance mechanisms.

To better understand the mechanism by which L718Q confers osimertinib resistance, Callegari *et al.* performed a comprehensive series of computational experiments comparing T790M+L718Q with T790M alone (Callegari *et al.*, 2018). The authors show that addition of L718Q does not alter the ionization state of C797, and thus does not alter the intrinsic reactivity of C797 to form a covalent bond with osimertinib. They also show that L718Q does not raise the activation free-energy required for adduct formation or alter the affinity of the receptor for osimertinib. However, MD simulations revealed that addition of L718Q stabilises a conformation where C797 and osimertinib are not close enough for the covalent bond to form. In EGFR with T790M+L718Q mutations, the fraction of conformations where C797 is close enough to the β -carbon of the acrylamide group of osimertinib to react is lower for compared to T790M alone (0.7% of structures for T790M+L718Q compared to 20.5% for T790M alone). Simulations show that this less reactive EGFR conformation observed in T790M+L718Q is stabilised by H-bonds between the acrylamide ring of osimertinib and Q718. Together, these data suggest that L718Q confers osimertinib resistance by stabilising a conformation that prevents covalent bond formation between C797 and osimertinib. Interestingly, *in vitro* experiments indicate that both Ex19Del+L718Q and L858R+L718Q are sensitive to afatinib, suggesting that afatinib could be used as a salvage therapy for patients harbouring L718Q (Ercan *et al.*, 2015).

1.3.3.1.4 G724S

Several case reports have identified G724S in osimertinib-refractory patients who previously experienced T790M-positive disease progression on either gefitinib or erlotinib (Oztan *et al.*, 2017; Peled *et al.*, 2017; Fassunke *et al.*, 2018). To establish G724S as an osimertinib resistance mechanism, Fassunke *et al.* expressed Ex19Del, G724S, and Ex19Del+G724S in NIH-3T3 cells and Ba/F3 cells and found that cells harbouring G724S were significantly less sensitive to osimertinib both in terms of EGFR phosphorylation and cell growth (Fassunke *et al.*, 2018). Interestingly, there is evidence to suggest that G724S might emerge from subclonal populations that exist prior to osimertinib treatment. In a case series of four patients, Fassunke *et al.* report that two patients had low levels of G724S prior to osimertinib

treatment whereas the other two patients had no detectable G724S. Following disease progression on osimertinib treatment all four patients had detectable G724S and no detectable T790M. Similar findings are reported by Peled *et al.*, who describe a patient with detectable G724S and T790M prior to osimertinib treatment, who showed no detectable T790M and an increased mutant allele frequency (MAF) of G724S following disease progression on osimertinib (Peled *et al.*, 2017).

Intriguingly, G724S mutations have only been identified in patients harbouring Ex19Del mutations (Oztan *et al.*, 2017; Fassunke *et al.*, 2018). Brown *et al.* show that osimertinib does not inhibit EGFR phosphorylation in cells expressing Ex19Del+G724S but potently inhibits EGFR phosphorylation in cells expressing L858R+G724S, indicating that G724S does not confer osimertinib resistance in the context of an L858R primary mutation (Brown *et al.*, 2019). For irreversible inhibitors to bind covalently to EGFR, they must first form a reversible complex with EGFR. When in this reversible complex with osimertinib, EGFR adopts a characteristic “bent” P-loop conformation which contributes to the affinity of osimertinib for EGFR as it enables the phenyl ring of F723 to make an energetically favourable contact with the indole ring of osimertinib (Yosaatmadja *et al.*, 2015). G724S rigidifies the P-loop of EGFR, preventing the formation of a stable “bent” P-loop conformation and displacing F723 from contact with osimertinib in both Ex19Del+G724S and L858R+G724S. However, binding-free energy calculations reveal that osimertinib reversibly binds more tightly to L858R compared to Ex19Del. Importantly, the binding-free energy calculated for L858R+G724S and Ex19Del alone are indistinguishable. This suggests that loss of F723-osimertinib contact in the L858R setting does not cause a sufficient reduction in binding affinity to prevent osimertinib from binding to L858R+G724S.

Although 746_750del accounts for approximately 67% of Ex19Del (Kobayashi and Mitsudomi, 2016), Brown *et al.* observed that in 15 out of 19 patients G724S mutations co-occurred with rare variants of Ex19Del, including substitution of the 7 amino acids from E746 to S752 for a serine residue (E746_752S>V) or isoleucine (E746_S752>I), an 8 amino acid deletion from S752 to I759 (S752_I759del), and a 6 amino acid deletion from L747 to S752 (L747_S752del) (Brown *et al.*, 2019). To investigate the reason for the increased representation of G724S in rare Ex19Del, Brown *et al.* focused on E746_S752>V. As previously observed in 746_750del,

E746_S752>V but not E746_S752>V+G724S was able to stabilise a favourable interaction between F723 and the indole ring of osimertinib. They also found that, just as with 746_750del, 746_S752>V stabilised an α C-helix “in” conformation compared to WT, which has previously been shown to increase dimerisation-dependent receptor activation (Shan *et al.*, 2012). Interestingly, they found that addition of G724S further stabilises the “in” α C-helix conformation compared to E746_S752>V alone. By contrast, addition of G724S to 746_750del causes less frequent “in” α C-helix conformations compared to 746_750del alone. This suggests that G724S in the background of a rare Ex19Del will increase dimerisation-dependent receptor activation, whereas G724S in the background of a common Ex19Del will decrease receptor activation.

1.3.3.1.5 G796D

A random mutagenesis screen in Ba/F3 cells revealed that G796D is able to confer resistance to CI-1033, a pan-ErbB inhibitor that forms a covalent bond at C797 in the same way as osimertinib (Avizienyte *et al.*, 2008). G796D has also been identified following disease progression on osimertinib in an L858R-positive NSCLC patient who had previously been treated with gefitinib until disease progression with T790M detection (Zheng *et al.*, 2017). As with G724S, there is evidence to suggest that G796D was present in a subclonal population before osimertinib treatment. Plasma samples taken before gefitinib treatment detected G796D at an MAF of 0.61%. Intriguingly, after disease progression on osimertinib G796D MAF increased to 1.91%, while L858R and T790M became undetectable (MAF pre-osimertinib treatment were 0.86% and 1.85% respectively). These data not only indicates that G796D confers resistance to osimertinib, but it also suggests that G796D may be an oncogenic mutation itself. In support of this hypothesis, expression of G796D in Ba/F3 cells conferred interleukin-3 (IL-3) independent growth at a slower rate compared to Ba/F3 cells expressing L858R, indicating mild oncogenic properties. G796 is adjacent to C797 and structural modelling of the EGFR kinase domain in complex with osimertinib showed that the side chain of mutated D796 would clash with osimertinib, leading to a steric and energetic repulsion that would result in loss of binding affinity (Zheng *et al.*, 2017). The ability of G796 to confer osimertinib

resistance was confirmed by dose response experiments and Western blot analysis, which revealed that G796D is resistant to osimertinib both in terms of cell growth and EGFR phosphorylation.

1.3.3.1.6 L792X

Mutations at L792, including L792F/Y/H, have been identified in *EGFR*-mutant NSCLC patients following disease progression on osimertinib (Chen *et al.*, 2017; Ou *et al.*, 2017; Fairclough *et al.*, 2019). Interestingly, these mutations are observed in *cis* with T790M but in *trans* with C797S, indicating the emergence of subclonal resistance mechanisms following treatment with osimertinib. Computational modelling indicates that mutated F792 would sterically interfere with a methoxy group on the phenyl ring of osimertinib, thereby disrupting the binding of osimertinib to EGFR (Ou *et al.*, 2017). By measuring MAPK signalling following osimertinib treatment, cells expressing L858R+T790M+L792F/H have been shown to harbour intermediate levels of osimertinib resistance compared to cells expressing either L858R+T790M or L858R+T790M+C797S (Fairclough *et al.*, 2019). L792F was also identified in an ENU mutagenesis screen as a resistance mechanism to afatinib in the context of a deletion of E709 and T710 with concomitant insertion of an aspartic acid (E709_T710insD) primary mutation (Kobayashi *et al.*, 2017). Subsequent experiments found that L792F also confers afatinib resistance in the context of Ex19Del or L858R primary mutations. However, as observed with osimertinib, L792F confers an intermediate resistance to afatinib compared to C797S.

1.3.3.2 EGFR-independent mechanisms of resistance

EGFR-independent mechanisms of resistance to osimertinib are similar to those seen in resistance to first-generation EGFRi. However, there are some differences in the frequency of specific resistance mechanisms, particularly depending on whether osimertinib is given as first- or second-line therapy following T790M-positive resistance to first generation EGFRi (Figure 1.7).

HER2 amplification has been identified in 2% and 5% of patients who have acquired resistance to first- and second-line osimertinib respectively (Figure 1.7) (Papadimitrakopoulou *et al.*, 2018; Ramalingam *et al.*, 2018a). As observed with *HER2*-mediated resistance to first-generation EGFRi, overexpression of *HER2* in a NSCLC cell line caused resistance to rociletinib and osimertinib (Ortiz-Cuaran *et al.*, 2016). *MET* amplification has also been reported in 4-15% and 5-50% of patients who have acquired resistance to first- and second-line osimertinib respectively (Figure 1.7) (Papadimitrakopoulou *et al.*, 2018; Ramalingam *et al.*, 2018a; Leonetti *et al.*, 2019a). *In vitro* experiments showed that overexpression of *MET* in third-generation EGFRi sensitive cell lines rescued sensitivity to these inhibitors and led to sustained phosphorylation of ERK and AKT despite continuing EGFRi treatment, indicating that *MET* amplification may drive resistance to EGFRi through reactivation of signalling pathways downstream of EGFR (Ortiz-Cuaran *et al.*, 2016). As observed in first-generation EGFRi resistant NSCLC, other mutations that bypass EGFR to reactivate downstream signalling networks to drive resistance to third-generation EGFRi have also been reported at lower frequencies (Figure 1.7). These include mutation of *KRAS* (Ortiz-Cuaran *et al.*, 2016), *BRAF*, and *PIK3CA*, as well as loss of *PTEN* (Papadimitrakopoulou *et al.*, 2018; Ramalingam *et al.*, 2018a). As with first-generation EGFRi, transformation from NSCLC to SCLC (Ham *et al.*, 2016) and EMT (Weng *et al.*, 2019) have been reported as resistance mechanisms to osimertinib in patients and in preclinical models respectively. Interestingly, mutations in genes encoding cell-cycle proteins such as cyclins D1, D2, and D3 have also been reported in 10% and 12% of patients who have acquired resistance to first- and second-line osimertinib respectively (Le *et al.*, 2018; Oxnard *et al.*, 2018; Papadimitrakopoulou *et al.*, 2018; Ramalingam *et al.*, 2018a; Zeng *et al.*, 2018). Oncogenic fusions such as *FGFR3-TACC3* have also been identified in 3-10% of patients who have acquired resistance to second-line osimertinib (Figure 1.7) (Le *et al.*, 2018; Oxnard *et al.*, 2018; Papadimitrakopoulou *et al.*, 2018; Ramalingam *et al.*, 2018a; Zeng *et al.*, 2018)

1.3.4 Clinical characteristics of common *EGFR* mutations in NSCLC

Although the common *EGFR* mutation L858R and Ex19Del are considered sensitive to the EGFRi discussed above, evidence suggests that these mutations are not equivalent and do not respond identically in the clinic.

Some studies have found that L858R is more commonly associated with the clinicopathological features of female sex, never smoking, and adenocarcinoma histology (Moriguchi *et al.*, 2006; Sasaki *et al.*, 2006; Sugio *et al.*, 2006). However, a study that pooled four trials to form the largest patient data set of these common mutations ($n = 714$) did not detect an association between L858R and any of these clinicopathological features (Lee *et al.*, 2015). The same pooled analysis reported that among patients who were not treated with EGFRi those with L858R mutations had longer OS compared to those with Ex19Del, suggesting that patients with Ex19Del have a poorer prognosis compared to those with L858R mutations. Interestingly, among patients treated with EGFRi, those with Ex19Del have a longer OS compared to those with L858R mutations (Jackman *et al.*, 2006; Riely *et al.*, 2006; Lee *et al.*, 2015). The mechanisms behind this difference in response are unclear; preclinical studies have shown that both mutations are almost identically sensitive to gefitinib treatment and clinical studies have found that the resistance mutation T790M occurs at equivalent frequencies in both L858R and Ex19Del patients (Mukohara *et al.*, 2005; Oxnard *et al.*, 2011; Katakami *et al.*, 2013). Similar mutation-specific effects have been reported in studies focusing on afatinib. Subgroup analysis of LUX-Lung 3 and LUX-Lung 6, which compared afatinib with chemotherapy in *EGFR*-mutant positive NSCLC patients, revealed that afatinib treatment provided a significant OS benefit for patients harbouring Ex19Del but not for patients harbouring L858R, indicating that afatinib may be particularly active against Ex19Del mutations (Sequist *et al.*, 2013; Wu *et al.*, 2014). However, significant differences in OS were not identified between mutation types in LUX-Lung 7, a phase IIB trial with a similar cohort size to LUX-Lung 3 and LUX-Lung 6 that compared afatinib with the first generation EGFRi gefitinib in NSCLC patients with Ex19Del or L858R mutations, and so the effect of mutation on clinical response to afatinib remains unclear (Park *et al.*, 2016). Mutation-specific response to therapy has also been observed with osimertinib treatment. Both the AURA3 and FLAURA

trials reported marginally lower HR for PFS for patients with Ex19Del compared to patients with L858R (0.34 vs. 0.46 and 0.43 vs. 0.51) but neither of these results were statistically significant (Mok *et al.*, 2017a; Soria *et al.*, 2018).

1.3.5 Rare EGFR mutations in NSCLC

Although rare *EGFR* mutations account for only ~15% of all *EGFR* mutations in NSCLC (Figure 1.5), the high incidence of lung cancer overall means over an estimated 30,000 new NSCLC diagnoses will harbour rare *EGFR* mutations every year (Harrison *et al.*, 2019). The following sections discuss rare single *EGFR* mutations that occur in NSCLC ranked by frequency, followed by a discussion of compound mutations in NSCLC. The sensitivities of the rare *EGFR* mutations discussed in the following sections as well as the common mutations L858R and Ex19Del are summarised in Table 1.2.

Mutation	First-generation		Second-generation			Third-generation		Exon-20 targetting			Dual EGFR-HER2
	Gefitinib	Erlotinib	Neratinib	Dacomitinib	Afatinib	Rociletinib	Osimertinib	Pozitotinib	TAK-788	TAS6417	Lapatinib
L858R	++	++		++	++		++				
Ex19Del	++	++		++	++		++				
Ex20Ins (insFQEA)		+							+		
Ex20Ins (others)									+		
G719X					++						
L861X					++						
S768X					++						
E709X					++						
Ex19Ins		+			+						

Table 1.2 - Summary of the sensitivities of EGFR mutations found in NSCLC to EGFRi. The sensitivity of the EGFR mutations discussed in this section to EGFRi is shown. Grey = unknown, red = resistant, yellow = partial sensitivity, green = sensitive, + = clinical evidence, ++ = clinical approval.

1.3.5.1 Exon 20 insertions

Exon 20 insertions (Ex20Ins) are the next most common *EGFR* mutations in in NSCLC after L858R and Ex19Del. Ex20Ins comprise a range of mutations that account for 4-10% *EGFR* mutations in NSCLC (Arcila *et al.*, 2013; Oxnard *et al.*, 2013; Yasuda *et al.*, 2013) Similar to Ex19Del, there are differences in the exact size and position of the insertion which ranges from 1-7 amino acids most commonly in the loop that follows the α C-helix (Yasuda *et al.*, 2013). Insertions in the loop

following the α C-helix form a wedge that “pushes” the α C-helix, effectively locking the helix in the inwardly rotated active conformation (Figure 1.4 A, Figure 1.4 B) (Eck and Yun, 2010; Yasuda *et al.*, 2013). Although 80-90% of Ex20Ins occur within this loop, the A763_Y764insFQEA mutation occurs within the α C-helix itself. A763_Y764insFQEA is structurally dissimilar to other Ex20Ins, and shifts the α C-helix towards its N-terminus, leading to an altered length of the β 3- α C loop (Yasuda *et al.*, 2013). Additionally, the FQEA insertion leads to an alanine residue at position 759 rather than an isoleucine (I759A). As the β 3- α C loop is the site of Ex19Del mutations and I759A is adjacent to L858R, A763_Y764insFQEA is proposed to activate EGFR by a mechanism similar to L858R or Ex19Del, as opposed to the mechanism more commonly observed in Ex20Ins. In particular, Yasuda *et al.* note that the I759A substitution caused by A763_Y764insFQEA would disrupt a cluster of hydrophobic residues (including I759, L747, L858, and L861) that stabilise the inactive conformation of the kinase domain.

The majority of NSCLC patients harbouring Ex20Ins are resistant to first- and second-generation EGFRi, with low RR of between 0-27% reported and a median PFS of <3 months (Sequist *et al.*, 2010b; Beau-Faller *et al.*, 2013; Naidoo *et al.*, 2015; Yang *et al.*, 2015a). Significant structural alterations in the P-loop and α C-helix caused by the Ex20Ins result in a relatively small drug binding pocket that sterically hinders first-generation EGFRi binding (Robichaux *et al.*, 2018). Furthermore, *in vitro* kinetic studies found that the Ex20Ins mutation D770_N771insNPG was able to induce kinase activity without causing a reduction in ATP affinity, hindering the competitive binding of first-generation EGFRi (Yasuda *et al.*, 2013). However, there is some evidence to suggest that specific Ex20Ins are sensitive to first- and second-generation EGFRi.

Patients harbouring the A763_Y764insFQEA insertion have demonstrated partial responses to erlotinib (Arcila *et al.*, 2013; Voon *et al.*, 2013; Naidoo *et al.*, 2015). As described earlier, A763_Y764insFQEA differs from the majority of Ex20Ins as it occurs within the α C-helix itself, as opposed to the loop following the α C-helix, and likely causes EGFR activation through a mechanism similar to Ex19Del and L858R compared to Ex20Ins that occur in the loop following the α C-helix (Yasuda *et al.*, 2013). This led to the hypothesis that A763_Y764insFQEA is also sensitive to first-generation EGFRi in a similar manner to Ex19Del and L858R. Experiments using

both Ba/F3 cells expressing A763_Y764insFQEA and a human NSCLC cell line harbouring endogenous A763_Y764insFQEA confirmed that A763_Y764insFQEA was significantly more sensitive to erlotinib in terms of cell growth and EGFR phosphorylation compared to other Ex20Ins mutations and cells with secondary T790M mutations.

Second-generation EGFRi have also shown efficacy for specific Ex20Ins mutations in preclinical studies. The efficacy of dacomitinib and afatinib were assessed against five different Ex20Ins mutations, revealing dacomitinib to be particularly effective against cells expressing D770delinsGY (Kosaka *et al.*, 2017). Remarkably, the presence of glycine at position 770 contributes substantially to dacomitinib sensitivity and the introduction of glycine at position 770 in two dacomitinib-resistant Ex20Ins mutations significantly increased their sensitivity to dacomitinib. The authors suggest that the smaller size of the side-chain in glycine compared to aspartic acid at position 770 restores conformational changes in the α C-helix that facilitate inhibitor binding which are lost in Ex20Ins mutations due to the repositioning of D770, which sterically hinders H-bonds between R776 and A767. However, most common Ex20Ins mutations lack a glycine at 770 and D770delinsGY itself is relatively rare, meaning there will be limited benefit gained from the clinical development of dacomitinib treatment for Ex20Ins patients.

Similar to first- and second-generation EGFRi, preclinical evidence suggests that third-generation EGFRi will not be effective for all Ex20Ins but may have activity against specific mutations. In one study, PDX models harbouring P772_H773insDNP and H773_V774insNPH mutations showed poor response to rociletinib and osimertinib (Yang *et al.*, 2016). However, in another study, focusing on xenograft models harbouring either D770_N771insSVD or V769_D770InsASV, osimertinib elicited superior anti-tumour activity compared to afatinib or erlotinib (Floc'h *et al.*, 2018). In contrast to D770delinsGY, D770_N771insSVD and V769_D770InsASV are relatively common, accounting for 22% and 17% of all Ex20Ins mutations. This suggests that there may be clinical benefit from the use of osimertinib in Ex20Ins patients, and a phase II clinical trial studying osimertinib treatment in Ex20Ins mutant NSCLC (NCT03414814) is currently ongoing.

Together, these data show although existing EGFRi may not be effective for all Ex20Ins mutations, patients harbouring specific Ex20Ins may benefit from treatment with existing EGFRi.

Several inhibitors have been developed that have the capacity to target Ex20Ins mutations. The most clinically advanced of these inhibitors is poziotinib, which was initially assessed in NSCLC patients with common *EGFR* mutations who developed acquired resistance to gefitinib or erlotinib but showed minimal clinical activity (Han *et al.*, 2017). Poziotinib differs structurally from other EGFRi; it has a flexible quinazoline core and small linking groups that, based on 3D modelling, has been predicted to bind tightly to the restricted drug-binding pocket of Ex20Ins mutants (Robichaux *et al.*, 2018). Expression of seven different Ex20Ins mutations in Ba/F3 cells revealed that poziotinib had an average IC₅₀ value of 1 nM, making poziotinib approximately 100 times more potent than osimertinib and 40 times more potent than afatinib *in vitro*. Poziotinib also showed durable anti-tumour effects against *in vivo* models of three Ex20Ins mutations. Although poziotinib potently inhibits Ex20Ins mutations, it has also demonstrated activity against WT-EGFR *in vitro*, raising concerns that poziotinib may suffer from dose-limiting effects similar to those observed with afatinib. Preliminary data from an ongoing phase II clinical trial of poziotinib reported a promising RR of 64% in 11 NSCLC patients harbouring Ex20Ins mutations (NCT03066206) (Robichaux *et al.*, 2018). However, in 2018 preliminary data from the larger ZENITH20 phase II trial (NCT03066206) led the FDA withhold breakthrough therapy designation poziotinib. In late 2019, a press release from the company that owns poziotinib, Spectrum Pharmaceuticals, stated that poziotinib failed to reach its primary endpoint in the first cohort of patients enrolled in the trial (Precision Oncology News, 2019). Out of the 115 patients in the first cohort, 17 had a response and 62 had SD, with an objective response rate (ORR) of 14.8%. Notably, 63% of patients experienced grade 3-4 toxicities which resulted in 68% of patients requiring dose reductions to subtherapeutic doses. However, both phase II clinical trials for poziotinib remain ongoing and are investigating alternative dosing schedules. It will therefore be necessary to wait for mature data before conclusions can be made regarding the use of poziotinib for Ex20Ins patients.

In addition to poziotinib, several other compounds that inhibit Ex20Ins mutations are being investigated. Mobocertinib (TAK-788) is an irreversible inhibitor that selectively targets Ex20Ins over WT-EGFR, and has shown activity in Ba/F3 cells expressing 14 different Ex20Ins mutations (Gonzalvez *et al.*, 2016). Mobocertinib was also shown to induce tumour regression in a PDX NSCLC model harbouring an Ex20Ins mutation. A phase I/II clinical trial (NCT02716116) established the tolerability of TAK-788 with an adverse event profile similar to other EGFRi and has now moved to an expansion phase seeking to determine ORR (Doebele *et al.*, 2018). In April 2020 Mobocertinib was granted Breakthrough Therapy Designation by the FDA (Takeda, 2020).

Another covalent inhibitor, TAS6417, binds irreversibly to C797 has selectivity for Ex20Ins over WT-EGFR (Hasako *et al.*, 2018). Using Ba/F3 cells and NIH-3T3 cells, Hasako *et al.* showed that TAS6417 was effective against six different Ex20Ins in terms of cell growth and EGFR phosphorylation. Owing to the lack of human NSCLC cell lines harbouring endogenous Ex20Ins, transcription activator-like effector nuclease (TALEN) mutagenesis was used to introduce D770_N771insSVD into the H1975 human NSCLC cell line, and subsequently remove the endogenous L858R/T790M EGFR, thereby engineering a human NSCLC cell line with Ex20Ins at the endogenous level (H1975-D770_N771insSVD) (Hasako *et al.*, 2018). Subsequent *in vitro* and *in vivo* experiments with H1975-D770_N771insSVD confirmed the activity of TAS6417 against this mutation. Notably, although potent inhibition of EGFR was detected in the tumours of mice bearing H1975-D770_N771insSVD tumours, there was minimal effect observed on WT-EGFR phosphorylation within the skin tissue, demonstrating the mutation-selectivity of TAS6417. A dose-finding phase I/IIa clinical trial assessing TAS6417 in Ex20Ins mutant NSCLC is currently ongoing (NCT04036682).

Another study has identified Compound 1A, a covalent inhibitor that also binds irreversibly to C797 with activity against Ex20Ins and selectivity over WT-EGFR (Jang *et al.*, 2018). Structure-guided design based on original pyrimidine core of osimertinib combined with biological evaluation led to the identification of Compound 1A. Unlike the osimertinib, Compound 1A possesses additional groups that form more extensive interactions with a deep hydrophobic pocket at the back of the ATP-binding site of EGFR. Compound 1A had anti-proliferative effects against Ba/F3

cells expressing three different Ex20Ins and a patient-derived NSCLC cell line harbouring an P772_H773insPNP mutation. Despite promising *in vitro* data, issues of poor oral bioavailability (11%) and short half-life (0.5 h) need to be addressed before Compound 1A is assessed *in vivo*.

In summary, although current clinical responses among Ex20Ins patients remains poor, recent developments indicate improvements in our ability to treat these patients. Use of existing EGFRi in specific Ex20Ins that show sensitivity to these inhibitors represents an exciting potential treatment strategy for these patients, and focused clinical trials are urgently needed to assess the efficacy of this approach. Furthermore, the rapid development of compounds capable of inhibiting a broader spectrum of Ex20Ins with selectivity over WT suggests that we are seeing the “first-generation” of EGFRi for Ex20Ins patients. Continued preclinical and clinical work in this space should elicit clinical benefit for patients in the near future.

1.3.5.2 G719X

G719X mutations account for ~1.5-3% of all *EGFR* mutations in NSCLC, with substitutions to S, A, C, and D reported (Kobayashi and Mitsudomi, 2016). G719 is in the P-loop, which contributes to the hydrophobic cluster surrounding L858 that stabilises the inactive conformation of the kinase domain (Figure 1.4 A) (Yun *et al.*, 2007). In the inactive conformation, the P-loop requires a flexibility that favours a glycine at position 719. Substitution of G719 for any non-glycine residue rigidifies the P-loop and thus weakens the hydrophobic interactions that stabilise the inactive α C-helix “out” conformation. Furthermore, Shan *et al.* predict that a rigidified P-loop caused by G719S would reduce the flexibility of the β 3- α C loop and suppress local disorder at the α C-helix region, thus increasing the propensity of the mutant receptor to dimerise (Shan *et al.*, 2012). *In vitro* kinase assays showed that G719S was 10 times more active compared to WT (Yun *et al.*, 2007).

Preclinical evidence has shown that G719A mutations are less sensitive to the first-generation EGFRi gefitinib and erlotinib, as well as the third-generation EGFRi osimertinib, compared to Ex19Del (Kobayashi *et al.*, 2015). However, cells expressing G719A have been found to be sensitive to the second-generation EGFRi

afatinib and neratinib both in terms of cell growth and EGFR phosphorylation, with IC_{90} values of 0.9 nM and 1.1 nM respectively. Cells expressing G719A almost entirely lost EGFR phosphorylation when treated with 10 nM afatinib, whereas EGFR phosphorylation was retained following treatment with 1 μ M of first- or third-generation EGFRi.

This lack of sensitivity to first-generation EGFRi is supported by clinical data. In the largest clinical study of rare *EGFR* mutations, Chiu *et al.* observed that although patients with single G719X showed some response to EGFRi treatment (36.8% RR, 6.3 months median PFS, $n = 78$), these patients were substantially less sensitive to therapy compared to those with L858R (67.5% RR, 10.4 months median PFS, $n = 256$) or Ex19Del mutations (RR = 65.3%, 13.5 months median PFS, $n = 222$) (Chiu *et al.*, 2015).

However, as observed in preclinical studies, second-generation EGFRi have shown activity in patients harbouring the G719X mutation. A phase II clinical trial of neratinib (NCT00266877) observed PR in three out of four patients harbouring G719X and 40 weeks' SD in the fourth (Sequist *et al.*, 2010b). Furthermore, post-hoc analysis of data from 32 patients pooled from LUX-Lung 2, LUX-Lung 3, and LUX-Lung 6 trials revealed clinical activity of afatinib in G719X patients (Yang *et al.*, 2015a). Across 8 patients harbouring single G719X mutations and 6 with complex G719X mutations, afatinib treatment resulted in 77.8% RR and 13.8 months median PFS, which in January 2018 led the FDA to broaden the indication for afatinib to include NSCLC patients that harbour G719X mutations (FDA, 2018c).

Interestingly, in contrast to preclinical observations, a recent phase II trial has suggested that osimertinib may also have clinical activity in this patient population, with 52.6% RR reported in 19 patients harbouring G719X mutations (Ahn *et al.*, 2018a). However, larger trials will be required to determine whether osimertinib can provide significant survival benefits compared to afatinib treatment.

1.3.5.3 L861X

L861X mutations account for around 3% of *EGFR* mutations in NSCLC, with substitutions to Q and R reported (Roengvoraphoj *et al.*, 2013). L861 is located in the activation loop and forms part of a cluster of hydrophobic residues that stabilise the inactive conformation (Figure 1.4 A) (Yasuda *et al.*, 2013; Banno *et al.*, 2016). By contrast, L861Q is able to form new H-bonds near the C-terminal of the α C-helix that stabilise the active conformation of the kinase domain (Shan *et al.*, 2012). Banno *et al.* expressed L861Q in the murine pro-B Ba/F3 cell line, which is dependent on IL-3 for cell growth (Banno *et al.*, 2016). Expression of L861Q conferred IL-3 independent growth in Ba/F3 cells. Furthermore, kinetic experiments revealed that L861Q has a higher affinity for ATP compared to WT-EGFR (Carey *et al.*, 2006). Taken together, these data indicate that L861Q is an oncogenic mutation.

Preclinical studies have shown that L861Q is resistant to first-generation EGFRi, but sensitive to afatinib and osimertinib (Banno *et al.*, 2016). Western blot analysis of cells expressing L861Q showed that EGFR remained phosphorylated following treatment with 100 nM erlotinib but was inhibited following treatment with 100 nM osimertinib or 10 nM afatinib. These observations are supported by clinical data. Patients with L861Q mutations have shown a diminished response to first-generation EGFRi compared to those with Ex19Del or L858R mutations (Chiu *et al.*, 2015). Chui *et al.* observed L861Q patients achieved a 40% RR and 8.1 months median PFS following treatment with first-generation EGFRi, compared to 67.5% RR and 10.4 months median PFS for L858R mutations, and 65.3% RR and 13.5 months median PFS for Ex19Del mutations. Afatinib treatment achieved higher RR in L861Q patients compared to first-generation EGFRi, with post-hoc analysis of the LUX-Lung trials showing 56% RR and 8.2 months median PFS following afatinib treatment in 12 patients with single L861Q point mutations, three patients with L861Q+G719X, and one patient with L861Q+Ex19Del complex mutations (Yang *et al.*, 2015a). This led to afatinib receiving FDA approval for L861Q mutant positive NSCLC (FDA, 2018c). Osimertinib has also shown activity in L861Q patients, with 77.8% PR reported in a phase II trial for osimertinib ($n = 9$) (Ahn *et al.*, 2018b).

1.3.5.4 S768X

S768I mutations are very rare, accounting for 0.5-1% of *EGFR* mutations in NSCLC, and most commonly occur as “compound” mutations with additional mutations in the *EGFR* gene (Kobayashi and Mitsudomi, 2016; Leventakos *et al.*, 2016). S768 lies within the α C-helix (Figure 1.4 A, Figure 1.4 B) and likely stabilises the inwardly rotated active conformation by improving the hydrophobic packing between the α C-helix and the adjacent β 9 strand (Shan *et al.*, 2012). Expression of S768I alone in Ba/F3 cells conferred IL-3 independent growth, suggesting that S768I is an oncogenic driver (Banno *et al.*, 2016).

In vitro experiments have shown that first-generation and third-generation are ineffective against S768I compared to L858R (Banno *et al.*, 2016). However, afatinib treatment causes a reduction in EGFR phosphorylation and cell viability in cells expressing S768I mutations comparable to that observed in cells expressing L858R.

Despite preclinical evidence demonstrating the ineffectiveness of first-generation EGFRi against S768I, clinical studies of first-generation EGFRi in patients harbouring S768I mutations are less clear. Some studies have reported intermediate sensitivity and PR (Masago *et al.*, 2010; Kobayashi *et al.*, 2013; Hellmann *et al.*, 2014; Leventakos *et al.*, 2016), whilst others have reported no response and progressive disease (Asahina *et al.*, 2006; Pallan *et al.*, 2014). The propensity of S768I to co-occur with other EGFR mutations may explain this variability of response, with clinical data suggesting that single S768I mutations are less responsive to first-generation EGFRi compared to S786I that co-occurs with additional EGFR mutations. Leventakos *et al.* report 3 months PFS following erlotinib treatment for a patient with S768I alone compared with 30 months PFS for a patient with S768I+L858R mutations (Leventakos *et al.*, 2016). Similarly, Chui *et al.* report 33% RR in patients harbouring single S768I mutations ($n = 7$) compared with 50% RR in patients who harbour S768I as part of a complex EGFR mutation ($n = 10$) following erlotinib treatment (Chiu *et al.*, 2015).

As observed in preclinical experiments, afatinib shows activity in patients harbouring S768I mutations (Yang *et al.*, 2015a). Post-hoc analysis of the LUX-Lung 2, LUX-Lung 3 and LUX-Lung 6 trials, found that afatinib treatment achieved 100% RR and

14.7 months median PFS for 8 patients harbouring S768I, leading to afatinib receiving FDA approval for this indication. Despite these promising results, it is important to note that only 1 out of the 8 S768I patients studied by Yang *et al.* had a single S768I, with the other 7 harboured complex mutations of S768I in combination with either L858R or G719X. Clinical trials focusing on patients with single S768I mutations will be essential to establish afatinib as a reliable therapy for this indication.

1.3.5.5 E709X

E709 lies within the N-lobe, towards the N-terminus of the β 1 strand that immediately precedes the P-loop (Figure 1.4 B). Although mutations at E709 have been reported in 1.48% of *EGFR*-mutation positive NSCLC patients, this frequency may be underreported as this class of mutations are not detectable by many commercially available diagnostic kits (Wu and Shih, 2016; Russo *et al.*, 2019). E709X mutations encompass delE709-T710insD as well as substitution mutations to A, G, K, or V, of which E709K is the most common. Interestingly, although delE709-T710insD has been reported as the only mutation present on *EGFR* in a tumour, substitution mutations at E709 are most frequently observed as compound mutations, with a recent study finding that over 75% of E709 substitutions existed as compound mutations (Wu and Shih, 2016; Kohsaka *et al.*, 2017). Stable expression of E709X mutations conferred IL-3 independent growth in Ba/F3 cells and enabled the mouse fibroblast cell line NIH-3T3 to form foci in a focus formation assay, indicating that these mutations are oncogenic drivers (Kobayashi *et al.*, 2015).

Ba/F3 cells were used to assess the sensitivity of E709K and delE709-T710insD against 7 different EGFRi (Kobayashi *et al.*, 2015). These experiments showed that both E709K and delE709-T710insD were significantly less sensitive to gefitinib, erlotinib, and osimertinib compared to cells expressing Ex19Del, with delE709-T710insD showing the greatest resistance to these inhibitors. However, E709K and delE709-T710insD showed sensitivity to the second-generation inhibitors afatinib and neratinib comparable to that of Ex19Del, both in terms of cell growth and EGFR

phosphorylation. This suggests that second-generation EGFRi have the greatest affinity for rare E709X mutations compared to first- or third-generation inhibitors and may be useful treatment options for patients harbouring these mutations.

As E709X mutations are not detectable by many commercially available diagnostic kits, clinical data regarding this class of mutations is extremely limited (Wu and Shih, 2016; Russo *et al.*, 2019). In line with preclinical observations, first-generation EGFRi displayed minimal activity in 4 patients harbouring delE709_T710insD mutations with a 25% RR (Kobayashi and Mitsudomi, 2016). Interestingly, Kobayashi *et al.* report a higher 53% RR for 15 patients with E709X complex mutations. Also in line with preclinical observations, a clinical study reported a pronounced response to afatinib, with E709X patients achieving a TTF of >12 months (Heigener *et al.*, 2015). However, all patients harbouring E709X in this study had complex mutations with additional L858R or G719X mutations and so the predictive and prognostic implications of E709X as a single mutation in patients remains unclear.

1.3.5.6 Exon 19 insertions

Insertions in exon 19 have also been reported, accounting for ~1% of all *EGFR* mutations in NSCLC (He *et al.*, 2012a). However, this number may be under representative as exon 19 insertions may not be detected by mutation-specific assays used at some academic centres (MacConaill *et al.*, 2009). Exon 19 insertions usually start at codon 744 or 745 and are almost always six amino acids in length (He *et al.*, 2012a). Although the specific amino acids inserted vary, the sequence PVAI is conserved in all reported exon 19 insertions. Additionally, all exon 19 insertions have two shared effects on the structure of the kinase domain. First, the insertion of the 6 amino acids causes a shift that adds a 6-residue sequence to the β 3- α C loop that connects the β 3-strand to the α C-helix (Figure 1.4 A). Second, the residues present at positions 746 and 747 are changed. The insertion of a 6-residue sequence to the loop connecting the β 3-strand to the α C-helix is unlikely to have a significant structural impact, as this loop is flexible in WT-EGFR. Similarly, alteration of E746 is unlikely to have any major effect as it is exposed on the solvent-facing

surface of the kinase domain. However, L747 is part of a cluster of hydrophobic residues that stabilise the inactive conformation of the kinase domain. In a case series of 11 patients with exon 19 insertion mutations all patients had a proline at position 747 rather than a leucine (He *et al.*, 2012a). This L747P substitution is likely to prevent the formation of these hydrophobic interactions and thereby destabilise the inactive conformation of the kinase domain.

Preclinical studies have shown that Ex19Ins are similar to Ex19Del in terms of their sensitivity to EGFRi (He *et al.*, 2012b). Expression of two different Ex19Ins mutations in Ba/F3 cells revealed a sensitivity to gefitinib and afatinib that was comparable to Ba/F3 cells expressing Ex19Del. Western blot analysis of NIH-3T3 cells expressing the same mutations found that EGFR inhibition following treatment with either inhibitor was also similar between Ex19Ins and Ex19Del. Kohsaka *et al.* assessed the sensitivity of Ba/F3 cells expressing *EGFR* with an insertion of the 6 amino acids VPVAIK between E745 and K746 (E745_K746insVPVAIK) against a panel of EGFRi, and found that cells expressing E745_K746insVPVAIK were marginally less sensitive to first-, second-, and third-generation inhibitors compared with Ex19Del (Kohsaka *et al.*, 2017).

Ex19Ins mutations are not commonly screened as part of routine diagnosis and so there is very little clinical data pertaining to this class of mutations. In a case series of 4 patients, He *et al.* report PR and time-to-progression of >12 months in 3 patients treated with afatinib ($n = 1$) or erlotinib ($n = 2$) (He *et al.*, 2012b). The fourth patient was treated with XL647, an experimental EGFRi of uncertain activity. These data support their preclinical findings and indicate that patients with Ex19Ins are sensitive to first- and second-generation EGFRi. Despite these promising data, several case studies report more varied responses to first-generation EGFRi ranging from a relatively short PFS of 5.9 months to a much longer 24 months (Iyevleva *et al.*, 2014; Park *et al.*, 2014; Kobayashi and Mitsudomi, 2016; Su *et al.*, 2017). This high variability in response highlights the urgent need for the routine use of diagnostic techniques capable of detecting these mutations and larger, focused clinical trials to establish the most efficacious treatment strategy for patients harbouring this class of mutations.

1.3.5.7 Compound mutations

Compound mutations (also referred to as “complex” mutations) occur when more than one mutation is detected on the same *EGFR* allele. In patients, compound mutations have been reported as “common + common” (e.g. L858R + Ex19Del), “common + rare” (e.g. L858R + G719C), or “rare + rare” (e.g. L861Q + G719C). In NSCLC, compound mutations have been reported to account for 5-15% of all *EGFR* mutations (Wu *et al.*, 2011; Kobayashi *et al.*, 2013; Liu *et al.*, 2013; Peng *et al.*, 2015). Interestingly, certain mutations have a propensity to occur as part of a compound mutation. In one study, over 75% of E709X mutations and over 90% of G719X mutations were identified as part of compound mutations (Kohsaka *et al.*, 2017). Kohsaka *et al.* used a focus formation assay to show that compound mutations are more oncogenic than their constituent single mutations. They also found that this increased oncogenicity only occurred when the compound mutations were present in *cis*, and not in *trans*.

Kohsaka *et al.* profiled the *EGFR*i sensitivity of 106 Ba/F3 cell lines expressing either *EGFR* compound mutations, in *cis* or in *trans*, or the corresponding *EGFR* single mutations (Kohsaka *et al.*, 2017). They found that each compound mutation showed an *EGFR*i sensitivity that was intermediate compared to that of either constituent *EGFR* mutation alone. For example, the IC_{50} value for gefitinib treatment the complex mutation L858R+E709K (125.5 nM) was higher compared to L858R alone (4.4 nM) but lower compared to E709K alone (340.8 nM). Interestingly, although this trend was also observed when cells were treated with osimertinib (IC_{50} values were 0.2 nM for L858R+E709K, <0.1 nM for L858R, and 5.6 nM for E709K) this trend was not observed with afatinib treatment, which showed equally potent activity (IC_{50} <0.1 nM) against all mutations regardless of whether they were single or complex.

In line with these observations, several clinical studies have reported that patients harbouring compound mutations show more durable response to first-generation *EGFR*i therapy compared to those with single rare mutations (Beau-Faller *et al.*, 2013; Cheng *et al.*, 2015; Wu and Shih, 2016). Patients with common + rare compound mutations have significantly longer median PFS following treatment with first-generation *EGFR*i compared to those with single rare mutations (7.4 vs. 1.3 months respectively) (Baek *et al.*, 2015). However, median PFS reported for

patients with common + rare mutations is lower than the median PFS typically observed for patients with single common mutations following treatment with first-generation EGFRi. This supports the preclinical finding that common + rare compound mutations show a sensitivity that is intermediate compared to either constituent mutation (Kohsaka *et al.*, 2017). Patients with rare + rare complex mutations also have significantly longer median PFS compared to those with single rare mutations (11.9 vs. 6.5 months) (Chiu *et al.*, 2015). Interestingly, the specific mutations that co-occur together appears to influence EGFRi sensitivity; patients harbouring G719X+L861Q achieved a higher RR compared to those harbouring G719X+S768I (88.9% vs. 50%). Patients harbouring common + common mutations show a median PFS of 9.5-16.5 months, which is similar to those harbouring either common mutation alone (Hata *et al.*, 2010; Xu *et al.*, 2016). Notably, patients whose compound mutations harbour mutations associated with EGFRi resistance have particularly poor clinical responses, with a median PFS of just 1.4 months reported for patients harbouring compound mutations containing either T790M or Ex20Ins (Zhang *et al.*, 2018). Despite the relatively high frequency of complex mutations, the heterogeneous nature of this class of mutations makes it challenging to determine the most effective treatment strategy for each individual patient. Preclinical data from Kohsaka *et al.* suggests that afatinib would be an effective strategy for this patient population, however there is no clinical data pertaining to the use of afatinib in patients with complex mutations. Large, prospective trials focused on compound mutations would facilitate a better understanding of the effect of complex mutations on response to therapy and would enable the leveraging of preclinical data in the search for better treatment strategies.

1.3.6 EGFR mutations in GBM

EGFR is among the most commonly altered genes in GBM (Brennan *et al.*, 2013). Notably, EGFR mutations that occur in GBM are most commonly found in the extracellular domain (Zandi *et al.*, 2007). This differs from EGFR mutations found in NSCLC, which most commonly occur in the intracellular domain. A large in-frame deletion in the extracellular domain of EGFR, known as EGFR-vIII is the most

common and well-studied GBM-associated EGFR mutant (Jeuken *et al.*, 2009), although less common point mutations in the extracellular domain have also been identified in GBM (Lee *et al.*, 2006; Cerami *et al.*, 2012; Brennan *et al.*, 2013; Gao *et al.*, 2013; Tate *et al.*, 2018). In the following sections, I discuss the structural features of GBM-associated EGFR mutations and approaches to target these mutations therapeutically. Mutations are discussed in order of frequency. The sensitivities of the *EGFR* mutations discussed in the following sections are summarised in Table 1.3.

Mutation	First-generation		Second-generation			Third-generation		Dual EGFR-HER2	Antibodies	
	Gefitinib	Erlotinib	Neratinib	Dacomitinib	Afatinib	Rociletinib	Osimertinib	Lapatinib	ABT-414	mAb806
EGFR-vIII	Red	Red	Green	Grey	Yellow	Grey	Green	Green	Grey	Green
A289V	Yellow	Yellow	Grey	Grey	Green	Red	Yellow	Green	Grey	Green
R108X	Yellow	Yellow	Grey	Grey	Green	Red	Yellow	Green	Grey	Green
G598V	Yellow	Yellow	Grey	Grey	Green	Red	Yellow	Green	Grey	Green
L62R	Yellow	Yellow	Grey	Grey	Green	Red	Yellow	Green	Grey	Green

Table 1.3 - Summary of the sensitivities of EGFR mutations found in GBM to EGFRi. The sensitivity of the EGFR mutations discussed in this section to EGFRi is shown. Grey = unknown, red = resistant, yellow = partial sensitivity, green = sensitive.

1.3.6.1 EGFR-vIII

EGFR-vIII is a large in-frame deletion in the extracellular domain of *EGFR* spanning exons 2-7 which encode domains I and II (Wong *et al.*, 1992). It is most commonly identified in glial tumours, but has also been detected in lung (Okamoto *et al.*, 2003), prostate (Olapade-Olaopa *et al.*, 2000), breast (Ge *et al.*, 2002), and head and neck cancers (Sok *et al.*, 2006). Loss of a large portion of the extracellular domain prevents EGFR-vIII from binding ligands. However, it is thought that deletion of domain II may prevent the formation of the closed inactive conformation of the extracellular domain due to the loss of the intramolecular tether (Su Huang *et al.*, 1997). Furthermore, it has been shown that transient EGFR-vIII homodimers are stabilised by disulphide bonds through N-terminal cysteine residues that are exposed in EGFR-vIII receptors (Ymer *et al.*, 2011). EGFR-vIII is associated with constitutive phosphorylation of EGFR at around 10% of the activity of ligand-stimulated WT-EGFR (Su Huang *et al.*, 1997). This low level of phosphorylation is

believed to lead to a much slower rate internalisation and degradation of EGFR-vIII compared to WT, leading to constitutive membrane-localisation of the mutant receptor (Su Huang *et al.*, 1997; Grandal *et al.*, 2007). Strikingly, even EGFR-vIII that are internalised are recycled back to the membrane rather than being degraded. Despite this, EGFR-vIII is insufficient to form tumours in *in vivo* models and always occurs in patients with concurrent amplification of *EGFR* (Frederick *et al.*, 2000; Ding *et al.*, 2001). Additional oncogenic aberrations, such as RAS mutations or PTEN loss, are required for oncogenesis (Ding *et al.*, 2001; Zhu *et al.*, 2009). Interestingly, EGFR-vIII has been shown to preferentially activate the PI3K pathway over the MAPK pathway, demonstrating that mutant variants of EGFR have altered downstream signalling networks (Moscatello *et al.*, 1998; Li *et al.*, 2004; Huang *et al.*, 2007).

Several other large deletions have also been detected at lower frequencies, occurring exclusively in GBM. EGFR-vI and EGFR-vII are deletions of the N-terminal region of exons 1-12 and of exons 14-15 respectively (Humphrey *et al.*, 1991; Wong *et al.*, 1992). These deletion mutations give rise to truncated proteins that are believed to be oncogenic. EGFR-vIV and EGFR-vV are intracellular deletions of exons 25-27 and exons 25-28 respectively that differ to the extracellular deletion mutations in that they are still able to bind ligand (Frederick *et al.*, 2000). Two variations of EGFR-vIV have been reported: EGFR-vIVa and EGFR-vIVb which harbour deletions of exons 25-27 and exons 25-26 respectively (Pines *et al.*, 2010). Both EGFR-vIV variants increase kinase activity compared to WT, becoming hyperphosphorylated following stimulation with EGF, and promote oncogenic phenotypes. Interestingly, EGFR-vIV activates distinct signalling networks compared to EGFR-vIII.

Experiments using the Ba/F3 model system found that cell growth in cells expressing EGFR-vIII was less sensitive to erlotinib treatment compared to cells expressing L858R or 746_750del (Ji *et al.*, 2006a). Barkovich *et al.* showed that erlotinib achieves lower kinase-site occupancy in EGFR-vIII compared with WT-EGFR, 746_750del, or L858R (Barkovich *et al.*, 2012). Furthermore, EGFR-vIII releases erlotinib more rapidly compared to WT-EGFR, whereas 746_750del and L858R released erlotinib more slowly compared to WT-EGFR. The dual EGFR-HER2 inhibitor lapatinib has shown significantly greater potency against EGFR-vIII

compared to erlotinib (Vivanco *et al.*, 2012). However, when Vivanco *et al.* assessed the clinical efficacy of lapatinib in a multicentre trial of 44 GBM patients they found that lapatinib did not achieve sufficient intratumoural concentration to inhibit EGFR. Afatinib has been shown to inhibit EGFR-vIII phosphorylation in cell line models, but did not slow tumour growth *in vivo* (Vengoji *et al.*, 2019). Neratinib is able to reduce the volume of tumours expressing EGFR-vIII *in vivo* and a clinical trial assessing the use of neratinib in GBM patients is currently ongoing (NCT02977780) (Ji *et al.*, 2006b). Osimertinib is highly brain-penetrant and was found to have activity against EGFR-vIII in the preclinical setting (Cross *et al.*, 2014; Kwatra *et al.*, 2017). Osimertinib was able to inhibit EGFR signalling in an EGFR-vIII positive cell line model and provide a 47% increase in OS in mice intracranially implanted with EGFR-vIII positive cells compared to vehicle control or lapatinib. However, in a case report of a glioblastoma patient a EGFR-vIII positive lesion was found to progress despite osimertinib treatment (Makhlin *et al.*, 2019). A phase I/II trial is currently ongoing assessing the use of osimertinib in GBM (NCATS 1-UH2-TR001370-01).

ABT-414 is an anti-EGFR antibody-drug conjugate comprised of the monoclonal antibody mAb806 and the toxin monomethyl auristatin F (MMAF), which inhibits tubulin assembly (Phillips *et al.*, 2016). mAb806 binds to a short cysteine-loop on EGFR between C287-C302 that is buried in WT-EGFR but exposed in EGFR-vIII (Johns *et al.*, 2004). After binding to EGFR, ABT-414 is internalised and intracellular proteases cause the release of MMAF which leads to cell death (Gan *et al.*, 2012). A phase I trial showed that ABT-414 can bind to EGFR in intracranial tumours (Gan *et al.*, 2013). A phase II/III study is currently assessing the addition of ABT-414 to radiotherapy combined with temozolomide, an alkylating agent commonly used in the treatment of GBM (NCT02573324). Additionally, an ongoing phase II trial is evaluating the efficacy of ABT-414 alone or with temozolomide compared with single-agent temozolomide or lomustine, another alkylating agent commonly used in the treatment of GBM (NCT02343406).

1.3.6.2 A289X

Substitutions at A289 are the most common point mutations in GBM, with substitutions to D, T, and V reported (Brennan *et al.*, 2013). A289 is located in domain II of the extracellular domain and directly contributes to intramolecular interactions that are believed to be autoinhibitory between domain I and II when in the inactive conformation (Bessman *et al.*, 2014). The precise mechanism by which A289X mutations promote oncogenicity is unclear. Lee *et al.* found that A289V caused constitutive phosphorylation of EGFR and promoted anchorage independent growth of NIH-3T3 cells in the absence of exogenous EGF, indicating that A289V is ligand-independent and oncogenic (Lee *et al.*, 2006). However, Bessman *et al.* report that A289V receptors remained monomeric in the absence of EGF (Bessman *et al.*, 2014). Instead, Bessman *et al.* find that A289X mutations increase the affinity of the receptor for the ligand 5-fold compared to WT. They suggest that A289X mutations weaken interactions between domains I and II that constrain the orientation of domain I with respect to the ligand in the WT receptor. The effect of this would be to increase the sensitivity of EGFR to lower concentrations of EGF or other ligands. Nevertheless, A289X mutations are oncogenic and cells harbouring them are highly dependent on them for survival (Vivanco *et al.*, 2012).

Mutations at A289 are most commonly reported in GBM. Clinical trials focusing on GBM patients have shown that gefitinib and erlotinib poorly inhibit EGFR signalling in tumour tissue (Lassman *et al.*, 2005; Hegi *et al.*, 2011). *In vitro* experiments have shown that cells harbouring point mutations A289 are more sensitive to lapatinib compared to erlotinib both in terms of EGFR phosphorylation and cell growth, however lapatinib does not reach sufficient intratumoural concentrations in GBM patients to inhibit EGFR (Vivanco *et al.*, 2012). In their large scale preclinical study of EGFR mutations' sensitivity to EGFRi, Kohsaka *et al.* report that cells expressing A289X mutations are less sensitive to first-, second-, and third-generation EGFRi compared to L858R and Ex19Del, but more sensitive than T790M (Kohsaka *et al.*, 2017). This indicates that there may be use for EGFRi that are capable of inhibiting EGFR in intracranial tumour tissue in patients.

Preclinical experiments found that mAb806 was able to bind A289V significantly better than WT-EGFR (Binder *et al.*, 2018). *In vivo* experiments showed that mAb806 reduced tumour volume in mice bearing A289V expressing tumours to a level comparable with mice harbouring EGFR-vIII expressing tumours. These data indicate that mAb806-based therapies might be useful for patients harbouring mutations at A289.

1.3.6.3 Rare *EGFR* mutations in GBM

R108X mutations are also identified in GBM, with substitutions for K and G reported (Lee *et al.*, 2006; Cerami *et al.*, 2012; Gao *et al.*, 2013). R108 lies within domain I and contributes to intramolecular interactions that are believed to be autoinhibitory between domain I and II when the receptor is in the inactive conformation (Bessman *et al.*, 2014). As with A289V the exact mechanism by which R108K confers oncogenicity is unclear. Expression of R108K in NIH-3T3 cells conferred anchorage-independent growth and constitutive phosphorylation of EGFR in the absence of EGF (Lee *et al.*, 2006). However, R108K receptors have also been shown to remain monomeric in the absence of ligand (Bessman *et al.*, 2014). Bessman *et al.* propose that R108K causes activation of EGFR through the same ligand-dependent mechanism as A289V, which is in contrast to the ligand-independent effects reported by Lee *et al.*. Interestingly, R108K has an even higher ligand-binding affinity compared to A289V, with a 20-fold increase in affinity over WT-EGFR.

G598 is located at the contact between domains II and IV and G598V mutations have been reported in GBM (Lee *et al.*, 2006). Western blot analysis showed that G598V is basally phosphorylated in serum-free conditions and is also responsive to EGF stimulation. NIH-3T3 cells expressing G598V were able to grow in anchorage-independent conditions and form tumours in nude mice, indicating that it is an oncogenic mutation. However, the mechanism by which G598V confers oncogenicity is unknown.

L62R has been identified in GBM as a single mutation and in NSCLC as part of complex mutations (Cerami *et al.*, 2012; Gao *et al.*, 2013; Tate *et al.*, 2018). Although L62R has been identified as an oncogenic mutation, able to confer IL-3

independent growth in Ba/F3 cells, it is not known how L62R confers oncogenicity (Kohsaka *et al.*, 2017; Tate *et al.*, 2018).

There is very little data pertaining to the sensitivity of R108X, G598V, and L62R mutations to EGFRi. All 3 mutations are most commonly reported in GBM, which has shown poor response to EGFRi in clinical studies and for which no EGFRi are currently approved (Gao *et al.*, 2018). R108K, G598V, and L62R have all been shown to have a similar EGFRi sensitivity profile to one another; they are all less sensitive to first-, second-, and third generation EGFRi compared to L858R and 746_750del but more sensitive to these inhibitors compared to T790M (Kohsaka *et al.*, 2017). This indicates that EGFRi with intracranial activity may be effective for patients harbouring these mutations.

MD and elastic network modelling (ENM) have indicated that R108K and G598V mutations favour a conformation that renders the mAb806 binding site accessible (Orellana *et al.*, 2019). In support of this, *in vitro* experiments demonstrated that mAb806 bound to R108K and G598V significantly better compared to WT-EGFR. Finally, mAb806 potently inhibited tumour growth in mice bearing tumours expressing R108K or G598V mutations compared with mice bearing WT-EGFR, highlighting mAb806 as a potential therapy for patients harbouring these mutations.

1.4 Conclusions and aims

Although oncogenic mutations in *EGFR* are common and occur in multiple cancer types, the mechanisms by which different mutations cause aberrant EGFR activation varies greatly. Different EGFR mutants also show distinct responses to targeted therapies, which translates into dramatic variation in the clinical response observed in patients depending on the specific EGFR mutant present (Figure 1.8). Furthermore, resistance mechanisms to targeted therapy can be highly divergent, with multiple secondary EGFR mutations reported to confer EGFRi resistance in patients. A greater understanding of the different EGFR mutants that occur in cancer, either as activating mutations or as resistance mutations, is essential to improving the therapeutic outcomes for patients harbouring these mutants. Through

rational drug design and the repurposing of existing inhibitors, exciting new treatment strategies have been recently identified for patients harbouring Ex20Ins: a class of EGFR mutations that has long been recognised as a driver of oncogenesis, but until recently has been untreatable with targeted agents. However, as these novel therapies approach the clinic potential mechanisms of acquired resistance and approaches to overcome resistant disease remain unclear.

Considering the disparity in clinical response observed for patients harbouring different EGFR mutants, identifying the optimal kinase inhibitor for distinct EGFR mutants may improve treatment options for patients. Therefore, this thesis seeks to study EGFR mutants in a pan-cancer approach, aiming to provide a deeper understanding of the biology of different EGFR mutants and identify novel therapeutic strategies for patients harbouring these mutants. Furthermore, as EGFRi that are capable of targeting Ex20Ins mutants progress through clinical trials, it is essential that potential resistance mechanisms to these inhibitors are anticipated and approaches to overcome acquired resistance are investigated. To address these challenges, this thesis also seeks to characterise potential resistance mechanisms to EGFRi in the Ex20Ins setting and establish candidate salvage therapies for acquired resistance to Ex20Ins-targeting EGFRi.

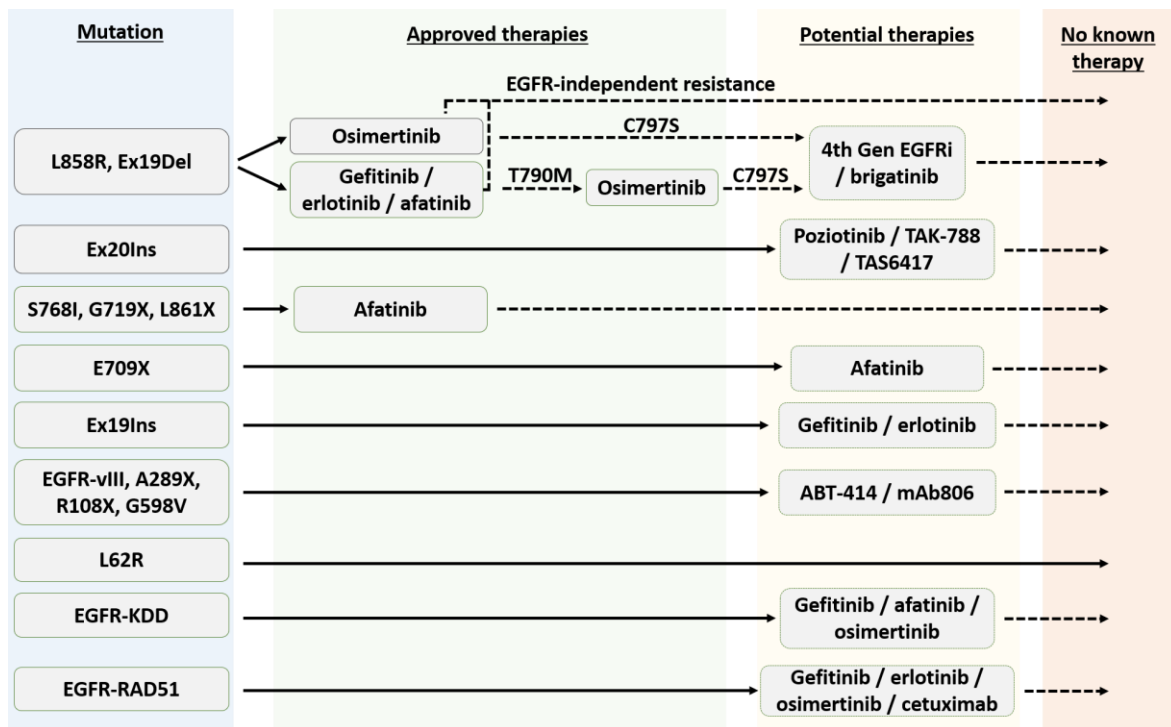


Figure 1.8 – Current clinical options for patients harbouring EGFR mutations. Dashed arrows indicate acquired resistance. Figure produced using Microsoft Powerpoint.

Project aims:

1. Establish an isogenic panel of cells expressing EGFR mutants from across cancer types.
2. Examine the sensitivities of distinct EGFR mutants to different small molecule inhibitors.
3. Identify mechanisms of resistance to pozitotinib and TAS6417 in Ex20Ins setting and investigate possible approaches to overcome this resistance.

Chapter 2

Materials and Methods

2.1 Mammalian cell culture

2.1.1 Cell lines and maintenance

All cell lines were maintained at 37°C in an atmosphere of 95% air/5% CO₂ and >95% humidity. The cell lines used in this project, their growth medium, supplements, selection antibiotics, and source are listed in Table 2.1. With the exception of growth medium for MCF10A cells, all growth media were supplemented with 10% (v/v) foetal bovine serum (FBS), 100 units/ml penicillin, and 100 mg/ml streptomycin. MCF10A cells were grown in DMEM with 5% (v/v) horse serum (HS), 100 units/ml penicillin, 100 mg/ml streptomycin, and the additional supplements listed in Table 2.1.

Adherent cell lines were passaged to new growth vessels upon reaching ~80% confluency. To passage adherent cells, cells were washed once with phosphate buffered saline (PBS) and detached by addition of a 0.05% (w/v) Trypsin/0.02% (w/v) Ethylenediaminetetraacetic acid (EDTA) solution (sufficient volume to cover the surface of the cell monolayer) followed by incubation for 1 – 5 min at 37°C. Trypsin was neutralised by the addition of fresh growth medium containing FBS and cells were then transferred to new growth vessels. Suspension cell lines were passaged when they reached a density of $\sim 1.5 \times 10^6$ cells / ml. To passage suspension cells, cells were pipetted up and down to mix the culture to a homogenous density, and a subculture was transferred to new growth vessels.

All cell lines were regularly tested for the presence of mycoplasma using MycoAlert Mycoplasma Detection kit (Lonza).

Cell line	Growth medium	Supplements	Selection antibiotic	Source
Phoenix Ecotropic	DMEM	10% (v/v) FBS	100 ng/ml cholera toxin, 200 µg/ml hygromycin	Gift (M. Katan)
HEK293T	DMEM	10% (v/v) FBS	-	ATCC (CRL-3216)
NIH-3T3	DMEM	10% (v/v) FBS	-	Gift (M. Katan)
NIH-3T3 + pFB-EGFRm	DMEM	10% (v/v) FBS	200 µg/ml hygromycin	-
H3122	RPMI 1640	10% (v/v) FBS	-	-
H3122 + pFB-EGFRm	RPMI 1640	10% (v/v) FBS	200 µg/ml hygromycin	-
MCF10A	DMEM	5% (v/v) HS, 20 ng/ml EGF, 0.5 mg/ml hydrocortisone, 100 ng/ml cholera toxin, 10 µg/ml insulin	-	Gift (R. Natrajan)
MCF10A + pFB-EGFRm	DMEM	5% (v/v) HS, 20 ng/ml EGF, 0.5 mg/ml hydrocortisone, 100 ng/ml cholera toxin, 10 µg/ml insulin	200 µg/ml hygromycin	-
Ba/F3	RPMI 1640	10% (v/v) FBS, 5 ng/ml IL-3	-	Gift (R. Marais)
Ba/F3 + pFB-EGFRm	RPMI 1640	10% (v/v) FBS	1 mg/ml hygromycin	-
Ba/F3 + pFB-EGFRm + SRC constructs	RPMI 1640	10% (v/v) FBS	1 mg/ml hygromycin, 2 µg/ml puromycin	-
PC9	RPMI 1640	10% (v/v) FBS	-	ECCAC (#90071810)
PC9 EGFR-T790M	RPMI 1640	10% (v/v) FBS, 1 µM gefitinib	-	-
PC9 + SRC constructs	RPMI 1640	10% (v/v) FBS	400 µg/ml hygromycin	-

Table 2.1 – Cell lines and growth conditions. pFB-EGFRm includes all mutant EGFR constructs and WT-EGFR. SRC constructs includes SRC-WT, SRC-T338I and pBABE-puro empty vector. FBS, foetal bovine serum; HS, horse serum; EGF, epidermal growth factor; IL-3, interleukin-3.

2.1.2 Cell counting

To count cells, 10 μ l of cell suspension was mixed with 10 μ l of a 0.4% (w/v) Trypan blue solution and the number of viable cells / ml was recorded using either a Countess II (Thermo Fischer Scientific) or Luna II (Logos Biosystems) automated cell counter.

2.1.3 Storage of cell lines

After counting, cells were centrifuged at 300 x g for 5 min to form a pellet. This pellet was then resuspended in FBS/10% (v/v) dimethyl sulfoxide (DMSO; Sigma) at a final density of 1×10^6 cells / ml. 1 ml aliquots were then transferred to cryovials (Thermo Fischer Scientific) and stored in -80°C overnight before moving to liquid nitrogen for long-term storage.

To recover cells from long-term storage, cryovials were placed in a 37°C water bath until thawed. Contents were then transferred to culture flasks containing prewarmed medium and left in the incubator overnight. Medium was changed the following day to remove residual DMSO.

2.1.4 Generation of stable cell lines using retrovirus

2.1.4.1 Generation of retrovirus to infect murine cell lines

Phoenix Ecotropic cells were used to produce retrovirus for infecting murine cells. 1 million cells were seeded per T25 flask to achieve 60-70% confluency the following day. 24 hours (h) after seeding, cells were transfected with 3 – 10 μ g of insert plasmid (Table 2.2) using branched polyethylenimine (PEI; Sigma-Aldrich) as a transfection reagent at a 1:4 (DNA:PEI) ratio. For each plasmid, PEI was diluted in 520 μ l of serum-free DMEM and incubated at room temperature (RT) for 20 min. DNA was then added to this mix and incubated at RT for a further 20 min to allow plasmid-PEI complexes to form. 5 ml DMEM was then added to this mixture.

Medium was removed from flasks containing Phoenix Ecotropic cells and the plasmid-PEI-DMEM mix was added on to the cells to initiate transfection. Medium was changed once 24 h after transfection. Viral supernatants were collected 48 h or 72 h post-transfection, filtered through 0.45 µm syringe-driven filters (Merck Millipore) to remove cellular debris, and either used immediately or stored at -80°C.

2.1.4.2 Generation of retrovirus to infect human cell lines

HEK293T cells were used to produce retrovirus or lentivirus to infect human cell lines. 10 million cells were seeded per T175 flask to achieve 60 – 70% confluency the following day. 24 h after seeding, cells were transfected with, 30 µg retrovirus packaging plasmid (pUMVC), 3.75 µg envelope plasmid (pCMV-VSV-G), and 30 µg insert plasmid (an 8:1:8 ratio) (Table 2.2). PEI was used as a transfection reagent at a 1:4 (DNA:PEI) ratio with the total amount of plasmid DNA transfected. Plasmids and PEI were diluted separately in 1 ml of 0.9% (w/v) NaCl solution, mixed by pipetting, and incubated for 10 min at RT. Equal volumes of plasmid and PEI mixtures were combined in a single tube, mixed by pipetting, and incubated at RT for a further 10 min to allow plasmid-PEI complexes to form. Medium was removed from flasks containing HEK293T cells and replenished with 20 ml fresh DMEM. Plasmid-PEI mixture was then added to the flasks in a dropwise manner. Medium was changed once 24 h after transfection. Viral supernatants were collected 72 h post-transfection, filtered through 0.45 µm syringe-driven filters to remove cellular debris, and either used immediately or stored at -80°C.

2.1.4.3 Infection of target cell lines

For infection of adherent cells, cells were seeded 24 h prior to infection. After 24 h, medium was removed from target cells and replaced with viral supernatant diluted with the appropriate amount of growth medium specific to the target cells. Polybrene (Sigma-Aldrich), a cationic polymer used to enhance infection, was added to the cells at a final concentration of 8 µg/ml. Target cells were incubated with virus for 6 h or 24 h, following which virus-containing medium was replaced with fresh growth

medium. After a further 48 h, cells were treated with either 2-3 µg/ml puromycin (Sigma-Aldrich) or 100 – 1000 µg/ml hygromycin (Invivogen). The concentration of selection antibiotic used was determined independently for each cell line by assaying dose-response in uninfected cell lines. The minimum concentration of antibiotic required to cause 100% cell death in uninfected cells within 7 days was used. Prior to any downstream experiments, infected cells were maintained in selection antibiotic for 14 days. Stable cell lines were maintained in selection antibiotic for growth and expansion, but antibiotic was removed for experiments.

2.2 Molecular biology techniques

2.2.1 Bacterial transformation

XL-10-Gold ultracompetent bacteria (Agilent) were thawed on ice. 50 µl aliquots of XL-10-Gold ultracompetent bacteria were mixed with 10 ng of plasmid DNA and incubated for 30 min on ice. Bacteria were then transformed by heat shock for 30 seconds at 42°C and incubated on ice for a further 2 min. 950 µl Luria-Bertani broth (LB broth; 5 g/L NaCl, 10 g/L bacto tryptone, 5 g/L yeast extract) was then added to the transformation reaction. Reactions were then incubated at 37°C with shaking at 225 rpm for 16 h. 50 – 300 µl of transformed bacteria were spread onto LB-agar (LB broth, 15 g/L agar) plates containing 100 µg/ml ampicillin and incubated at 37°C for 16 h.

2.2.2 Plasmid preparation

A list of the plasmids used in this project is provided in Table 2.2. Single bacterial colonies were isolated and used to inoculate a 5 ml culture of LB-broth with 100 µg/ml ampicillin. Cultures were incubated at 37°C with shaking at 225 rpm for 16 h. For small scale plasmid preparation, 1 – 5 ml of bacterial culture was centrifuged at 6800 x g for 3 min and plasmid DNA was isolated from the bacterial pellet using

QIAprep Spin Miniprep kit (QIAGEN) following manufacturer's instructions. For larger scale plasmid preparation, 200 µl of the initial 5 ml culture was used to inoculate a 200 ml culture of LB-broth with 100 µg/ml ampicillin at 37°C for 16 h. This culture was then centrifuged at 4700 x g for 15 min and DNA was isolated from the bacterial pellet using HiSpeed Plasmid Maxi Kit (QIAGEN).

Plasmid	Bacterial resistance	Mammalian resistance	Source	Description	Reference
pBABE-puro-EGFR-WT	Ampicillin	Puromycin	Addgene (#11011)	WT-EGFR insert used to clone into pFB-Hygro expression vector	(Greulich <i>et al.</i> , 2005)
pFB-Hygro	Ampicillin	Hygromycin	Gift (M. Katan)	Empty vector backbone for retrovirus	-
pUMVC	Kanamycin	-	Addgene (#8449)	Packaging plasmid for producing retrovirus particles	(Stewart <i>et al.</i> , 2003)
pCMV-VSV-G	Ampicillin	-	Addgene (#8454)	Envelope plasmid for producing retrovirus particles	
pBABE-puro	Ampicillin	Puromycin	Gift (R. Marais)	Empty vector backbone for retrovirus	-
pBABE-SRC-Rescue	Ampicillin	Hygromycin	Addgene (#26983)	WT c-SRC insert for retrovirus	(Zhang <i>et al.</i> , 2009)
pBABE-SRC-Dasatinib-resistant	Ampicillin	Hygromycin	Addgene (#26980)	SRC with T338I gatekeeper mutation insert for retrovirus	

Table 2.2 – Plasmids and selectable markers

2.2.3 Glycerol stock

Glycerol stocks were prepared for the long-term storage of transformed bacteria. Liquid bacterial culture was mixed 1:1 with 50% (v/v) glycerol solution and stored at -80°C. To recover cultures from long term storage, glycerol stocks were removed from -80°C and kept on dry ice. A small amount of the stored culture was retrieved using a sterile pipette tip. The culture was then spread on LB-agar plates with 100 µg/ml ampicillin and incubated at 37°C for 16 h.

2.2.4 Agarose gel electrophoresis

1% (w/v) agarose gels were prepared by dissolving 1 g agarose in 100 ml TAE (2 M tris, 57.1 mM glacial acetic acid, 50 mM EDTA) and adding 0.5 µg/ml ethidium bromide. DNA samples were mixed with 6X DNA Loading Dye (Thermo Fischer Scientific) and loaded on to the gel. Electrophoresis was performed in TAE running buffer for 1 – 1.5 h. DNA bands were visualised using a UV transilluminator or a ChemiDoc Touch gel dock (BioRad). DNA bands were excised by scalpel and extracted by QIAquick Gel Extraction Kit (QIAGEN) following manufacturer's instructions.

2.2.5 Sanger sequencing

Samples were sequenced using Eurofins Genomic tube sequencing service. Sequence alignment was performed using the online tool Benchling (<https://benchling.com/>). A list of primers used for sequencing is shown in Table 2.3.

2.2.6 Generation of mutant EGFR expression constructs

2.2.6.1 Cloning

Full-length WT-EGFR was purchased from Addgene (pBABE-puro-EGFR-WT, #11011). This was sequenced and sub-cloned into the pFB retroviral vector (Stratagene) for mammalian expression using In-Fusion HD kits (Clontech) following the manufacturer's instructions.

EGFR was amplified by PCR from pBABE-puro-EGFR-WT (Addgene plasmid #11011) using pFB-EGFR FW and pFB-EGFR RV primers shown in Table 2.3. Additional overhangs complementary to the cloning site of the destination pFB vector were introduced on either side of the *EGFR* gene. PCR was performed using CloneAmp HiFi PCR Premix (Clontech) according to manufacturer's instructions. PCR reaction mixtures contained 12.5 µl CloneAmp HiFi PCR Premix, 0.25 µM forward primer, 0.25 µM reverse primer, and 80 ng of pBABE-puro-EGFR-WT. Reaction mixtures were made up to a final volume of 25 µl using sterile distilled water. PCR reactions were performed on a thermocycler with 35 cycles of denaturation (98°C for 10 seconds), annealing (55°C for 15 seconds), and extension (72°C for 20 seconds) followed by a single final elongation step of 72°C for 5 min. PCR reactions were then purified using NucleoSpin PCR Clean-up kits (Takara Bio) following manufacturer's instructions.

pFB was linearised by digestion with BamHI, and isolated by agarose gel electrophoresis and gel extraction using QIAquick Gel Extraction kits (QIAGEN). The *EGFR* PCR product with complementary overhangs was then cloned into the linearised pFB using In-Fusion HD kits (Clontech) following the manufacturer's instructions. Cloning reactions contained 2 µl In-Fusion HD Enzyme Premix, 100 ng of linearized pFB, and 75 ng of purified *EGFR* PCR product. Reactions were made up to a final volume of 10 µl using sterile distilled water. Reactions were incubated at 50°C for 15 min, placed on ice and then used to transform bacteria. Following transformation, plasmid DNA was isolated from bacterial colonies and sequenced by Sanger sequencing to confirm presence of *EGFR* using primers shown in Table 2.3.

Gene	Sequence (5' - 3')	Reference
In-Fusion HD cloning kit		
pFB-EGFR FW	TGCCGGATCGAATTGAGTGTGGTGGTACATCATGCG	
pFB-EGFR RV	TTCTGCTCGAGGATCTGCTCCAATAAATTCAGTGC	
pFB-EGFR sequencing		
EGFR-1	TCGATCCTCCCTTTATCCAGC	
EGFR-2	AACCTGCAGATCATCAGAGGA	
EGFR-3	TGACTGCTGCCACAACCAG	
EGFR-4	AACTGCACCTCCATCAGTG	
EGFR-5	GAAAACAGCTGCAAGGCCAC	
EGFR-6	ATCCAAACTGCACCTACGGATG	
EGFR-7	ATGAAGCCTACGTGATGGCC	
EGFR-8	AGAGTGATGTCTGGAGCTACG	
EGFR-9	ACGTCACGGACTCCCCTC	
EGFR-10	AGGCAGCCACCAAATTAGC	
pBABE-SRC sequencing		
pBABE5'	CTTTATCCAGCCCTCAC	Weinberg Lab
Src-1	ATGGGGAGCAGCAAGAG	
Src-2	GGGAACCTTCTTGGTCC	
Src-3	AGGGCTGCTTTGGAGAG	
Src-4	GGACAACGAGTACACAG	
Src-5	CTGGAGGACTACTTCACC	
Genomic PCR and sequencing: EGFR		
EGFR Genomic 1F	ATGCGACCCTCCGGGACG	
EGFR Genomic 1R	CCTTCAGTCCGGTTTTATTTGC	
EGFR Genomic 2F	CGAAAATTCCTATGCCTTAGC	
EGFR Genomic 2R	GCTTCGTCTCGGAATTTGC	
EGFR Genomic 3F	CACAACCAGTGTGCTGCAG	
EGFR Genomic 3R	GAGATCGCCACTGATGGAG	
EGFR Genomic 4F	GGTGAATTTAAAGACTCACTCTCC	
EGFR Genomic 4R	GGTCCCAAACAGTTTTTTCCAG	
EGFR Genomic 5F	GGAGATAAGTGATGGAGATGTG	
EGFR Genomic 5R	CGTCAATGTAGTGGGCAC	
EGFR Genomic 6F	CCATGAACATCACCTGCAC	
EGFR Genomic 6R	CTCAAGAGAGCTTGGTTGG	
EGFR KD F1	AGCTTGTGGAGCCTCTTACACC	(Kosaka <i>et al.</i> , 2004)
EGFR KD R1	TAAAATTGATTCCAATGCCATCC	
EGFR Genomic 7F	CGGAAGAGAAAGAATACCATGC	
EGFR Genomic 7R	GGTAGAAGTTGGAGTCTGTAGG	
EGFR Genomic 8F	GCGCTACCTTGTCATTCAGG	
EGFR Genomic 8R	GCTGATTGTGATAGACAGGATTCTG	
EGFR Genomic 9F	CCAGTGCCTGAATACATAAACC	
EGFR Genomic 9R	TGCTCCAATAAATTCAGTCTTTG	

Table 2.3 – Primer sequences for sequencing, PCR amplification, and cloning.

2.2.6.2 Site-directed mutagenesis

Site-directed mutagenesis (SDM) was used to introduce specific *EGFR* mutations into the pFB-EGFR expression vector. Mutations were introduced using either New England Biolabs Q5 SDM kit or Agilent Technologies QuikChange Lightning Site-Directed Mutagenesis Kit. Primers used for SDM were designed using NEBasechanger (<https://nebasechanger.neb.com/>) or QuikChange Primer Design (<https://www.chem.agilent.com/store/primerDesignProgram.jsp>), respectively. Primer sequences are shown in Table 2.4 and Table 2.5.

Amino Acid Change	Nucleotide Change	Direction	Sequence (5' - 3')
L62R	T185G	F	GGTAATTTCCAAATTCACCGGACCACCTCACAGTTATT
		R	AATAACTGTGAGGTGGTCCGTGGGAATTTGGAAATTACC
R108G	A322G	F	TCGTAGTACATATTTCTCCGATGATCTGCAGGTTTTCC
		R	GGAAAACCTGCAGATCATCGGAGGAAATATGTACTACGA
R252C	C754T	F	CGTCTCGGAATTTGCAGCAGACCAGGCAGTC
		R	GACTGCCTGGTCTGCTGCAAATTCGGAGACG
A289D	C866A	F	ACTTCTTCACGCAGGTGTACCAAAGCTGTATTTG
		R	CAAATACAGCTTTGGTGACACCTGCGTGAAGAAGT
A289T	G865A	F	CACGCAGGTGGTACCAAAGCTGTATTTGCCCT
		R	AGGGCAAATACAGCTTTGGTACCACCTGCGTG
A289V	C866T	F	ACTTCTTCACGCAGGTGTACCAAAGCTGTATTTG
		R	CAAATACAGCTTTGGTGTCACCTGCGTGAAGAAGT
G598V	G1793T	F	TTTCTCCCATGACTACTGCCGGGCAGGTC
		R	GACCTGCCCGGCAGTAGTCATGGGAGAAA
G719A	G2156C	F	CGAACGCACCGGAGGCCAGCACTTTGATC
		R	GATCAAAGTGCTGGCCTCCGGTGCGTTCCG
G719C	G2155T	F	CGAACGCACCGGAGCACAGCACTTTGATCTT
		R	AAGATCAAAGTGCTGTGCTCCGGTGCGTTCCG
L858R	T2573G	F	CCCAGCAGTTTGGCCCGCCAAAATCTGTGA
		R	TCACAGATTTTGGGCGGGCCAAACTGCTGGG
L861Q	T2582A	F	TCCGCACCCAGCTGTTTGGCCAGCC
		R	GGCTGGCCAAACAGCTGGGTGCGGA
L861R	T2582G	F	TCCGCACCCAGCCGTTTGGCCAGCC
		R	GGCTGGCCAAACAGCTGGGTGCGGA
E746_A750del		F	TCCCGTCGCTATCAAGACATCTCCGAAAGCCA
		R	TGGCTTTCGGAGATGTCTTGATAGCGACGGGA
L747_T751del		F	AATTCGTCGCTATCAAGGAATCTCCGAAAGCC
		R	GGCTTTCGGAGATTCTTGATAGCGACGGGAATT

Table 2.4 – Primer sequences for QuikChange Lightning Site-directed Mutagenesis kit.

Amino Acid Change	Nucleotide Change	Direction	Sequence (5' - 3')
E709K	G2125A	F	GATCTTGAAGAAAAGTGAATTCAAAAAG
		R	CTCAAGAGAGCTTGGTTG
A767_V769dupASV		F	CGTGGCCAGCGTGGACAACCCC
		R	CTGGCCATCACGTAGGCTTCATCGAGG
N771_H773dupNPH		F	CCACAACCCCCACGTGTGCCGC
		R	GGGTTGTCCACGCTGGCCATCACG
S768_D770dupSVD		F	GGACAGCGTGGACAACCCCCAC
		R	ACGCTGGCCATCACGTAGGCTTC

Table 2.5 – Primer sequences for Q5 Site-directed Mutagenesis kit.

Reactions using the QuikChange Lightning kit contained 50 ng template DNA, 125 ng forward primer, 125 ng reverse primer, 1 µl dNTP mix, 5 µl of 10X reaction buffer, and 1.5 µl of QuikSolution reagent. Reactions were made up to a final volume of 50 µl using sterile distilled water and 1 µl of QuikChange Lightning Enzyme was added. After an initial denaturation step of 95°C for 2 min, reactions were subjected to 18 cycles of denaturation (95°C for 20 seconds), annealing (60°C for 10 seconds), and extension (68°C for 5 min 30 seconds) followed by a final elongation step of 68°C for 5 min. Reactions were then treated with 2 µl *Dpn* I and incubated at 37°C for 5 min to digest unmutated template plasmid.

Reactions using the Q5 SDM kit contained 12.5 µl Q5 Hot Start High-Fidelity 2X Master Mix, 0.5 µM forward primer, 0.5 µM reverse primer, and 10 ng template DNA. Reactions were made up to 25 µl using sterile distilled water. After an initial denaturation step of 98°C for 30 seconds, reactions were subjected to 25 cycles of denaturation (98°C for 10 seconds), annealing (57-69°C for 30 seconds), and extension (72°C for 5 min 30 seconds) followed by a final elongation step of 72°C for 2 min. To digest unmutated template DNA, 1 µl PCR product was mixed with 5 µl 2X KLD reaction buffer, 1 µl KLD Enzyme Mix, and 3 µl sterile distilled water and incubated at RT for 5 min.

Following mutagenesis, reactions were used to transform bacteria. Plasmid DNA was isolated from bacterial colonies and the presence of the desired mutations and absence of additional mutations was confirmed by Sanger sequencing using primers provided in Table 2.3.

2.2.7 Generation of mutant SRC expression constructs

SRC-WT and SRC-T338I constructs were isolated from the pBABE-Hygro vector by restriction digest with BamHI and Sall, followed by agarose gel electrophoresis and gel extraction using QIAquick Gel Extraction kits (QIAGEN). The pBABE-puro vector was linearized using BamHI and Sall and was then purified by agarose gel electrophoresis and gel extraction. SRC fragments and linearized pBABE-puro were ligated using Quick Ligase (NEB). Ligation reactions contained 97 ng of each SRC fragment and 150 ng of linearized pBABE-puro made up to a total volume of 20 μ l using nuclease-free water (Thermo Fischer Scientific). Reactions were incubated at RT for 5 min, chilled on ice, and used to transform bacteria. Following transformation, plasmid DNA was isolated from bacterial colonies and successful cloning screened by agarose gel electrophoresis and confirmed by Sanger sequencing using primers shown in Table 2.3.

2.2.8 Genomic DNA extraction from Ba/F3 clones isolated from ENU screens to identify acquired *EGFR* mutations

To isolate genomic DNA from cell lines, cells were centrifuged at 300 x g for 5 min to pellet. Cell pellets were kept at -20°C for storage. Genomic DNA was extracted from pellets using DNeasy Blood and Tissue Kit (QIAGEN) following manufacturer's instructions. DNA concentration was assessed by measuring absorbance using a DS-11 spectrophotometer (DeNovix).

2.2.9 Polymerase chain reaction of *EGFR* extracted from Ba/F3 clones isolated from ENU screens to identify acquired *EGFR* mutations

Polymerase chain reactions (PCR) were performed using the GoTaq DNA Polymerase enzyme (QIAGEN). Reaction mixtures contained 1X GoTaq reaction buffer, 1.5 mM MgCl₂, 0.2 mM of each dNTP, 0.4 μ M forward primer, 0.4 μ M reverse

primer, 50 ng template DNA, and 0.5 units of GoTaq DNA polymerase. Reactions were made up to a final volume of 20 µl with molecular biology grade water. Reactions were performed with an initial denaturation step at 94°C for 2 min, followed by 40 cycles of denaturation (94°C for 30 seconds), annealing (56°C for 30 seconds), and extension (72°C for 30 seconds). This was followed by a final extension step (72°C for 10 min). Prior to Sanger sequencing PCR products were visualised by agarose gel electrophoresis and treated with ExoSAP-IT clean-up reagent (Thermo Fischer Scientific) following manufacturer's instructions. Primers used for amplification of *EGFR* are shown in Table 2.3.

2.2.10 Droplet digital polymerase chain reaction (ddPCR) to confirm presence of *EGFR* T790M mutation in gefitinib-resistant PC9 cells

Genomic DNA was isolated as described in section 2.2.8 and 200 ng was digested with HindIII (New England Biosciences) for 1 hour at 37°C. The droplet digital PCR (ddPCR) reaction was performed with 10 ng of digested DNA, sequence-specific FAM/HEX labelled probes and ddPCR Supermix (Bio-Rad). Probes for *EGFR* T790M were commercially available (BioRad). Reactions contained 3 µl of digested DNA (10 ng), 1 µl of *EGFR*-WT HEX probe, 1 µl *EGFR*-T790M FAM probe, 10 µl ddPCR Mastermix (UTP), and 6 µl water. PCR reactions were emulsified into droplets using a QX-100 droplet generator (Bio-rad) according to manufacturer's instructions. Emulsified PCR reactions were performed in 96-well plates using G-Storm GS4 thermal cycler (G-Storm) by incubation at 95°C for 10 minutes followed by 40 cycles of 95°C for 15 seconds and 60°C for 60 seconds, and then a final 10 minute incubation at 98°C. Fluorescence was read using QX-100 droplet reader and results were analysed using QuantaSoft software (Bio-Rad). The fractional abundance was determined using the following formula:

$$\left(\frac{\text{Number of mutant droplets}}{\text{Number of mutant droplets} + \text{number of wildtype droplets}} \right) * 100$$

2.3 Protein analysis techniques

2.3.1 Protein extraction and quantification

Prior to protein harvest, adherent cells were washed once with ice-cold PBS. Suspension cells were collected from suspension, pelleted by centrifugation at 300 x g for 5 min, resuspended in ice-cold PBS, and pelleted again. Proteins were extracted in RIPA lysis buffer (50mM Tris.HCl, pH 7.6, 150mM NaCl, 1% NP40, 0.1% sodium dodecyl sulphate (SDS), 0.5% sodium deoxycholate) containing Halt Protease and Phosphatase Inhibitor Cocktail with EDTA (Pierce, Thermo Fisher Scientific). Lysates were incubated for 15 min on ice and mixed by vortexing every 2 min. Lysates were then centrifuged at 15,000 x g for 15 min, 4°C to remove cellular debris and the supernatant was transferred to a fresh tube and stored at -20°C.

Protein concentration was measured by bicinchoninic acid (BCA) assay (Pierce, Thermo Fisher Scientific) according to manufacturer's instructions. A Spectramax M5 plate reader (Molecular Devices) was used to measure absorbance at a wavelength of 562 nm.

2.3.2 Sodium dodecyl sulphate-polyacrylamide gel electrophoresis

10 – 40 µg of protein lysate were prepared with 10X NuPAGE Sample Reducing Agent and 4X NuPAGE LDS Sample Buffer (Thermo Fisher Scientific) and boiled for 5 min at 95°C. Proteins were separated on 4-12% gradient gels (Novex, Thermo Fisher Scientific) using sodium dodecyl sulphate-protein agarose gel electrophoresis (SDS-PAGE). Electrophoresis was performed at 120 V for 90 min.

2.3.3 Western blotting

Protein gels were transferred to methanol-soaked polyvinylidene fluoride (PVDF) membranes either by wet transfer for 3 h at 30 V using transfer buffer (Tris 25 mM, glycine 192 mM, methanol 20% v/v, pH 8.3) or by semi-dry transfer for 1 minute at

20 V, followed by 4 min at 23 V and 2 min at 25 V using an iBlot 2 semi-dry blotting machine (Thermo Fisher Scientific).

To prevent non-specific antibody binding, membranes were blocked for 30 min at RT with shaking at 45 rpm using blocking buffer (5% (w/v) milk/Tris-buffered saline (TBS)/0.01% (v/v) Tween or 5% (w/v) bovine serum albumin (BSA)/TBS/0.01% (v/v) Tween). Membranes were then incubated with primary antibodies in blocking buffer at 4°C overnight with shaking, washed 3 times with wash buffer (TBS/0.01% (v/v) Tween) for 10 min at RT with shaking, then incubated with secondary antibodies in blocking buffer for 1 h. Membranes were washed again 3 times and then developed using Supersignal West Pico Plus Chemiluminescent Substrate (Pierce, Thermo Fisher Scientific). Bands were visualised either by exposure to x-ray film or captured using a ChemiDoc Touch gel dock (BioRad). Primary and secondary antibodies and blotting conditions are listed in Table 2.6.

To strip membranes of bound antibodies, membranes were washed once for 5 min at RT with wash buffer, incubated with Restore Plus Western Blot Stripping Buffer (Thermo Fisher Scientific) for 15 min and washed again for 5 min with wash buffer. Stripped membranes were re-probed with new antibodies as described above beginning with membrane blocking.

Target	Species and clonality	Source	Blocking buffer and dilution
EGFR pY1173	Rabbit monoclonal	Cell Signalling Technology #4407	BSA 1:1000
EGFR pY1068	Rabbit polyclonal	Cell Signalling Technology #2234	BSA 1:1000
EGFR pY845	Rabbit polyclonal	Cell Signalling Technology #2231	BSA 1:1000
EGFR	Rabbit polyclonal	Cell Signalling Technology #2232	Milk 1:1000
SRC pY416	Rabbit polyclonal	Cell Signalling Technology #2101	BSA 1:1000
SRC	Rabbit polyclonal	Cell Signalling Technology #2108	Milk 1:1000
α -Tubulin	Mouse monoclonal	Sigma-Aldrich #T5168	Milk 1:10,000
Anti-rabbit HRP	Goat monoclonal	Cell Signalling Technology #7074	Milk 1:1000 – 1:10,000
Anti-mouse HRP	Goat polyclonal	SignalChem #G32-62G-1000	Milk 1:10,000

Table 2.6 – Primary and secondary antibodies.

2.4 Phenotypic assays

2.4.1 Chemical inhibitor preparation and storage

The chemical inhibitors used in this project are shown in Table 2.7. To prepare stocks of inhibitors, powders were resuspended in DMSO at a concentration of 1 – 10 mM depending on the solubility of the compound. After resuspension, inhibitors were aliquoted and stored at -20°C .

Compound	Source	Compound cont.	Source
Afatinib	LC Labs #A-8644	LY2603618	Selleckchem #S2626
Alisertib	Selleckchem #S1133	MK2206	Selleckchem #S1078
AZD5363	Selleckchem #S8019	MK-8776	Selleckchem #S2735
BEZ235	LC Labs #N-4288	Momelotinib	Selleckchem #S2219
BGJ398	Selleckchem #S2183	Navitoclax	Selleckchem #S1001
BI 2536	Selleckchem #S1109	Neratinib	LC Labs #N-6404
Binimetinib	LC Labs #B-2332	Niclosamide	Selleckchem #S3030
BMS345541	Sigma Aldrich #B9935	NVP-AEW541	Selleckchem #S1034
Bosutinib	LC Labs #B-1788	NVP-TAE226	Selleckchem #S2820
BX-795	Sigma Aldrich #SML0694	NVP-TAE684	Selleckchem #S1108
Cediranib	LC Labs #C-4300	Osimertinib	Selleckchem #S7297
Ceritinib	Selleckchem #S7083	Palbociclib	Selleckchem #S1116
Cilengitide trifluoroacetate	Selleckchem #S7077	Pazopanib	LC Labs #P-6706
Crizotinib	LC Labs #C-7900	PF562271	Selleckchem #S2890
Silmitasertib	Selleckchem #S2248	Ponatinib	LC Labs #P-7022
Dabrafenib	Selleckchem #S2807	Pozotinib	Stratech #S7358-SEL
Dasatinib	LC Labs #D-3307	Rapamycin	LC Labs #R-5000
EAI045	Selleckchem #S8242	Regorafenib	LC Labs #R-8024
Entrectinib	Selleckchem #S7998	Rociletinib	LC Labs #R-3692
Erlotinib	LC Labs #E-4997	Rucaparib	Selleckchem #S1098
Foretinib	LC Labs #F-4185	Saracatinib	Selleckchem #S1006
Galunisertib	Selleckchem #S2230	SB203580	Selleckchem #S3400
Gefitinib	LC Labs #G-4408	SH-4-54	Selleckchem #S7337
GSK126	Selleckchem #S7061	Sorafenib	LC Labs #S-8599
GW441756	Selleckchem #S2891	SP600125	Selleckchem #S7979
Imatinib	LC Labs #I-5577	Sunitinib	LC Labs #S-8877
JQ1	Selleckchem #S7110	Talazoparib	Selleckchem #S7048
Lapatinib	LC Labs #L-4899	TAS6417	MedChemExpress #HY-112299
Lenvatinib	LC Labs #L-5400	Trametinib	LC Labs #T-8123
Linsitinib	LC Labs #L-5814	Vandetanib	LC Labs #V-9402
Luminespib	LC Labs #N-5300	XAV-939	Selleckchem #S1180

Table 2.7 – Chemical compounds.

2.4.2 Cell viability assays

Cells were seeded at 1000 – 4000 cells / well in 96-well plates. For adherent cells, medium was removed after 24 h, and replaced with fresh medium containing the appropriate drug concentration or vehicle control. For suspension cells, 50 µl of drug at 2X the appropriate concentration was added to 50 µl of cells on the same day as seeding. 72 h after drug treatment, cell viability was estimated by measuring ATP concentration using Cell Titre Glo (Promega), following manufacturer's instructions. Luminescence was measured using a Victor X5 plate reader (PerkinElmer). Raw luminescence values were normalised against the vehicle control. Four-parameter non-linear regression curve-fitting was performed using GraphPad Prism 7 or GraphPad Prism 8 software to calculate the IC₅₀ value.

2.4.3 Growth curve by confluency

Cells were seeded into 96-well plates at 500 cells / well and confluency was measured using a Celigo Imaging Cytometer (Nexcelom). 24 h after seeding medium was changed to either fresh medium or fresh medium containing 50 ng/ml EGF. Medium was changed twice weekly.

2.4.4 Colony formation assay

Cells were seeded at low density (2000 cells / well) in a 6-well plate. After 24 h, medium was replaced with fresh medium containing the appropriate drug concentration or vehicle control. Medium and drug were replaced every 3 days. After 2 weeks, medium was aspirated and cells were fixed using Carnoy's solution (3:1 Methanol:Acetic acid). Fixative was removed and cells were allowed to dry before staining with a 1% (w/v) crystal violet solution (Sigma-Aldrich). Plates were imaged using a ChemiDoc system (Bio-Rad).

2.4.5 Spheroid growth assay

Cells were seeded into Ultra-low Binding Round Bottom 96-well plates (Corning) at 1000 cells/well. Plates were then centrifuged at 1000 x g for 10 min and incubated for 24 h to allow spheroid formation. After 24 h, drug or vehicle was added at the indicated doses bringing the total volume of the well to 100 μ l. Spheroid area was quantified at the indicated time points using an ImageXpress high-content microscope (Molecular Devices) and a Celigo Imaging Cytometer (Nexcelom). Spheroid viability was assessed at the indicated time points by Cell Titre Glo.

2.4.6 IL-3 independent growth curve

Ba/F3 cells were collected from suspension culture. To remove IL-3 from cells, cells were pelleted, resuspended in PBS, and pelleted again. Cells were then resuspended in RPMI without IL-3 and counted.

For the growth curves presented in Figure 3.8, cells were seeded in 96-well plates at 2000 cells / well and cell viability was measured at the indicated time points by Cell Titre Glo.

For the growth curves presented in Figure 3.11 and Figure 4.10 B, cells were seeded into 6-well plates at a density of 1×10^5 / ml in a total volume of 3 ml. 100 μ l of culture was taken from each well upon seeding and cell viability was measured by Cell Titre Glo (Day 0 cell viability reading). At each indicated time point, a further 100 μ l of culture was taken from each well and cell viability was measured by Cell Titre Glo (Day x cell viability reading). The difference between the cell viability at each time point (Day x) and the cell viability upon seeding (Day 0) was used to calculate the volume of culture required to seed a new well at the original seeding density using the following formula:

$(\text{Cell viability Day } x / \text{Cell viability Day } 0) / 3000 = \text{Volume to carry forward to new well } (\mu\text{l})$

Each new well was then made up to a final volume of 3 ml with RPMI without IL-3. Population doubling was calculated for each time point using the following formula:

$\text{Log}^2(\text{Cell viability Day } x / \text{Cell viability Day } 0)$

Cumulative population doubling was calculated for each time point by summing the population doubling of all previous time points.

2.5 Screening techniques

2.5.1 EGFR inhibitor screen

EGFRi included in the EGFRi screen are gefitinib, erlotinib, afatinib, neratinib, rociletinib, osimertinib, poziotinib, TAS6417, and lapatinib. Master library plates containing each EGFRi at a concentration of 10 μM , 5 μM , 2.5 μM , 1 μM , 500 nM, and 100 nM in DMSO were prepared and stored at -80°C until required. Cell lines were seeded at 4000 cells per well in 96-well plates. Master plates were defrosted at RT and cells were treated with inhibitors to a final concentration of 1 μM , 500 nM, 250 nM, 100 nM, and 50 nM. After 72 h cell viability was measured using Cell Titre Glo. For data analysis, 2 technical replicate plates were plate normalised against their respective vehicle control treated cells before calculating the average cell viability across replicate plates. Three biological replicates were performed for each EGFRi screen.

2.5.2 Small molecule inhibitor screen

The chemical compounds used in the small molecule inhibitor screen are listed in Table 4.1. Master library plates containing inhibitors at a concentration of 5 μM (or 500 nM for luminespib) in DMSO were prepared and stored at -80°C until required. Cell lines were seeded at 4000 cells per well in 96-well plates. Master plates were defrosted at RT and cells were treated with inhibitors to a final concentration of 500 nM (or 50 nM for luminespib). After 72 h cell viability was measured using Cell Titre Glo. For data analysis, 2 technical replicate plates were plate normalised against their respective vehicle control treated cells before calculating the average cell viability across replicate plates. Two biological replicates were performed for each

small molecule inhibitor screen.

2.5.3 N-ethyl-N-nitrosourea mutagenesis screen

Stock N-ethyl-N-nitrosourea (ENU; Sigma-Aldrich) was prepared as 100 mg/ml aliquots and stored at -80°C until required. 66 – 100 million Ba/F3 cells were treated with 100 µg/ml ENU for 24 h. After 24 h, medium containing ENU was removed from the cells by centrifugation at 300 x g for 5 min, cells were washed 3 times with PBS, and fresh medium was added to the cells. After a further 24 h cells, poziotinib or TAS6417 at the desired concentration was added to the cells. Cells were distributed over 3 – 5 96-well plates at 50,000 cells/well. Plates were monitored regularly by visual inspection under a microscope. Once cells reached confluency in a 96-well plate they were transferred to a 24-well plate. Inhibitor concentration remained consistent throughout. Once cells grew to confluency in a 24-well plate a frozen aliquot of cells for future experiments was prepared and a cell pellet was collected for genomic DNA extraction. The cell pellet was stored at -20°C prior to extraction of genomic DNA and subsequent Sanger sequencing to check for presence of *EGFR* mutations.

Chapter 3

Generation of a panel of isogenic cell lines expressing cancer-associated *EGFR* mutants

3.1 Introduction

In order to study differences between *EGFR* mutations observed across cancer types it is necessary to first identify cancer-associated mutations and second an appropriate model system to study them in. Cancer-associated *EGFR* mutations can be determined by examining the frequency of *EGFR* mutations occurring in patients from across all cancer types and selecting the most commonly recurrent. Once cancer-associated mutations have been identified, one could study the functional effects of these mutations either by using human cancer cell lines that endogenously harbour the *EGFR* mutations of interest or by engineering a model cell line to express mutant *EGFR*. This study utilises the latter approach for two reasons. First, for many of the less common *EGFR* mutants there are no commercially available cell lines that endogenously harbour these mutants. Second, heterogeneity in the genetic or epigenetic background between different cancer cell lines may make it challenging to identify characteristics of particular *EGFR* mutants, such as sensitivity to a kinase inhibitor or an ability to increase cellular growth, as there may be variations between cell lines in *EGFR*-independent characteristics, such as growth rate or co-occurring mutations. Although utilising exogenous expression of *EGFR* mutants in a model cell line circumvents issues of inherent variation in *EGFR*-independent characteristics, there are disadvantages with this approach. For example, utilising viral transduction to exogenously express *EGFR* mutants could lead to the genomic integration of the *EGFR* construct within another gene, causing genomic rearrangements that may have phenotypic effects. Additionally, a model cell line is further from the clinical scenario that is being modelled compared to a human cancer cell line that endogenously harbours an oncogenic *EGFR* mutant. This may lead to observations that are artefactual and specific to model system that are not seen in human cancer cell lines or patients. To tackle these challenges, this project seeks to first utilise model cell lines as a tool for rapid functional screens and will ultimately validate observations from these models in more physiologically relevant human cancer cell lines.

This project uses an experimental pipeline for comparative analysis of functional differences between *EGFR* mutants found in patients in order to identify the most

effective inhibitors for distinct EGFR mutants (Figure 3.1). The experimental pipeline is broken down into 3 parts:

1. A panel of expression vectors encoding cancer-associated *EGFR* mutants are generated by site directed mutagenesis (SDM). A subset of *EGFR* mutant vectors are expressed into model cell lines and experimental conditions are tested to identify an assay system where a phenotype that is dependent on EGFR signalling can be measured. Once an assay system where an EGFR-dependent phenotype can be measured has been identified, the entire panel of *EGFR* mutant vectors are expressed into the model cell line and comparable EGFR expression levels are confirmed by western blot.
2. The sensitivity or resistance of all EGFR mutants to 9 EGFRi and 53 other small molecule inhibitors is investigated to establish the optimal inhibitor for distinct EGFR mutants. Full dose-response experiments are used to validate the hits from the small molecule inhibitor screen.
3. The mechanisms underpinning the sensitivity or resistance of specific EGFR mutants to different inhibitors are examined.

This chapter describes the first section of this experimental pipeline: identification of the *EGFR* mutations of interest; generation of expression vectors for these mutations; optimisation of a model system to study these mutations; and the generation of a panel of cell lines expressing the different *EGFR* mutants.

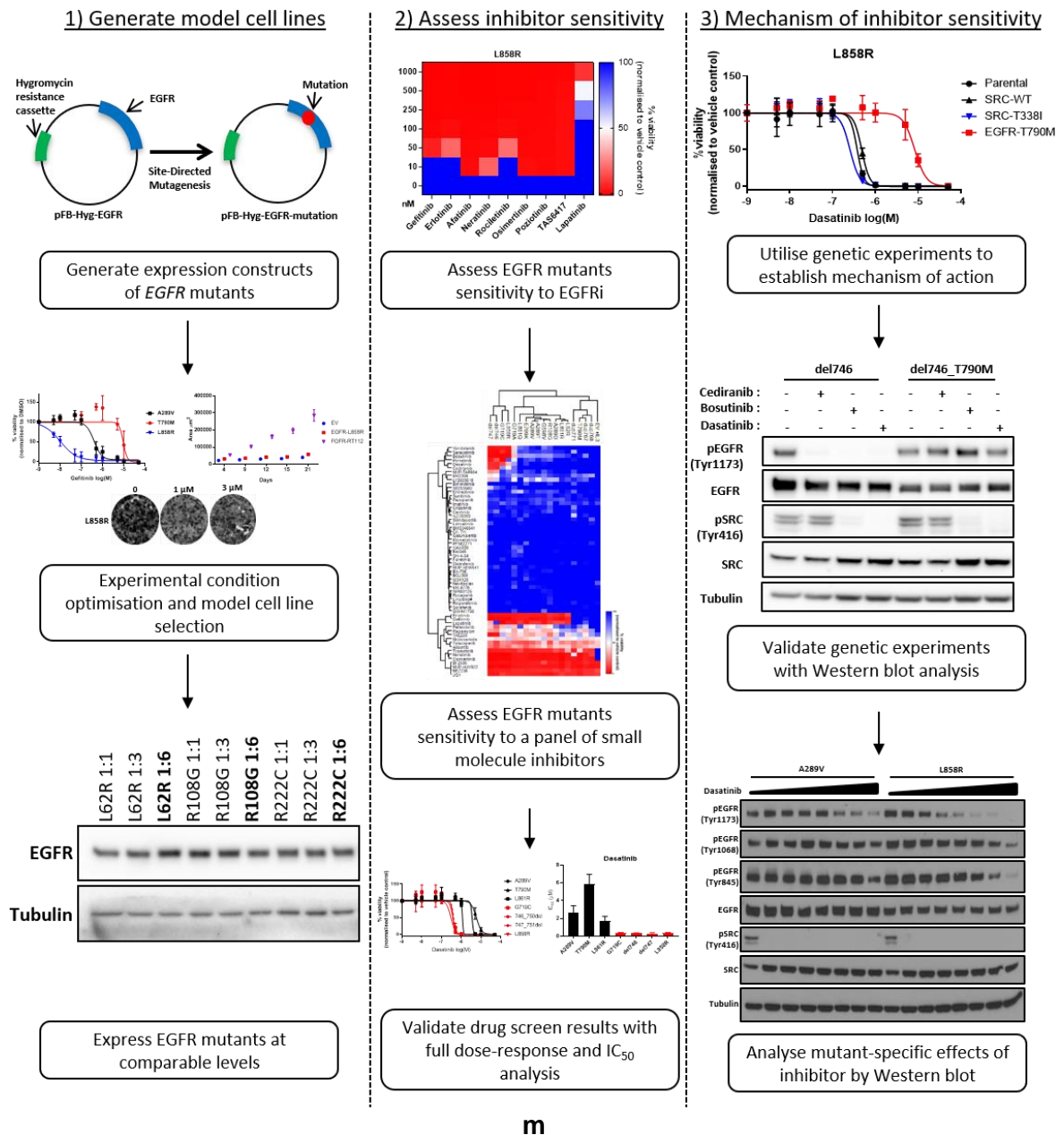


Figure 3.1 – Outline of proposed experimental pipeline to characterise *EGFR* mutations from across cancer types. 1) Expression vectors for the *EGFR* mutations of interest are generated by site-directed mutagenesis. A model cell line where an *EGFR*-dependant phenotype can be measured is identified and all *EGFR* mutations of interest are expressed in the model cell line at comparable expression levels. 2) Following the establishment of model cell lines, the sensitivity of the different *EGFR* mutants to EGFRi and other small molecule inhibitors is assessed. IC_{50} = half-maximal inhibitory concentration. 3) The mechanisms underlying the differences in inhibitor sensitivity are investigated. Mutant-specific effects of inhibitors are evaluated by western blot.

3.2 Selection of cancer-associated *EGFR* mutations for inclusion in the study

Large-scale cancer sequencing efforts of patient tumour specimens have revealed a plethora of *EGFR* mutations along the full length of the gene. These data can be accessed through online databases such as cBioPortal; a Web resource which facilitates integration of cancer genome sequencing data from large-scale sequencing studies such as The Cancer Genome Atlas, International Cancer Genome Consortium, and MSK-IMPACT Clinical Sequencing Cohort (Cerami et al., 2012; Gao et al., 2013; Zehir et al., 2017). *EGFR* mutations across all cancer types were analysed using cBioPortal at the beginning of this project (October 2016). Mutations were ranked by their frequency of occurrence to identify recurrent mutations that occur in hotspots and may be oncogenic (Vogelstein et al., 2013; Chen et al., 2018). These hotspots may represent “driver” mutations that confer a growth advantage to the cell harbouring the mutation. My functional experiments seek to delineate driver mutations versus “passenger” mutations which can also occur within oncogenes but do not confer a growth advantage (Merid et al., 2014). The evolutionary advantage conferred by driver mutations in oncogenes means that these mutations are enriched in tumours. Therefore selecting the *EGFR* mutations that occur most frequently in tumour samples should lead to the selection of *EGFR* mutations most likely to be oncogenic. The 19 most common recurrent mutations in *EGFR* were selected for functional characterisation (Table 3.1, Figure 3.2). Although Ex20Ins are the most frequently occurring class of *EGFR* mutations after the common mutations Ex19Del and L858R, the heterogenous nature of Ex20Ins meant that no single Ex20Ins mutation was prevalent enough to be accounted for in the 19 most frequent mutations in the cBioPortal database. Therefore, the Ex20Ins mutations A767_769dupASV (dup767), S768_dupSVD (dup768), and N771_H773dupNPH (dup771) were included in the study (Table 3.1). These particular Ex20Ins mutations were selected as I have access to human NSCLC cell lines that endogenously harbour these mutations, which could serve to validate results observed in the model cell line. These human NSCLC cell lines are very rare, making them a valuable resource for studying this class of *EGFR* mutations. Additionally the first- and third-generation gatekeeper mutations T790M and C797S

were included in the study, bringing the total of *EGFR* mutations included in this study to 24.

Mutation	Cancer Type
L62R	Brain, Breast, Lung
R108G/K	Brain, Stomach, Lung
R222C/L	Brain, Skin, Sarcoma, Colon, Lung
R252C/H	Brain, Prostate, Colon, Stomach
A289D/T/V	Brain, Breast, Lung, Head and Neck
G598V	Brain, Oesophageal
E709K	Lung, Urothelial, Skin, Brain, Breast
G719A/C	Lung, Urothelial, Breast, Brain
S768X	Lung, Breast, Colorectal
746_750del (Ex19del)	Lung, Urothelial
747_751del (Ex19del)	Lung
A767_769dupASV (Ex20Ins)	Lung, Brain, Liver, Urothelial, Head and Neck
S768_dupSVD (Ex20Ins)	Lung, Head and Neck
N771_H773dupNPH (Ex20Ins)	Lung, Urothelial, Head and Neck
L858R	Lung, Rectal
L861R/Q	Lung, Colon, Brain

Table 3.1 – Mutations included in this study and their associated cancer types. Mutations were selected from cBioPortal filtering for all cancer types with no overlapping samples (Cerami et al., 2012; Gao et al., 2013). The most frequent 19 mutations were selected. Three Ex20Ins mutations were also included. WT, T790M, and C797S were included in the panel as controls (not shown).

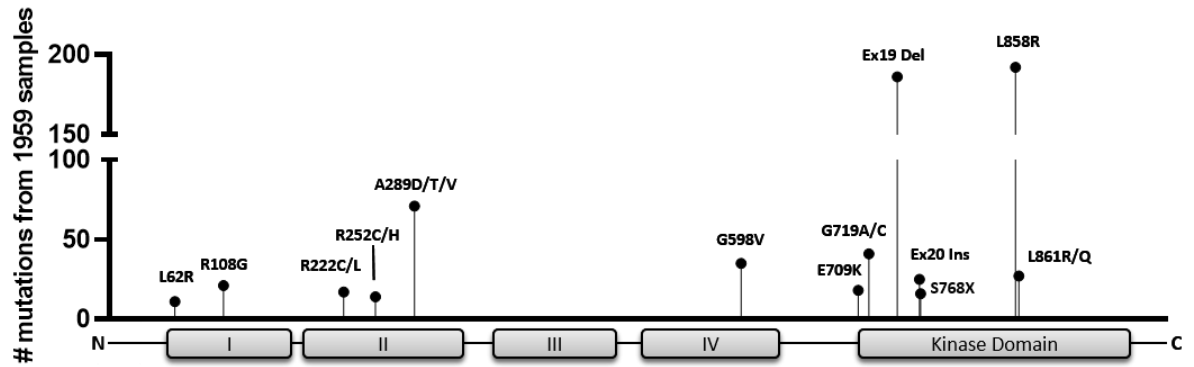


Figure 3.2 - The frequency of *EGFR* mutations selected for study in this project. Lollipop plot displaying the frequency of *EGFR* mutations selected from cBioPortal filtering for all cancer types with no overlapping samples (Cerami et al., 2012; Gao et al., 2013). The y-axis shows the number of samples from individual patients each mutation was detected in. The location of each mutation within the domains of *EGFR* is indicated by the grey bar at the bottom of the lollipop plot. From left to right, the grey bar represents the different domains of *EGFR* from N-terminus to C-terminus. Mutations were ranked by frequency and the most frequently recurrent 19 mutations were selected. A767_769dupASV, N771_H773dupNPH, and S768_dupSVD were also included. Ex19Del includes 746_750del and 747_751del. Ex20Ins includes A767_769dupASV, N771_H773dupNPH, and S768_dupSVD. WT, T790M, and C797S were also included in the panel as controls (not shown).

3.3 Generation of expression vectors encoding *EGFR* mutations

For the generation of stable cell lines which express *EGFR* mutants, a plasmid containing full-length WT-*EGFR* was purchased from Addgene (#11011). This was sequenced and subcloned into the pFB retroviral vector (Stratagene) for mammalian expression. SDM was used to introduce the mutations of interest, which were subsequently confirmed by Sanger sequencing (Appendix Figure 7.1). In total, plasmids encoding 24 *EGFR* mutants were generated including the 19 most frequent mutations identified using cBioPortal (Figure 3.2), three Ex20Ins mutations, and the gatekeeper mutations T790M and C797S. Experimental details are provided in section 2.2.6.

3.4 Identification of an optimal model cell line to study cancer-associated EGFR mutations

This project aims to improve our ability to treat patients whose tumours harbour *EGFR* mutations by identifying the most effective inhibitors for distinct *EGFR* mutants. To achieve this, it is necessary to identify a model cell line that has a dependence on *EGFR* signalling for a particular phenotype, such as cell survival or growth. Measuring the effect that inhibitor treatment has on this phenotype would provide insights into the sensitivity of *EGFR* mutants to different inhibitors. To identify a model cell line suitable for studying the sensitivity of *EGFR* mutants to different inhibitors, a small subset of *EGFR* mutants were first expressed in NIH-3T3 murine fibroblast, H3122 NSCLC, MCF10A mammary epithelial, and Ba/F3 murine pro-B cells which were then assessed for their ability to confer an *EGFR*-dependent phenotype.

3.4.1 NIH-3T3

The murine fibroblast cell line NIH-3T3 was evaluated as a model system as it has previously been used to characterise the signalling networks and oncogenicity of different *EGFR* mutants in multiple studies (Greulich *et al.*, 2005; Lee *et al.*, 2006; Pines *et al.*, 2010). A subset of 7 *EGFR* mutants (L62R, R252C, A289T, A289V, G598V, G719A, T790M, and L858R) were expressed in NIH-3T3 cells along with empty vector (EV) and WT-*EGFR* controls (Figure 3.3 A). These mutants were selected as they occur across different regions of the protein (Figure 3.2) and include mutants that have previously been shown to be oncogenic in *in vivo* experiments (i.e. A289V and L858R) (Greulich *et al.*, 2005; Lee *et al.*, 2006). They also include mutants that have previously been shown in studies utilising exogenous expression of *EGFR* mutants in model cell lines to be sensitive to first-generation *EGFRi* (i.e. L858R) (Lynch *et al.*, 2004; Tracy *et al.*, 2004) and resistant to first-generation *EGFRi* (i.e. T790M) (Kobayashi *et al.*, 2005).

To assess whether NIH-3T3 cells are a suitable model for investigating the sensitivity of *EGFR* mutants to different small molecule inhibitors, I first sought to

establish whether these cells recapitulated gefitinib dose responses reported in preclinical studies of human NSCLC cell lines and model cell lines expressing these EGFR mutants (Lynch *et al.*, 2004; Ono *et al.*, 2004; Tracy *et al.*, 2004; Kohsaka *et al.*, 2017). To examine the sensitivity of NIH-3T3 cells expressing different EGFR mutants to gefitinib, cells were treated with gefitinib at a range of concentrations for 72 h following which cell viability was measured using Cell Titre Glo (Figure 3.3 B). The resulting dose-response curves were used to calculate the half maximal inhibitory concentration (IC₅₀) values: the dose of inhibitor required to reduce cell viability by 50% when compared to vehicle-treated control. Analysis of the IC₅₀ values from this experiment showed that the EV cell line had a higher IC₅₀ value upon gefitinib treatment compared to cells expressing WT-EGFR (IC₅₀ = 14.02 μM vs 10.65 μM respectively) (Figure 3.3 C). This is expected as western blot analysis found that EV NIH-3T3 cells do not express EGFR and therefore are not dependent on EGFR signalling (Figure 3.3 A). NIH-3T3 cells expressing L858R had a significantly lower IC₅₀ value upon gefitinib treatment compared to cells expressing WT-EGFR (IC₅₀ = 6.82 μM vs 10.65 μM respectively) (Figure 3.3 C), which is in line with published data showing that L858R is more sensitive to inhibition by gefitinib compared to WT-EGFR in Cos-7 cells (Lynch *et al.*, 2004). However, despite expressing mutant EGFR, the panel of NIH-3T3 cell lines each had IC₅₀ values of >6 μM. This contrasts with published data which found that the human NSCLC cell line H3255, which harbours an endogenous L858R mutation in EGFR, has an IC₅₀ value of 0.04 μM upon treatment with gefitinib (Tracy *et al.*, 2004). To further investigate the relative lack of gefitinib sensitivity in NIH-3T3 cells expressing EGFR mutants compared with a mutant EGFR dependent NSCLC cell line, the gefitinib dose-response experiment was repeated in the human NSCLC cell line PC9, which endogenously harbours the gefitinib-sensitive 746_750del (del746) mutation (Figure 3.3 B). Comparative analysis of IC₅₀ values revealed that PC9 cells were significantly more sensitive to gefitinib compared with NIH-3T3 cells expressing L858R (IC₅₀ = 0.43 μM vs 6.82 μM respectively) (Figure 3.3 C). To confirm that gefitinib treatment was inhibiting EGFR phosphorylation in NIH-3T3 cells, cells expressing either the gatekeeper mutation T790M or L858R were treated with 1 μM gefitinib for 6 h prior to lysis. Western blot analysis revealed that as expected EGFR phosphorylation was not inhibited in cells expressing T790M but was potently inhibited in cells expressing L858R (Figure 3.3 E). These data indicates that,

although L858R was significantly more sensitive to gefitinib compared to WT-EGFR in NIH-3T3 cells, the relative insensitivity of NIH-3T3 cells expressing L858R compared to PC9 cells (Figure 3.3 B and Figure 3.3 C) is not due to lack of EGFR inhibition, but rather the result of a reduced dependence of NIH-3T3 cells on EGFR signalling for survival.

Previous studies have shown that NIH-3T3 cells expressing oncogenic EGFR mutants proliferate more rapidly compared to NIH-3T3 cells expressing WT-EGFR (Pines *et al.*, 2010). To test whether expression of EGFR mutants included in this study conferred a growth advantage to NIH-3T3 cells, proliferation was assessed over a 7-day period by measuring confluence in a 96-well plate (Figure 3.3 F). This revealed no clear difference in proliferation between EV, WT-EGFR, or EGFR-mutant expressing NIH-3T3 cells which provides further evidence that under growth conditions in normal growth media, NIH-3T3 cells are not dependent on oncogenic EGFR signalling for cell growth.

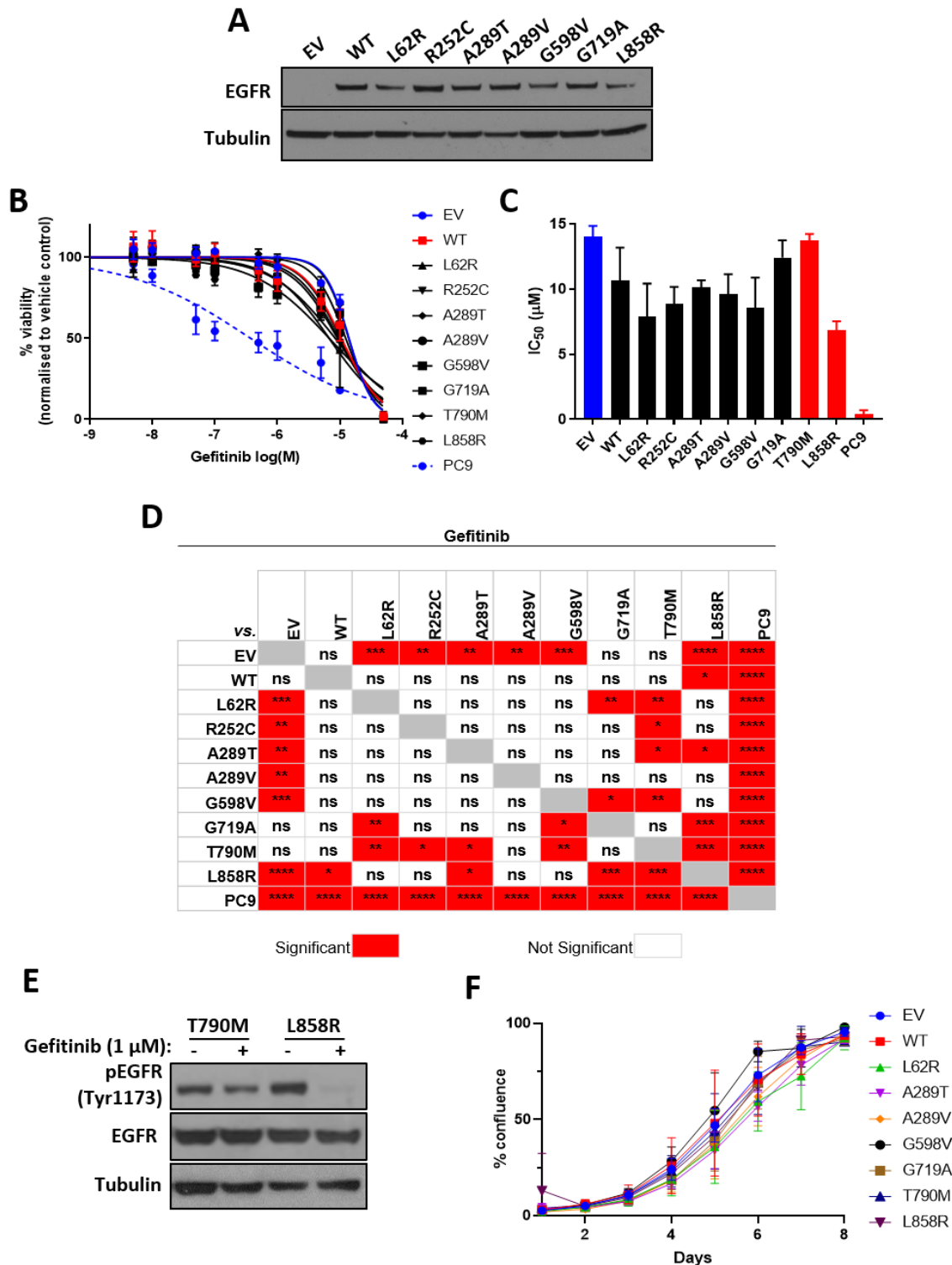


Figure 3.3 – Effect of expression of EGFR mutants on gefitinib sensitivity and proliferation in NIH-3T3 cells. (A) Western blot analysis confirmed expression of EGFR mutants in NIH-3T3 cells. $n = 1$ biological replicate. EV = empty vector, WT = wild type. (B) Dose-response curves for NIH-3T3 cells expressing different EGFR mutants and PC9 cells upon treatment with gefitinib. Cell viability is normalised to vehicle control (DMSO). (C) Bar chart showing IC_{50} values for NIH-3T3 cells expressing different EGFR mutants and PC9 cells upon treatment with gefitinib calculated from B. (D) Statistical significance for the indicated pairwise comparisons of IC_{50} values was calculated by Tukey's multiple

comparisons test. * = $p < 0.05$, ** = $p < 0.01$, *** = $p < 0.001$, **** = $p < 0.0001$, ns = not significant. (E) Western blot analysis of EGFR phosphorylation at Y1173 in NIH-3T3 cells expressing EGFR-T790M or EGFR-L858R following 1 h gefitinib treatment. $n = 1$ biological replicate. (F) Growth curve for NIH-3T3 cells expressing different EGFR mutants. (B, C, F) Values represent mean \pm standard deviation from $n = 3$ biological replicates.

I hypothesised that the lack of EGFR-dependence may be due to incomplete activation of EGFR in NIH-3T3 cells in normal growth media. To test this hypothesis, gefitinib dose-response experiments were repeated in the presence of 50 ng/ml EGF ligand (Figure 3.4 A). Analysis of the IC_{50} values showed that EV cells and cells expressing T790M were significantly less sensitive to gefitinib compared to WT-EGFR whilst the remaining mutations had similar IC_{50} values compared to WT-EGFR (Figure 3.4 B, Figure 3.4 C). Notably, the IC_{50} value for L858R was still >100 -fold higher than has previously been reported in H3255 cells which endogenously harbour an L858R mutation (4.48 μ M vs 0.04 μ M respectively) (Tracy *et al.*, 2004). The proliferation experiment was also repeated with 50 ng/ml EGF added to the cells 24 h after seeding to investigate whether the addition of EGF to the growth media would lead to an EGFR-dependent growth advantage in NIH-3T3 cells expressing EGFR mutants. However, no clear differences in proliferation were observed between EV, WT-EGFR, or EGFR-mutant expressing NIH-3T3 cells (Figure 3.4 D). Together, these data demonstrate that addition of EGF to the media does not alter EGFR-dependent growth or gefitinib sensitivity in NIH-3T3 cells expressing EGFR mutations.

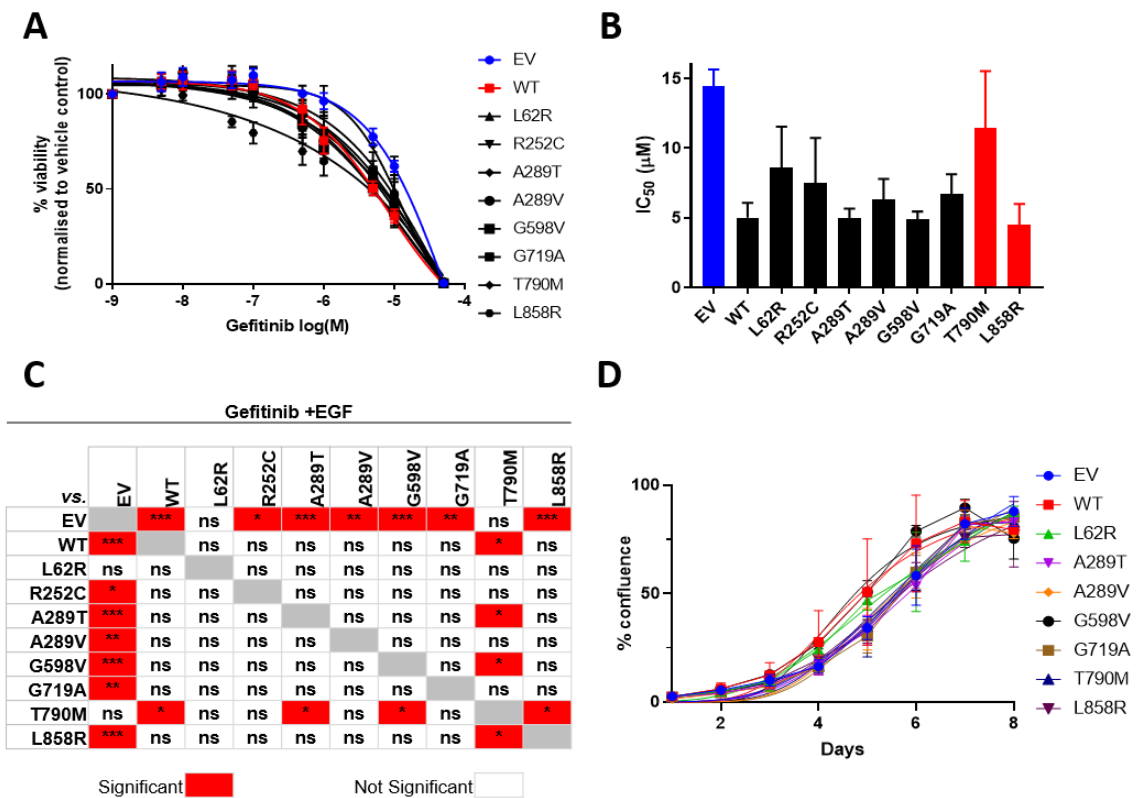


Figure 3.4 – Effect of expression of EGFR mutations on gefitinib sensitivity and proliferation in NIH-3T3 cells in the presence of EGF. (A) Dose-response curves for NIH-3T3 cells expressing different EGFR mutants upon treatment with gefitinib and 50 ng/ml EGF. Cell viability is normalised to vehicle control (DMSO). EV = empty vector, WT = wild type. (B) Bar chart showing IC₅₀ values for NIH-3T3 cells upon treatment with gefitinib and 50 ng/ml EGF calculated from A. (C) Statistical significance for the indicated pairwise comparisons of IC₅₀ values was calculated by Tukey’s multiple comparisons test . * = p<0.05, ** = p<0.01, *** = p<0.001, ns = not significant. (D) Growth curve for NIH-3T3 cells expressing different EGFR mutants grown with 50 ng/ml EGF added 24 h after seeding. (A, B, D). Values represent mean ± standard deviation from *n* = 3 biological replicates.

I next sought to examine whether altering the seeding conditions of the cells could lead to an EGFR-dependent phenotype by using colony formation assays and spheroid growth assays. Colony formation assays require cells to overcome low seeding densities, which may reduce autocrine and paracrine signalling as well as cell-cell interactions, in order to grow. Additionally, colony formation assays can be run over 14 days, compared to the 72 h used for the previous dose-response experiments, which may exacerbate any differences between the EGFR mutants. I hypothesised that the presence of oncogenic EGFR might provide a growth advantage in a colony formation assay that would cause the cells to display gefitinib sensitivity more consistent with previously published clinical and preclinical data

(Lynch *et al.*, 2004; Paez *et al.*, 2004; Tracy *et al.*, 2004). However, colony formation assays did not detect differences in gefitinib sensitivity between the EGFR mutants (Figure 3.5 A). Notably, NIH-3T3 cells expressing L858R were resistant to gefitinib, forming colonies in 1 μ M of the inhibitor. These data demonstrates that use of colony formation assays does not produce an EGFR-dependent phenotype.

Growing cells as spheroids requires cells to overcome anchorage independent growth, nutrient gradients, and hypoxia (Hirschhaeuser *et al.*, 2010) which I hypothesised may give cells expressing oncogenic EGFR mutants a growth advantage over EV or WT-EGFR expressing cells. To test whether growing cells as spheroids would lead to an EGFR-dependent phenotype, cells were seeded in ultra-low attachment round-bottom plates and centrifuged to form spheroids. After 24 h cells were treated with DMSO, 100 nM gefitinib, or 1 μ M gefitinib. Following 72 h treatment, cell viability was measured using Cell Titre Glo. Cells expressing EGFR mutants did not show a significant increase in cell viability compared to EV cells after 72 h DMSO treatment (Figure 3.5 B). However, gefitinib treatment caused a significant decrease in cell viability compared to DMSO, indicating that spheroid growth may be EGFR-dependent in NIH-3T3 cells expressing EGFR mutants (Figure 3.5 C). Although cell viability of EGFR expressing NIH-3T3 cells grown as spheroids was significantly reduced by gefitinib treatment, the actual reduction in cell viability was modest; even the 1 μ M dose of gefitinib only resulted in a ~1.4-fold reduction in cell viability compared with DMSO. This modest reduction in cell viability following a high dose of gefitinib suggests that spheroid growth in NIH-3T3 cells is not highly dependent on EGFR signalling. By contrast, 1 μ M gefitinib treatment of PC9 cells grown as spheroids caused a 40-fold reduction in cell viability compared with DMSO, demonstrating that spheroid growth in PC9 cells is highly dependent on EGFR signalling (Figure 3.5 C).

To further investigate whether expression of EGFR mutants conferred a spheroid growth advantage in NIH-3T3 cells, spheroid growth was tracked by measuring spheroid area using microscopy, rather than cell viability, over a longer time period. Spheroid growth of NIH-3T3 cells expressing L858R was tracked over 21 days and compared with NIH-3T3 cells expressing an oncogenic FGFR3-TACC3 fusion (RT112) as a positive control (Lamont *et al.*, 2011). This experiment showed that the spheroid area of NIH-3T3 cells expressing the RT112 FGFR3-TACC3 fusion

increased ~5-fold after 21 days compared to NIH-3T3 cells expressing L858R, which did not grow as a spheroid (Figure 3.5 D). Taken together, these data indicate that NIH-3T3 cells expressing mutant EGFR do not grow as spheroids.

It was therefore concluded that NIH-3T3 cells are insufficiently dependent on exogenously expressed EGFR for investigating the effects of inhibitor treatment in distinct EGFR mutants and I therefore began working to identify a different model cell line for use in this thesis.

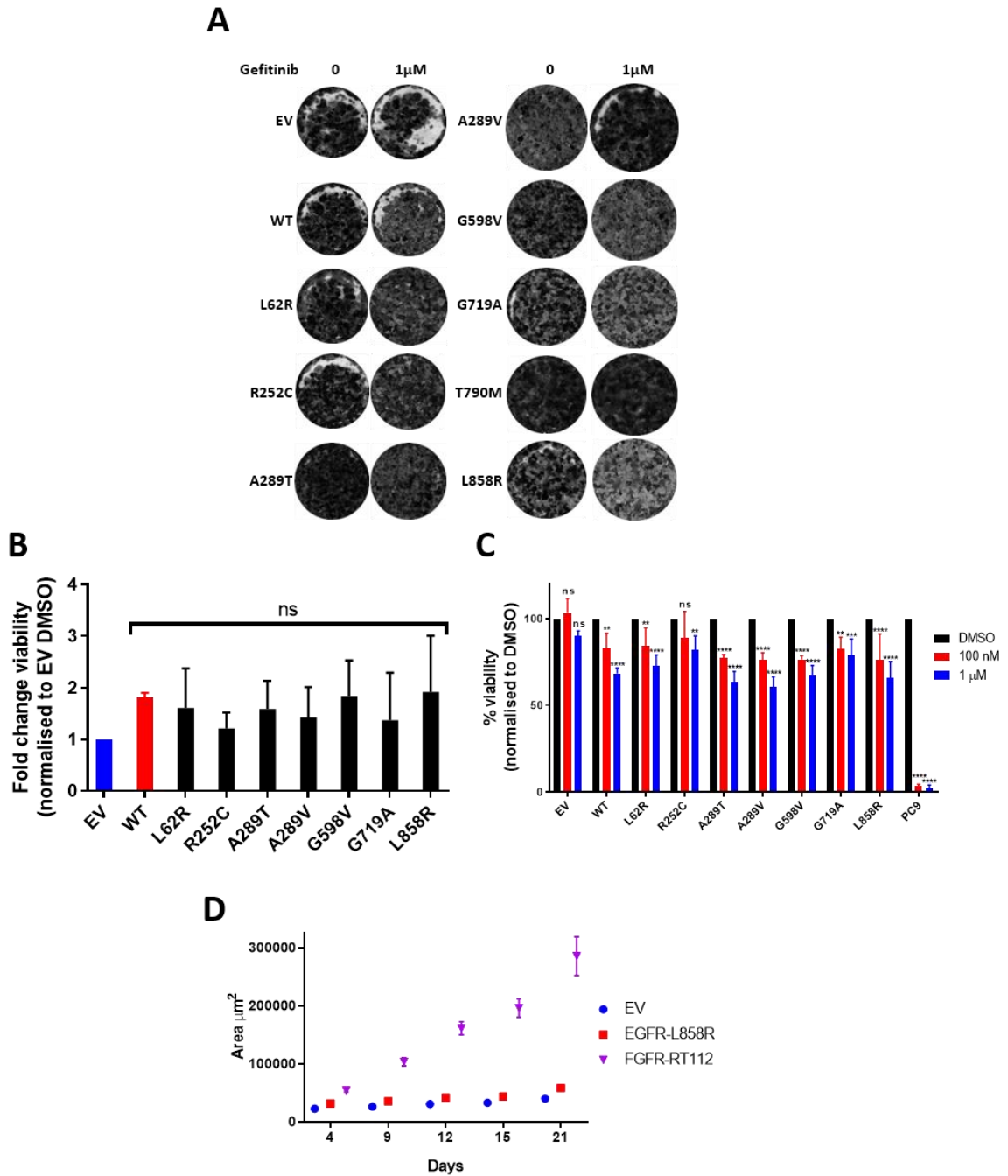


Figure 3.5 – Effect of altering cell culture conditions to increase EGFR-dependence in NIH-3T3 cells expressing EGFR mutants. (A) Representative images of long-term colony formation assays in the NIH-3T3 cell line panel upon treatment with gefitinib or DMSO control at the indicated doses for 2 weeks. Images are $n = 1$ biological replicates. EV = empty vector, WT = wild type. (B) Bar chart showing fold change viability of NIH-3T3 cells expressing the indicated EGFR mutants when grown as spheroids upon treatment with DMSO for 72 h. Cell viability was measured by Cell Titre Glo and shown as fold change compared to EV NIH-3T3 cells. Statistical significance was calculated by Dunnett’s multiple comparisons test comparing each cell line against EV DMSO. All comparisons were not significant (ns). Values represent mean \pm standard deviation from $n = 3$ biological replicates. (C) Bar chart

showing cell viability of NIH-3T3 cells expressing the indicated mutants grown as spheroids following 72 h treatment with 100 nM or 1 μ M gefitinib as indicated. Cell viability for each mutant is normalised to its own vehicle control (DMSO). Statistical significance was calculated by Dunnett's multiple comparisons test comparing 100 nM or 1 μ M gefitinib treatment with DMSO treatment within each mutant. ** = $p < 0.01$, *** = $p < 0.001$, **** = $p < 0.0001$, ns = not significant. Values represent mean \pm standard deviation from $n = 3$ biological replicates. (D) Increase in spheroid area of NIH-3T3 cells expressing the indicated constructs over 21 days. Error bars represent standard deviation from three technical replicates, $n = 1$ biological replicate.

3.4.2 H3122

H3122 is a human NSCLC cell line that harbours an EML4-ALK fusion. The cells are dependent on ALK signalling for survival and are sensitive to ALK inhibitors (ALKi) such as crizotinib and ceritinib (Friboulet *et al.*, 2014; Yamaguchi *et al.*, 2014). Yamaguchi *et al.* identified EGFR overexpression as a resistance mechanism to crizotinib in H3122 cells (Yamaguchi *et al.*, 2014). It was therefore hypothesised that expression of the EGFR mutants included in this study (Table 3.1) in H3122 cells may confer resistance to ALKi, consequently making the cells dependent on the mutant EGFR for survival. This dependency on EGFR could then be exploited to determine the kinase inhibitor sensitivity of different EGFR mutants. To test this hypothesis, a pilot set of mutants including A289V, T790M, and L858R were expressed in H3122, along with EV and WT-EGFR controls (Figure 3.6 A). A reduced set of mutants was used compared to the NIH-3T3 experiments in order to enable more rapid testing of different model systems. A289V, T790M, and L858R were selected for the following reasons: A289V is the most common GBM mutation in the panel of EGFR mutants included in this study, and has previously been reported in studies utilising exogenous expression of A289V in Ba/F3 cells as partially sensitive to gefitinib (Kohsaka *et al.*, 2017); T790M is a common gefitinib resistance mutation occurring in NSCLC previously reported in studies of a human NSCLC cell line harbouring endogenous T790M as resistant to gefitinib (Kosaka *et al.*, 2006); L858R is a common NSCLC mutation previously reported in studies of a human NSCLC cell line harbouring endogenous L858R as sensitive to gefitinib (Tracy *et al.*, 2004).

To test whether expression of these EGFR mutants was able to confer ALKi resistance, the cells were treated with the ALKi ceritinib at a range of concentrations for 72 h before cell viability was measured using Cell Titre Glo (Figure 3.6 B). None of the EGFR mutations were able to confer resistance to ceritinib, with no significant differences in IC₅₀ value detected between parental H3122 cells, EV, WT-EGFR, or EGFR-mutant expressing H3122 cells (Figure 3.6 C). As with NIH-3T3 cells, it was hypothesised that this lack of EGFR-dependent phenotype may be due incomplete activation of EGFR in normal growth media. To test this hypothesis, the ceritinib dose-response experiments were repeated with 50 ng/ml EGF added to the cells simultaneously with ceritinib (Figure 3.6 D). However, there were no significant differences in IC₅₀ value between parental H3122 cells, EV, WT-EGFR, or EGFR-mutant expressing H3122 cells, although H3122 cells expressing either EV, A289V, T790M, or L858R had a non-significant ~2-fold increase in IC₅₀ value compared to parental and WT-EGFR expressing H3122 cells (Figure 3.6 E). Interestingly, treating the cells with EGF decreased sensitivity to ceritinib in all H3122 cells, including EV and parental cells (Figure 3.6 F). Reduced ceritinib sensitivity in all H3122 cells upon EGF treatment suggests that parental H3122 cells express endogenous EGFR at low levels, which is supported by western blot data showing low levels of EGFR present in EV cells (Figure 3.6 A) and was also shown in parental H3122 cells by Yamaguchi *et al.* (Yamaguchi *et al.*, 2014). These data suggested that it would be challenging to engineer an EGFR-dependent phenotype by using ALK inhibition in H3122 cells and thus it was concluded that H3122 cells would not be a suitable cell line for studying EGFR mutants.

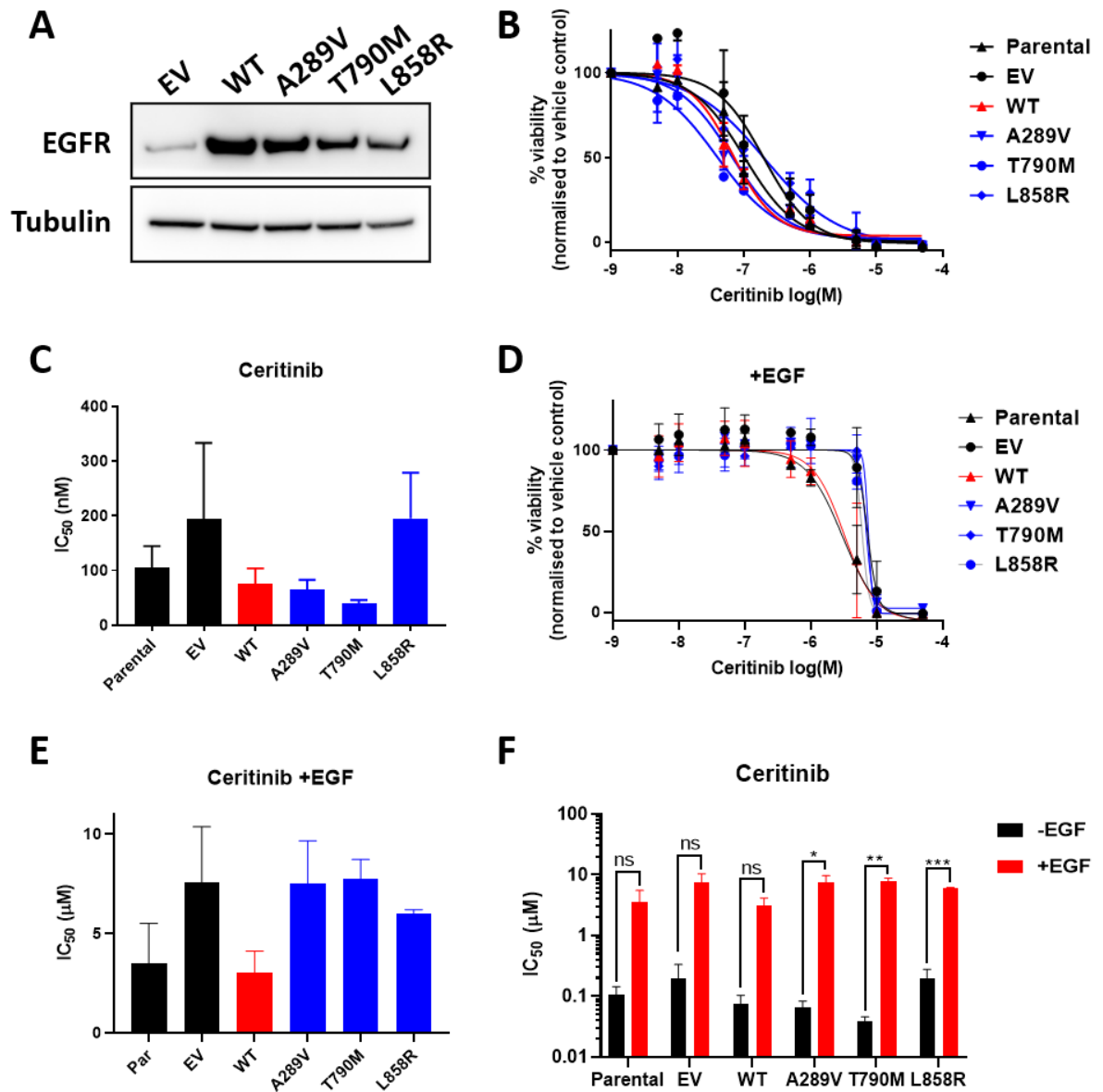


Figure 3.6 – H3122 cells assessed as a model for studying EGFR mutations. (A) Western blot analysis confirmed expression of EGFR mutations in H3122 cells. $n = 1$ biological replicate. EV = empty vector, WT = wild type. (B) Dose-response curves for H3122 cell lines upon treatment with ceritinib. Cell viability is normalised to vehicle control (DMSO). (C) Bar chart showing IC_{50} values for H3122 cells upon treatment with ceritinib calculated from B. Statistical significance was calculated by Tukey's multiple comparisons test. All comparisons were not significant. (D) Dose-response curves for H3122 cell lines upon treatment with ceritinib and 50 ng/ml EGF. Cell viability is normalised to vehicle control (DMSO). (E) Bar chart showing IC_{50} values for H3122 cells upon treatment with ceritinib and 50 ng/ml EGF calculated from D. Statistical significance was calculated by Tukey's multiple comparisons test. All comparisons were not significant. (F) Bar chart showing IC_{50} values for H3122 cells upon treatment with ceritinib with or without 50 ng/ml EGF. Statistical significance for the indicated pairwise comparisons was calculated by t-test. * = $p < 0.05$, ** = $p < 0.01$, *** = $p < 0.001$, ns = not significant. (B, C, D, E, F) Values represent mean \pm standard deviation from $n = 2$ biological replicates.

3.4.3 MCF10A

MCF10A is a non-transformed human mammary epithelial cell line that has previously been used to study EGFR mutants (Bessette *et al.*, 2015) and was therefore assessed as a model to study this panel of EGFR mutants (Table 3.1). The same pilot set of EGFR mutants tested in H3122 cells were also expressed in MCF10A cells (Figure 3.7 A). A dose-response experiment revealed that MCF10A cells expressing T790M were the least sensitive to gefitinib ($IC_{50} = 18.22 \mu M$), MCF10A cells expressing L858R were the most sensitive to gefitinib ($IC_{50} = 56 \text{ nM}$). MCF10A cells expressing A289V or WT-EGFR showed similar gefitinib sensitivity to one another ($IC_{50} = 552 \text{ nM}$ and 664 nM respectively) that was intermediate compared to MCF10A cells expressing either T790M or L858R. This concurs with previous observations that T790M confers resistance to gefitinib (Kosaka *et al.*, 2006), that L858R is highly sensitive to gefitinib (Tracy *et al.*, 2004), and that A289V exhibits a partial sensitivity to gefitinib (Kohsaka *et al.*, 2017). Statistical analysis found that MCF10A cells expressing L858R, A289V, or WT-EGFR have 325-, 33-, and 27-fold lower IC_{50} value respectively compared to T790M but did not find a significant difference in IC_{50} between MCF10A cells expressing L858R, A289V, or WT-EGFR (Figure 3.7 C, Figure 3.7 D). The fact that there was no significant difference detected between the IC_{50} values for L858R and both WT-EGFR and A289V upon gefitinib treatment, despite the dose-response curve indicating that L858R is more sensitive to gefitinib compared to WT-EGFR and A289V, suggests that analysis of IC_{50} values may not be most appropriate approach for assessing the sensitivity of different EGFR mutants to the same inhibitor. Rather, analysis of the full dose-response curve, as opposed to the single data point derived from IC_{50} calculations, may provide a more refined assessment of the efficacy of an inhibitor against different EGFR mutants. The agreement of these results with published data suggests that MCF10A cells may be a useful model for studying different EGFR mutations (Lynch *et al.*, 2004; Tracy *et al.*, 2004; Kosaka *et al.*, 2006; Kohsaka *et al.*, 2017). To further test the MCF10A model system, the cells were treated with the third-generation EGFRi osimertinib (Figure 3.7 E). These data showed that T790M was more sensitive to osimertinib compared with gefitinib ($IC_{50} = 318 \text{ nM}$ vs 18.22

μM respectively), and that L858R was more sensitive compared to WT-EGFR and the other EGFR mutations (Figure 3.7 F). Both of these observations are consistent with published data from studies utilising exogenous expression of T790M and L858R in Ba/F3 cells and are consistent with published data demonstrating that osimertinib is able to overcome T790M-mediated resistance, further demonstrating that MCF10A cells could be an appropriate model for investigating the small molecule inhibitor sensitivities in distinct EGFR mutants (Cross *et al.*, 2014; Kohsaka *et al.*, 2017).

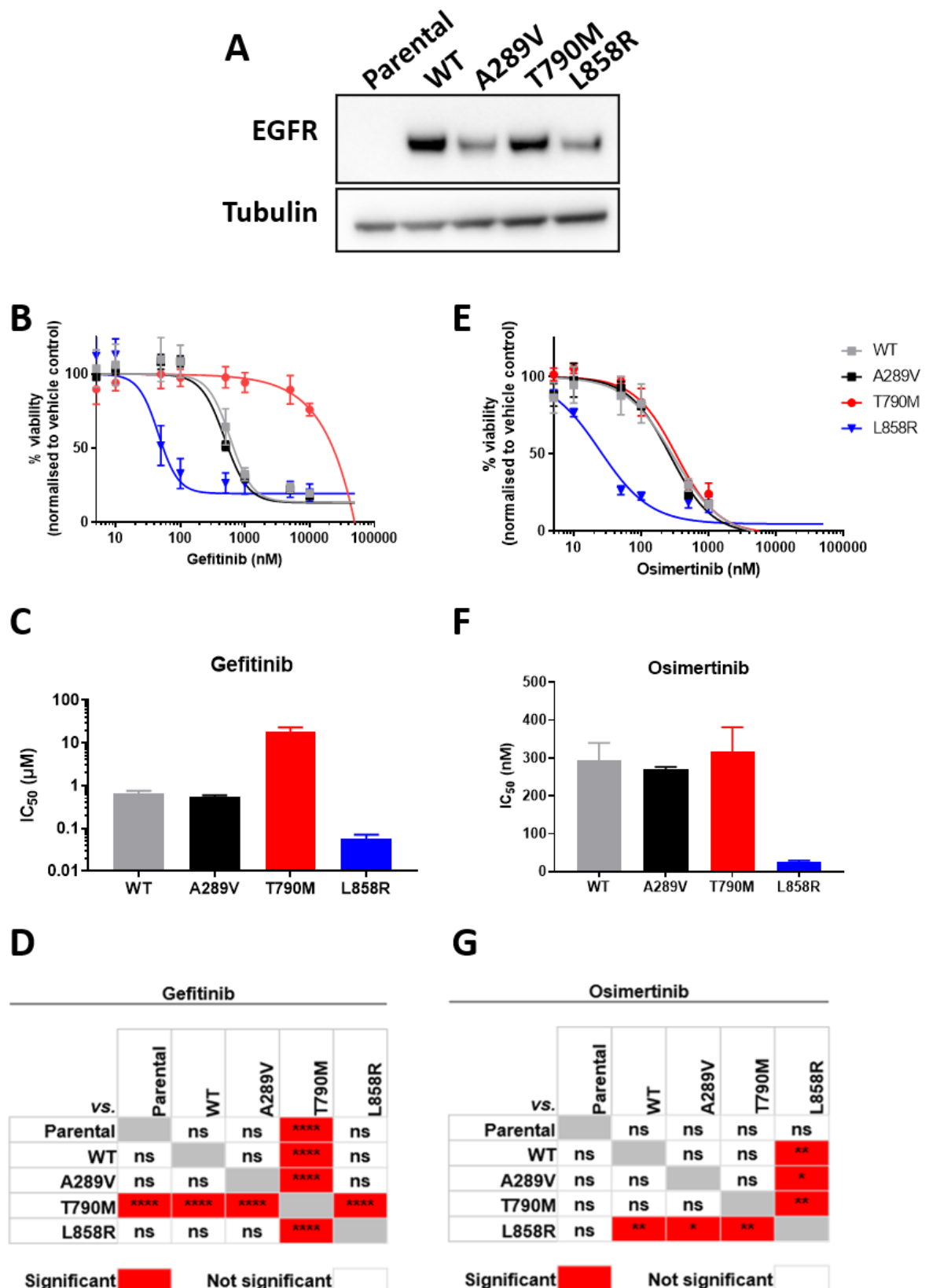


Figure 3.7 - MCF10A cells assessed as a model for studying EGFR mutations. (A) Western blot analysis confirmed expression of EGFR mutations in MCF10A cells. $n = 1$ biological replicate. EV = empty vector, WT = wild type. (B) Dose-response curves for MCF10A cell lines upon treatment with gefitinib. Cell viability is normalised to vehicle control

(DMSO). $n = 3$ biological replicates. (C) Bar chart showing IC_{50} values for MCF10A cells upon treatment with gefitinib calculated from B. $n = 3$ biological replicates. (D) Statistical significance for the indicated pairwise comparisons of IC_{50} values was calculated by 2-way ANOVA followed by Tukey's multiple comparisons test. **** = $p < 0.0001$, ns = not significant. (E) Dose-response curves for MCF10A cell lines upon treatment with osimertinib. Cell viability is normalised to vehicle control (DMSO). $n = 2$ biological replicates. (F) Bar chart showing IC_{50} values for MCF10A cells upon treatment with osimertinib calculated from E. $n = 2$ biological replicates. (G) Statistical significance for the indicated pairwise comparisons of IC_{50} values was calculated by 2-way ANOVA followed by Tukey's multiple comparisons test. * = $p < 0.05$, ** = $p < 0.01$, ns = not significant. (B, C, E, F) Values represent mean \pm standard deviation.

3.4.4 Ba/F3

Ba/F3 is an IL-3 dependent murine pro-B cell line. It has been widely used to study oncogenes, including *EGFR*, *HER2* and *ALK*, as the expression of an oncogene can result in IL-3 independent growth that renders the Ba/F3 cells dependent on the oncogene for cell growth (Kobayashi *et al.*, 2015; Koga *et al.*, 2018; Yoda *et al.*, 2018). These cells have been used to assess the sensitivity of oncogenic mutations in exon 18 of *EGFR* to different EGFRi (Kobayashi *et al.*, 2015). To establish whether Ba/F3 cells could be used to study EGFR mutants in this study, the pilot set of EGFR mutants that was used to assess H3122 cells and MCF10A cells was similarly expressed in Ba/F3 cells along with WT-EGFR and EV controls (Figure 3.8 A).

The ability of the *EGFR* mutant constructs to confer IL-3 independent growth in the Ba/F3 cells was assessed by removing IL-3 from the growth media and tracking their viability over 2 weeks using Cell Titre Glo (Figure 3.8 B). The cell viability of EV cells grown in the presence of 5 ng/ml IL-3 and WT-EGFR cells grown in the presence of 50 ng/ml EGF increased rapidly until day 4, after which cell viability decreased. By contrast, EV cells without IL-3 and WT-EGFR cells without EGF did show any increase in cell viability. Cell viability increased for Ba/F3 cells expressing T790M and L858R following IL-3 withdrawal, although slower compared to EV +IL-3 and WT-EGFR +EGF, with T790M and L858R reaching a peak in cell viability at day 6 compared to day 4 for EV +IL-3 and WT-EGFR +EGF (Figure 3.8 C). Cell viability also increased for Ba/F3 cells expressing A289V following IL-3 withdrawal, although slower than T790M and L858R, with cell viability still increasing at day 13

(Figure 3.8 C). These data demonstrate that expression of the 3 EGFR mutants was able to confer IL-3 independent growth in Ba/F3 cells, whereas expression of WT-EGFR is not. This suggests that growth of Ba/F3 cells in IL-3 independent conditions is dependent on mutant EGFR signalling.

To confirm that growth of Ba/F3 cells expressing mutant EGFR in IL-3 independent conditions was dependent on EGFR signalling, Ba/F3 cells expressing A289V, T790M, or L858R were tested for their sensitivity to gefitinib (Figure 3.8 D). Dose-response experiments showed that Ba/F3 cells expressing T790M were the least sensitive to gefitinib ($IC_{50} = 8.8 \mu\text{M}$), cells expressing L858R were the most sensitive to gefitinib ($IC_{50} = 12 \text{ nM}$), and cells expressing A289V have an intermediate sensitivity to gefitinib compared to Ba/F3 cells expressing either T790M or L858R ($IC_{50} = 454 \text{ nM}$). Statistical analysis found that Ba/F3 cells expressing L858R and A289V have a 733- and 20-fold lower IC_{50} value compared to T790M respectively but did not find a significant difference in IC_{50} between Ba/F3 cells expressing A289V or L858R (Figure 3.8 E). These data indicate that the IL-3 independent growth of Ba/F3 cells expressing these EGFR mutants is dependent on EGFR signalling. Furthermore, the sensitivities observed in these experiments are consistent with data from the MCF10A cells described in Figure 3.7 as well as previously published data from preclinical *in vitro* experiments (Tracy *et al.*, 2004; Kohsaka *et al.*, 2017) and clinical studies (Lynch *et al.*, 2004; Kosaka *et al.*, 2006). Taken together, these data indicate that Ba/F3 cells will be a suitable model to investigate the most effective inhibitor for distinct EGFR mutants.

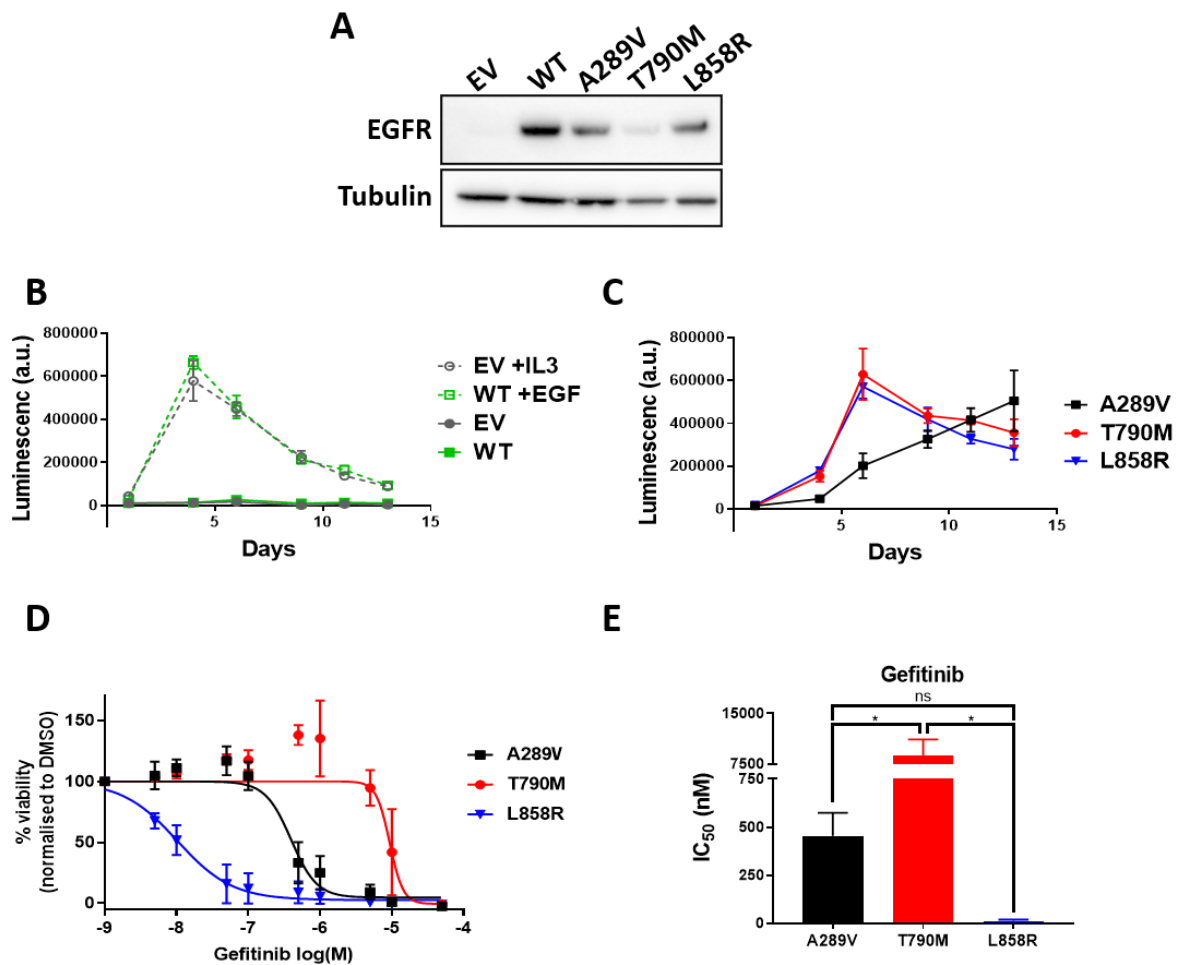


Figure 3.8 – Ba/F3 cells assessed as a model for studying EGFR mutations. (A) Western blot analysis confirmed expression of EGFR mutations in Ba/F3 cells. $n = 1$ replicate. EV = empty vector, WT = wild type. (B) Cell viability of Ba/F3 cells expressing WT-EGFR or EV following removal of IL-3 from the growth media. $n = 3$ biological replicates. (C) Cell viability of Ba/F3 cells expressing A289V, T790M, or L858R following removal of IL-3 from the growth media. $n = 3$ biological replicates. (D) Dose-response curves for Ba/F3 cell lines upon treatment with gefitinib. Cell viability is normalised to vehicle control (DMSO). $n = 2$ biological replicates. (E) Bar chart showing IC₅₀ values for Ba/F3 cells upon treatment with gefitinib calculated from C. Statistical significance was calculated by Tukey's multiple comparisons test comparing T790M with A289V and L858R. * = $p < 0.05$, ns = not significant. $n = 2$ biological replicates. (B, C, D) Values represent mean \pm standard deviation.

3.5 Generation of a Ba/F3 panel expressing EGFR mutations

These results show that of the 4 cell line models evaluated, MCF10A and Ba/F3 recapitulate known gefitinib sensitivities of certain EGFR mutants and may therefore be appropriate models for investigating the most effective inhibitors for distinct EGFR mutants. As MCF10A media requires the addition of EGF, which could be a

confounding factor as the response of different EGFR mutants to EGF is unknown, Ba/F3 cells were selected as the model system of choice for my thesis. A pipeline was therefore designed to generate an expanded panel of Ba/F3 cells expressing different EGFR mutants (Figure 3.9). As overexpression of WT-EGFR is itself known to be oncogenic (Carraway and Sweeney, 2002), it was important that EGFR mutants have comparable expression levels to ensure that phenotypic and signalling differences observed are due to the specific mutant under study and not due to differences in receptor expression levels. To ensure that the different EGFR mutants were expressed to the same level, each EGFR mutant was stably transduced in Ba/F3 cells using 3 different viral titres. After infection, cells were selected for 14 days using 1 mg/ml hygromycin. At this point, lysates were generated and EGFR expression assessed by western blot. For each mutant, 1 cell line was selected from the 3 cell lines produced using different viral titres on the basis of comparable EGFR expression between the different EGFR mutants. These cell lines were then assessed for their ability to grow in IL-3 independent conditions. After 2 weeks of IL-3 independent growth, cell lines were considered stable and EGFR expression levels confirmed again by western blot.

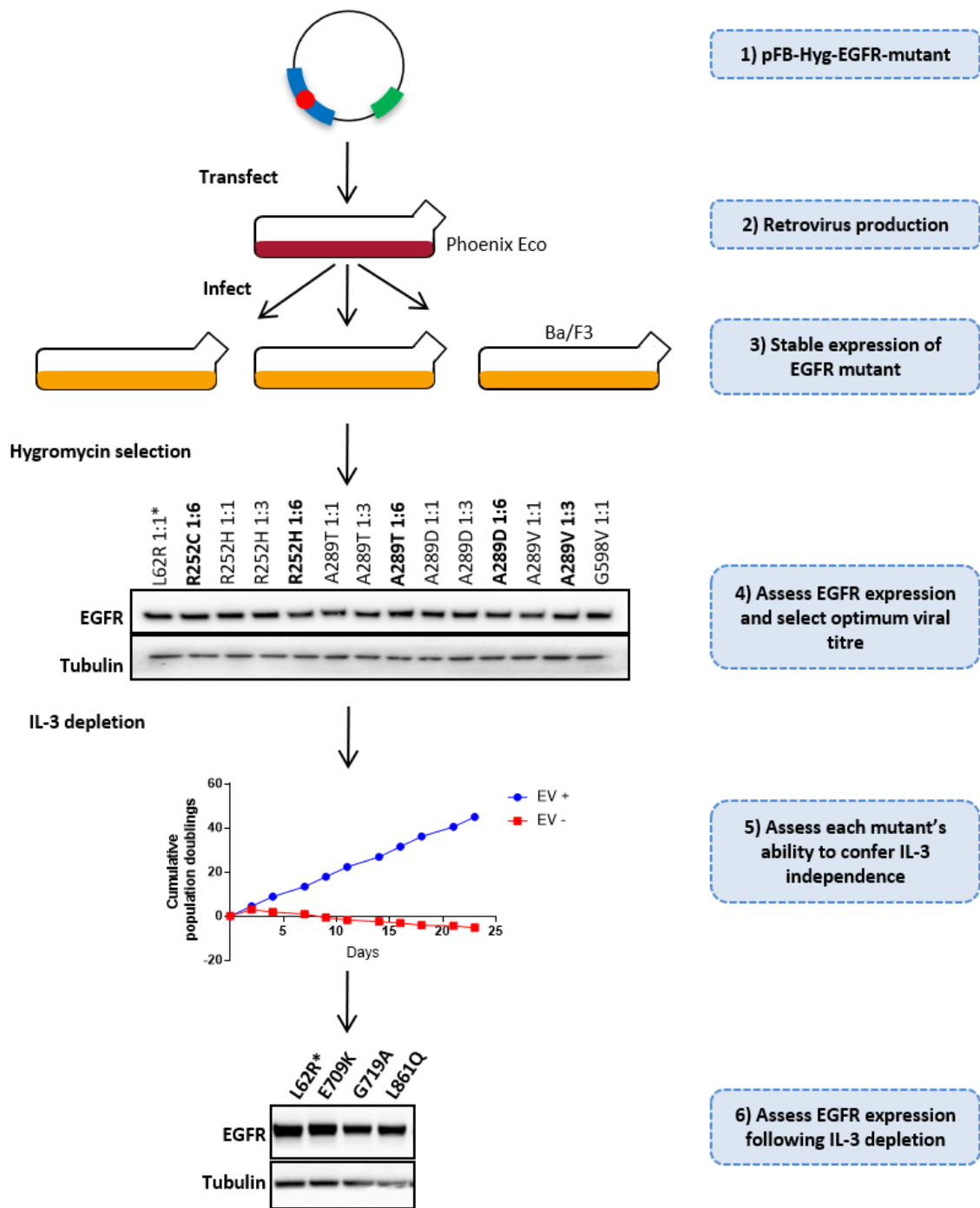


Figure 3.9 – Workflow for generating an expanded panel of mutant EGFR- expressing Ba/F3 cells. 1, 2) Expression constructs for the different EGFR mutants are packaged into retroviruses by transfection into Phoenix Eco cells. 3) Retrovirus is harvested from Phoenix Eco cells and three different viral titres are used to infect Ba/F3 cells to ensure equal expression of EGFR. 4) Following hygromycin selection, EGFR expression is assessed by western blot. For each mutant, 1 cell line was selected for IL-3 depletion from the 3 cell lines produced using different viral titres on the basis of comparable EGFR expression between the different EGFR mutants (selected cell lines are highlighted in bold). 5) The ability of each EGFR mutant to confer IL-3 independent growth is assessed. 6) After 2 weeks of IL-3 independent growth, cells were considered stable, and EGFR expression is confirmed again by western blot.

An expanded panel of 19 *EGFR* mutants was expressed in Ba/F3 cells using 3 viral titres (mutants are listed in Table 3.1. E709K, L861Q, dup767, dup768, and dup771 were not included at this stage). Western blot analysis revealed that there was negligible difference in the *EGFR* expression levels between cell lines generated with different viral titres (Figure 3.10). Therefore, the lowest viral titre was selected from each mutant to be taken forward for IL-3 depletion, as these cell lines will likely have had the fewest genomic integration events and therefore the lowest likelihood of unknown genetic changes. Although del746, 747_751del (del747), L858R, and L861R showed lower *EGFR* expression compared to the rest of the *EGFR* mutants (Figure 3.10), the cell lines transduced using different viral titres used for each of these mutants showed negligible variation in *EGFR* expression compared with one another and so the cell line transduced using the lowest viral titre was taken forward for IL-3 deprivation.

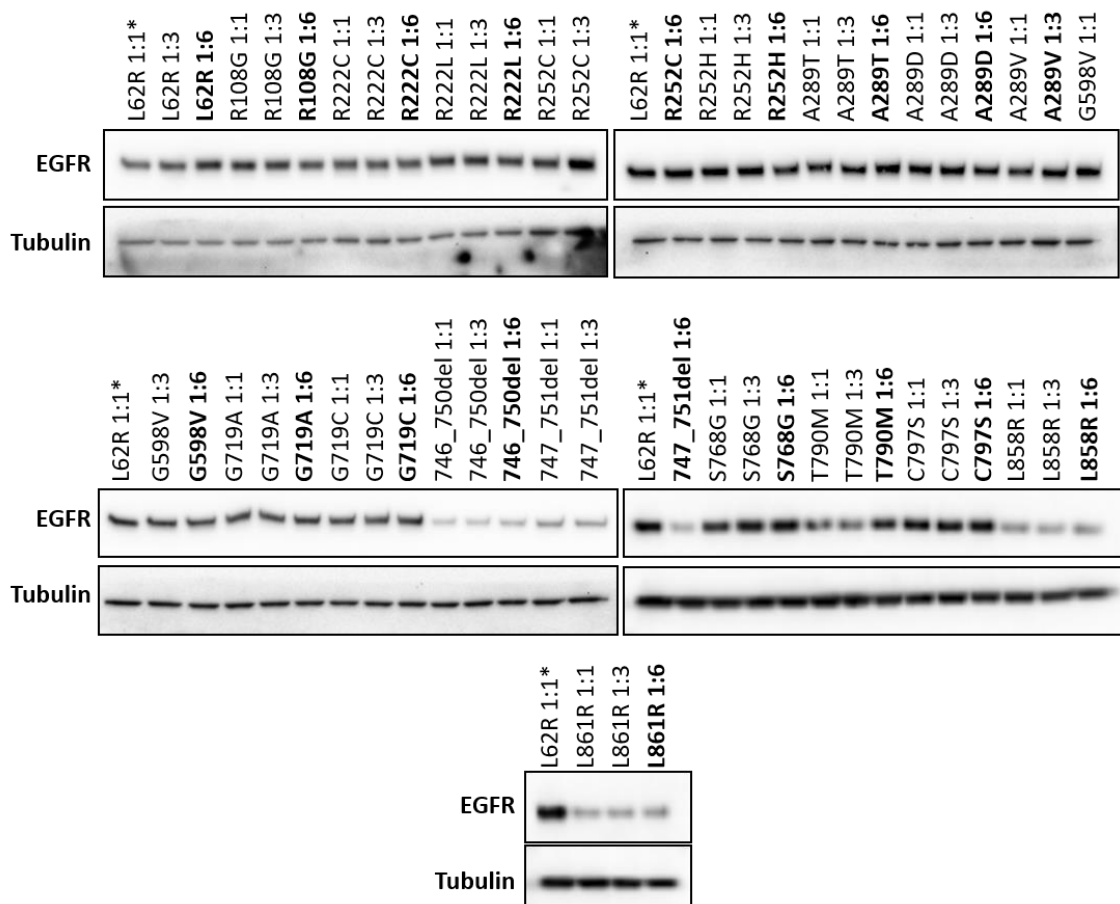


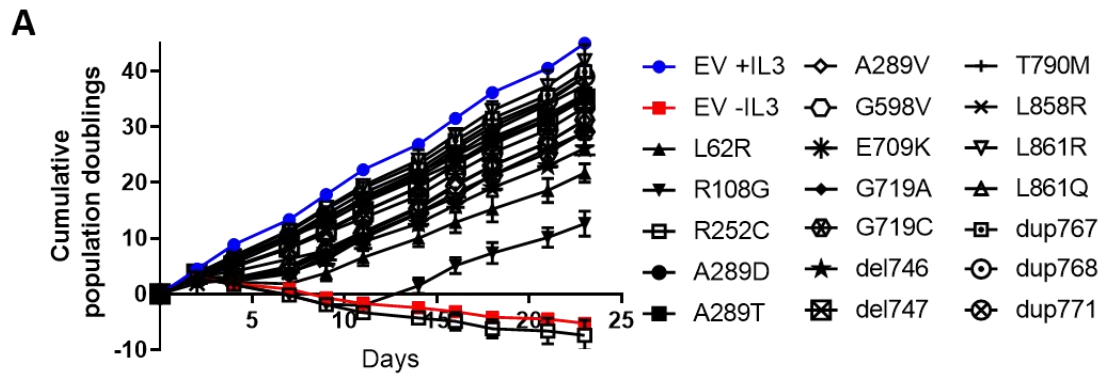
Figure 3.10 – Optimisation of *EGFR* expression levels in Ba/F3 cells prior to IL-3 depletion. Three different viral titres were utilised in order to ensure comparable expression of *EGFR* mutants. Virus was diluted in RPMI at ratios of 1:1, 1:3, and

1:6 prior to use in infection. Cell lysates were analysed by western blot to compare EGFR expression levels between the different viral titres. L62R 1:1 was used as a reference on all gels and is highlighted with an asterisk. Bold text indicates the cell lines that were taken forward for IL-3 deprivation. $n = 1$ biological replicate.

3.6 Growth properties of EGFR-mutant expressing Ba/F3 cells under IL-3 deprivation.

The ability of each mutation to confer IL-3 independent growth in Ba/F3 cells was assessed using a protocol described by Greulich *et al.* (Greulich *et al.*, 2012). This protocol differs from the one used in Figure 3.8 B in that it involves splitting the cells back to their original seeding density at the indicated time points and calculating cumulative population doubling. This prevents cells from saturating the media and cell viability subsequently decreasing, as was observed in Figure 3.8 B. A further 5 EGFR mutants were included at this stage: E709K, L861Q, dup767, dup768, and dup771 (Table 3.1). As different viral titres made negligible difference to EGFR expression (Figure 3.10) only the lowest viral titre was used to transduce these mutants into Ba/F3 cells. Utilising the Greulich *et al.* protocol for measuring growth revealed that 18 of the 24 EGFR mutants were able to confer IL-3 independence (Figure 3.11 A). R252C did not confer IL-3 independence (Figure 3.11 A). For Ba/F3 cells expressing R222C, R222L, R252H, S768G, or C797S, no cells grew following removal of IL-3. Interestingly, R108G took longer to confer IL-3 independence compared with the other EGFR mutants. This indicates that R108G may be less oncogenic compared to the majority of EGFR mutants, although further *in vivo* experiments will be required to confirm this. After 2 weeks of IL-3 independent growth, cells were considered stable. Western blot analysis confirmed comparable levels of EGFR expression (Figure 3.11 C), including del746, del747, L858R, and L861R, which had previously shown lower levels of EGFR expression compared to other EGFR mutants (Figure 3.10). This suggests that IL-3 deprivation resulted in an increase in EGFR expression in these cell lines. To investigate changes in EGFR expression levels following IL-3 deprivation, lysates collected from Ba/F3 cells expressing A289V, T790M, and L858R mutants before and after IL-3 deprivation were compared by western blot (Figure 3.11 D). This showed a clear increase in

EGFR expression following 2 weeks' IL-3 independent growth in all 3 cell lines, demonstrating that EGFR expression levels increase following IL-3 deprivation.



B

Mutant	Day											
	0	2	4	7	9	11	14	16	18	21	23	
EV +IL3	ns	*	***	****	****	****	****	****	****	****	****	****
L62R	ns	ns	ns	ns	*	**	**	**	**	**	**	**
R108G	ns	ns	ns	ns	ns	ns	ns	ns	**	**	**	**
R252C	ns	ns	ns	ns	ns	ns	ns	ns	ns	ns	ns	ns
A289D	ns	ns	ns	ns	*	**	*	*	*	**	**	**
A289T	ns	ns	**	****	****	****	****	****	****	****	****	****
A289V	ns	ns	ns	*	**	**	**	**	**	**	**	**
G598V	ns	ns	ns	*	**	**	**	**	**	**	**	**
E709K	ns	ns	ns	*	**	**	**	**	**	**	**	**
G719A	ns	ns	**	**	**	**	**	**	**	**	**	**
G719C	ns	ns	ns	ns	*	**	**	**	**	**	**	**
del746	ns	ns	*	***	****	****	****	****	****	****	****	****
del747	ns	ns	**	****	****	****	****	****	****	****	****	****
dup767	ns	ns	*	****	****	****	****	****	****	****	****	****
dup768	ns	ns	*	****	****	****	****	****	****	****	****	****
dup771	ns	ns	*	****	****	****	****	****	****	****	****	****
T790M	ns	ns	*	****	****	****	****	****	****	****	****	****
L858R	ns	ns	*	****	****	****	****	****	****	****	****	****
L861R	ns	ns	*	****	****	****	****	****	****	****	****	****
L861Q	ns	ns	*	**	**	**	**	**	**	**	**	**

Significant ■ Not Significant □

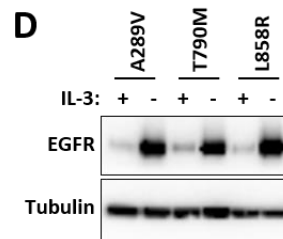
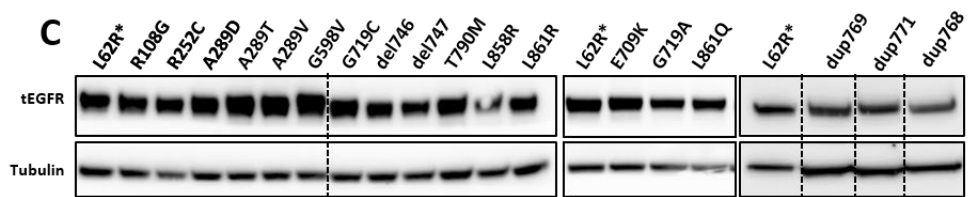


Figure 3.11 – A panel of 18 EGFR mutants confer IL-3 independent growth in Ba/F3 cells. (A) Proliferation of Ba/F3 cell lines expressing different EGFR mutants upon

IL-3 withdrawal. Cell viability was measured by Cell Titre Glo at the indicated times. Values represent mean \pm standard deviation from $n = 3$ biological replicates. EV = empty vector, WT = wild type. (B) Statistical significance was calculated using the Holm-Sidak multiple comparisons test comparing each mutant with EV -IL3 at the indicated time points. * = $p < 0.05$, ** = $p < 0.01$, *** = $p < 0.001$, **** = $p < 0.0001$, ns = not significant. (C) Western blot showing comparable EGFR expression levels in Ba/F3 cell lines following 2 weeks' IL-3 independent growth. L62R was used as a reference on all gels and is highlighted with an asterisk. $n = 1$ biological replicate. (D) Western blot showing EGFR expression in Ba/F3 cells harbouring the indicated EGFR mutants before and after IL-3 deprivation. Lysates collected before IL-3 deprivation are indicated with a "+", lysates collected after IL-3 deprivation are indicated with a "-". $n = 1$ biological replicate.

3.7 Discussion

Large-scale tumour sequencing efforts have led to the identification of many different *EGFR* mutations along the full length of the gene and in multiple cancer types (Cerami et al., 2012; Gao et al., 2013). However, studying the differences between *EGFR* mutations is challenging as there are few cell lines available that harbour endogenous *EGFR* mutants, in particular the less common variants. Furthermore, different cell lines are not isogenic and can have differences in phenotypes, such as growth rate or dependency on EGFR signalling. Such variations make it difficult to deconvolute effects caused by differences in the biology of distinct EGFR mutants and effects caused by the genetic and epigenetic diversity between cell lines. To address these challenges, researchers have utilised exogenous expression of *EGFR* mutations in model cell lines to study different EGFR mutants (Pines et al., 2010; Bessette et al., 2015; Kobayashi et al., 2015). Recently, innovative techniques employing TALEN (Hasako et al., 2018) or CRISPR-Cas9 (Floc'h et al., 2018) technology have been used to introduce mutations into the endogenous *EGFR* allele of human cancer cell lines, which are discussed further in chapter 6. In this chapter, cancer-associated *EGFR* mutants were identified from the online database cBioPortal and expression vectors for these mutants were generated by SDM (Cerami et al., 2012; Gao et al., 2013). Next, a series of experiments identified Ba/F3 cells as the optimal model system with which

to study these *EGFR* mutants. Finally, an expanded panel of *EGFR* mutants were stably expressed in Ba/F3 cells for further characterisation.

First, NIH-3T3 cells were examined as a model system to study *EGFR* mutants. NIH-3T3 cells have previously been used to study the distinct signalling networks observed between different *EGFR* mutants (Pines *et al.*, 2010). For this project, it was important to identify a phenotype that was dependent on *EGFR*, as this would enable the determination of the optimal inhibitors for different *EGFR* mutants. However, a series of pilot experiments presented in this chapter were not able to identify a phenotype that was dependent on *EGFR* in NIH-3T3 cells. Addition of EGF to the media was assessed in an attempt to drive *EGFR* activation in *EGFR*-mutant expressing cells that may lead to an *EGFR* dependent phenotype. Although addition of EGF did not lead to gefitinib sensitivities consistent with published data, it did lead to significantly increased gefitinib sensitivity in WT-*EGFR* expressing NIH-3T3 cells compared with EV cells. Indeed, under EGF supplemented conditions WT-*EGFR* expressing NIH-3T3 cells were similarly sensitive to gefitinib compared to NIH-3T3 cells expressing L858R (IC_{50} values = 5.01 μ M and 4.48 μ M for WT-*EGFR* and L858R respectively). A possible explanation for this is the comparable levels of *EGFR* phosphorylation observed between NIH-3T3 cells expressing WT-*EGFR* and L858R following EGF stimulation (Greulich *et al.*, 2005). Although L858R has higher levels of *EGFR* phosphorylation in the absence of EGF stimulation, following EGF stimulation both WT-*EGFR* and L858R have similar levels of *EGFR* phosphorylation. Similarly, Greulich *et al.* showed that WT-*EGFR* expressing NIH-3T3 cells grown in the presence of EGF were more sensitive to gefitinib treatment compared to NIH-3T3 cells expressing an Ex20Ins mutant that is known to be resistant to gefitinib treatment. Together, these data indicate that when grown in the presence of EGF, NIH-3T3 cells expressing WT-*EGFR* do show some sensitivity to gefitinib. This may explain the significantly increased gefitinib sensitivity of WT-*EGFR* expressing NIH-3T3 cells compared to EV cells which express no *EGFR*. Previous studies have shown that NIH-3T3 cells expressing *EGFR* mutants are able to grow in anchorage independent conditions in soft agar assays and form tumours in mice (Lee *et al.*, 2006). Soft agar assays are not sufficiently high-throughput for the experiments proposed in this thesis (Figure 3.1) and so spheroid growth assays were investigated as a more high-throughput method of assessing non-adherent

growth. However, the NIH-3T3 cells expressing EGFR mutants used in this thesis did not grow as spheroids. Additionally, previous studies have shown that expression of mutant *EGFR* in NIH-3T3 cells increases cell proliferation (Pines *et al.*, 2010). This effect was not observed in the data presented in this chapter. A possible explanation for this is differences in the overall levels of EGFR expression. High levels of EGFR expression are known to be oncogenic (Carraway and Sweeney, 2002), and so it is possible that NIH-3T3 cells used in this chapter had lower levels of EGFR expression compared to previous studies (Pines *et al.*, 2010). It should also be noted that the EGFR mutants studied by Pines *et al.* were not included in this chapter (EGFR-vIII and EGFR-vIV), and so it is possible that the increased proliferation of NIH-3T3 cells following expression of mutant EGFR is specific to these mutants and similar increases in proliferation are not observed with the mutants included in this chapter. Another possible approach to increase EGFR dependence in this model system would be to serum starve the cells overnight and then stimulate them with EGF in serum-free media. This approach would stop all other cell signalling and leave only the EGFR pathway active. Any phenotype observed under these conditions would necessarily be EGFR-dependent. However, this approach could also confound results as serum starvation leads to cell cycle arrest (Cruz *et al.*, 2019). Furthermore, high-concentration EGF stimulation without any other cell signalling present differs significantly to the clinical scenario and may obscure observations driven by factors such as ligand-independent activation of EGFR.

A reduced set of EGFR mutants were then used to assess the H3122, MCF10A, and Ba/F3 cell lines for their ability to display an EGFR-dependant phenotype. H3122 cells are human NSCLC cells that harbour an EML4-ALK fusion. Given that roughly half of the EGFR mutations included in this study (Table 3.1) are most commonly reported in NSCLC, H3122 cells were a potentially ideal model system as they would more closely replicate the clinical scenario compared with NIH-3T3 cells, which are murine fibroblasts. As WT-EGFR overexpression has been reported as a resistance mechanism to ALKi in H3122 cells (Yamaguchi *et al.*, 2014), it was hypothesised that expression of mutant EGFR in H3122 cells would similarly confer resistance to ALKi. This ALKi resistance would be EGFR-dependent, which could then be leveraged to study differences in kinase inhibitor sensitivity between EGFR

mutants. However, expression of WT- and mutant *EGFR* constructs in H3122 cells did not confer ALKi resistance. This differs to published data which has found overexpression of WT-EGFR to be a mechanism of resistance to ALKi (Yamaguchi *et al.*, 2014). Yamaguchi *et al.* identified overexpression of EGFR as an ALKi resistance mechanism in H3122 cells that had been chronically exposed to escalating doses of the ALKi crizotinib up to 1 μ M over the course of 12 weeks after which clonal populations were derived under 1 μ M crizotinib treatment over the course of a further 10 weeks. By contrast, in this study EGFR was stably transduced by retroviral infection. The long period of selection used by Yamaguchi *et al.* may have allowed cells to adapt to altered signalling pathways that would enable EGFR overexpression to compensate for loss of ALK signalling and thereby confer resistance to ALKi, whereas this opportunity for adaptation is lacking when EGFR is ectopically transduced. MCF10A cells expressing EGFR mutants displayed gefitinib sensitivities that were consistent with previously published data using cell lines such as Cos-7, Ba/F3, and H3225 (Tracy *et al.*, 2004; Kobayashi *et al.*, 2005; Kohsaka *et al.*, 2017). This promising data was followed by results that showed that T790M was more sensitive to osimertinib compared with gefitinib, and that L858R was more sensitive to osimertinib compared with T790M. Both of these observations are consistent with published data from studies utilising exogenous expression of EGFR mutants in Ba/F3 cells (Kohsaka *et al.*, 2017). These results demonstrating that EGFR mutants expressed in MCF10A cells recapitulate published preclinical and clinical data indicate that MCF10A cells display dependency on exogenously expressed EGFR and therefore could be a good model for studying EGFR mutants. Similar consistency with previously published data was observed with Ba/F3 cells expressing EGFR mutants. As MCF10A media is supplemented with EGF, and the effect of EGF on different EGFR mutants is unknown, Ba/F3 cells were chosen as the model system used for this project and 24 EGFR mutants were subsequently transduced in Ba/F3 cells.

Included in this panel were the first- and third-generation EGFRi resistance-mutations T790M and C797S. These mutations were included as single mutations without an additional oncogenic activating EGFR mutations. This differs from what is observed in the clinic, where T790M and C797S are always identified as secondary mutations following disease progression on first- or third-generation

EGFRi therapy in patients whose tumours harbour primary activating mutations in EGFR, such as L858R or Ex19Del. T790M and C797S were included in the panel of mutants studied in this thesis without additional activating mutations as controls to provide information on how an inhibitor may be binding to EGFR. T790M prevents reversible inhibitors, such as gefitinib and erlotinib, from binding to EGFR by both steric hindrance and increasing the affinity of the receptor for ATP (Yun *et al.*, 2008). C797S prevents inhibitors that irreversibly bind to EGFR by covalent modification of C797 from inhibiting EGFR (Paasche *et al.*, 2010; Capoferri *et al.*, 2015). Including T790M and C797S in the panel of EGFR mutations would therefore provide information on whether an inhibitor is binding to EGFR via reversible ATP competition or by irreversible covalent modification. T790M and C797S were included as single mutations as this removes any confounding effect that the presence of primary activating mutations may have on inhibitor sensitivity. Although no differences have been observed between Ex19Del+T790M and L858R+T790M or Ex19Del+C797S and L858R+C797S in terms of EGFRi sensitivity, differences in osimertinib sensitivity have been observed between L858R+G724S and Ex19Del+G724S (Oztan *et al.*, 2017; Peled *et al.*, 2017; Fassunke *et al.*, 2018; Brown *et al.*, 2019b). This raises the possibility that the presence of a primary mutation could influence whether T790M or C797S confers resistance to a particular inhibitor. Including these mutations as single mutations removes this possibility and provides a clear indication of the binding mode of an inhibitor. However, including these mutations as single mutations prevents conclusions being made about the effect that T790M or C797S would have on inhibitor sensitivity in the context of a specific primary activating mutation. This would therefore need to be assessed on a case-by-case basis by generating a cell line expressing T790M or C797S in addition to each individual activating mutation of interest.

18 out of the 24 EGFR mutants were shown to confer IL-3 independent growth in Ba/F3 cells. Interestingly, there was a delay before R108G was able to confer IL-3 independent growth compared to the other EGFR mutants. These data are consistent with previous observations regarding point mutations at R108. Lee *et al.* showed that NIH-3T3 cells expressing R108K mutant EGFR formed fewer colonies in an anchorage independent growth experiment compared to NIH-3T3 cells expressing A289V mutant EGFR (Lee *et al.*, 2006). They also found that R108K

expressing NIH-3T3 cells formed smaller tumours in mice compared to NIH-3T3 cells expressing A289V. Together these data suggest that R108X mutants are less oncogenic compared to A289V. However, as discussed in chapter 1 the mechanism by which R108X substitutions confer oncogenic activity is unclear: Lee *et al.* report that R108K mutants are phosphorylated in the absence of ligand, whereas Bessman *et al.* found that R108K mutants are monomeric in the absence of ligand and propose that R108K promotes a ligand-dependent activation of EGFR (Bessman *et al.*, 2014). Furthermore, although the data from Lee *et al.* suggests that R108K is less oncogenic compared to A289V, Bessman *et al.* report R108K to have a 20-fold higher affinity for EGF compared to A289V. To understand the mechanism by which R108X mutations cause oncogenic EGFR activation, future work should focus on understanding the structural consequences of the substitution and the impact this has on the kinase activity of EGFR.

Expression of R222C, R222L, R252C, R252H, S768G, or C797S did not enable growth of Ba/F3 cells in the absence of IL-3 (described in section 3.6), indicating that these mutants may not confer oncogenic activity to EGFR. In the case of C797S, this may be due to the fact that this substitution is a resistance-causing mutation, rather than an oncogenic driver mutation. The mechanism by which C797S confers resistance to EGFRi differs to that of T790M, which did confer IL-3 independent growth in Ba/F3 cells despite also being a resistance-causing mutation rather than an oncogenic driver. T790M confers resistance to first-generation EGFRi, which bind reversibly to EGFR through competition with ATP, by increasing the affinity of the receptor for ATP (Yun *et al.*, 2008). This increase in ATP affinity is consistent with observations that cells expressing T790M alone have higher basal EGFR phosphorylation compared to cells expressing WT-EGFR (Godin-Heymann *et al.*, 2007). Together, these data indicate that T790M may increase the kinase activity of EGFR compared to WT-EGFR and may account for the ability of cells expressing T790M alone to confer IL-3 independent growth to Ba/F3 cells in this chapter. C797S confers resistance to EGFRi through a different mechanism compared to T790M. Substitution of the nucleophilic cysteine residue (C797) for a less nucleophilic serine residue (C797S) prevents EGFRi from binding covalently to EGFR (Paasche *et al.*, 2010; Capoferri *et al.*, 2015). This mechanism of action has no impact on the kinase activity of EGFR and may explain why cells expressing

C797S alone were not able to confer IL-3 independence to Ba/F3 cells in this chapter. Although S768I has been shown to confer IL-3 independent growth to Ba/F3 cells (Banno *et al.*, 2016), S768G has not. Furthermore, S768I occurs more frequently in patients compared to S768G. Taken together, these data indicate that S768G may be a passenger mutation and not confer oncogenic activity to EGFR. Similarly, R222C, R222L, R252C, and R252H, which also did not confer IL-3 independent growth to Ba/F3 cells, are all identified in patients at low frequencies (Figure 3.2) and may therefore be passenger mutations. This highlights that not all recurrent mutations detected in tumours are oncogenic drivers (Merid *et al.*, 2014). In contrast with findings described in section 3.6, a recent study has shown that Ba/F3 cells expressing R222C were able to grow in IL-3 independent conditions and form tumours in mice (Kim *et al.*, 2020). As discussed earlier, a possible explanation for this discrepancy between this published data and findings described in section 3.6 is the overall expression levels of R222C in the cells. High levels of EGFR expression have been shown to be oncogenic (Carraway and Sweeney, 2002), and so it is possible that expression levels of R222C were higher in the Ba/F3 cells used by Kim *et al.* compared to those used in this thesis, which would explain the differences observed in IL-3 independent growth.

Taken together, data presented in this chapter describe the pan-cancer identification of cancer-associated *EGFR* mutants and the generation of a model system with which to study these mutants (Figure 3.1). A panel of 18 Ba/F3 cell lines expressing different EGFR mutants at comparable levels. As discussed in chapter 1, durable response to anti-EGFR therapy remains elusive for many patients whose tumours harbour less common EGFR mutants. A panel of isogenic cell lines expressing different EGFR mutants, such as the panel described here, could be used to profile the sensitivity of EGFR mutants against a library of EGFRi and other small molecule inhibitors to identify the most efficacious inhibitor for distinct EGFR mutants, potentially identifying novel treatment strategies for patients whose tumours harbour EGFR mutants. Furthermore, this panel of mutant EGFR expressing cell lines could also be used to investigate the possibility of exploiting downstream signalling dependencies of distinct EGFR mutants. It has previously been shown that different EGFR mutants activate distinct downstream signalling networks (Moscatello *et al.*, 1998; Li *et al.*, 2004; Huang *et al.*, 2007). Exploiting the dependency of distinct

EGFR mutants on differentially activated downstream signalling networks could be an effective treatment strategy against EGFR mutants that do not respond well to currently available EGFRi. The establishment of a panel of EGFR-expressing Ba/F3 cells described in this chapter will facilitate studies of the sensitivities of these mutants to different kinase inhibitors, which is described in the next chapter.

Chapter 4

Intracellular mutations of EGFR are sensitive to a subset of broad-spectrum kinase inhibitors

4.1 Introduction

The studies discussed in chapter 1 describe how different EGFR mutants have distinct responses to specific EGFRi. Given that there are many EGFRi either currently approved or in development, identifying the most efficacious EGFRi for distinct EGFR mutants could improve the therapeutic options available to patients with less well-characterised mutants. This approach has led to the identification of afatinib as an effective EGFRi for the treatment of patients whose tumours harboured S768I, G719X, or L861Q mutations, greatly improving the therapeutic outlook for these patients who showed poor response to other EGFRi available at the time (OS = 19.4 months for afatinib vs 12 months for gefitinib) (Watanabe *et al.*, 2014; Yang *et al.*, 2015a). The use of afatinib in this patient group was identified by preclinical studies utilising Ba/F3 cells to assess the sensitivity of these mutations to a panel of EGFRi, which was supported by post-hoc analysis of 3 clinical trials that found a durable response to afatinib in patients harbouring these mutants (Kobayashi *et al.*, 2015; Yang *et al.*, 2015a). However, for many EGFR mutants there is still no approved EGFRi (Figure 1.8). Therefore, there is a need to understand the response of EGFR mutants to EGFRi that are currently approved or are in development. Previous studies have assessed the sensitivity of EGFR mutants to 5 EGFRi: gefitinib, erlotinib, afatinib, rociletinib, and osimertinib (Kohsaka *et al.*, 2017). However, there are more EGFRi that are clinically available or under development that have not been tested against a large panel of EGFR mutants. Neratinib, for example, has shown clinical efficacy in patients harbouring G719X mutations (Sequist *et al.*, 2010b). Lapatinib also has been shown to more potently inhibit extracellular domain mutants compared with intracellular domain mutants (Vivanco *et al.*, 2012). Neither of these inhibitors has been tested against a large panel of EGFR mutants. Furthermore, there are now several EGFRi capable of targeting Ex20Ins mutants that have not been assessed more broadly against other EGFR mutants. Therefore, I sought to profile the sensitivity of the EGFR mutants represented in my Ba/F3 model against a larger panel of EGFRi than previously reported (Figure 4.1 A).

Additionally, previous studies have found that cells expressing certain EGFR mutants are sensitive to broad-spectrum kinase inhibitors such as dasatinib (Formisano *et al.*, 2015; Duong-Ly *et al.*, 2016) (Figure 4.1 B). However, these studies were restricted to a group of Ex19Del mutants and a limited number of intracellular domain point mutations. Therefore, it is not known if this sensitivity is observed more broadly across the different EGFR mutants observed in cancer, including mutations that occur in the extracellular domain. Previous work has also shown that different EGFR mutants can activate distinct downstream signalling networks (Moscatello *et al.*, 1998; Pines *et al.*, 2010). This raises the possibility that EGFR mutants that respond poorly to EGFRi could be targeted by inhibiting pathways downstream of EGFR that are aberrantly activated in a mutant-specific manner (Figure 4.1 C). In this chapter, a small molecule inhibitor screen is used to address several unanswered questions. First, do the broad-spectrum inhibitors identified in previous studies have activity against other EGFR mutants that were not included in these studies (Formisano *et al.*, 2015; Duong-Ly *et al.*, 2016)? Second, are there additional small molecule inhibitors that have mutant-specific activity against EGFR which have not previously been investigated (Figure 4.1 B)? Third, do certain EGFR mutants have downstream signalling dependencies that can be exploited therapeutically (Figure 4.1 C)?

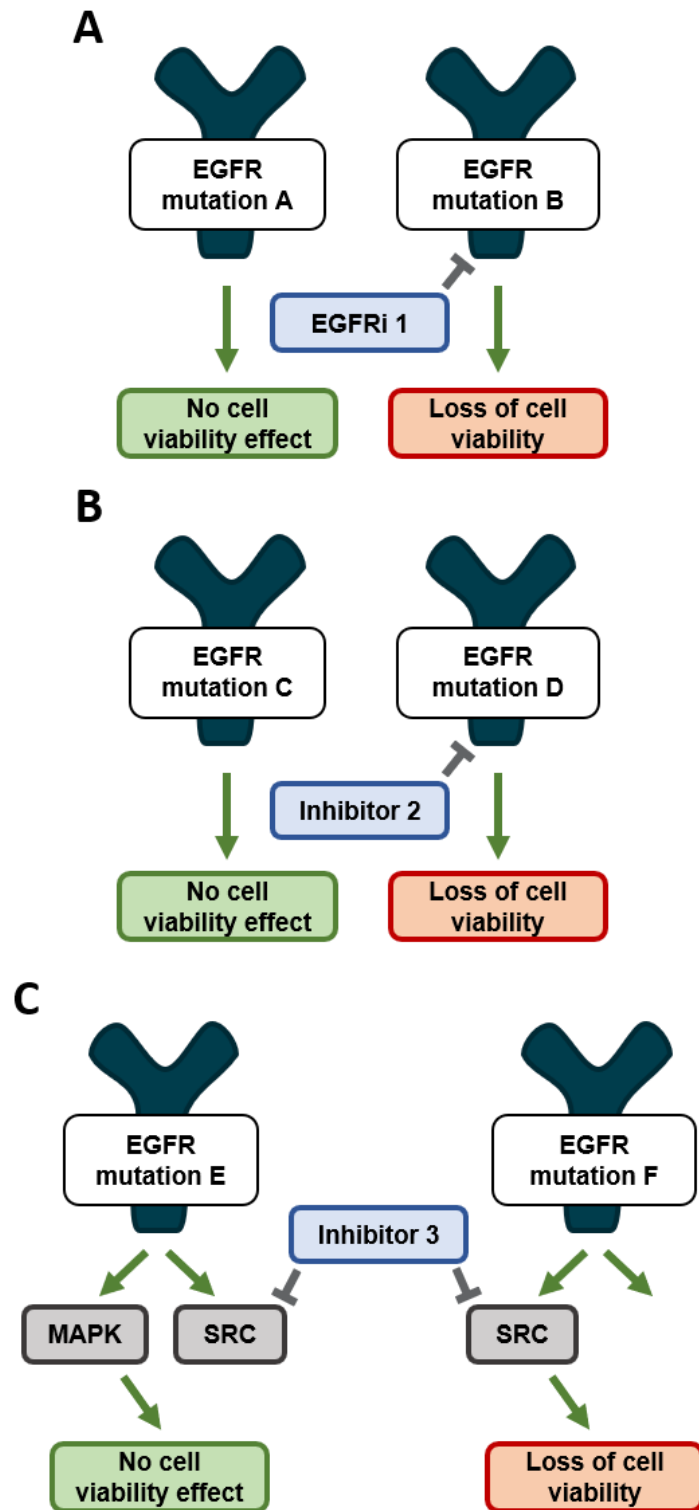


Figure 4.1 – Aims of EGFRi and small molecule inhibitor screen. (A) The EGFRi screen aims to identify EGFRi that are active against EGFR mutants that have not yet been assessed for their sensitivity to all EGFRi. (B,C) The small molecule inhibitor screen has two aims: (B) to identify small molecule inhibitors that are able to inhibit EGFR phosphorylation and elucidate the specific EGFR mutants that these inhibitors are capable of binding to; (C) investigate the possibility that different EGFR mutants activate distinct signalling pathways that can be exploited therapeutically.

4.2 EGFRi and small molecule inhibitor screen set-up

In order to screen all 18 EGFR mutants against the maximum number of compounds in a short time frame, library plates for EGFRi and small molecule inhibitor compounds were established. For the EGFRi library plates, 9 EGFRi (gefitinib, erlotinib, afatinib, neratinib, rociletinib, osimertinib, poziotinib, TAS6417, and lapatinib) were prepared at 6 doses (final concentrations: 10, 50, 100, 250, 500, and 1000 nM). For the small molecule inhibitor library plates, 58 compounds (Table 4.1) were prepared at a final concentration of 500 nM (or 50 nM for luminespib). Inhibitors were selected to target a wide range of major signalling pathways and kinases in order to broadly profile the kinase dependencies of different EGFR mutants in a high-throughput manner. In addition to selective inhibitors, such as osimertinib and ceritinib, broad-spectrum inhibitors, such as pazopanib and ponatinib, were also included. The inclusion of broad-spectrum inhibitors enables the interrogation of multiple signalling pathways, with the intention to identify kinase dependencies by triaging overlapping targets of effective broad-spectrum compounds. The screens were performed in an analogous method to dose-response experiments described in chapter 3: cells were seeded in 96-well plates and treated with the indicated dose of inhibitor for 72 h following which cell viability was measured using Cell Titre Glo. For the EGFRi screen, each experiment was performed in biological triplicate. For the small molecule inhibitor screen, each experiment was performed in biological duplicate with the intention to validate any hits from the screen with full dose-response experiments.

Compound	Target	Major pathway
Gefitinib	EGFR	EGFR
Erlotinib	EGFR	
Neratinib	EGFR and HER2	
Osimertinib	EGFR	
EAI045	EGFR	
Lapatinib	HER2, EGFR	
Vandetanib	Broad spec: VEGFR2/3, EGFR, FGFR1	SRC
Dasatinib	Broad spec: SFKs, BCR-ABL, PDGFR α	
Saracatinib	SRC	
Bosutinib	SRC	Broad spectrum tyrosine kinase inhibitors
Cediranib	Broad spec: VEGFR, Flt1/4, KIT	
Ponatinib	Broad spec: ABL, PDGFR α , FGFR	
Foretinib	Broad spec: HGFR, VEGFR, MET	
Imatinib	Broad spec: BCR-ABL, KIT, PDGFR	
Lenvatinib	Broad spec: VEGFR, FGFR, PDGFR	
Pazopanib	Broad spec: PDGFR α , VEGFR, KIT, FGFR	
Sunitinib	Broad spec: PDGFR α , VEGFR, KIT	
Regorafenib	Broad spec: VEGFR, PDGFR β	
SP600125	Broad spec: JNK, Aurora A	
Sorafenib	Broad spec: VEGFR, PDGFR α , RAF	
Momelotinib	JAK 1, JAK2	
SH-4-54	Pan-STAT	Ras/MAPK pathway
Niclosamide	STAT3	
Dabrafenib	BRAF V600E	PI3K/AKT/mTOR pathways
Binimetinib	MEK1/2	
Trametinib	MEK1/2	
MK2206	AKT	
AZD5363	AKT	IGF1R
BEZ235	PI3K, mTOR	
Rapamycin	mTORC1	
Linsitinib	IGF1R	FGFR
NVP-AEW541	IGF1R, IR	
BGJ398	FGFR	ALK
Crizotinib	ALK, MET, ROS1	
Ceritinib	ALK	
NVP-TAE684	ALK	Trk receptors
Entrectinib	TrkA/B/C, ROS1, ALK	
GW441756	TrkA, c-Raf1, CDK	FAK
TAE226	FAK, PYK2, IR, IGF-1R, FAK	
PF562271	FAK, AKT, CDKs	p38 MAPK signalling
SB203580	p38 MAPK	
Galunisertib	TGF β receptor I	TGF β
Cilengitide trifluoroacetate (Cil. Tri.)	Integrins ($\alpha\beta$ 3 and $\alpha\beta$ 5)	Integrins
Talazoparib	PARP	PARP
Rucaparib	PARP	
LY2603618	CHK1	CHK1
MK-8776	CHK1	
BMS345541	IKK-2, IKK-1	NF- κ B and TBK1 signalling
BX-795	PDK1, TBK1, IKK	
XAV-939	Tankyrase 1/2	Wnt/ β -catenin signalling
Navitoclax	Bcl-xL, Bcl-2, Bcl-w	Bcl2-family proteins
GSK126	EZH2	EZH2 methyltransferase
JQ1	BRD1-4	BET bromodomain family
Silmitasertib	Casein Kinase 2	CK2
Luminespib	Hsp90	Hsp90
Palbociclib	CDK4/6	
Alisertib	Aurora A	Cell cycle regulators
BI 2536	PLK1	

Table 4.1– Inhibitors used in the small molecule inhibitor screen. The major cellular targets of the compounds are indicated. Compounds are grouped based on their targets or related pathways. Broad spec = broad spectrum.

4.3 Assessment of the sensitivity of EGFR mutants to a panel of EGFR inhibitors

The EGFRi screen was performed on 18 EGFR mutants and data from this screen is presented in a series of heatmaps displaying percentage cell viability normalised to vehicle control (DMSO) in Figure 4.2. This viability data was also used to calculate IC₅₀ values (Figure 4.3).

The EGFRi screen showed that the common EGFR mutants (del746, del747, and L858R) are sensitive to lower doses of the first-generation EGFRi gefitinib and erlotinib compared to the gatekeeper mutant T790M (Figure 4.2). This aligns with well-established preclinical and clinical data that Ex19Del and L858R are sensitive to first-generation EGFRi, and that T790M confers resistance to these inhibitors (Lynch *et al.*, 2004; Yu *et al.*, 2013). G719A is less sensitive to both gefitinib and erlotinib (IC₅₀ = 255.95 nM and 254 nM respectively) compared to G719C (IC₅₀ = 24.43 nM and 10.95 nM respectively), confirming previous observations (Figure 4.3 A) (Kohsaka *et al.*, 2017). L62R, R108G, A289D/T/V, G598V, E709K, L861R and L861Q are all ~12 – 15-fold less sensitive to gefitinib and erlotinib compared to the common EGFR mutants, but are more sensitive compared to T790M (Figure 4.3 B). As expected, all 3 Ex20Ins mutants are resistant to gefitinib and erlotinib with IC₅₀ values of >1 µM upon treatment with either inhibitor. As the highest dose used in the EGFRi screen is 1 µM it was not possible to calculate precise gefitinib and erlotinib IC₅₀ values for the Ex20Ins mutants or T790M with this experiment. There is no significant difference between gefitinib and erlotinib sensitivity for any EGFR mutant, with the exception of del747 which is more sensitive to gefitinib compared with erlotinib (IC₅₀ = 6.46 nM vs. 12.5 nM respectively) (Figure 4.3 B).

The majority of EGFR mutants were equally sensitive to the second-generation EGFRi afatinib (IC₅₀ = ~5 nM) with the exception of T790M and all 3 Ex20Ins mutants, which had IC₅₀ values ~40-fold higher compared to the other EGFR mutants (Figure 4.3 C). Similar trends were observed with neratinib: the majority of EGFR mutants displayed similar sensitivity to neratinib compared to one another (IC₅₀ = ~20 – 40 nM) whereas T790M and the 3 Ex20Ins mutants were less sensitive to neratinib, with IC₅₀ values ~10-fold higher compared to the other EGFR mutants

(Figure 4.3 C). G719A, G719C, and L858R all showed similar sensitivity to both neratinib and afatinib ($IC_{50} = \sim 5$ nM for G719A, G719C, and L858R upon treatment with either neratinib or afatinib) (Figure 4.3 C). Dup767 also showed similar sensitivities to both neratinib and afatinib ($IC_{50} = 162$ nM and 174 nM respectively). All other mutants showed reduced sensitivity to neratinib compared to afatinib (Figure 4.3 C).

The common EGFR mutants del746, del747, and L858R were all comparably sensitive to the third-generation EGFRi osimertinib ($IC_{50} = \sim 5$ nM for each mutant) (Figure 4.3 D). G719C was ~ 3 -fold less sensitive to osimertinib ($IC_{50} = 13.68$ nM) compared with the common EGFR mutants and was more sensitive to osimertinib compared with G719A ($IC_{50} = 74.71$ nM) (Figure 4.3 A). As expected T790M showed an increased sensitivity to osimertinib ($IC_{50} = 72.13$ nM) compared to gefitinib, erlotinib, ($IC_{50} = >1$ μ M for both) and afatinib ($IC_{50} = 277.55$ nM). L62R, R108G, A289D/T/V, G598V, E709K, L861R, and L861Q were all ~ 7 -fold more sensitive to osimertinib compared to gefitinib or erlotinib, but ~ 8 -fold less sensitive to osimertinib compared to afatinib (Figure 4.3 E). Of the 3 Ex20Ins mutants, dup767 was the most sensitive to osimertinib ($IC_{50} = 39.14$ nM compared with 195.47 nM and 189.21 nM for dup769 and dup771 respectively) although these differences were not statistically significant. All 3 Ex20Ins mutants were more sensitive to osimertinib compared to gefitinib and erlotinib. Rociletinib, another third-generation EGFRi, showed a similar pattern of sensitivity compared to osimertinib but with a reduced potency (Figure 4.2, Figure 4.3 D).

All EGFR mutants were highly sensitive to poziotinib at the lowest dose tested (10 nM), with the exception of T790M (Figure 4.2). T790M showed a 10-fold decrease in sensitivity to poziotinib compared to all other mutants but was more sensitive to poziotinib compared with osimertinib ($IC_{50} = 48.24$ nM vs. 72.13 nM respectively). TAS6417 had ~ 2 – 14-fold less potent effects on cell viability compared to poziotinib in all mutants with the exception of G719A, G719C, del746, del747, and L858R which all showed equal sensitivity to TAS6417 compared with poziotinib (Figure 4.3 F).

As previously observed, lapatinib was more effective against the extracellular domain mutants A289D, A289V, and G598V ($IC_{50} = 337.03$ nM, 224.79 nM, and

148.82 nM respectively) compared with the intracellular mutants del746 and L858R ($IC_{50} = >1 \mu\text{M}$ and 496.89 nM respectively) (Figure 4.3 G) (Vivanco *et al.*, 2012). Interestingly, this trend is not continued with all intracellular domain mutants: G719A and G719C showed the highest sensitivity to lapatinib ($IC_{50} = 37.26$ nM and 16.58 nM respectively), and L861R and L861Q were also more sensitive to lapatinib ($IC_{50} = 185.88$ nM and 196.48 nM respectively) compared with A289D and A289V.

An interesting observation from this screen is the sensitivity of different substitutions at the same amino acid position. For example, G719A is consistently less sensitive to all EGFRi in this experiment compared to G719C, with the exception of poziotinib and the second-generation EGFRi afatinib and neratinib (Figure 4.3 A). This effect has previously been shown for a subset of the EGFRi presented here (Kohsaka *et al.*, 2017). A similar difference is also observed between del746 and del747, with del746 less sensitive to gefitinib, erlotinib, neratinib, rociletinib, and lapatinib compared to del747, although none of these differences are statistically significant. The differential sensitivity of patients harbouring distinct Ex19Del variants has previously been reported. Chung *et al.* have reported a lower ORR to first-generation EGFRi for patients with Ex19Del starting at 746 compared with those starting at 747 (Chung *et al.*, 2012). However, other groups have found the opposite tendency (Lee *et al.*, 2013; Kaneda *et al.*, 2014).

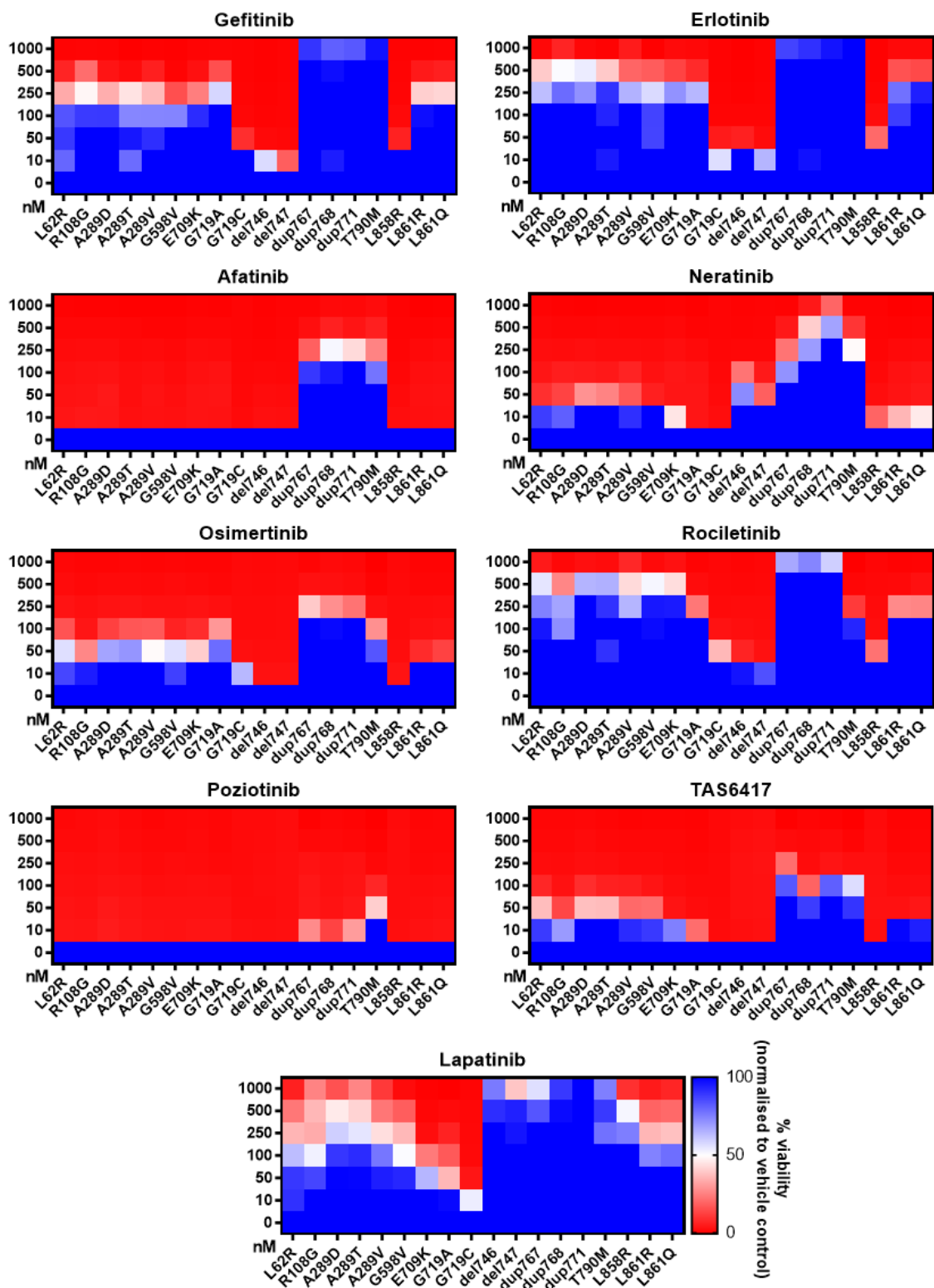


Figure 4.2 – An EGFRi screen reveals the sensitivity of EGFR mutants to a panel of EGFRi. A series of heatmaps showing cell viability of Ba/F3 cells expressing the indicated EGFR mutants upon treatment with the indicated inhibitors. Cell viability was measured by Cell Titre Glo and normalised to vehicle control (DMSO). Values represent mean from $n = 3$ biological replicates.

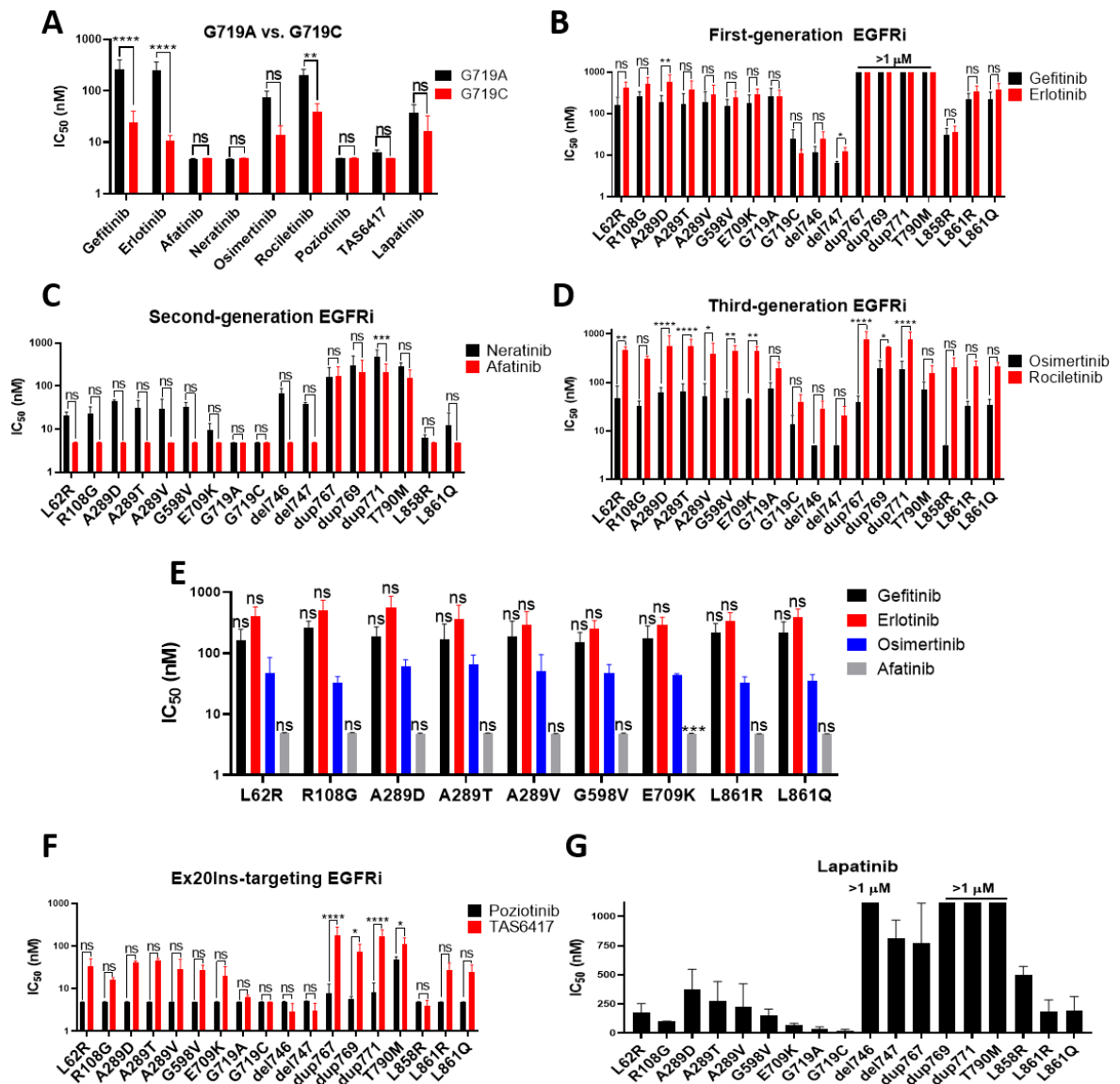


Figure 4.3 – IC₅₀ analysis of the EGFRi screen. (A) Bar chart showing IC₅₀ values for Ba/F3 cells expressing G719A or G719C upon treatment with the indicated EGFRi. (B) Bar chart showing IC₅₀ values for Ba/F3 cells expressing the indicated EGFR mutants upon treatment with gefitinib or erlotinib. (C) Bar chart showing IC₅₀ values for Ba/F3 cells expressing the indicated EGFR mutants upon treatment with afatinib or neratinib. (D) Bar chart showing IC₅₀ values for Ba/F3 cells expressing the indicated EGFR mutants upon treatment with osimertinib or rociletinib. (E) Bar chart showing IC₅₀ values for Ba/F3 cells expressing the indicated EGFR mutants upon treatment with gefitinib, erlotinib, osimertinib, or afatinib. (F) Bar chart showing IC₅₀ values for Ba/F3 cells expressing the indicated EGFR mutants upon treatment with pozotinib or TAS6417. (G) Bar chart showing IC₅₀ values for Ba/F3 cells expressing the indicated EGFR mutants upon treatment with lapatinib. (A, B, C, D, E, F, G) IC₅₀ was calculated from Figure 4.2 using four-parameter non-linear regression analysis performed on GraphPad Prism 8. Values represent mean ± standard deviation from *n* = 3 biological replicates. (A, B, C, D, F) Statistical significance for the indicated pairwise comparisons was calculated by 2-way ANOVA followed by Sidak's multiple

comparisons test. * = $p < 0.05$, ** = $p < 0.01$, *** = $p < 0.001$, **** = $p < 0.0001$, ns = not significant. (E) Statistical significance was calculated by Dunnett's multiple comparisons test comparing each inhibitor with osimertinib within each mutant. *** = $p < 0.001$, ns = not significant .

4.4 A small molecule inhibitor screen reveals mutant-specific sensitivities

The small molecule inhibitor screen was performed on 18 EGFR mutants as well as EV Ba/F3 cells grown in media supplemented with IL-3. The data for the small molecule inhibitor screen is presented in a heatmap displaying percentage cell viability normalised to vehicle control (DMSO) in Figure 4.4. Pearson's correlation performed to assess the reproducibility of the targeted small molecule inhibitor screen showed that biological replicates displayed strong correlation ($r^2 > 0.85$) in all experiments (Figure 4.5). Some of the EGFRi included in the EGFRi screen were also present on the small molecule inhibitor screen (gefitinib, erlotinib, neratinib, osimertinib, and lapatinib). The activity of EGFRi against the different EGFR mutants were consistent between the EGFRi screen and the small molecule inhibitor screen (Figure 4.2, Figure 4.3, Figure 4.4). Several compounds were found to be lethal for all EGFR mutants and the EV control: the bromodomain and extraterminal (BET) inhibitor JQ1; the dual PI3K-AKT inhibitor BEZ235; the polo-like kinase 1 (PLK1) inhibitor BI 2536; and the heat shock protein 90 (Hsp90) inhibitor luminespib. As these inhibitors displayed non-selective toxicity they were not pursued any further. A number of inhibitors had no activity at the 500 nM dose tested against any cell line (indicated by the black box on Figure 4.4). Interestingly, G719C, del746, del747, and L858R formed a cluster revealing an increased sensitivity to the TKIs dasatinib, saracatinib, bosutinib, cediranib, and vandetanib compared to the rest of the EGFR mutants (indicated by the blue box on Figure 4.4). G719C, del746, and del747 also showed an increased sensitivity to ponatinib compared with the rest of the EGFR mutants, whereas L858R did not.

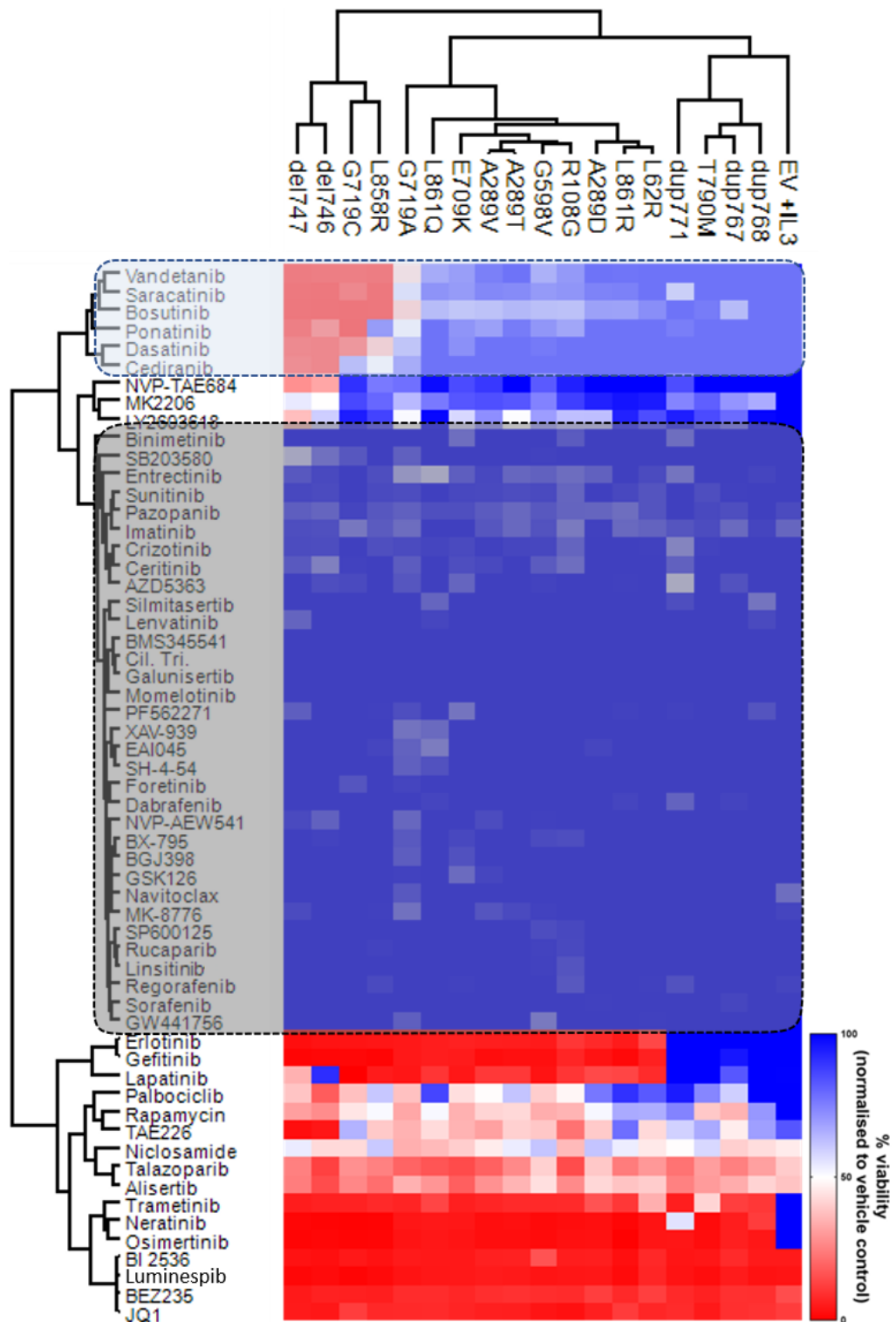


Figure 4.4 - Small molecule inhibitor screen reveals mutant-specific sensitivities to 6 broad-spectrum TKIs. A heatmap showing cell viability of Ba/F3 cells expressing the indicated EGFR mutants upon treatment with 500 nM of the indicated inhibitors (or 50 nM luminespib). Cell viability was measured by Cell Titre Glo and normalised to vehicle control (DMSO). 2-way hierarchical clustering based on Euclidean distance was performed using Perseus software. Values are mean of $n = 2$ biological replicates. EV = empty vector.

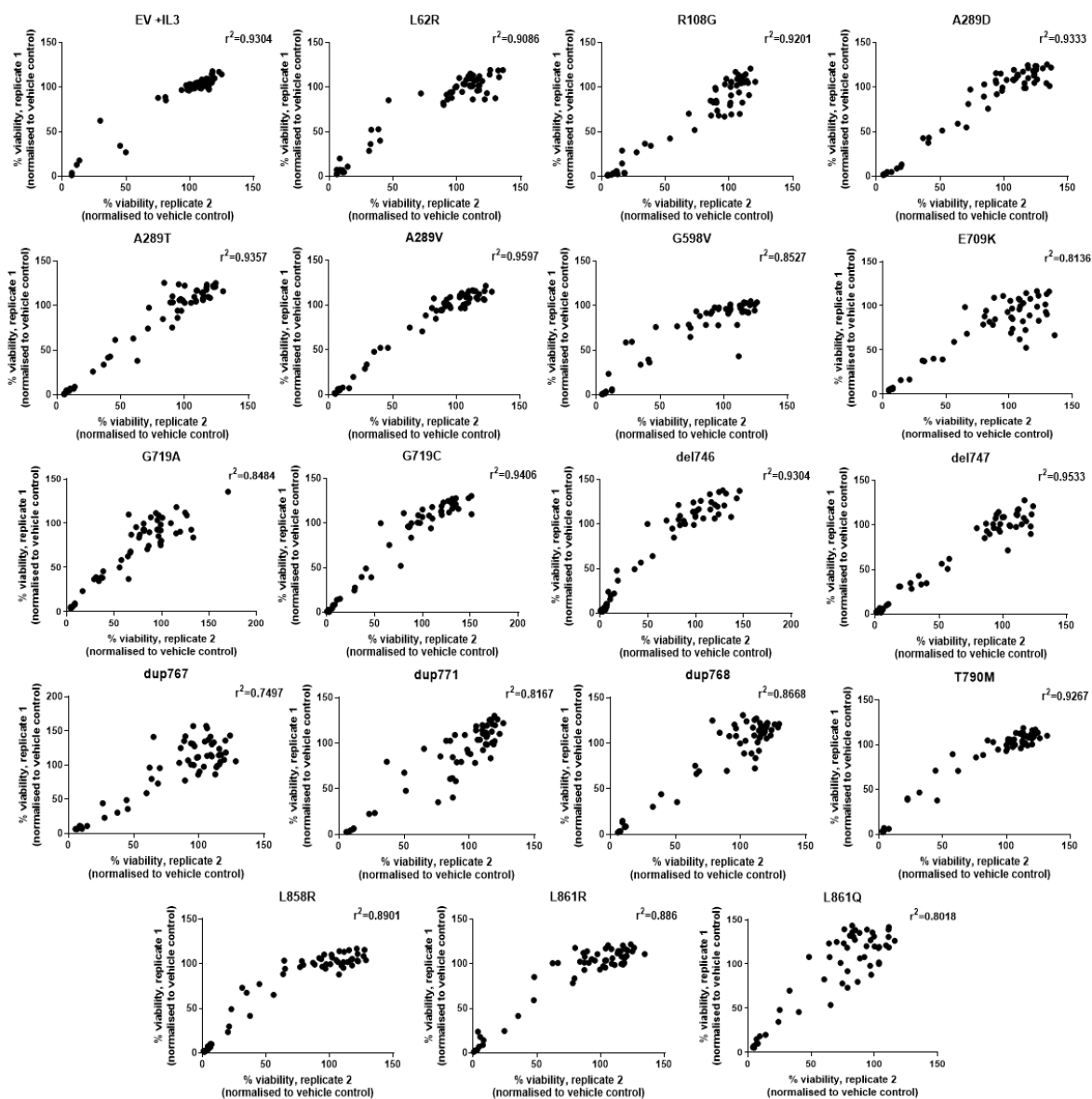


Figure 4.5 - Pearson's correlation analysis of drug screen replicates. Scatterplots showing the Pearson's correlation coefficient (r^2) between cell viability data for 2 biological replicates of the drug screen was calculated for each cell line using GraphPad Prism 8. The r^2 value is displayed for each cell line.

To validate the small molecule inhibitor screen results, full dose-response experiments for dasatinib, saracatinib, bosutinib, cediranib, vandetanib, and ponatinib were performed on the cell lines expressing sensitive EGFR mutants (G719C, del746, del747, L858R) (Figure 4.6). A289V, T790M, and L861R were selected as resistant mutants for comparison. These experiments revealed that sensitive mutants had a ~5 – 20-fold decrease in IC_{50} value compared to the resistant mutants. Consistent with observations from the small molecule inhibitor

screen (Figure 4.4), L858R showed a ponatinib sensitivity comparable to the resistant mutants and did not group with G719C, del746, and del747 (Figure 4.6 A). Together, these data identify mutant-specific activity of dasatinib, saracatinib, bosutinib, cediranib, and vandetanib against G719C, del746, del747, and L858R compared with the remainder of the EGFR mutants included in this study. Additionally, ponatinib is identified as having mutant-specific activity against G719C, del746, and del747 compared with the remainder of the EGFR mutants included in this study.

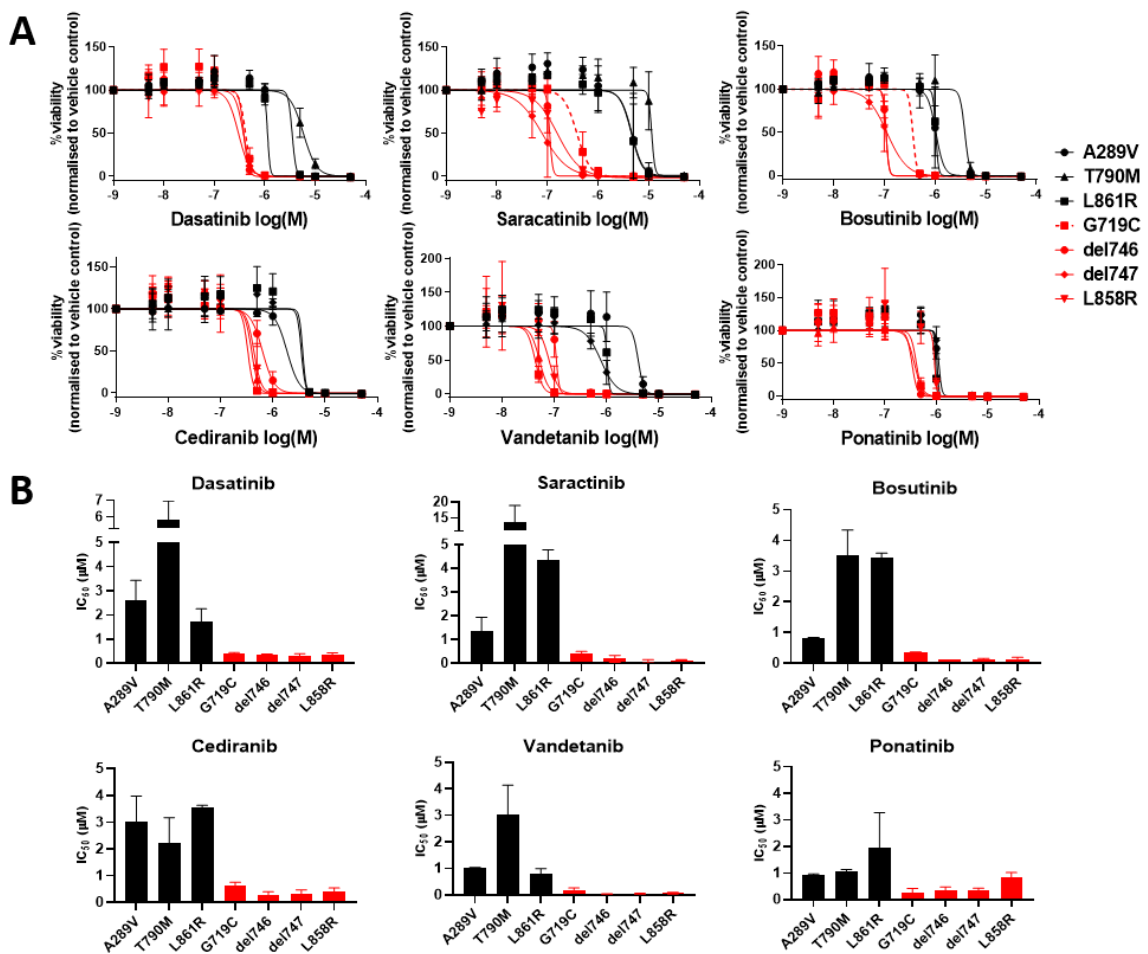


Figure 4.6 – Specific EGFR mutants show increased sensitivity to 6 broad-spectrum TKIs compared to other mutants. (A) Dose-response curves for Ba/F3 cells expressing the indicated EGFR mutants upon treatment with dasatinib, saracatinib, bosutinib, cediranib, vandetanib, or ponatinib. Cell viability was measured by Cell Titre Glo and normalised to vehicle control (DMSO). **(B)** Bar charts showing the IC₅₀ values for Ba/F3 cells expressing the indicated EGFR mutants upon treatment with dasatinib, saracatinib, bosutinib, cediranib, vandetanib, or ponatinib calculated from A. IC₅₀ was calculated using four-parameter non-linear regression analysis

performed on GraphPad Prism 8. (A, B) Values represent mean \pm standard deviation from $n = 3$ biological replicates.

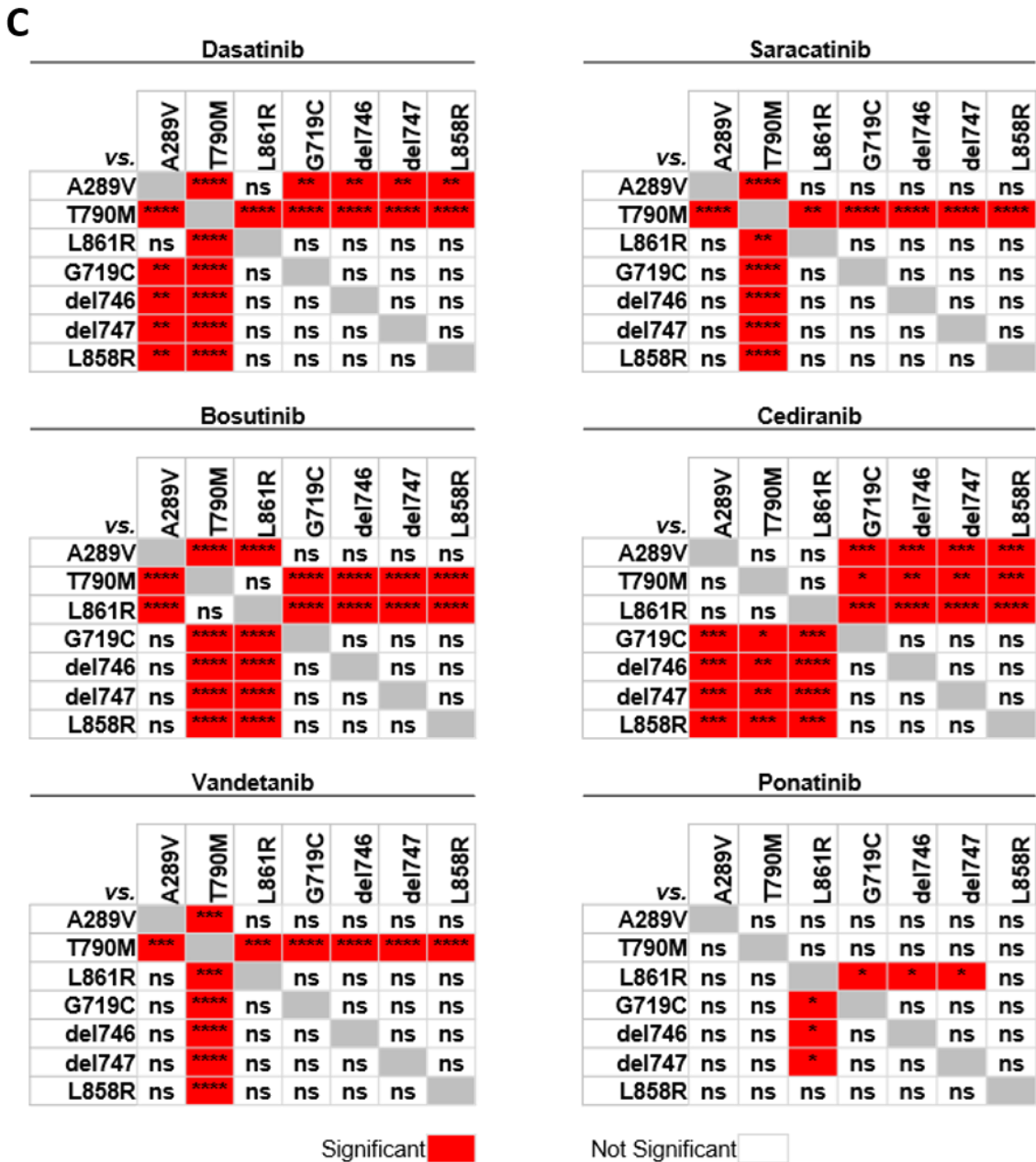


Figure 4.6 (cont.) – Specific EGFR mutants show increased sensitivity to 6 broad-spectrum TKIs compared to other mutants. (C) Statistical significance for the indicated pairwise comparisons of IC₅₀ values was calculated by Tukey's multiple comparisons test. * = $p < 0.05$, ** = $p < 0.01$, *** = $p < 0.001$, **** = $p < 0.0001$, ns = not significant.

4.5 Analysis of small molecule inhibitor screen hits determines putative shared targets

Dasatinib, saracatinib, bosutinib, cediranib, vandetanib, and ponatinib are all broad-spectrum multi-target TKIs (Roskoski, 2015; Kim *et al.*, 2017). Dasatinib, saracatinib, bosutinib, and ponatinib were initially developed as SRC/Abl inhibitors, while cediranib and vandetanib were initially developed as inhibitors of the VEGFR family. To explore the mechanism underlying the mutant-specific inhibitor sensitivity observed in Figure 4.4 and Figure 4.6, the shared protein targets of the 6 broad-spectrum TKIs were identified using a kinase selectivity overlap analysis (Figure 4.7). Overlap analysis was performed using the Kinase inhibitor Experiments Omnibus (KiEO) database, which collates kinase selectivity data from published kinase inhibitor profiling studies. This analysis revealed ABL1, discoidin domain receptor 2 (DDR2), protein-tyrosine kinase 6 (PTK6), and the SFKs SRC and YES1 as common targets of these 6 broad-spectrum TKIs (Figure 4.7) (Fabian *et al.*, 2005; Apsel *et al.*, 2008; Karaman *et al.*, 2008; O'Hare *et al.*, 2009; Remsing Rix *et al.*, 2009; Anastassiadis *et al.*, 2011; Davis *et al.*, 2011; Metz *et al.*, 2011; Uitdehaag and Zaman, 2011; Dar *et al.*, 2012; McTigue *et al.*, 2012; Uitdehaag *et al.*, 2014; Duong-Ly *et al.*, 2016; Wei *et al.*, 2016). It was initially decided to investigate whether SRC inhibition was the cause of increased sensitivity to these 6 broad-spectrum TKIs for the following reasons. First, G719C, del746, del747, and L858R all most commonly occur in NSCLC and overexpression or hyperactivity of SRC has previously been observed in NSCLC patients (Masaki *et al.*, 2003). Second, SRC and EGFR are able to activate one another in a bi-directional manner (Oude Weernink *et al.*, 1994; Maa *et al.*, 1995; Sato *et al.*, 1995; Weernink and Rijksen, 1995). Third, SRC is the most commonly implicated SFK member in cancer (Yeatman, 2004), and has been shown to be active in NSCLC cell lines harbouring Ex19Del or L858R mutations in EGFR, with combinations of SRC and EGFR inhibition showing synergistic effect (Song *et al.*, 2006; Zhang *et al.*, 2007). It was therefore hypothesised that G719C, del746, del747, and L858R may have an increased dependency on SRC signalling compared to other EGFR mutants, leading to an increased sensitivity to these inhibitors as they each target SRC (Figure 4.1 C). Additionally, previously published data from cell-free kinase assays

has shown that dasatinib, saracatinib, and bosutinib can bind to certain intracellular EGFR mutants (Formisano *et al.*, 2015). It was therefore also hypothesised that sensitivity to these inhibitors may be caused by inhibition of EGFR (Figure 4.1 B). To determine whether these inhibitors were targeting EGFR, SRC, or both, I treated del746 with each inhibitor for 6 h prior to lysis and analysed the lysates by western blot. This analysis revealed that all 6 inhibitors reduced EGFR phosphorylation and 3 inhibitors reduced SRC phosphorylation (Figure 4.8). A series of experiments was therefore designed to determine whether it was the inhibition of EGFR or inhibition of SRC that was causing the increased sensitivity of the mutants to these inhibitors.

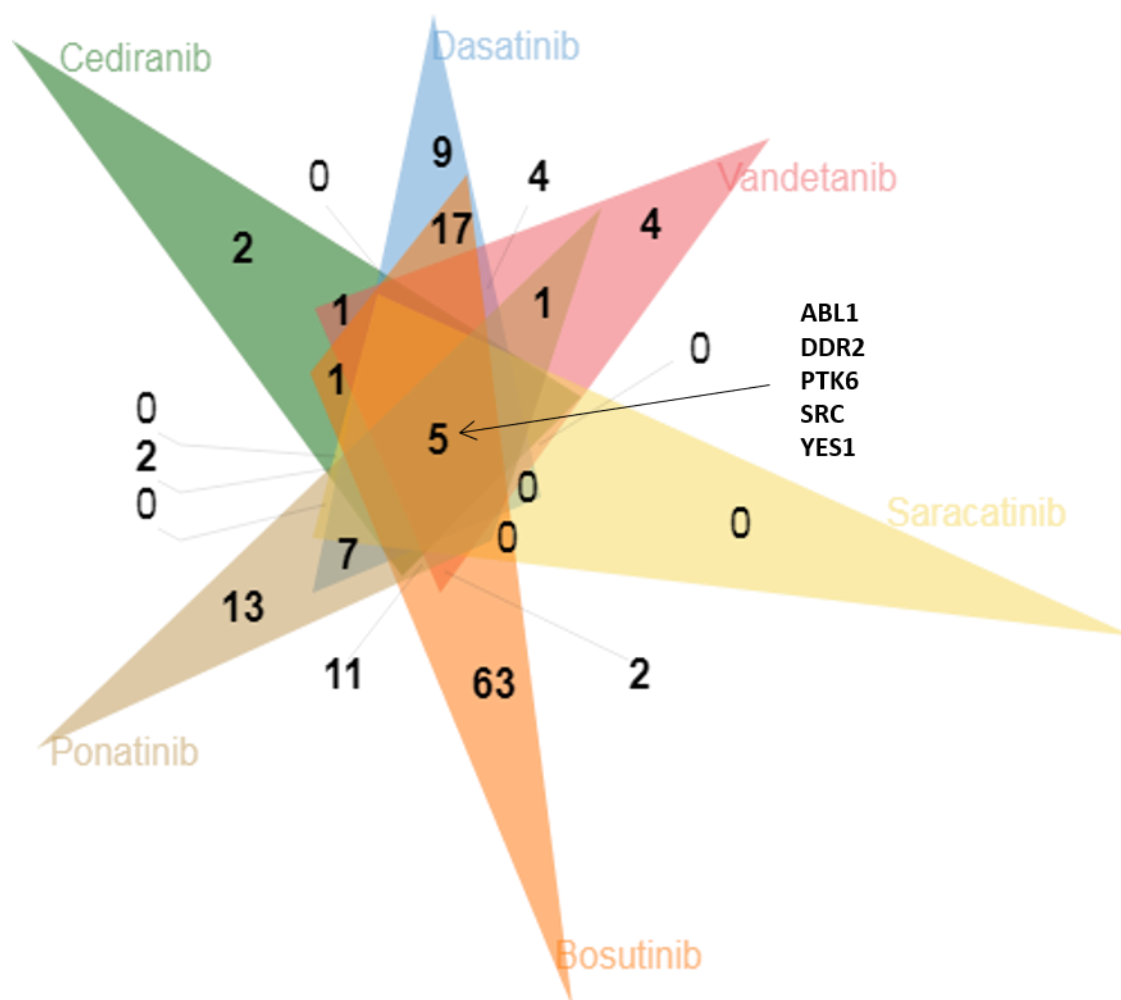


Figure 4.7 – Shared targets of hits from the small molecule inhibitor screen. Targets of kinase inhibitors were identified using published kinase selectivity datasets collated in the KiEO database. Numbers indicate the numbers of inhibitors identified. The Venn diagram was generated using the ‘Overlap Analysis application’ within the KiEO database (<http://35.172.151.213/KIEOv1.0/>). KiEO considers a kinase a target

of an inhibitor if the $IC_{50}/K_d/K_i \leq 1 \mu\text{M}$ or the Percent of inhibition over Control $\leq 15\%$ from the assays. The overlap analysis was performed on the shared targets of the compounds that pass this threshold.

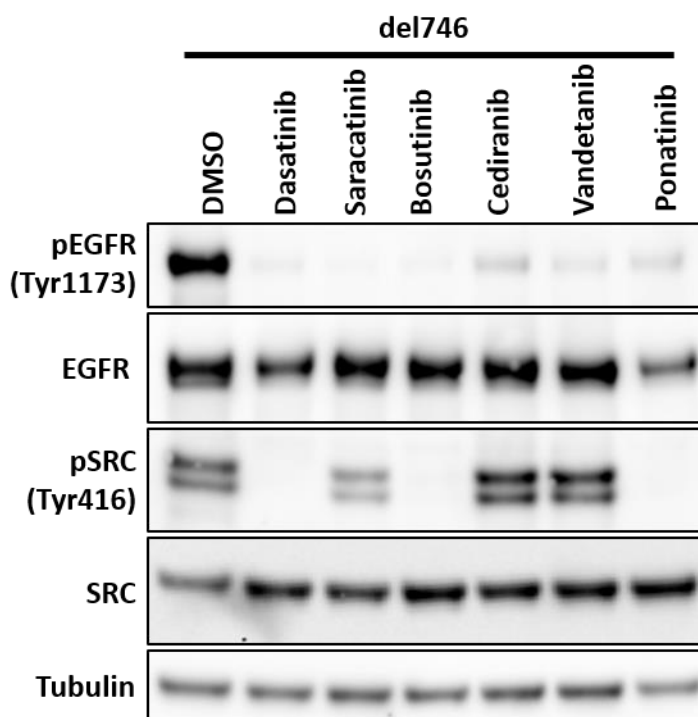


Figure 4.8 – All 6 hits from the small molecule inhibitor screen reduce EGFR phosphorylation and 3 reduce SRC phosphorylation. Western blot showing EGFR phosphorylation and SRC phosphorylation in Ba/F3 cells expressing del746 upon treatment with $2 \mu\text{M}$ of the indicated inhibitor for 6 h. Tubulin was used as a loading control. Blots shown are representative of $n = 2$ biological replicates.

4.6 Generation of SRC and EGFR gatekeeper mutant cell lines

To establish whether inhibition of SRC or inhibition of EGFR was the cause of sensitivity to the 6 broad-spectrum TKIs identified in the small molecule inhibitor screen, rescue experiments were performed by expressing constructs encoding mutant alleles of *SRC* and *EGFR* that do not allow inhibitor binding, known as gatekeeper mutants, in the cell lines harbouring sensitive EGFR mutants. If the broad-spectrum TKIs are causing loss of cell viability by inhibition of SRC or EGFR, then expression of these gatekeeper mutants will rescue the sensitivity of the Ba/F3 cells harbouring sensitive EGFR mutants to the broad-spectrum TKIs, as the gatekeeper mutant will prevent the TKIs from binding to its target.

The SRC-T338I mutation is a gatekeeper mutation that has been shown to prevent dasatinib from binding to SRC (Zhang *et al.*, 2009). Constructs containing either WT chicken SRC (SRC-WT) or chicken SRC-T338I were subcloned into pBABE-puro vectors (Figure 4.9 A). The original SRC constructs were in pBABE-hygro vectors obtained from the Joan Massagué lab via Addgene. These constructs were packaged into retroviruses and stably expressed in Ba/F3 cells expressing del746, del747, and L858R. SRC expression was confirmed by Western blot (Figure 4.9 B). SRC expression had minimal effect on EGFR expression levels. To confirm that the SRC-T338I constructs were preventing dasatinib from binding to SRC as previously reported, each cell line was lysed following 6 h treatment with 500 nM dasatinib. Western blot analysis of these lysates showed that dasatinib treatment resulted in potent inhibition of SRC phosphorylation in cell lines expressing SRC-WT, but no inhibition of SRC phosphorylation in cell lines expressing SRC-T338I (Figure 4.9 C).

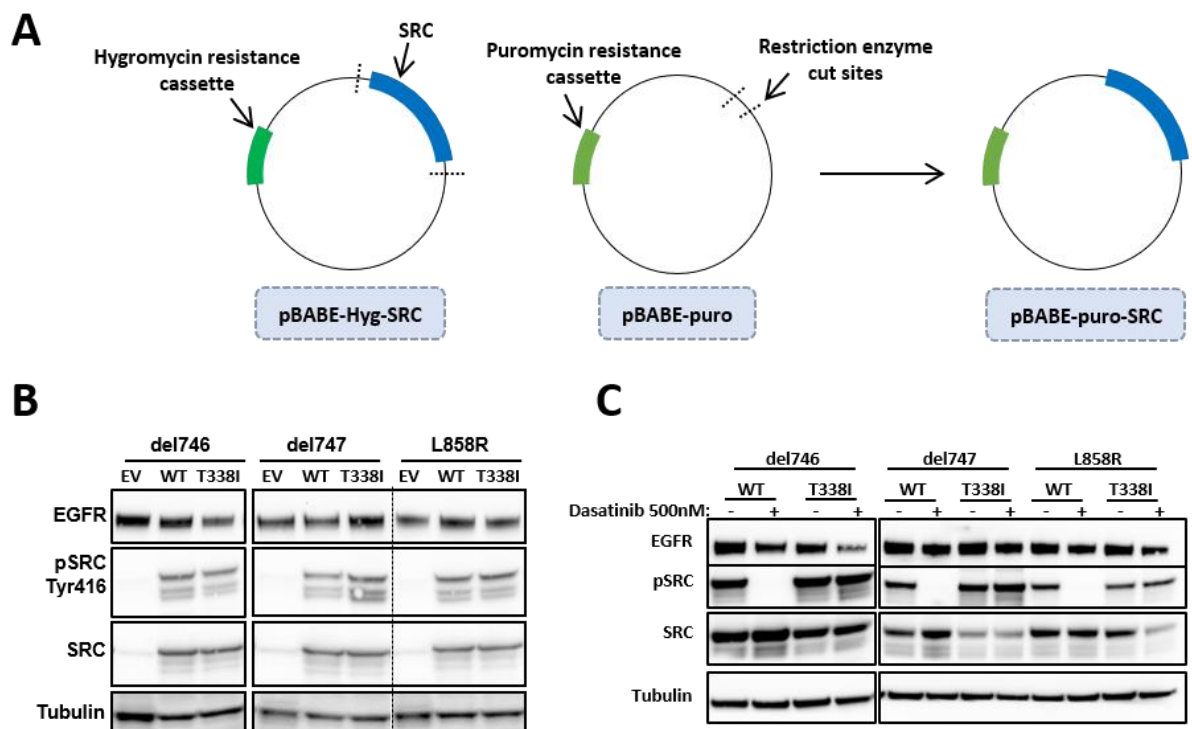


Figure 4.9 – Generation of SRC gatekeeper cell lines. (A) Workflow for generating pBABE-puro expression vectors for SRC-WT and SRC-T338I. Briefly, the SRC gene was isolated from pBABE-hygro expression constructs by restriction digest and agarose gel purification. SRC was then cloned into a pBABE-puro expression vector linearised using the same restriction enzymes. (B) Stable expression of EV, SRC-WT, and SRC-T338I constructs in Ba/F3 cells harbouring del746, del747, or L858R

was confirmed by western blot. Blots shown are $n = 1$ biological replicates. EV = empty vector, WT = wild type. (C) Western blot showing EGFR expression levels and SRC phosphorylation in Ba/F3 cells harbouring the indicated EGFR mutants and expressing either SRC-WT or SRC-T338I upon treatment with 500 nM dasatinib or vehicle control (DMSO) as indicated for 6 h. Blots shown are representative of $n = 2$ biological replicates. (B, C) Tubulin was used as a loading control.

As described in chapter 1, the EGFR T790M gatekeeper mutation has been shown to prevent the binding of inhibitors such as gefitinib (Yun *et al.*, 2008). T790M was therefore used as a gatekeeper mutation to use to prevent the 6 broad-spectrum TKIs identified in the small molecule inhibitor screen binding to EGFR. To establish EGFR-gatekeeper mutation cell lines, I employed a second round of SDM using the expression constructs for del746, del747, and L858R as templates in order to generate expression constructs with a secondary T790M gatekeeper mutation in EGFR (Figure 4.10 A). It was later discovered that del746+T790M had an additional unintended K1099E mutation. These were then packaged into retroviruses and transduced by infection into parental Ba/F3 cells. As described in section 3.5, after infection cells were selected with 1 mg/ml hygromycin for 2 weeks. Following this, IL-3 was removed from the cells' media and the population doubling of cells was tracked at the indicated time points (Figure 4.10 B). This showed that expression of del746+T790M, del747+T790M, and L858R+T790M in Ba/F3 cells conferred IL-3 independence, indicating that cells expressing T790M-containing double mutants are able to grow in a mutant EGFR-dependent manner comparable to their single-mutant counterparts. Western blot analysis showed that each double-mutant cell line had a lower expression of EGFR compared to the single-mutant cell lines (Figure 4.10 C). Despite this reduced expression, cells expressing secondary T790M mutants were found to be resistant to gefitinib treatment as has previously been reported (Figure 4.10 D) (Yun *et al.*, 2008). Also in line with published data, cells expressing secondary T790M mutants were found to be sensitive to osimertinib (Figure 4.10 D) (Cross *et al.*, 2014).

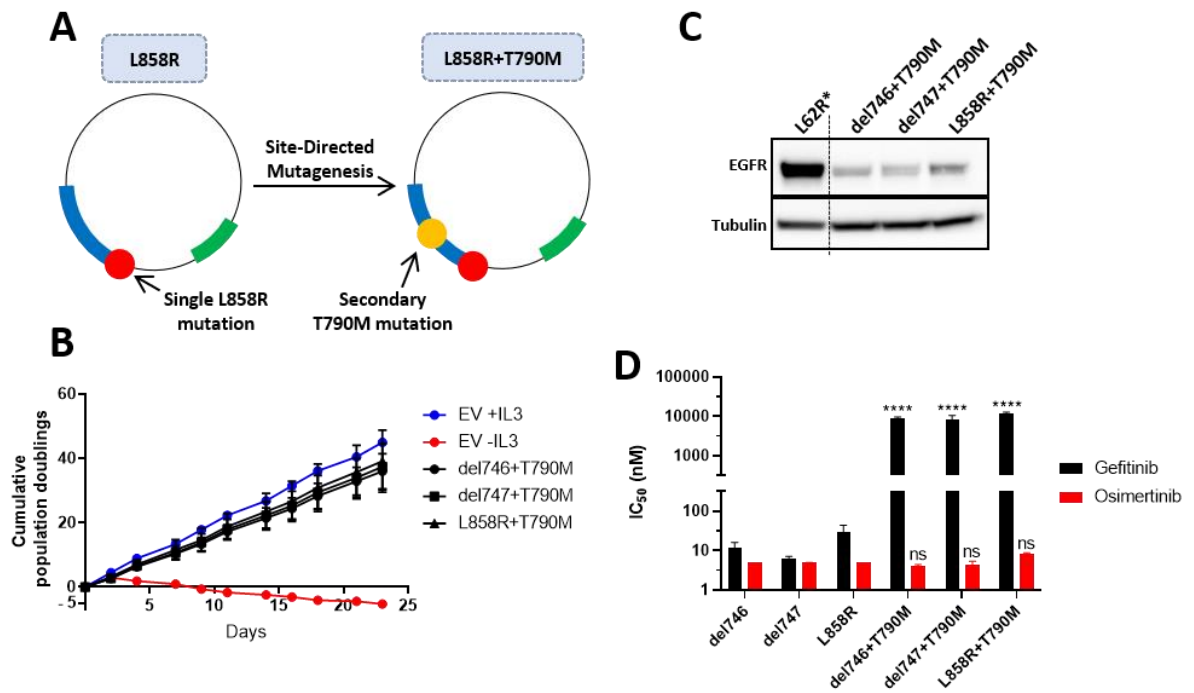


Figure 4.10 – Generation of EGFR gatekeeper cell lines. (A) Workflow for generating expression vectors for del746, del747, and L858R with secondary T790M mutations by site-directed mutagenesis. (B) Proliferation of Ba/F3 cell lines expressing different EGFR mutants upon IL-3 withdrawal. Cell viability was measured by Cell Titre Glo at the indicated times. EV = empty vector. (C) EGFR expression levels of Ba/F3 cells expressing del746+T790M, del747+T790M, and L858R+T790M were assessed by western blot. L62R was used as a reference and is highlighted with an asterisk. Tubulin was used as a loading control. Blots shown are $n = 1$ biological replicates. (D) Bar chart showing IC₅₀ values for Ba/F3 cells expressing the indicated EGFR mutants upon treatment with gefitinib or osimertinib. Cells were treated a dose range of gefitinib or osimertinib for 72 h. Viability was measured by Cell Titre Glo and normalised to vehicle control (DMSO). IC₅₀ was calculated using four-parameter non-linear regression analysis performed on GraphPad Prism 8. Statistical significance for the indicated pairwise comparisons was calculated by 2-way ANOVA followed by Tukey's multiple comparisons test comparing each mutant with its +T790M counterpart. **** = $p < 0.0001$, ns = not significant. (B, D) Values represent mean \pm standard deviation from $n = 3$ biological replicates.

4.7 SRC-gatekeeper mutant does not confer resistance to broad-spectrum TKIs identified in small molecule inhibitor screen

To examine whether inhibition of SRC signalling caused sensitivity to the broad-spectrum TKIs identified in the small molecule inhibitor screen, the sensitivity of Ba/F3 cells harbouring del746, del747, or L858R expressing either SRC-WT or SRC-T338I to the 6 broad-spectrum TKIs was compared. Dose-response experiments showed no appreciable difference between parental cells and cells expressing SRC-WT, suggesting that stable expression of SRC-WT does not affect the sensitivity of cells to these inhibitors (Figure 4.11). Additionally, dose-response experiments showed that expression of SRC-T338I did not cause a decrease in sensitivity to the broad-spectrum TKIs compared to expression of SRC-WT. Statistical analysis of the IC₅₀ values showed no significant differences between del746, del747, and L858R cells expressing either SRC-WT or SRC-T338I (Figure 4.12). These data indicate that inhibition of SRC signalling is not the mechanism leading to sensitivity to the broad-spectrum TKIs identified in the small molecule inhibitor screen for Ba/F3 cells expressing del746, del747, or L858R. Despite this, there was a clear shift to the left in the dose-response curve of del746 cells expressing SRC-T338I compared with del746 cells expressing SRC-WT upon dasatinib treatment (Figure 4.11). This indicates that the expression of SRC-T338I did not decrease, but rather increased the sensitivity of del746 cells to dasatinib compared to the expression of SRC-WT. The mechanism underpinning the increased dasatinib sensitivity of del746 cells expressing SRC-WT is investigated in section 4.9. Taken together, these data suggest that the increased sensitivity of del746, del747, and L858R to the broad-spectrum TKIs identified in the small molecule inhibitor screen is not caused by a mutant-specific dependency on the SRC signalling pathway that can be exploited therapeutically (Figure 4.1).

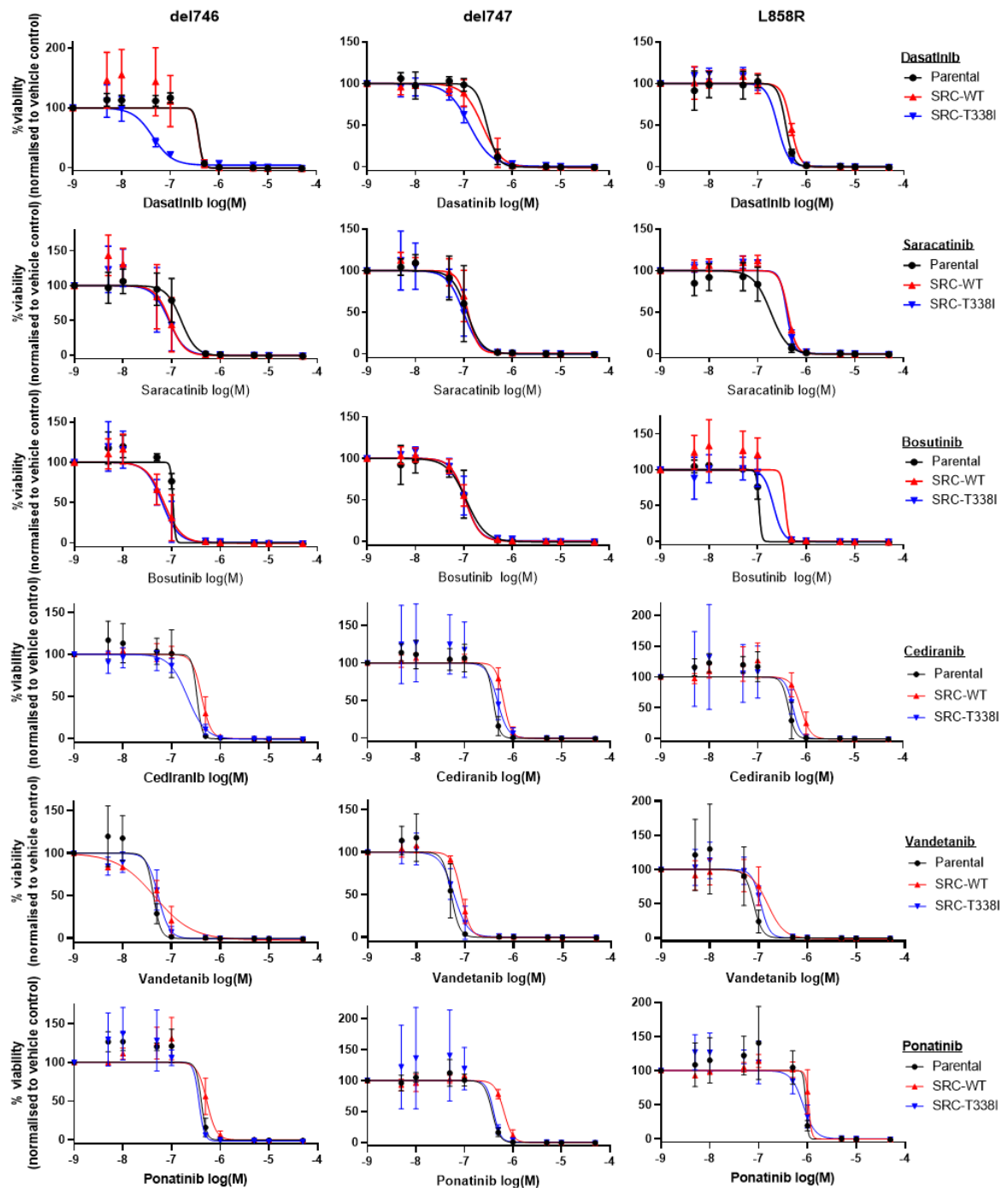


Figure 4.11 - Expression of SRC-T338I does not rescue sensitivity to dasatinib, saracatinib, bosutinib, cediranib, vandetanib, or ponatinib in Ba/F3 cells expressing del746, del747, or L858R. Dose-response curves for Ba/F3 cells harbouring del746, del747, or L858R expressing either no SRC construct (parental), SRC-WT, or SRC-T338I upon treatment with dasatinib, saracatinib, bosutinib, cediranib, vandetanib, or ponatinib at the indicated doses for 72 h. Viability was measured by Cell Titre Glo and normalised to vehicle control (DMSO). For dasatinib, saracatinib, cediranib, vandetanib, and ponatinib values represent mean \pm standard deviation from $n = 3$ biological replicates. For bosutinib values represent mean \pm standard deviation from $n = 2$ biological replicates. WT = wild type.

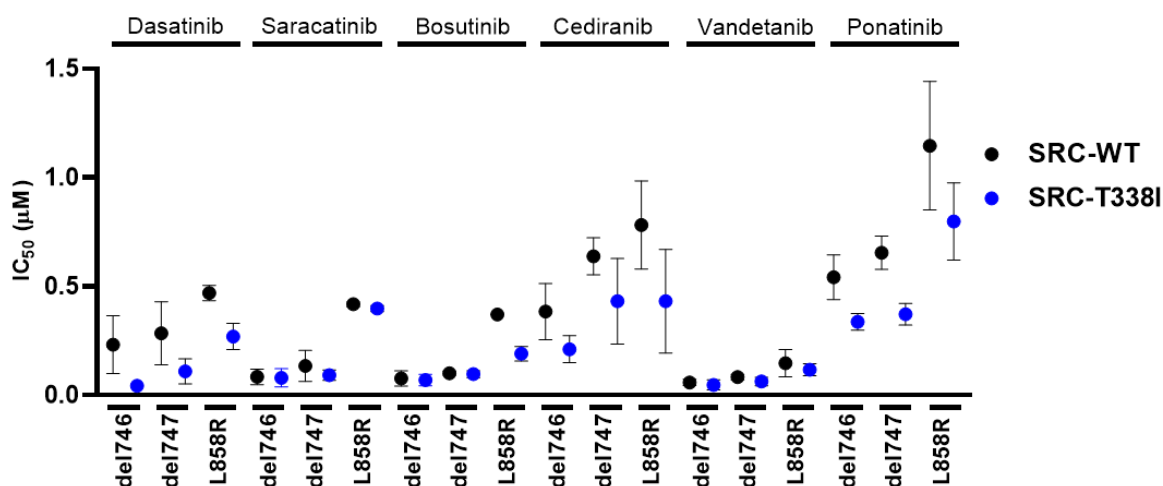


Figure 4.12 – IC₅₀ analysis shows that expression of SRC-T338I does not rescue sensitivity to dasatinib, saracatinib, bosutinib, cediranib, vandetanib, or ponatinib in Ba/F3 cells expressing del746, del747, or L858R. Plot showing IC₅₀ values of Ba/F3 cells expressing the indicated EGFR mutants and either SRC-WT or SRC-T338I upon treatment with dasatinib, saracatinib, bosutinib, cediranib, vandetanib, or ponatinib. IC₅₀ was calculated from Figure 4.11 using four-parameter non-linear regression analysis performed on GraphPad Prism 8. Statistical significance between SRC-WT and SRC-T338I for each mutant upon treatment with each inhibitor was calculated by Sidak's multiple comparisons test. All comparisons were not significant. For dasatinib, saracatinib, cediranib, vandetanib, and ponatinib values represent mean ± standard deviation from *n* = 3 biological replicates. For bosutinib values represent mean ± standard deviation from *n* = 2 biological replicates. WT = wild type.

4.8 EGFR-gatekeeper mutation confers resistance to broad-spectrum TKIs identified in small molecule inhibitor screen

To investigate whether inhibition of EGFR signalling caused sensitivity to the broad-spectrum TKIs identified in the small molecule inhibitor screen, the sensitivity of parental del746, del747, and L858R cells was compared with cells harbouring a secondary T790M mutation in EGFR (del746+T790M, del747+T790M, and L858R+T790M). Dose-response experiments showed that cells harbouring secondary T790M mutations had reduced sensitivity to dasatinib, saracatinib, bosutinib, cediranib, and vandetanib compared to parental cells (Figure 4.13). Analysis of the IC₅₀ values showed that cells harbouring secondary T790M mutations had ~8 – 60-fold higher IC₅₀ values higher compared to parental cells

when treated with dasatinib, saracatinib, bosutinib, cediranib, and vandetanib (Figure 4.14). The effect of secondary T790M mutations on ponatinib sensitivity was less pronounced. Dose-response curves indicated a slight decrease in ponatinib sensitivity for del746+T790M and del747+T790M compared with del746 and del747 respectively (Figure 4.13), although there were no significant differences in IC₅₀ values (Figure 4.14). Together, these data indicate that ponatinib exerts a moderate effect on cell viability in del746 and del747 expressing Ba/F3 cells through the inhibition of EGFR. There was no appreciable change in ponatinib sensitivity between L858R cells and L858R+T790M cells (Figure 4.13, Figure 4.14). This is consistent with results presented in Figure 4.6 showing that L858R has a ponatinib sensitivity comparable to that of the resistant EGFR mutants. These data indicate that, with the exception of ponatinib, the increased sensitivity of Ba/F3 cells harbouring del746, del747, or L858R to the broad-spectrum TKIs identified in the small molecule inhibitor screen is caused by a loss of EGFR signalling.

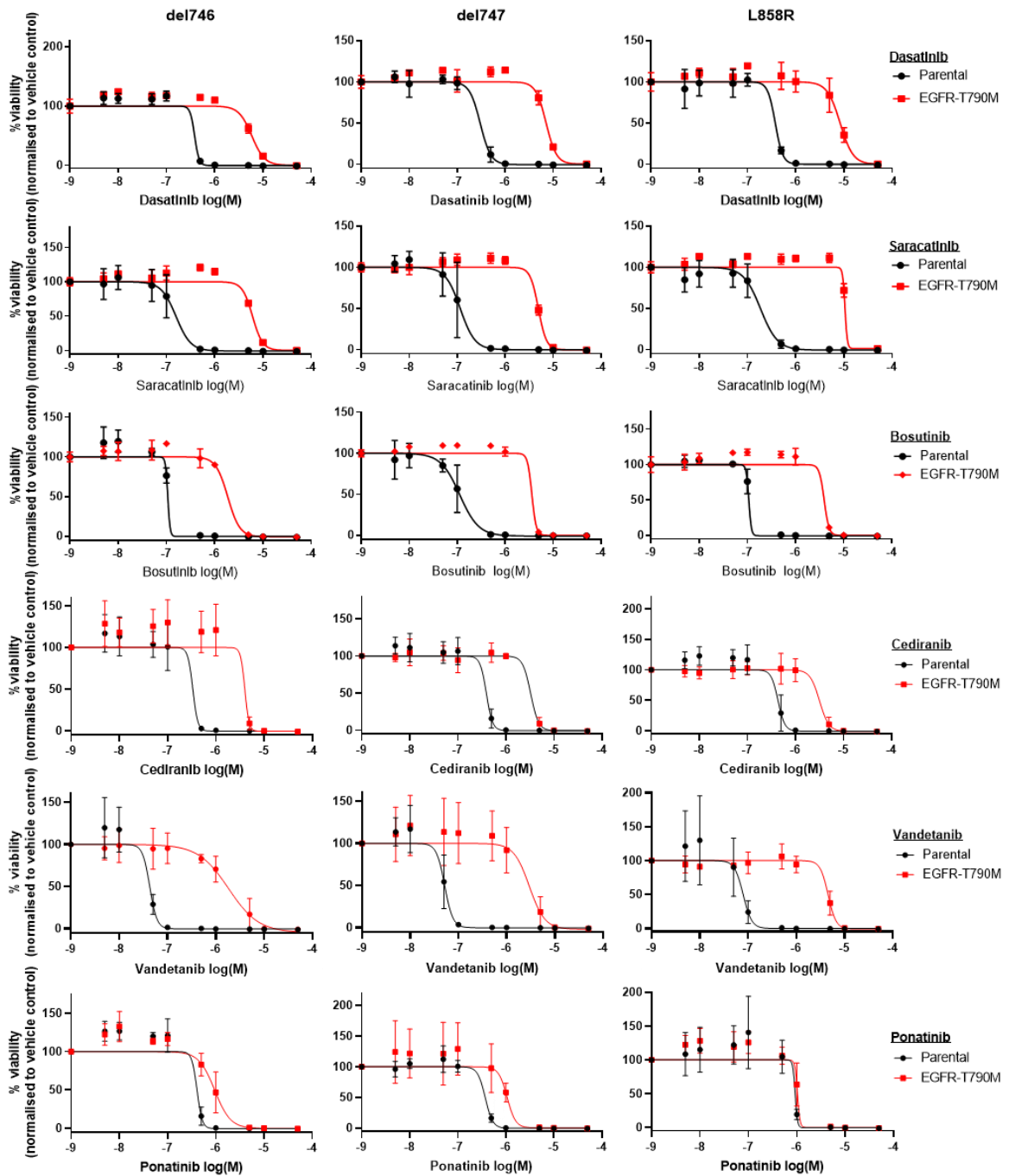


Figure 4.13 – Expression of EGFR-T790M rescues the sensitivity of Ba/F3 cells harbouring del746, del747, or L858R to dasatinib, saracatinib, bosutinib, cediranib, and vandetanib. Dose-response curves for Ba/F3 cells harbouring del746, del747, or L858R with or without a secondary EGFR-T790M mutation upon treatment with dasatinib, saracatinib, bosutinib, cediranib, vandetanib, or ponatinib at the indicated doses for 72 h. Viability was measured by Cell Titre Glo and normalised to vehicle control (DMSO). Values represent mean \pm standard deviation from $n = 3$ biological replicates.

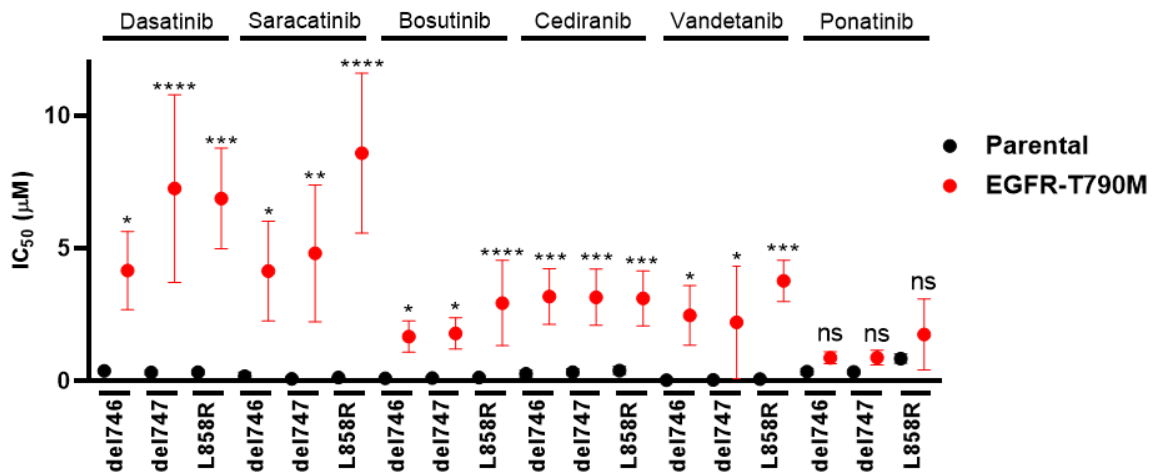


Figure 4.14 – IC₅₀ analysis shows that expression of EGFR-T790M in Ba/F3 cells harbouring del746, del747, or L858R rescues sensitivity to dasatinib, saracatinib, bosutinib, cediranib, and vandetanib. Plot showing IC₅₀ values of Ba/F3 cells expressing the indicated EGFR mutants with or without a secondary EGFR-T790M mutation upon treatment with dasatinib, saracatinib, bosutinib, cediranib, vandetanib, or ponatinib. IC₅₀ was calculated from Figure 4.13 using four-parameter non-linear regression analysis performed on GraphPad Prism 8. Statistical significance was calculated by Sidak’s multiple comparisons test. Stars represent significance of Parental vs EGFR-T790M within each cell line and inhibitor. * = $p < 0.05$, ** = $p < 0.01$, *** = $p < 0.001$, **** = $p < 0.0001$, ns = not significant. Values represent mean \pm standard deviation from $n = 3$ biological replicates.

4.9 SRC can act as a dasatinib “sink”

Unexpectedly, expression of SRC-T338I caused a clear shift to the left in the dose-response curve of del746 cells treated with dasatinib compared to del746 cells expressing SRC-WT (Figure 4.15 A). Although there was no significant difference in IC₅₀ values between del746 cells expressing SRC-T338I or SRC-WT (Figure 4.12), the shift to the left in the dose-response curve upon dasatinib treatment indicated an increase in dasatinib sensitivity in del746 cells expressing SRC-T338I compared to SRC-WT. It was hypothesised that this may be due to an increase of free dasatinib in the SRC-T338I expressing cells compared to SRC-WT expressing cells leading to increased inhibition of EGFR. Based on the observations in Figure 4.7, Figure 4.11 and Figure 4.13, a model was proposed where in SRC-WT expressing cells dasatinib can bind to both EGFR and SRC (Figure 4.15 B). However, in SRC-T338I expressing cells dasatinib is unable to bind the SRC

gatekeeper mutant and therefore there is more dasatinib available within the cell to bind to EGFR. This would result in increased inhibition of EGFR phosphorylation at lower doses of dasatinib in SRC-T338I expressing cells compared to SRC-WT expressing cells, which would account for the increased dasatinib sensitivity observed in SRC-T338I expressing cells (Figure 4.15 A). To test this hypothesis, del746 cells expressing SRC-WT or SRC-T338I were treated with a dose range of dasatinib for 6 h prior to lysis. Western blot analysis of these lysates showed that SRC phosphorylation was inhibited at 10 nM of dasatinib in del746 cells expressing SRC-WT, whereas as expected cells expressing SRC-T338I had sustained SRC phosphorylation following treatment with 1000 nM of dasatinib (Figure 4.15 C). In contrast, EGFR phosphorylation was inhibited at 250 nM dasatinib in SRC-T338I expressing cells whereas 500 nM of dasatinib was required to cause a similar level of EGFR inhibition in SRC-WT expressing cells. Together, these data indicate that SRC-WT may act as a “sink” for dasatinib. Increased free dasatinib in SRC-T338I expressing cells may explain the increased sensitivity to dasatinib observed in Figure 4.15 A and Figure 4.15 C. However, to establish this the differences in free dasatinib concentrations between SRC-WT and SRC-T338I expressing cells would have to be measured. Additionally, *in vitro* kinase assays would need to be employed to demonstrate that there was indeed increased dasatinib binding to EGFR in SRC-T338I expressing cells compared to SRC-WT cells.

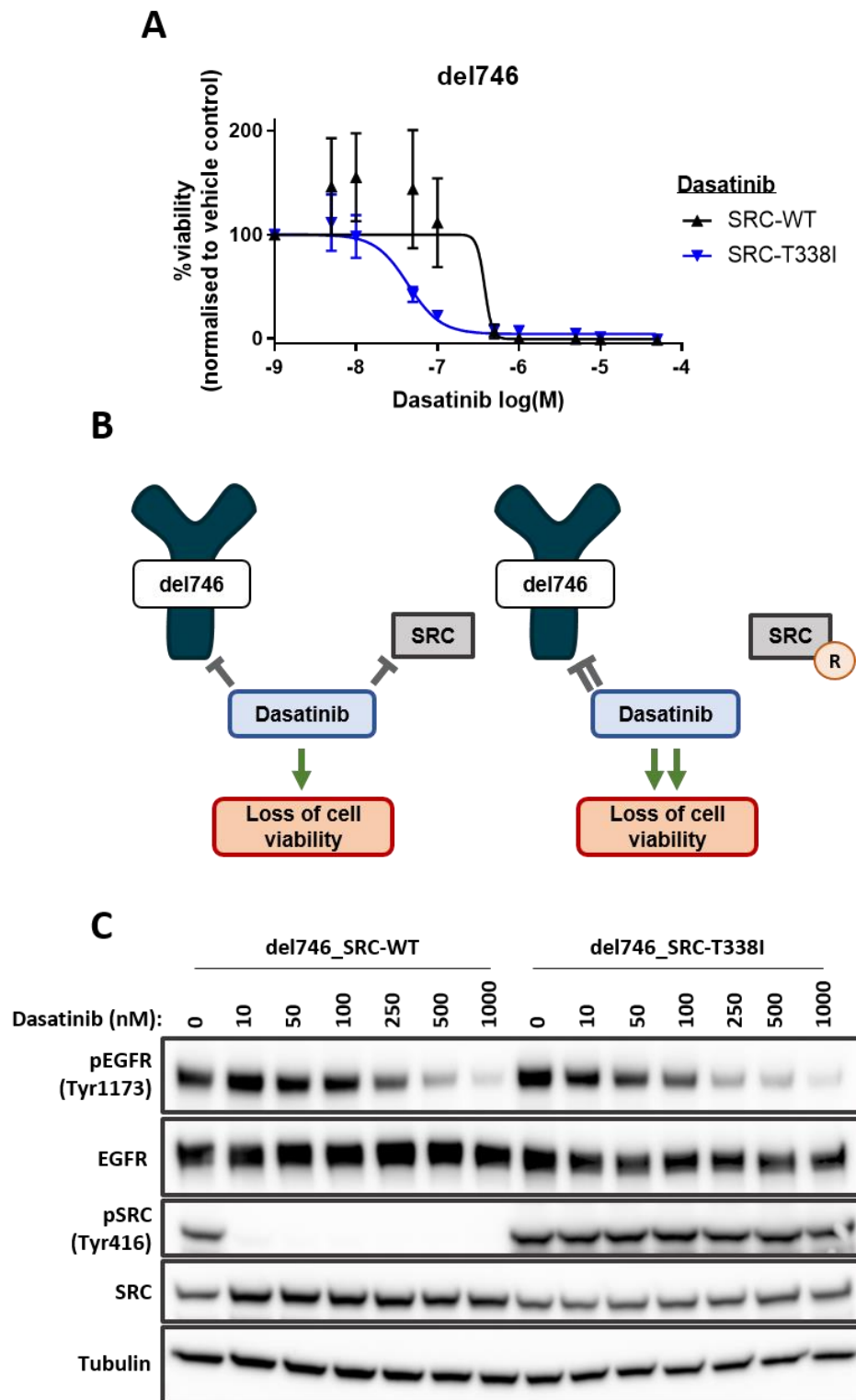


Figure 4.15 – SRC can act as a dasatinib “sink”. (A) Dose-response curves for Ba/F3 cells harbouring del746 expressing either no SRC construct (parental), SRC-WT, or SRC-T338I upon treatment with dasatinib at the indicated doses for 72 h. Viability was measured by Cell Titre Glo and normalised to vehicle control (DMSO). Values represent mean \pm standard deviation from $n = 3$ biological replicates. WT = wild type. (B) A schematic of the proposed mechanism for increased dasatinib sensitivity in del746 cells expressing SRC-T338I. In cells expressing SRC-WT dasatinib binds

both SRC and EGFR. In cells expressing SRC-T338I dasatinib cannot bind to SRC and so therefore there is more cytoplasmic dasatinib available to bind to EGFR compared to cells expressing SRC-WT. This causes inhibition of EGFR at lower doses of dasatinib resulting in loss of cell viability at lower dasatinib doses in the SRC-T338I expressing cells compared to the SRC-WT expressing cells. (C) Western blot showing EGFR phosphorylation and SRC phosphorylation in Ba/F3 cells harbouring a del746 EGFR mutant and expressing either SRC-WT or SRC-T338I upon treatment with the indicated dose of dasatinib for 6 h. Tubulin was used as a loading control. Blots shown are representative of $n = 2$ biological replicates.

4.10 EGFR-T790M prevents EGFR inhibition by broad-spectrum TKIs identified in small molecule inhibitor screen

Having observed that expression of EGFR-T790M rescues the sensitivity of cells expressing del746, del747, or L858R to the hits from the small molecule inhibitor screen (Figure 4.13, Figure 4.14), western blot analysis confirmed that this effect was caused by an inability of a selection of the broad-spectrum TKIs to inhibit EGFR phosphorylation in cells harbouring secondary T790M mutations. Treatment of cells expressing del746 or L858R, with or without secondary T790M mutations, with cediranib, bosutinib, or dasatinib for 6 h showed that EGFR phosphorylation was reduced by each inhibitor in cells without T790M but was sustained in cells with T790M (Figure 4.16). These signalling data further provide evidence supporting that the sensitivity of del746, del747, and L858R to the broad-spectrum TKIs identified in the small molecule inhibitor screen is caused by inhibition of EGFR phosphorylation.

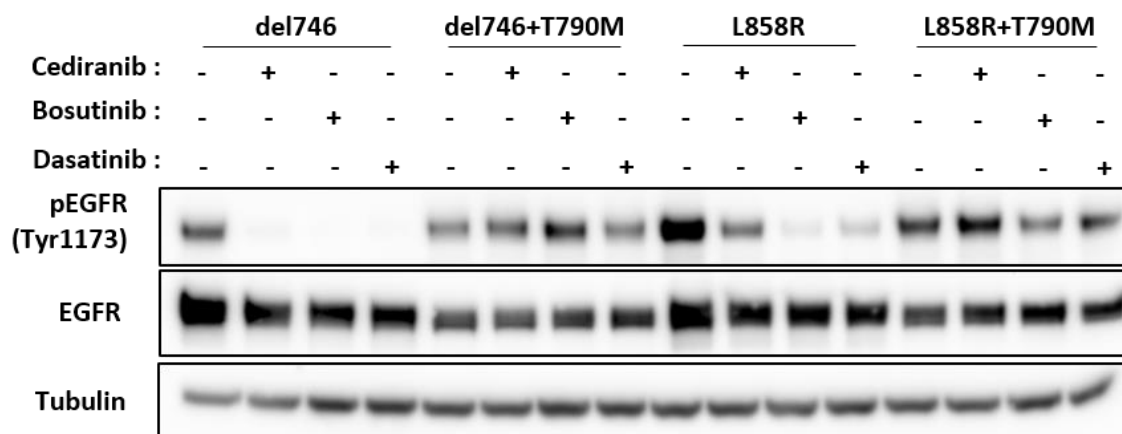


Figure 4.16 - Expression of EGFR-T790M prevents EGFR inhibition following treatment with kinase inhibitors. Western blot showing phosphorylation of EGFR in Ba/F3 cells expressing del746 or L858R, with or without secondary T790M mutations, following 6 h treatment with 2 μ M of the indicated inhibitor. Tubulin was used as a loading control. Blots shown are representative of $n = 2$ biological replicates.

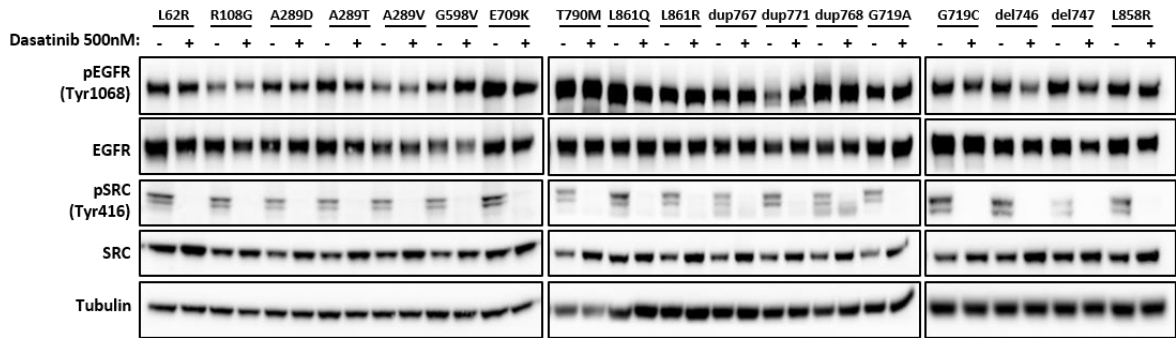
4.11 A289V is inhibited at lower doses of dasatinib compared to L858R

Having established that inhibition of EGFR phosphorylation is the cause of sensitivity to the broad-spectrum TKI identified in the small molecule inhibitor screen, I next sought to understand why certain EGFR mutants were more sensitive to these inhibitors compared to others. To test whether there were any signalling differences between EGFR mutants following treatment with the broad-spectrum TKIs identified in the small molecule inhibitor screen, dasatinib was selected as an exemplar inhibitor for the 6 broad-spectrum TKI and the effect of dasatinib treatment against all mutants was examined. Dasatinib was selected from the 6 broad-spectrum TKIs as Figure 4.6 demonstrated dasatinib is active against all sensitive mutants and Figure 4.13 showed that expression of the T790M gatekeeper mutation rescued the sensitivity of sensitive mutants to dasatinib. This is exemplary of the other broad-spectrum TKIs identified from small molecular inhibitor screen except ponatinib which does not show increased activity against L858R (Figure 4.6) compared with the resistant EGFR mutants and does not show a significant rescue phenotype following expression of T790M in Ba/F3 cells harbouring del746, del747, or L858R (Figure 4.14). All EGFR mutant expressing cells were treated with 500 nM

dasatinib for 6 h prior to lysis. 500 nM dasatinib was used as this is the dose used in the small molecule inhibitor screen: the dose upon which sensitive mutants had a cell viability of 0% and resistant mutants had a cell viability of ~100%. Western blot analysis of these lysates showed that SRC phosphorylation was inhibited in all cells (Figure 4.17 A). As previous experiments had already established that SRC phosphorylation did not contribute to the sensitivity of the cells to dasatinib, and loss of SRC phosphorylation is observed equally across all EGFR mutants regardless of the specific mutant's sensitivity to dasatinib, this effect likely does not explain the increased sensitivity of G719C, del746, del747, and L858R to dasatinib. Dasatinib treatment had little effect on EGFR phosphorylation at this dose (Figure 4.17 A). However, a slight reduction in EGFR phosphorylation was observed in G719C, del746, and del747 following dasatinib treatment compared to DMSO control. This indicated that there were differences in the reduction of EGFR phosphorylation between mutants upon dasatinib treatment, but these differences were small when observing response to a single dose of 500 nM dasatinib. It was hypothesised that these differences may be more apparent over a larger dose range. To test this hypothesis, A289V, a dasatinib-resistant mutant, and L858R, a dasatinib-sensitive mutant, were treated with a dose range of dasatinib for 6 h. SRC phosphorylation and phosphorylation of EGFR at 3 different phospho-sites was measured by western blot (Figure 4.17 B). SRC phosphorylation was potently inhibited at all doses in both mutants, further suggesting that SRC signalling is not the mechanism of sensitivity to dasatinib in these cells. EGFR phosphorylation was reduced at lower doses of dasatinib in cells expressing L858R compared to cells expressing A289V. In L858R expressing cells, EGFR phosphorylation at all 3 phospho-sites measured was clearly reduced at 750 nM of dasatinib. By contrast, in cells expressing A289V the same dose of dasatinib caused no change in EGFR phosphorylation compared to DMSO control at any phospho-site measured (Figure 4.17 B). This indicates that the increased sensitivity of L858R compared with A289V to dasatinib treatment is due to an increased sensitivity of L858R to EGFR inhibition by dasatinib. Figure 4.13 indicates that EGFR inhibition is the mechanism that leads to an increased sensitivity in cells expressing del746, del747, or L858R to all of the broad-spectrum TKIs identified in the small molecule inhibitor screen, with the exception of ponatinib. Taken together with the signalling data presented in Figure 4.17 B, these data suggest that the sensitivity of these mutants to dasatinib, saracatinib, bosutinib,

cediranib, and vandetanib is also caused by an increased sensitivity to EGFR inhibition compared to other EGFR mutants as opposed to an increased dependency of these mutants on SRC signalling compared to other EGFR mutants.

A



B

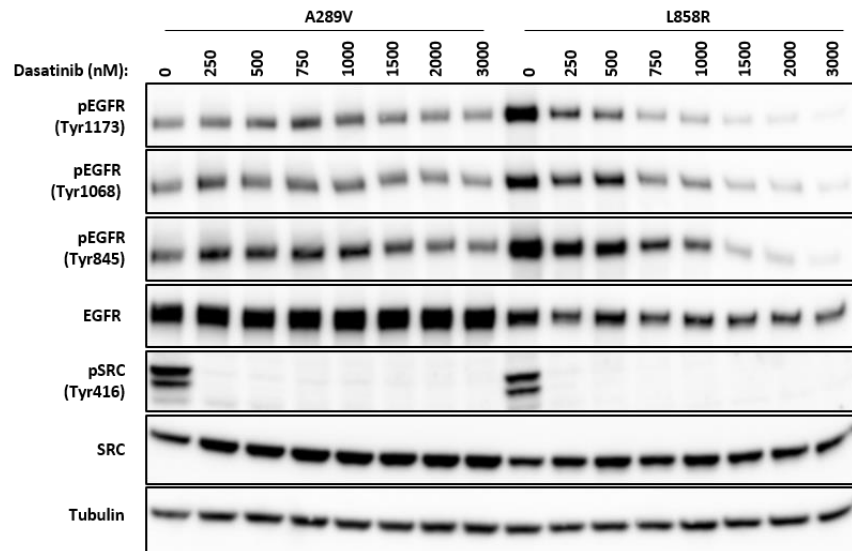


Figure 4.17 – Dasatinib treatment causes loss of SRC phosphorylation in sensitive and resistant EGFR mutants and loss of EGFR phosphorylation at lower doses in a sensitive mutants compared to a resistant mutants. (A) Western blot showing EGFR phosphorylation and SRC phosphorylation in Ba/F3 cells expressing the indicated EGFR mutants upon treatment with 500 nM dasatinib or vehicle control (DMSO) for 6 h. (B) Western blot showing EGFR phosphorylation at Tyr1173, Tyr1068, and Tyr845 and SRC phosphorylation in Ba/F3 cells expressing A289V or L858R upon treatment with the indicated dose of dasatinib or vehicle control (DMSO) for 6 h. (A, B) Tubulin was used as a loading control. Blots shown are representative of $n = 2$ biological replicates.

4.12 Increased sensitivity to small molecule inhibitor screen hits is also observed in a human NSCLC cell line

PC9 cells, a human NSCLC cell line harbouring a del746 mutation in EGFR, were used to validate the findings observed in the Ba/F3 model system. As Ba/F3 cells are murine pro-B cells that have been engineered to be dependent on exogenously expressed EGFR mutants for their growth, it is possible that findings observed in this model system are artefacts and specific to the model system. It is therefore important to confirm that findings from the Ba/F3 cells are also observed in human NSCLC cells that harbour endogenous EGFR mutants. To establish whether the broad-spectrum TKIs identified in the small molecule inhibitor screen targeted SRC or EGFR in PC9 cells, derivative PC9 cell lines expressing SRC-WT, SRC-T338I, or harbouring a secondary T790M mutation in EGFR were generated. To generate SRC-WT and SRC-T338I cell lines, pBABE-hygro constructs containing SRC-WT or SRC-T338I were packaged into retroviruses, along with an empty vector control, and transduced by infection into parental PC9 cells (performed by Simon Vyse, ICR). PC9 cells were then selected with hygromycin and western blotting was used to confirm the expression of the SRC constructs (Figure 4.18 A). To generate PC9 cells harbouring a secondary T790M mutation in EGFR (PC9 EGFR-T790M), PC9 cells were exposed to escalating doses of gefitinib up to 1 μ M (performed by Laura Pacini, ICR) (Figure 4.18 B). Previous studies have shown that culturing PC9 cells in escalating doses of gefitinib until cells acquire resistance to gefitinib leads to the emergence of PC9 cells that harbour a secondary T790M mutation in EGFR (Crystal *et al.*, 2014). The resultant cell line showed an increased resistance to gefitinib compared to parental PC9 cells (Figure 4.18 C). Presence of T790M was confirmed by droplet digital PCR (ddPCR) (performed by Laura Pacini, ICR) (Figure 4.18 D).

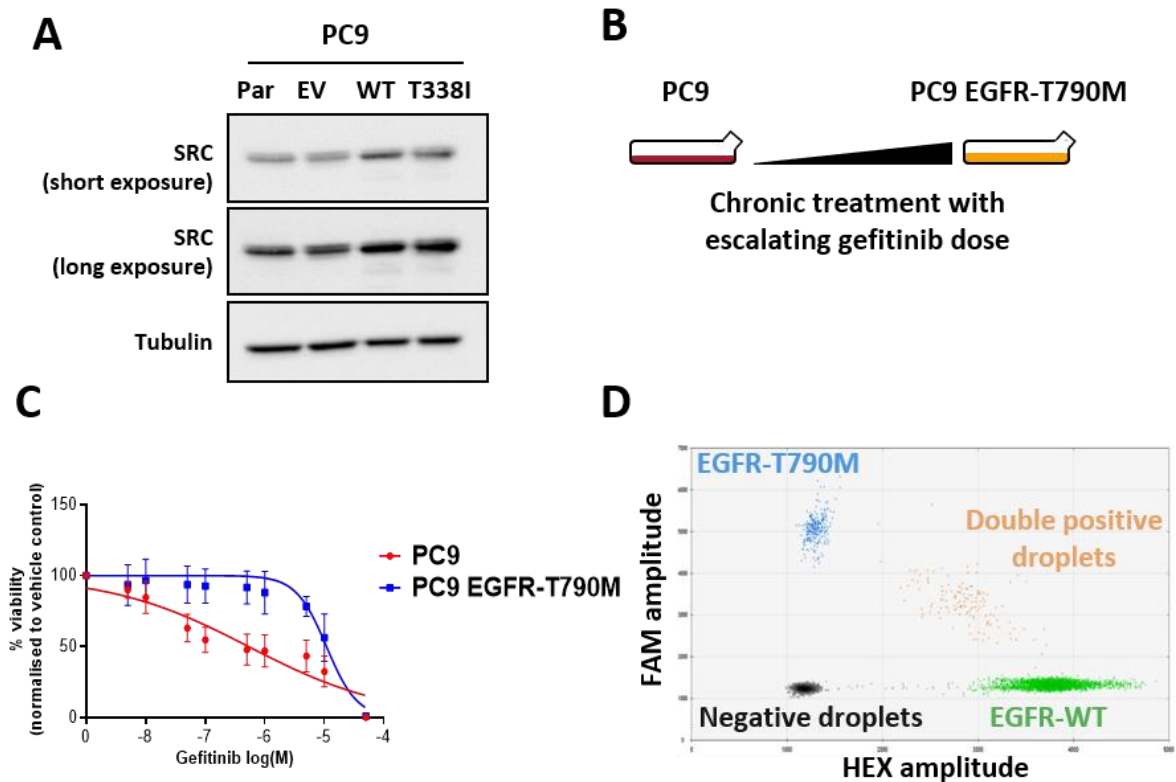


Figure 4.18 – Generation of derivative PC9 cell lines expressing SRC-WT, SRC-T338I, or harbouring a secondary T790M mutation in EGFR. (A) Western blot showing total SRC expression levels in PC9 cells harbouring the indicated constructs. Tubulin was used as a loading control. Blots are $n = 1$ biological replicate. Par = parental, EV = empty vector, WT = wild type. (Simon Vyse, ICR). (B) Schematic of the generation of T790M positive PC9 cells. Briefly, PC9 cells were treated with an IC_{50} dose of gefitinib (65 nM) and cultured until cells reached ~90% confluency. At this point cells were subcultured into a new culture vessel. 24 h after subculturing, the gefitinib dose was increased. This process was repeated until cells could grow in 1 μ M gefitinib (Laura Pacini, ICR). (C) Dose-response curves of PC9 cells and PC9 EGFR-T790M cells upon treatment with gefitinib. Cell viability was measured by Cell Titre Glo and normalised to vehicle control (DMSO). Values represent mean \pm standard deviation from $n = 3$ biological replicates. (D) Scatterplot of fluorescent signal from droplets from genomic DNA extracted from PC9 EGFR-T790M cells. Droplet populations are labelled as follows: EGFR-T790M FAM = blue, EGFR-WT HEX = green, Double positive droplets = orange, droplets lacking fluorescent signal (negative) = black. (Laura Pacini, ICR).

To establish whether inhibition of SRC signalling caused sensitivity to the 6 broad-spectrum TKIs identified in the small molecule inhibitor screen, PC9 cells harbouring either SRC-WT or SRC-T338I were assessed for their sensitivity to dasatinib, saracatinib, bosutinib, cediranib, vandetanib, and ponatinib by treating the cells with

a range of concentrations of each inhibitor for 72 h prior to cell viability measurement with Cell Titre Glo. There was no significant difference in IC_{50} values between PC9 SRC-WT cells and PC9 SRC-T338I cells for any inhibitor with the exception of dasatinib, where PC9 SRC-T338I cells had a significantly higher IC_{50} value compared to PC9 SRC-WT cells (1.70 μ M vs 0.22 μ M for PC9 SRC-T338I cells and PC9 SRC-WT cells respectively) (Figure 4.19 A). The decreased sensitivity of PC9 SRC-T338I cells to dasatinib treatment compared with PC9 SRC-WT cells contrasts with observations from the Ba/F3 model system where no significant differences in dasatinib sensitivity were detected between cells expressing SRC-WT and SRC-T338I (Figure 4.11, Figure 4.12) with the exception of Ba/F3 cells harbouring del746, where expression of SRC-T338I actually increased dasatinib sensitivity compared to expression of SRC-WT (Figure 4.15). In Ba/F3 cells expressing del746, SRC-WT appeared have a “sink” effect on dasatinib and expression of SRC-T338I reversed this effect leading to increased sensitivity of del746 cells expressing SRC-T338I compared to del746 cells expressing SRC-WT. By contrast, in PC9 cells expression of SRC-T338I decreases dasatinib sensitivity compared with SRC-WT. Together, these data indicate that PC9 cells have a dependency on SRC signalling that is not observed in Ba/F3 cells harbouring del746.

To investigate whether inhibition of EGFR signalling caused sensitivity to the 6 broad-spectrum TKI identified in the small molecule inhibitor screen the sensitivity of parental PC9 cells and PC9 EGFR-T790M cells to dasatinib, saracatinib, bosutinib, cediranib, vandetanib, and ponatinib was compared. As was observed in the Ba/F3 experiments, PC9 EGFR-T790M cells had significantly higher IC_{50} values compared to the parental cells for all inhibitors except ponatinib (Figure 4.19 B). Notably, the increase in IC_{50} value upon dasatinib treatment was greater between parental PC9 cells and PC9 EGFR-T790M cells (14.3-fold increase in IC_{50} value) compared with the increase in IC_{50} value between PC9 SRC-WT cells and PC9 SRC-T338I cells (7.7-fold increase in IC_{50} value). This suggests that the sensitivity of PC9 cells to dasatinib treatment is caused by a combination of SRC inhibition as well as EGFR inhibition and that inhibition of EGFR signalling has the larger impact on PC9 cell viability. This contrasts with observations from Ba/F3 cell harbouring del746, where EGFR inhibition appeared to be the sole determinant of dasatinib sensitivity (Figure 4.15). Possible mechanisms for the role of EGFR inhibition and

SRC inhibition in the sensitivity of PC9 cells to dasatinib are discussed in section 4.13 . Taken together these data indicate that, as was observed in the Ba/F3 model system, the primary mechanism leading to sensitivity to dasatinib, saracatinib, bosutinib, cediranib, and vandetanib is due to inhibition of EGFR signalling and not due to inhibition of SRC signalling.

As in the Ba/F3 experiments, this hypothesis was tested using dasatinib as an exemplar of the other broad-spectrum TKIs identified in the small molecule inhibitor screen. Parental PC9 cells and PC9 EGFR-T790M cells were treated with a dose range of dasatinib for 6 h prior to lysis. Western blot analysis showed that EGFR phosphorylation was inhibited at 1000 nM dasatinib in PC9 cells, whereas EGFR phosphorylation was sustained at 1000 nM dasatinib in PC9 EGFR-T790M cells (Figure 4.19 C). SRC phosphorylation was inhibited at 100 nM dasatinib in both cell lines. Together, these data demonstrate that, in the context of a human NSCLC cell line, del746 EGFR mutants are sensitive to inhibition by dasatinib.

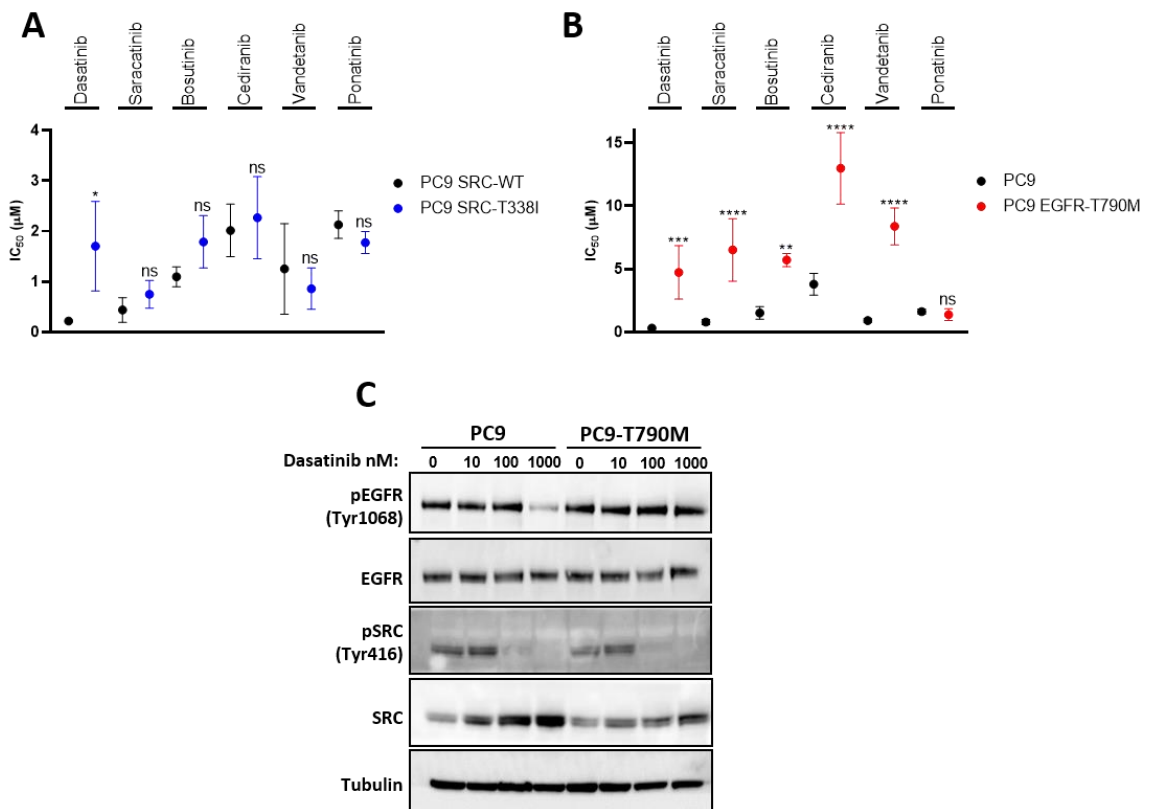


Figure 4.19 – EGFR-T790M rescues kinase inhibitor sensitivity in human PC9 NSCLC cells with endogenous del746. (A) Plot showing IC₅₀ values of PC9 cells expressing either SRC-WT or SRC-T338I upon treatment with dasatinib, saracatinib, bosutinib, cediranib, vandetanib, or ponatinib. (B) Plot showing IC₅₀ values of PC9 cells and

PC9 EGFR-T790M cells upon treatment with dasatinib, saracatinib, bosutinib, cediranib, vandetanib, or ponatinib. (A, B) Cells were treated with each inhibitor at a range of doses for 72 h. Viability was measured by Cell Titre Glo. IC₅₀ was calculated using four-parameter non-linear regression analysis performed on GraphPad Prism 8. Values represent mean ± standard deviation from $n = 3$ biological replicates. Statistical significance was calculated by Sidak's Multiple Comparisons test. * = $p < 0.05$, ** = $p < 0.01$, *** = $p < 0.001$, **** = $p < 0.0001$, ns = not significant. WT = wild-type. (C) Western blot showing EGFR phosphorylation and SRC phosphorylation in PC9 cells and PC9 EGFR-T790M cells upon treatment with the indicated doses of dasatinib for 6 h. Tubulin was used as a loading control. Blots shown are representative of $n = 2$ biological replicates.

4.13 Discussion

Assessing the sensitivity of EGFR mutants to available EGFRi has previously been used to identify the optimal EGFRi for distinct EGFR mutants and has resulted in the approval of afatinib for NSCLC patients harbouring S768I, G719X, or L861Q mutants; a patient population for whom there was previously no approved anti-EGFR therapy (Kobayashi *et al.*, 2015; Yang *et al.*, 2015a). This approach has also led to the identification of poziotinib as an EGFRi that is capable of inhibiting Ex20Ins mutations (Robichaux *et al.*, 2018). Large scale preclinical screening efforts have profiled the sensitivity of EGFR mutants to some clinically available EGFRi (Kohsaka *et al.*, 2017). However, not all clinically available EGFRi have been assessed and novel EGFRi currently under development have not been examined for use against a broad range of EGFR mutants. In this chapter, the sensitivity of 18 EGFR mutants from across all cancer types to seven EGFRi was examined including the Ex20Ins-targeting EGFRi poziotinib and TAS6417, which are assessed for their efficacy against a large panel of EGFR mutants for the first time here.

Interestingly, del747 appeared marginally more sensitive to gefitinib, erlotinib, and rociletinib compared to del746. Differences in the EGFRi sensitivities of patients harbouring distinct Ex19Del variants have previously been reported (Chung *et al.*, 2012; Lee *et al.*, 2013; Kaneda *et al.*, 2014), however the data is controversial and there is no consensus on the prognostic implications of different Ex19Del in terms of sensitivity to EGFRi. A notable observation described in this chapter is the

sensitivity of extracellular domain mutants to afatinib, osimertinib, poziotinib, and TAS6417. Extracellular domain mutants are most commonly observed in GBM; a disease that currently has no approved anti-EGFR therapies. These observations are particularly exciting as both afatinib and osimertinib have been shown to penetrate the blood-brain barrier (Hoffknecht *et al.*, 2015; Ahn *et al.*, 2019). Although afatinib had limited efficacy in an unselected cohort of GBM patients (Reardon *et al.*, 2014), data presented in this chapter indicates that GBM patients with EGFR mutations may be sensitive to afatinib. Future clinical investigation of afatinib should focus on GBM patients with extracellular domain mutations in EGFR to examine the possibility that afatinib would be effective in this population. A phase I/II clinical trial is currently assessing the efficacy of osimertinib in GBM (NCATS 1-UH2-TR001370-01). The data from this trial will help translate the findings presented in this thesis and elsewhere (Kohsaka *et al.*, 2017) into clinical practice. Future work should focus on *in vivo* experiments to determine the CNS activity of TAS6417 and poziotinib to urgently assess the utility of these inhibitors for this group of patients who currently have very limited therapeutic options. Another notable observation described in this chapter is that it is not the case that all extracellular mutants are sensitive to lapatinib while all intracellular mutants are not, as has previously been indicated (Vivanco *et al.*, 2012). Although data presented in this chapter confirmed previous data that lapatinib is more active against the extracellular mutants A289D, A289V, and G598V, compared with the intracellular mutant del746 (Vivanco *et al.*, 2012), it also demonstrated for the first time that G719A, G719C, L861R, and L861Q are more sensitive to lapatinib compared to A289D, with G719A and G719C being the most sensitive EGFR mutants tested.

One shortcoming of this study is the use of the Ba/F3 model system. Although Ba/F3 cells have been used extensively to study the sensitivity of EGFR mutants to EGFRi, human cancer cell lines harbouring endogenous EGFR mutants are more representative of the clinical scenario as they more faithfully replicate the genetic background observed in tumour tissues. Although it was possible to validate the data reported for del746 in the Ba/F3 model system using PC9 cells, the lack of human cancer cell lines harbouring less common EGFR mutants means that use of model systems is the only way to study these mutants in the preclinical setting. This highlights the need to generate new cell lines that harbour endogenous rare EGFR

mutants, which is discussed further in chapter 6. Another caveat is that the use of cell line models does not always mirror a drug's activity in patients. This is exemplified in Vivanco *et al.*'s study of lapatinib in GBM, which demonstrated that lapatinib potently inhibited extracellular domain EGFR mutants in GBM cell lines but did not achieve sufficient intratumoural concentrations to inhibit EGFR in GBM patients (Vivanco *et al.*, 2012). Similarly, poziotinib showed activity against cell line models harbouring T790M mutations (Cha *et al.*, 2012) but showed low activity in T790M-positive patients in a phase II clinical trial (Han *et al.*, 2017). These examples encourage caution when interpreting results from cell line models and highlight the necessity of *in vivo* and clinical studies. This is particularly pertinent when considering the results of this EGFRi screen, as the data indicates that afatinib, osimertinib, TAS6417, and poziotinib could all be effective treatment options for patients with extracellular domain mutants. As this class of mutants most commonly occurs in GBM, a disease for which there are no clinically approved anti-EGFR therapies available, these results are potentially very exciting. However, further *in vivo* studies will be essential to validate these inhibitors as potential treatment options for patients harbouring these mutants.

Data presented in this chapter also builds on previous studies which have shown that multi-target kinase inhibitors can inhibit certain EGFR mutants but were restricted to a limited selection of intracellular domain mutants (Formisano *et al.*, 2015; Duong-Ly *et al.*, 2016), identifying G719C, del746, del747, and L858R as more sensitive to dasatinib, saracatinib, bosutinib, cediranib, vandetanib, and ponatinib compared to the other EGFR mutants in the panel. As it has previously been shown that different EGFR mutants can activate distinct downstream signalling networks (Moscatello *et al.*, 1998; Pines *et al.*, 2010), a series of experiments was performed to provide evidence that this increased sensitivity was due to EGFR inhibition and not due to a mutant-specific dependency on SRC signalling. Data presented in this chapter indicate that the increased sensitivity of G719C, del746, del747, and L858R to the 6 broad-spectrum TKI identified in the small molecule inhibitor screen compared to the other EGFR mutants in the panel is caused by inhibition of EGFR signalling at lower inhibitor doses.

Notably, del746 cells expressing SRC-T338I were more sensitive to dasatinib compared with del746 cells expressing SRC-WT. Western blot analysis showed that

cells expressing SRC-T338I sustained EGFR phosphorylation at higher doses compared to cells expressing SRC-WT, but lost EGFR phosphorylation at lower doses compared to cells expressing SRC-WT. The inability of dasatinib to inhibit SRC-T338I and concurrent increased inhibition of EGFR indicates that SRC may be able to act as a “sink” for dasatinib, with increased cytoplasmic dasatinib available to inhibit EGFR in cells expressing SRC-T338I compared with those expressing SRC-WT causing increased dasatinib sensitivity. However, further kinetic experiments to confirm the increased binding of dasatinib to EGFR and decreased binding of dasatinib to SRC in cells expressing SRC-T338I are needed to confirm this hypothesis. By contrast, similar experiments performed in the human NSCLC cell line PC9, which harbours a del746 mutation in EGFR, identified a decreased dasatinib sensitivity in PC9 SRC-T338I cells compared to PC9 SRC-WT cells. A possible explanation for this discrepancy between the Ba/F3 model system and PC9 cells is that PC9 cells have an increased sensitivity to inhibition of SRC signalling that is independent of EGFR signalling. Previous studies have shown that SRC is active in human NSCLC cell lines that harbour a del746 mutation in EGFR, and that EGFR and SRC inhibitor combinations are synergistic (Song *et al.*, 2006; Zhang *et al.*, 2007). Furthermore, SRC signalling that is independent of EGFR signalling has been observed in PC9 cells with an acquired T790M mutation following chronic exposure to gefitinib (Yoshida *et al.*, 2014) or afatinib (Ichihara *et al.*, 2017). Together, these data suggest that the decreased dasatinib sensitivity of PC9 SRC-T338I cells compared to PC9 SRC-WT cells may be due to an inherent dependency of PC9 cells on SRC signalling that is independent of EGFR signalling. Importantly, the decrease in dasatinib sensitivity between PC9 EGFR-T790M cells and parental PC9 cells was greater than the decrease in dasatinib sensitivity between PC9 SRC-T338I cells and PC9 SRC-WT cells. This indicates that inhibition of EGFR by dasatinib has a greater impact on PC9 cell viability compared to inhibition of SRC by dasatinib. An important caveat to be aware of when interpreting data from these cell lines is the different approaches by which they were engineered. The SRC-WT and SRC-T338I expressing PC9 cells were generated by retroviral transduction of expression vectors encoding SRC-WT or SRC-T338I. PC9 cells harbouring a secondary EGFR-T790M mutation were generated by exposing PC9 cells to escalating concentrations of gefitinib until they were able to grow in 1 μ M of gefitinib. Exposure to increasing concentrations of gefitinib could have caused additional

alterations within the PC9 cells that were not detected which could affect the cells' sensitivity to the hits from the small molecule inhibitor screen. Additionally, it has been reported that PC9 cells can take different evolutionary routes to acquiring gefitinib resistance (Hata *et al.*, 2016). This raises the possibility of distinct clonal populations existing within the PC9 EGFR-T790M cells, which may affect the data generated using them.

Improvements to the design of the small molecule inhibitor screen could have led to the identification of more inhibitors with activity against EGFR mutants. In this chapter, a single concentration was used for all inhibitors with the exception of luminespib. A lower dose of luminespib was used as it has previously been shown to be highly to be a highly potent compound (Akahane *et al.*, 2016; Jorge *et al.*, 2018). Similar approaches could have been taken with the other inhibitors included in the screen; tailoring the concentration of each inhibitor based on known potencies. Such an approach would have ensured that each inhibitor was used at a concentration most likely to distinguish sensitive mutants from resistance mutants and may have led to the identification of more inhibitors with activity against EGFR mutants.

An interesting finding from the data presented here is the differences in inhibitor sensitivity observed between different substitutions of the same amino acid. For example, G719A was consistently less sensitive to EGFRi compared to G719C, with the exception of poziotinib and the second-generation EGFRi afatinib and neratinib. This trend was also observed in the small molecule inhibitor screen: G719A is less sensitive to saracatinib, bosutinib, cediranib, vandetanib and dasatinib compared to G719C. These results add to existing data showing that EGFR mutants, even those that occur at the same amino acid, do not respond equivalently to targeted therapy (Kobayashi and Mitsudomi, 2016). Future work focusing on the precise structural changes that are caused by subtly different mutations and the effect they have on inhibitor binding could improve our understanding of EGFR mutants and facilitate improvements in our ability to target them therapeutically.

Despite the availability of approved inhibitors for patients whose tumours harbour G719C, del746, del747, and L858R, the 6 broad-spectrum TKI identified in this chapter may have potential clinical application. First, it is possible that resistance

mechanisms to these inhibitors may be distinct from the known resistance mechanisms to approved first- and third-generation EGFRi. If this were the case, then it may mean that approved first- and third-generation EGFRi would be effective treatments following progression on first-line therapy using 1 of the 6 broad-spectrum TKI identified here. Such a strategy would add lines of therapy to a patient's treatment and could prolong the period in which a patient is responding to therapy. Second, as these inhibitors are broad-spectrum it is possible that they may improve patient responses through polypharmacology: utilising a single drug to target multiple signalling pathways (Antolin *et al.*, 2016). Use of these inhibitors target multiple signalling pathways in addition to EGFR could block bypass signalling pathways and thereby delay acquired resistance. Furthermore, cediranib, ponatinib, and vandetanib have been shown to also inhibit VEGF signalling (Roskoski, 2015; Kim *et al.*, 2017). Combined inhibition of EGFR signalling and VEGF signalling could target a tumour by blocking growth signalling within tumour cells and angiogenesis simultaneously. Finally, the ability to inhibit multiple targets may enable these inhibitors to overcome resistance in patients with unknown resistance mechanisms to first- and third-line EGFRi. Around 10% and 30-50% of acquired resistance to first- and third-generation EGFRi, respectively, occurs via an unknown mechanism (Westover *et al.* 2018; Leonetti *et al.*, 2019). Employing broad-spectrum inhibitors with proven activity against EGFR signalling could overcome these resistance mechanisms.

Of the 6 broad-spectrum TKI identified in this chapter, dasatinib has been most thoroughly investigated in NSCLC clinical trials (Johnson *et al.*, 2010; Kruser *et al.*, 2011). These trials included patients with both EGFR-mutant and KRAS-mutant NSCLC and reported modest efficacy (disease control rate = 43%). However, EGFR mutation status was not found to be predictive of response to dasatinib. Dasatinib treatment in patients with NSCLC exacerbated pleural effusions, a build-up of fluid in the pleural cavity surrounding the lungs (Froudarakis, 2012). Pleural effusions have also been observed in ALL and CML patients receiving dasatinib treatment (Brixey and Light, 2010). Despite this, prolonged treatment and clinical benefit from dasatinib therapy can be achieved with early identification and management of pleural effusions (Cortes *et al.*, 2017). Combination of dasatinib with EGFRi therapy in patients with molecularly unselected NSCLC is well tolerated, but no significant

disease control in EGFR-mutant NSCLC has been reported (Haura *et al.*, 2010; Johnson *et al.*, 2011; Creelan *et al.*, 2019). However, it is important to note that in the largest trial to assess dasatinib and EGFRi combination therapy the majority of patients harboured secondary T790M mutations (75%), indicating that dasatinib therapy may be ineffective in patients with this mutation (Johnson *et al.*, 2011). This finding is consistent with data reported in this chapter. The lack of molecular selection is an important caveat when considering these clinical trial results; notably, in a clinical trial of 33 unselected NSCLC patients receiving combined dasatinib and erlotinib treatment, PR (which was the best overall response reported in the study) was observed only in the 5 patients who harboured EGFR mutations. Additionally, combination of dasatinib and the third-generation EGFRi osimertinib has been shown to be highly effective against PC9 cells with acquired EGFRi resistance (Ichihara *et al.*, 2017; Watanabe *et al.*, 2017) and is currently being investigated in an ongoing phase I/II clinical trial (NCT02954523). Together, these data indicate that further clinical investigation of dasatinib, alone or in combination with EGFRi, in clinical cohorts selected for the sensitising mutations identified in this chapter (ie: G719C, del746, del747, and L858R) may identify clinical benefit in this population. Although there are no clinical data describing the efficacy of cediranib or bosutinib in NSCLC, bosutinib treatment has been shown to be well tolerated in patients with solid tumours (Daud *et al.*, 2012). Interestingly, a phase II clinical trial of saracatinib treatment in a molecularly unselected cohort of NSCLC patients found no correlation between clinical outcome and SRC expression (Laurie *et al.*, 2014). Furthermore, objective response was only observed in a patient with an Ex19Del mutation in EGFR. Together, these data suggest that the saracatinib sensitivity observed in this NSCLC patient was caused by inhibition of EGFR and not inhibition of SRC. This is consistent with observations described in this chapter and indicates that further clinical investigation of saracatinib in NSCLC patients with sensitising EGFR mutations is warranted. Ponatinib and vandetanib have shown efficacy in RET-rearranged NSCLC (Lee *et al.*, 2017b; Yoh *et al.*, 2017; Gainor *et al.*, 2020). Although there are no clinical data regarding the use of ponatinib for the treatment of EGFR-mutant NSCLC, a phase III clinical trial of molecularly unselected NSCLC patients observed greater clinical benefit in terms of both PFS and OS in patients with EGFR mutations (Heymach *et al.*, 2014). This observation indicates that NSCLC patients with EGFR mutations are sensitive to ponatinib treatment. Future

clinical studies focusing on NSCLC patients with EGFR mutations are essential to establish this.

Together, data presented in this chapter have built on published data to provide a more complete picture of the sensitivities of EGFR mutants from all cancer types to EGFRi and other small molecule inhibitors (Figure 4.1). A notable finding from this chapter is the efficacy of afatinib, osimertinib, poziotinib, and TAS6417 against extracellular domain mutants. Further investigation of these inhibitors in intracranial *in vivo* models is warranted to examine their CNS activity and clinical studies focusing on patients whose tumours harbour the sensitive EGFR mutants identified in this chapter are essential to establishing their efficacy in this population. Furthermore, data presented in this chapter has identified a number of small molecule inhibitors that inhibit EGFR on a mutant-specific basis. Future experiments should investigate the affinity of these inhibitors for distinct EGFR mutants by employing *in vitro* kinase assays such as those described by Carey *et al.* to demonstrate the increased affinity of erlotinib for del746 and L858R compared to WT-EGFR (Carey *et al.*, 2006). Such experiments could establish that the mutant-specific sensitivity observed in this chapter is caused by increased inhibitor binding to distinct EGFR mutants. Furthermore, the preclinical data demonstrating the sensitivity of specific EGFR mutants to these small molecule inhibitors supports preliminary observations from clinical trials that indicate their efficacy in patients. Taken together, these findings provide rationale for further clinical investigation focusing specifically on NSCLC patients whose tumours harbour the sensitising EGFR mutants identified in this chapter.

Chapter 5

Resistance mechanisms to EGFRi in exon 20 insertion mutant cells

5.1 Introduction

Although Ex20Ins mutations are the most frequent *EGFR* mutations after the common mutations L858R and Ex19Del, there are currently no approved targeted therapies for patients harbouring this class of mutations. Clinical studies have found that although responses to chemotherapy among patients with Ex20Ins mutations is similar to patients with L858R or Ex19Del mutations, patients harbouring Ex20Ins have a significantly shorter TTP when treated with the first-generation EGFRi erlotinib compared to patients harbouring L858R or Ex19Del (3 vs. 12 months, $p < 0.01$) (Naidoo *et al.*, 2015). This poor response to EGFRi is due to a combination of structural rearrangements caused by the Ex20Ins mutation that prevents EGFRi from binding to the ATP-binding site, and the ability of Ex20Ins mutant EGFR to induce kinase activity without reducing ATP affinity, which prevents EGFRi from outcompeting ATP in the kinase domain (Yasuda *et al.*, 2013; Robichaux *et al.*, 2018). Despite this, specific Ex20Ins mutants are sensitive to currently available EGFRi, as discussed in chapter 1. Preclinical studies have shown that Ba/F3 cells expressing D770delinsGY are sensitive to the second-generation EGFRi dacomitinib and afatinib (Kosaka *et al.*, 2017) and that xenograft models bearing D770_N771insSVD and V769_D770InsASV mutants are sensitive to the third-generation EGFRi osimertinib (Floc'h *et al.*, 2018). Additionally, clinical studies have found that patients harbouring the A763_Y764insFQEA insertion achieved partial responses to erlotinib (Arcila *et al.*, 2013; Voon *et al.*, 2013; Naidoo *et al.*, 2015). However, Ex20Ins are a heterogeneous class of mutations and the majority do not respond to currently available EGFRi (Sequist *et al.*, 2010b; Beau-Faller *et al.*, 2013; Naidoo *et al.*, 2015; Yang *et al.*, 2015a). To address this problem, a number of inhibitors that are capable of targeting Ex20Ins mutant EGFR have been developed (Vyse and Huang, 2019). Of these inhibitors, 3 are currently undergoing clinical investigation: poziotinib is being assessed in the ZENITH20 phase II trial (NCT03066206); TAS6417 is being investigated in a first-in-human phase I/IIa trial (NCT04036682); and mobocertinib is being studied in the EXCLAIM phase I/II trial (NCT02716116), preliminary results of which led to Breakthrough Therapy Designation from the FDA, and the EXCLAIM-2 phase III trial (NCT04129502), which is now enrolling patients.

Whilst the development of EGFRi capable of targeting Ex20Ins mutant EGFR may bring significant clinical benefit for patients harbouring these mutants, experience with previous generations of EGFRi in common sensitising EGFR mutants leads to the expectation that patients will develop acquired resistance to these inhibitors. As described in chapter 1, there are numerous resistance mechanisms to first-generation EGFRi, the most common of which is the T790M point mutation (Yu *et al.*, 2013). Although third-generation EGFRi are able to overcome T790M-mediated resistance to first-generation EGFRi, numerous resistance mechanisms to third-generation EGFRi have also been described, the most common of which is the C797S point mutation (Thress *et al.*, 2015; Papadimitrakopoulou *et al.*, 2018; Leonetti *et al.*, 2019b). In order to achieve durable responses with EGFRi therapy it is essential to identify mechanisms of acquired resistance and develop approaches to address resistant disease. As Ex20Ins-targeting EGFRi progress through clinical trials, preclinical studies aimed at identifying both potential resistance mechanisms to these inhibitors and salvage therapies to overcome acquired resistance will provide valuable information for the treatment of patients harbouring Ex20Ins mutant EGFR.

ENU mutagenesis screens have previously been used to identify candidate resistance mutations to the EGFRi dacomitinib, afatinib, and osimertinib (Ercan *et al.*, 2015; Kobayashi *et al.*, 2017, 2018). ENU is an alkylating agent that most commonly causes A->T transversion and AT->CG transitions, but has also been shown to cause GC->AT transitions (Coghill *et al.*, 2002; Nolan *et al.*, 2002). ENU is used to generate a large number of mutant alleles in a population of cells which are subsequently chronically treated with an inhibitor. This selects for mutant alleles that enable growth in the presence of the inhibitor and thereby facilitates the identification of resistance-causing mutations. In this chapter, ENU mutagenesis screens are used to identify candidate resistance-causing mutations to Ex20Ins-targeting EGFRi in Ba/F3 cells expressing dup767, dup768, or dup771 mutant EGFR and a small molecule inhibitor screen is used to identify potential salvage therapies.

5.2 Ba/F3 cells expressing Ex20Ins mutants are resistant to gefitinib but sensitive to poziotinib and TAS6417

Dose-response experiments were used to confirm that Ba/F3 cells expressing dup767, dup768, or dup771 Ex20Ins mutants are resistant to gefitinib, but are sensitive to poziotinib and TAS6417 (Figure 5.1 A), as previously described (Hasako *et al.*, 2018; Robichaux *et al.*, 2018). As expected, all Ex20Ins mutants were 35 – 72-fold more sensitive to TAS6417 and 611 – 800-fold more sensitive to poziotinib compared to gefitinib. Additionally, all Ex20Ins mutants were more sensitive to poziotinib compared to TAS6417 (Figure 5.1 B) (IC_{50} values for poziotinib and TAS6417 respectively = 3.27 nM vs 56.26 nM for dup767, 4.01 nM vs 44.17 nM for dup768, and 4.59 nM vs 81.61 nM for dup771). To confirm that these differences in sensitivity were due to inhibition of EGFR phosphorylation, Ba/F3 cells expressing the different Ex20Ins mutants were treated with a dose range of each inhibitor for 6 h. Western blot analysis confirmed that EGFR phosphorylation was not reduced in any Ex20Ins mutant expressing Ba/F3 cell line following treatment with doses up to 1 μ M of gefitinib (Figure 5.2). By contrast, EGFR phosphorylation was potently inhibited in all Ex20Ins mutant expressing Ba/F3 cell lines upon treatment with 10 nM poziotinib or 1 μ M TAS6417. Notably, in all Ex20Ins expressing Ba/F3 cell lines EGFR phosphorylation was inhibited at lower doses of poziotinib compared to TAS6417, which is consistent with cell viability data showing that all Ex20Ins expressing Ba/F3 cells are more sensitive to poziotinib compared with TAS6417. Taken together, these data confirm previously published data from Ba/F3 cells that Ex20Ins mutants are sensitive to poziotinib and TAS6417, but are resistant to gefitinib (Hasako *et al.*, 2018; Robichaux *et al.*, 2018).

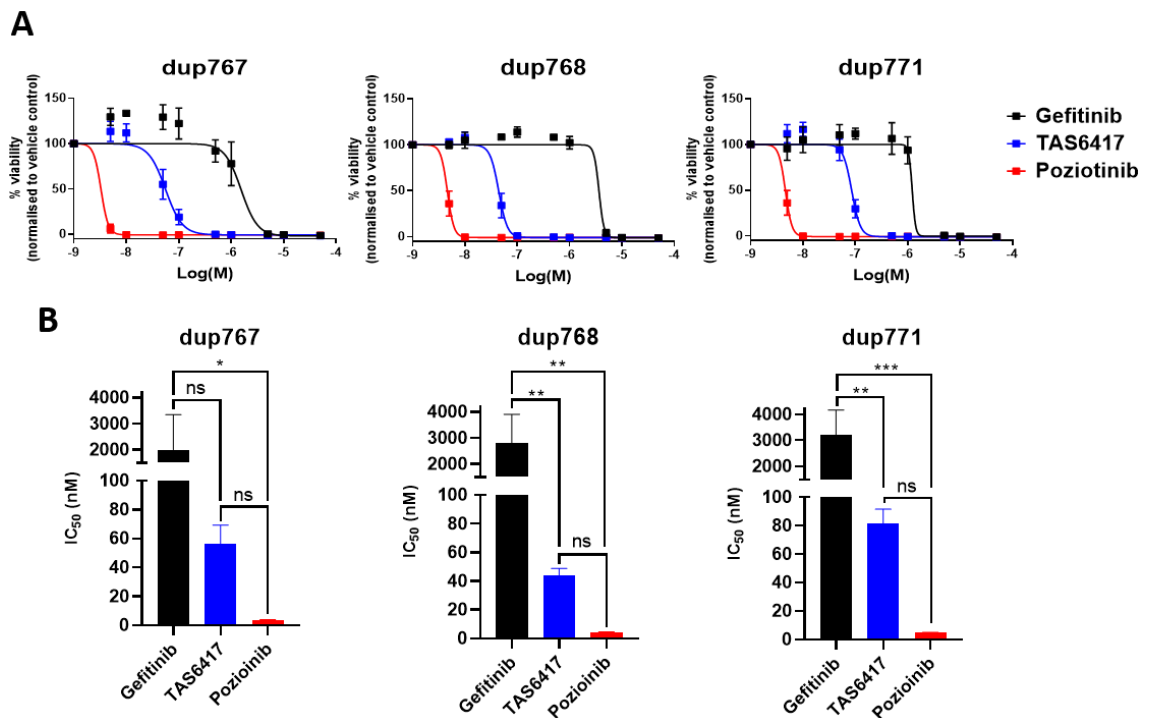


Figure 5.1 – Ex20Ins mutants are more sensitive to poziotinib and TAS6417 compared with gefitinib. (A) Dose-response curves for Ba/F3 cells expressing the indicated EGFR mutant upon treatment with gefitinib, TAS6417, or poziotinib. Cell viability was measured by Cell Titre Glo and normalised to vehicle control (DMSO). (B) Bar charts showing the IC₅₀ values for Ba/F3 cells expressing the indicated EGFR mutant upon treatment with gefitinib, TAS6417, or poziotinib calculated from A. IC₅₀ was calculated using four-parameter non-linear regression analysis performed on GraphPad Prism 8. Statistical significance for the indicated pairwise comparisons was calculated by Tukey’s multiple comparisons test. * = $p < 0.05$, ** = $p < 0.01$, *** = $p < 0.001$, ns = not significant. (A, B) Values represent mean \pm standard deviation from $n = 3$ biological replicates.

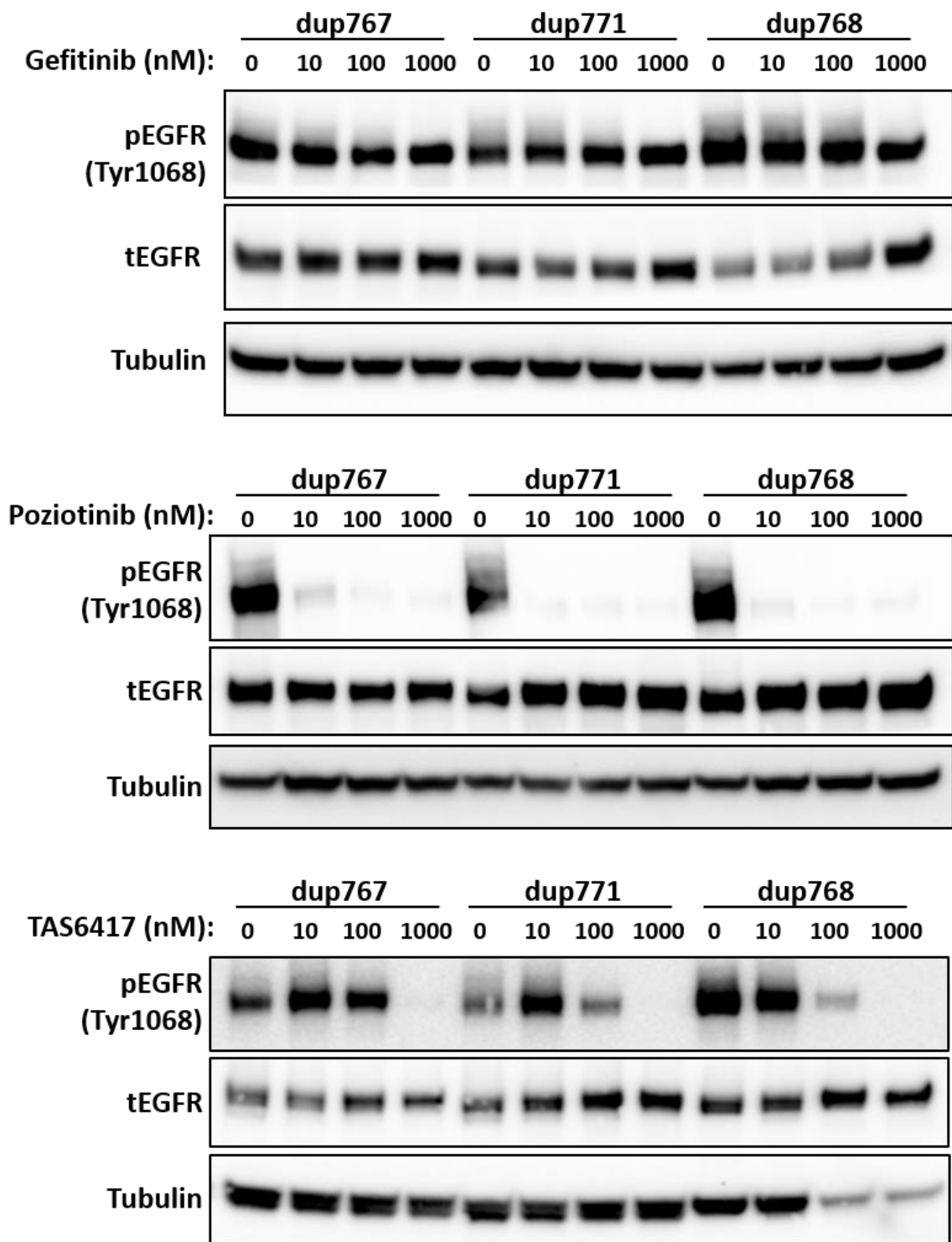


Figure 5.2 – Phosphorylation of Ex20Ins mutant EGFR is reduced by poziotinib and TAS6417 but not by gefitinib. Western blots showing EGFR phosphorylation in Ba/F3 cells expressing the indicated Ex20Ins EGFR mutants following 6 h treatment with gefitinib, TAS6417, or poziotinib at the indicated doses. Tubulin was used as a loading control. *n* = 1 biological replicates.

5.3 An ENU mutagenesis screen identifies potential resistance mechanisms to poziotinib and TAS6417 treatment

An ENU mutagenesis screen was employed to investigate resistance mechanisms to poziotinib and TAS6417 in Ba/F3 cells expressing Ex20Ins mutants. ENU mutagenesis screens were performed as previously described (Katayama *et al.*, 2015). Briefly, 66 – 100 million cells were treated with 100 µg/ml ENU for 24 h (Figure 5.3). Following this, ENU was removed from the cells by centrifugation and the cells were washed 3x with PBS before being allowed to recover in growth medium for 24 h. Cells were then divided into aliquots, treated with the appropriate inhibitor at the desired concentration, and distributed over 3 – 5 96-well plates at a density of 50,000 cells/well. 96-well plates were regularly monitored for signs of growth by visual inspection under a microscope and scaled up from 96-well plates into 24-well plates upon reaching confluency. Inhibitor concentration was kept constant throughout. Once cells reached confluency in 24-well plates a cell pellet was collected for DNA extraction and an aliquot of cells was frozen for future experiments.

To determine a selection dose to be used following ENU mutagenesis, IC_{99} for poziotinib and TAS6417 was calculated for each of the Ex20Ins-expressing Ba/F3 cell lines (IC_{99} upon treatment with poziotinib = 1.77 nM, 2.03 nM, and 2.38 nM for dup767, dup768, and dup771 respectively. IC_{99} upon treatment with TAS6417 = 20.27 nM, 24.07 nM, 45.17 nM for dup767, dup768, and dup771 respectively) (Figure 5.4). Based on these calculations, an initial selection dose of 2 nM was selected for poziotinib and 50 nM for TAS6417. However, selection using these doses resulted in cell growth in all wells which cells were distributed into. It was therefore concluded that 2 nM poziotinib and 50 nM TAS6417 are insufficient to select for resistant subpopulations. ENU mutagenesis was repeated and cells were selected with 10 nM poziotinib. However, this also resulted in cell growth in a large number of wells. Therefore, resistant subpopulations were selected for using 100 nM and 200 nM poziotinib and 500 nM TAS6417.

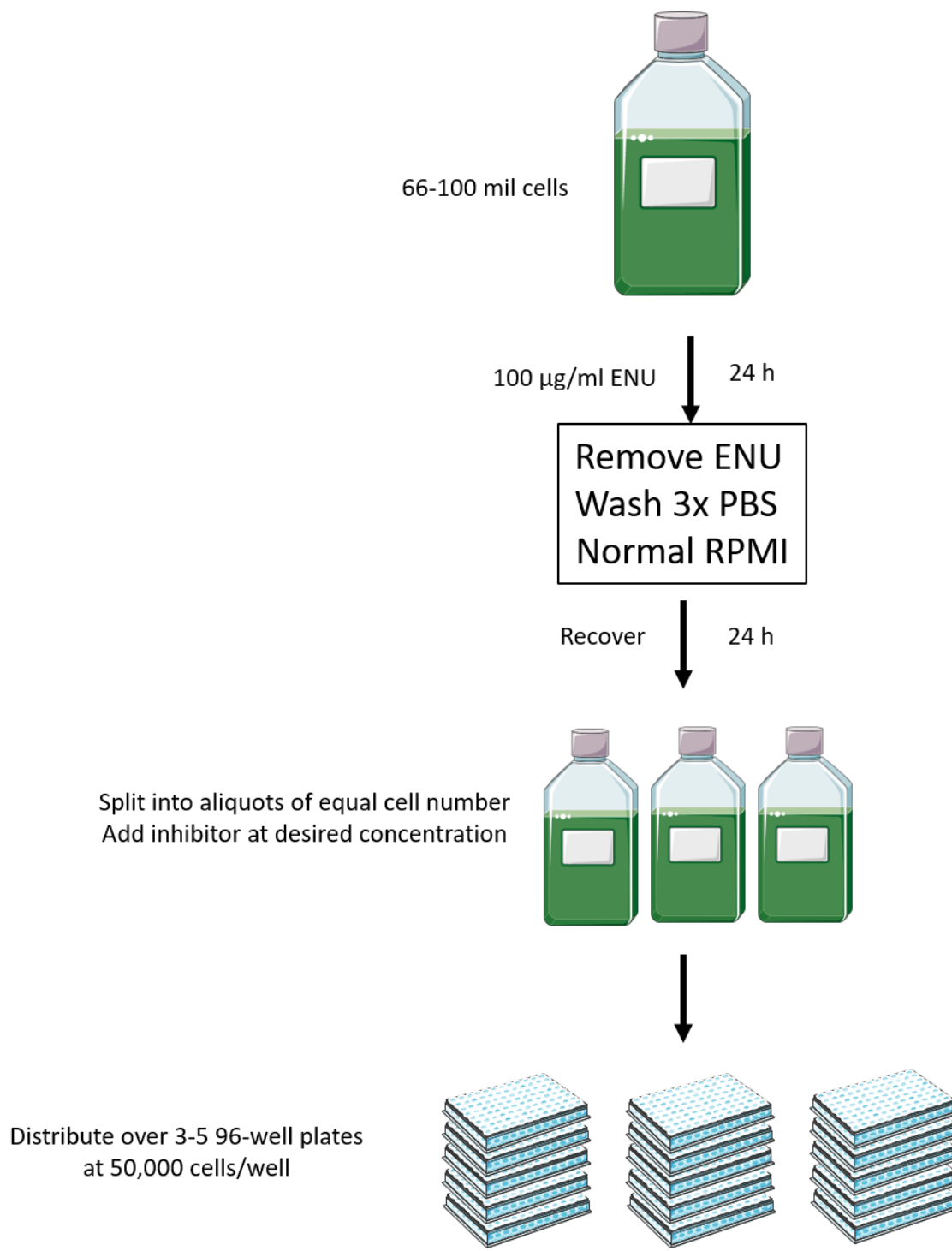


Figure 5.3 – Schematic of the ENU mutagenesis screens.

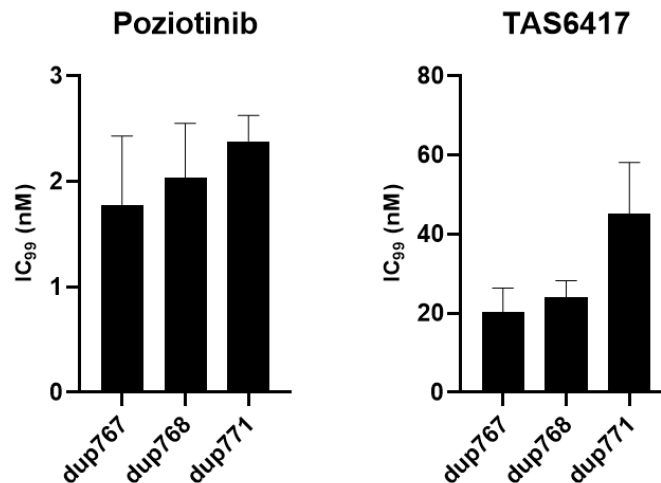


Figure 5.4 – IC₉₉ of Ex20Ins mutants to poziotinib and TAS6417. Bar charts showing the IC₉₉ of Ba/F3 cells expressing the indicated Ex20Ins mutants upon treatment with poziotinib or TAS6417 calculated from Figure 5.1 A. IC₉₉ was calculated using four-parameter non-linear regression analysis performed on GraphPad Prism 8. Values represent mean ± standard deviation from $n = 3$ biological replicates.

To investigate potential resistance mechanisms to poziotinib treatment in cells harbouring Ex20Ins, Ba/F3 cells expressing dup767, dup768, or dup771 were mutagenised by ENU treatment and exposed to 100 nM poziotinib to select for resistant subpopulations. Following ~1 – 4 weeks selection, a total of 57 resistant subpopulations were isolated from dup767 cells ($n = 20$), dup768 cells ($n = 23$), and dup771 cells ($n = 14$). DNA was extracted from each resistant subpopulation and the kinase domain of *EGFR* was amplified (Figure 5.5) and sequenced. In dup767 cells, 95% of resistant subpopulations sampled (19/20) harboured an additional T790M mutation (Figure 5.6 A). The remaining 5% (1/20) harboured an additional C797S mutation. In dup768 and dup771 ~70% of resistant subpopulations sampled harboured an additional T790M mutation (16/23 in dup768 and 10/14 in dup771). In both dup768 and dup771 cells the remaining ~30% of resistant subpopulations sampled had acquired an additional C797S mutation (7/23 in dup768 and 4/14 in dup771). These data indicate that T790M and C797S are able to confer resistance to poziotinib and suggests that the frequency of T790M or C797S occurrence varies depending on the specific Ex20Ins mutation present. To investigate whether increasing the selection dose of poziotinib would produce a different complement of mutations, the screen was repeated in dup771 cells using 200 nM poziotinib for

selection. A further 21 resistant subpopulations were isolated and for each resistant subpopulation DNA was extracted and the kinase domain of *EGFR* was amplified and sequenced. This revealed a small decrease in the frequency of T790M mutations and a small increase in the frequency of C797S mutations following selection with 200 nM poziotinib compared to 100 nM poziotinib (71% vs 62% of resistant subpopulations harboured additional T790M mutations and 29% vs 33% of resistant subpopulations harboured additional C797S mutations following selection with 100 nM and 200 nM poziotinib respectively), indicating that higher doses of poziotinib may decrease the relative frequency of T790M occurrence and increase the relative frequency of C797S occurrence (Figure 5.6 B). However, the differences in frequency are small and so additional replicates are required to confirm this. Interestingly, 1 resistant subpopulation was isolated using 200 nM poziotinib selection that had no other mutation in the *EGFR* kinase domain other than the dup771 Ex20Ins mutation. As ENU is a non-targeted mutagen, it is possible that this resistant subpopulation acquired an *EGFR* mutation outside of the kinase domain or a mutation in another gene that enables it to grow in the presence of 200 nM poziotinib, however further sequencing analysis is necessary to confirm this. Together, these data indicate that acquisition of either T790M or C797S is able to confer poziotinib resistance to these Ex20Ins mutants and that T790M is a more common mechanism of poziotinib resistance compared to C797S.

To examine potential resistance mechanisms to TAS6417 treatment in cells harbouring Ex20Ins mutants, Ba/F3 cells expressing dup768 or dup771 were mutagenised by ENU treatment and exposed to 500 nM TAS6417 to select for resistant subpopulations. A higher selection dose was used for TAS6417 compared with poziotinib as TAS6417 is less active against dup767, dup768, and dup771 compared with poziotinib (Figure 5.1, Figure 5.2, Figure 5.4). Following ~1 – 4 weeks selection, a total of 17 resistant subpopulations were isolated from dup768 cells ($n = 6$) and dup771 cells ($n = 11$). DNA was extracted from each resistant subpopulation and the kinase domain of *EGFR* was amplified and sequenced. Interestingly, in both dup768 and dup771 expressing Ba/F3 cells all resistant subpopulations sampled harboured C797S mutations and none harboured T790M (Figure 5.6 C). This differs from the poziotinib-resistant subpopulations, where additional T790M mutations were detected at a higher frequency compared to

C797S in all 3 Ex20Ins expressing Ba/F3 cells used, indicating that acquisition of C797S may confer a greater level of resistance to TAS6417 compared with T790M.

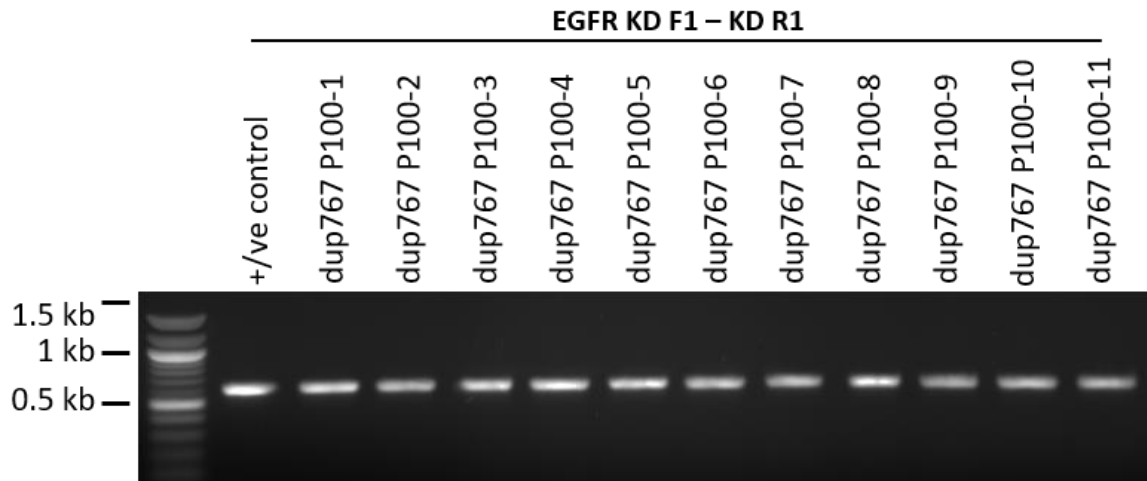


Figure 5.5 – Amplification of the *EGFR* kinase domain is confirmed by agarose gel. The kinase domain of *EGFR* was amplified using the indicated primers described in (Kosaka *et al.*, 2004) (sequences provided in Table 2.3). A plasmid encoding WT-*EGFR* was used as a positive control (+/ve control). “P100” indicates that the resistant subpopulation was selected using 100 nM poziotinib and the number after “P100” indicates the individual resistant subpopulation isolated from the screen.

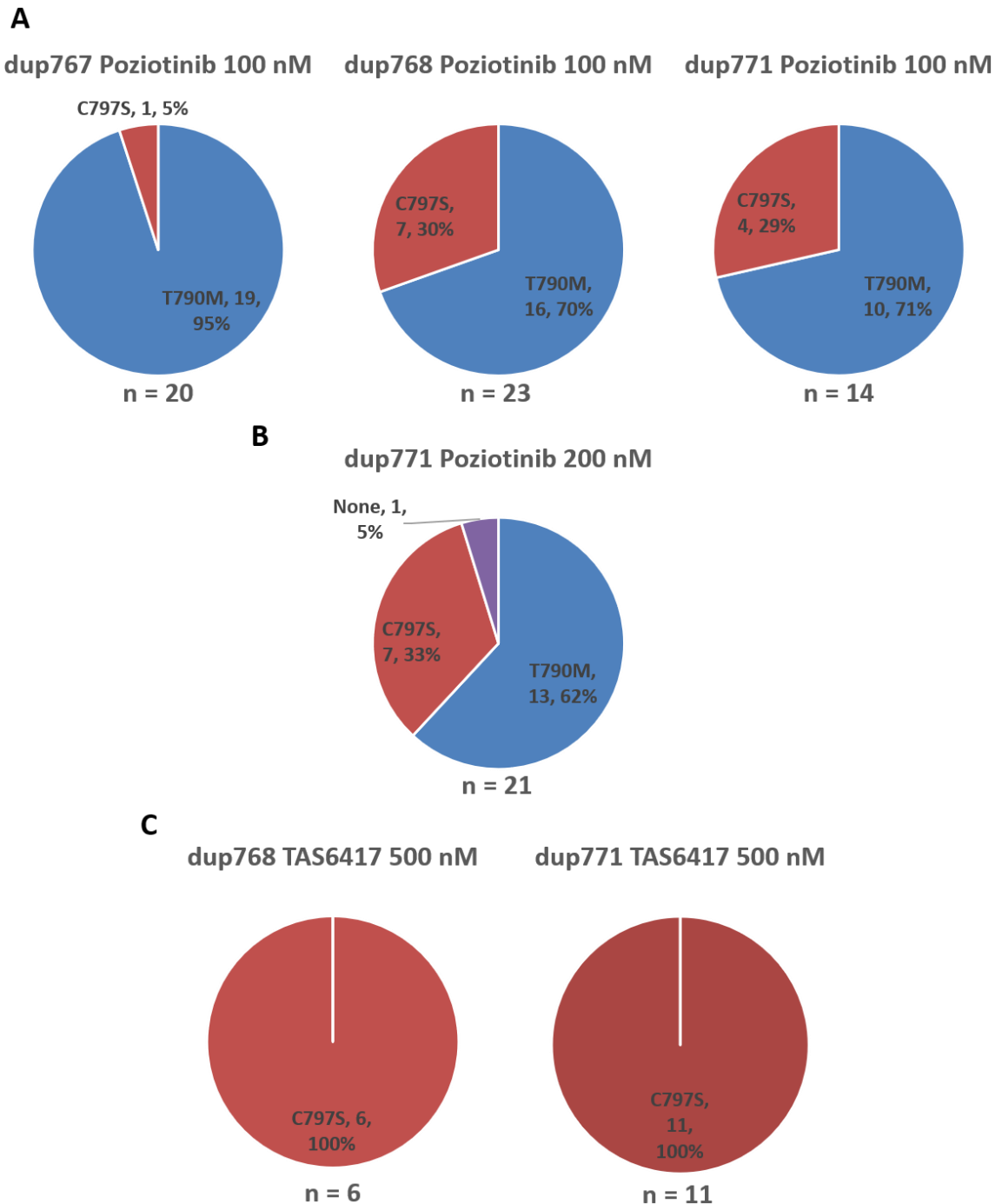


Figure 5.6 – Secondary mutations identified in resistant subpopulations isolated from ENU mutagenesis screens. (A) Pie charts showing the frequency of additional mutations identified in the EGFR kinase domain of Ba/F3 cells expressing dup767, dup768, or dup771 following ENU mutagenesis and chronic exposure to 100 nM poziotinib. (B) Pie chart showing the frequency of additional mutations identified in the EGFR kinase domain of Ba/F3 cells expressing dup771 following ENU mutagenesis and chronic exposure to 200 nM poziotinib. (C) Pie charts showing the frequency of additional mutations identified in the EGFR kinase domain of Ba/F3 cells expressing dup768 or dup771 following ENU mutagenesis and chronic exposure to 500 nM TAS6417.

5.4 T790M and C797S confer a similar level of resistance to poziotinib but C797S confers greater resistance to TAS6417 compared to T790M

Four resistant subpopulations were selected to further investigate the resistance mechanisms identified from the ENU mutagenesis screens: dup771 P100-4, dup771 P200-4, dup771 P200-8, and dup771 T500-1. Dup771 P100-4 was isolated using 100 nM poziotinib selection, dup771 P200-4 and dup771 P200-8 were both isolated using 200 nM poziotinib selection, and dup771 T500-1 was isolated using 500 nM TAS6417 selection. These resistant subpopulations were selected as they were all derived from dup771 cells, they include resistant subpopulations isolated from both poziotinib and TAS6417 ENU screens, from both poziotinib doses used, and they include 2 resistant subpopulations that harbour an additional T790M mutation and 2 resistant subpopulations that harbour an additional C797S mutation (summarised in Table 5.1). To confirm there were no additional *EGFR* mutations in these 4 resistant subpopulations other than those reported in Figure 5.6, the full *EGFR* gene was amplified using 4 amplicons in addition to the kinase domain (Figure 5.7). Sequencing of the full gene revealed no additional mutations in these resistant subpopulations other than the original dup771 mutation and the acquired T790M or C797S mutation reported in Figure 5.6.

Resistant subpopulation	Inhibitor	Dose (nM)	Primary mutation	Additional mutation
dup771 P100-4	Poziotinib	100	N771_H773dupNPH	T790M
dup771 P200-4	Poziotinib	200	N771_H773dupNPH	T790M
dup771 P200-8	Poziotinib	200	N771_H773dupNPH	C797S
dup771 T500-1	TAS6417	500	N771_H773dupNPH	C797S

Table 5.1 – Details of resistant subpopulations selected for further investigation. The name, inhibitor and dose used for selection, primary mutation, and additional mutation for the resistant subpopulations selected for further investigation.

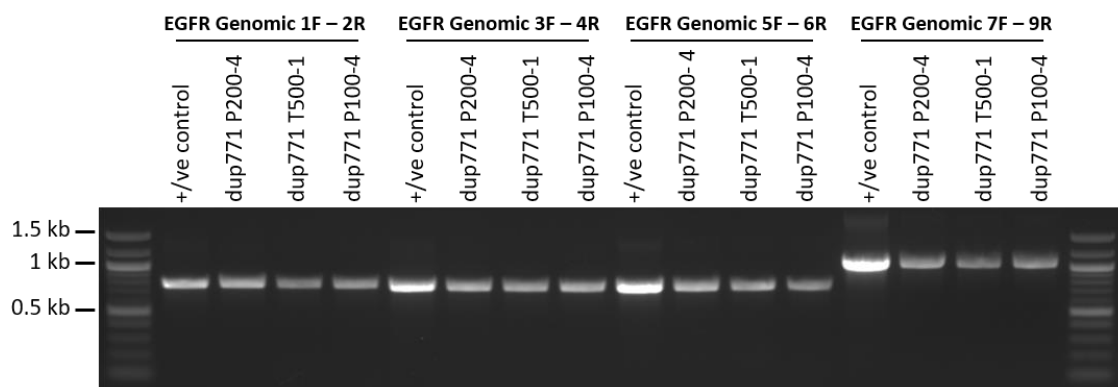


Figure 5.7 – Amplification of the whole *EGFR* gene is confirmed by agarose gel. Representative gel showing the amplification of the full *EGFR* gene using the indicated primers (sequences provided in Table 2.3). A plasmid encoding WT-*EGFR* was used as a positive control (+/ve control). “P100” indicates that the resistant subpopulation was selected using 100 nM poziotinib, “P200” indicates that the resistant subpopulation was selected using 200 nM poziotinib, “T500” indicates that the resistant subpopulation was selected using 500 nM TAS6417.

Dose-response experiments were performed on dup771 P100-4, dup771 P200-4, dup771 P200-8, and dup771 T500-1 to confirm resistance to poziotinib or TAS6417 (Figure 5.8 A). Additionally, the sensitivity of resistant subpopulations isolated following selection with poziotinib (dup771 P100-4, dup771 P200-4, and dup771 P200-8) to TAS6417 and the sensitivity of the resistant subpopulation isolated following selection with TAS6417 (dup771 T500-1) to poziotinib was also assessed to establish whether there was cross resistance conferred to the other Ex20Ins-targeting EGFRi. These experiments revealed that resistant subpopulations had ~89 – 184-fold increase in IC_{50} value upon poziotinib treatment compared to parental dup771 cells (IC_{50} = 797.60 nM, 717.74 nM, 407.82 nM, and 843.62 nM for dup771 P100-4, dup771 P200-4, dup771 P200-8, and dup771 T500-1 respectively compared to 4.59 nM for parental dup771 cells) (Figure 5.8 B). Interestingly, Ba/F3 cells engineered in chapter 3 to express T790M alone (Figure 3.11), hereafter referred to as parental T790M cells, were ~16-fold more sensitive to poziotinib treatment compared the resistant subpopulations harbouring additional T790M mutations dup771 P100-4 and dup771 P200-4 (IC_{50} = 797.60 nM and 717.74 nM for dup771 P100-4 and dup771 P200-4 respectively compared to 48.25 nM for

parental T790M cells). This indicates that the combination of T790M and dup771 reduces sensitivity to poziotinib compared to either mutation alone.

Resistant subpopulations also showed a ~5 – 117-fold increase in IC_{50} value upon TAS6417 treatment compared to parental dup771 cells (IC_{50} = 389.56 nM, 493.12 nM, 3.01 μ M, and 9.57 μ M for dup771 P100-4, dup771 P200-4, dup771 P200-8, and dup771 T500-1 respectively compared to 81.61 nM for parental dup771 cells) (Figure 5.8 B). Interestingly, resistant subpopulations harbouring additional C797S mutations (dup771 P200-8 and dup771 T500-1) were less sensitive to TAS6417 compared to resistant subpopulations harbouring additional T790M mutations (dup771 P100-4 and dup771 P200-4): dup771 P200-8 and dup771 T500-1 had ~7- and ~22-fold higher IC_{50} values respectively compared to the resistant subpopulations harbouring additional an T790M mutation. This indicates that C797S may be more effective at conferring resistance to TAS6417 compared to T790M and may explain why no resistant subpopulations harbouring additional T790M mutations were detected in Ba/F3 cells that were selected with TAS6417 following ENU mutagenesis (Figure 5.6 C). This contrasts with observations from the poziotinib dose-response experiments, which showed that resistant subpopulations harbouring additional T790M mutations had similar IC_{50} values compared to those harbouring additional C797S. Notably, parental T790M cells had an ~11-fold higher IC_{50} value compared to parental dup771 cells upon treatment with poziotinib (48.25 nM vs 4.59 nM for T790M and dup771 respectively) (Figure 5.8 D), whereas parental T790M cells only had a 1.34-fold higher IC_{50} value compared to dup771 upon treatment with TAS6417 (109.46 nM vs 81.61 nM for T790M and dup771 respectively), suggesting that T790M has a greater ability to confer resistance to poziotinib compared to TAS6427. Resistant subpopulations harbouring additional T790M mutations were more sensitive to TAS6417 compared with poziotinib, whereas resistant subpopulations harbouring additional C797S mutations were more resistant to TAS6417 compared with poziotinib (IC_{50} values for poziotinib vs TAS6417 = 797.60 nM vs 389.56 nM for dup771 P100-4, 717.75 nM vs 493.12 nM for dup771 P200-4, 407.83 nM vs 3.01 μ M for dup771 P200-8, and 843.62 nM vs 9.56 μ M for dup771 T500-1) (Figure 5.8 F). Interestingly, dup771 T500-1 had a significantly higher IC_{50} value compared to dup771 P200-8 upon TAS6417 treatment a despite both harbouring an additional C797S mutation (IC_{50} values =

9.57 μM and 3.01 μM for dup771 T500-1 and dup771 P200-8 respectively), indicating that there may be further factors affecting TAS6417 sensitivity in addition to the C797S mutation. Dup771 T500-1 was selected with 500 nM TAS6417, whereas dup771 P200-8 was selected with 200 nM poziotinib, raising the possibility that the differences in selection account for the variations in TAS6417 sensitivity.

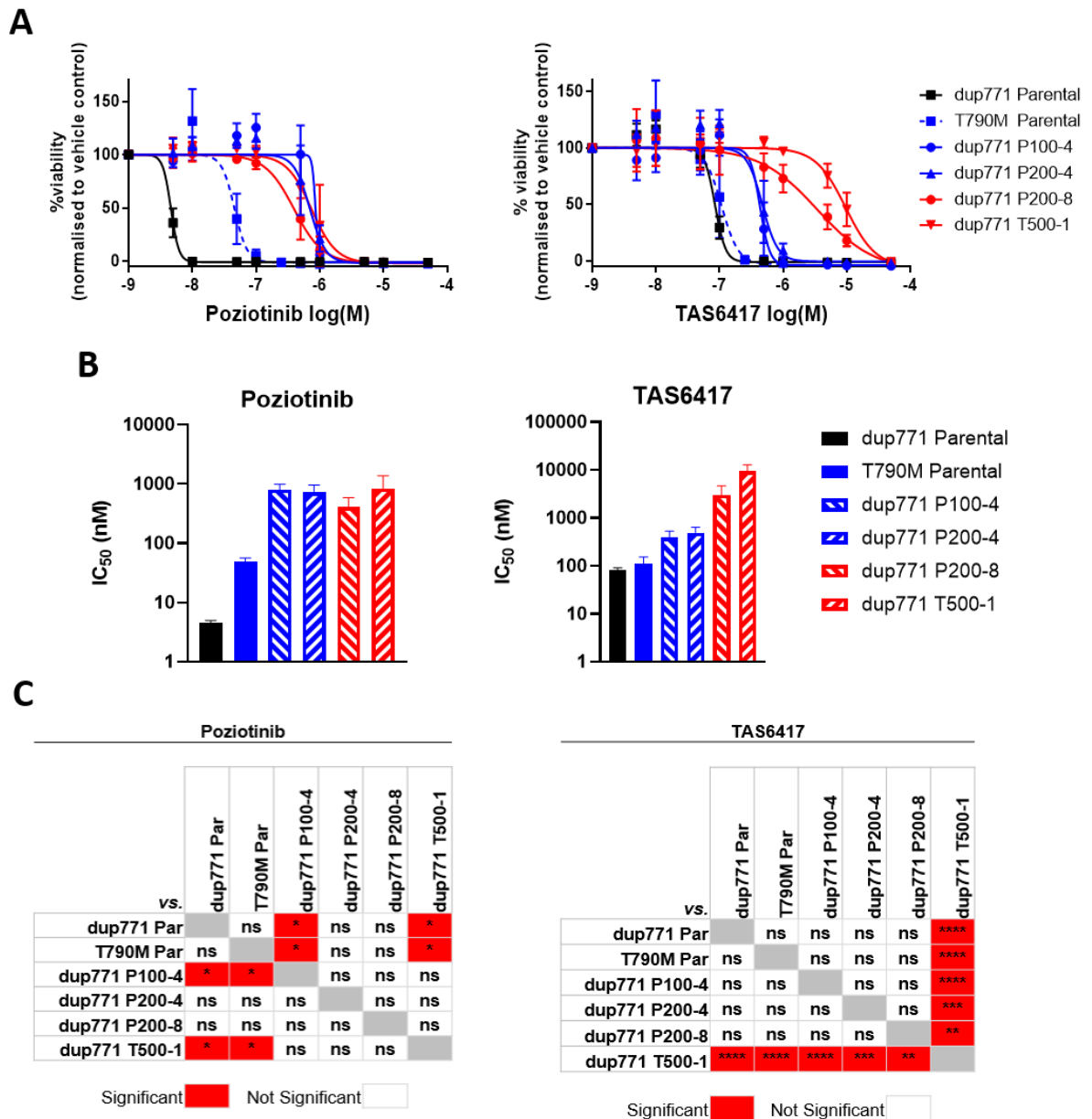


Figure 5.8 – Resistant subpopulations isolated from the ENU mutagenesis screens are resistant to poziotinib and TAS6417 compared with parental cells. (A) Dose-response curves for the indicated resistant subpopulations and Ba/F3 cells expressing dup771 or T790M upon treatment with TAS6417 or poziotinib. Cell viability was measured by Cell Titre Glo and normalised to vehicle control (DMSO). (B) Bar charts showing the IC₅₀ values for the indicated resistant subpopulations and Ba/F3 cells expressing dup771 or T790M upon treatment with TAS6417 or poziotinib calculated from A. IC₅₀ was calculated using four-parameter non-linear regression analysis performed on GraphPad Prism 8. (C) Statistical significance for the indicated pairwise comparisons of IC₅₀ values was calculated by Tukey's multiple comparisons test. * = p<0.05, ** = p<0.01, *** = p<0.001, **** = p<0.0001, ns = not significant.

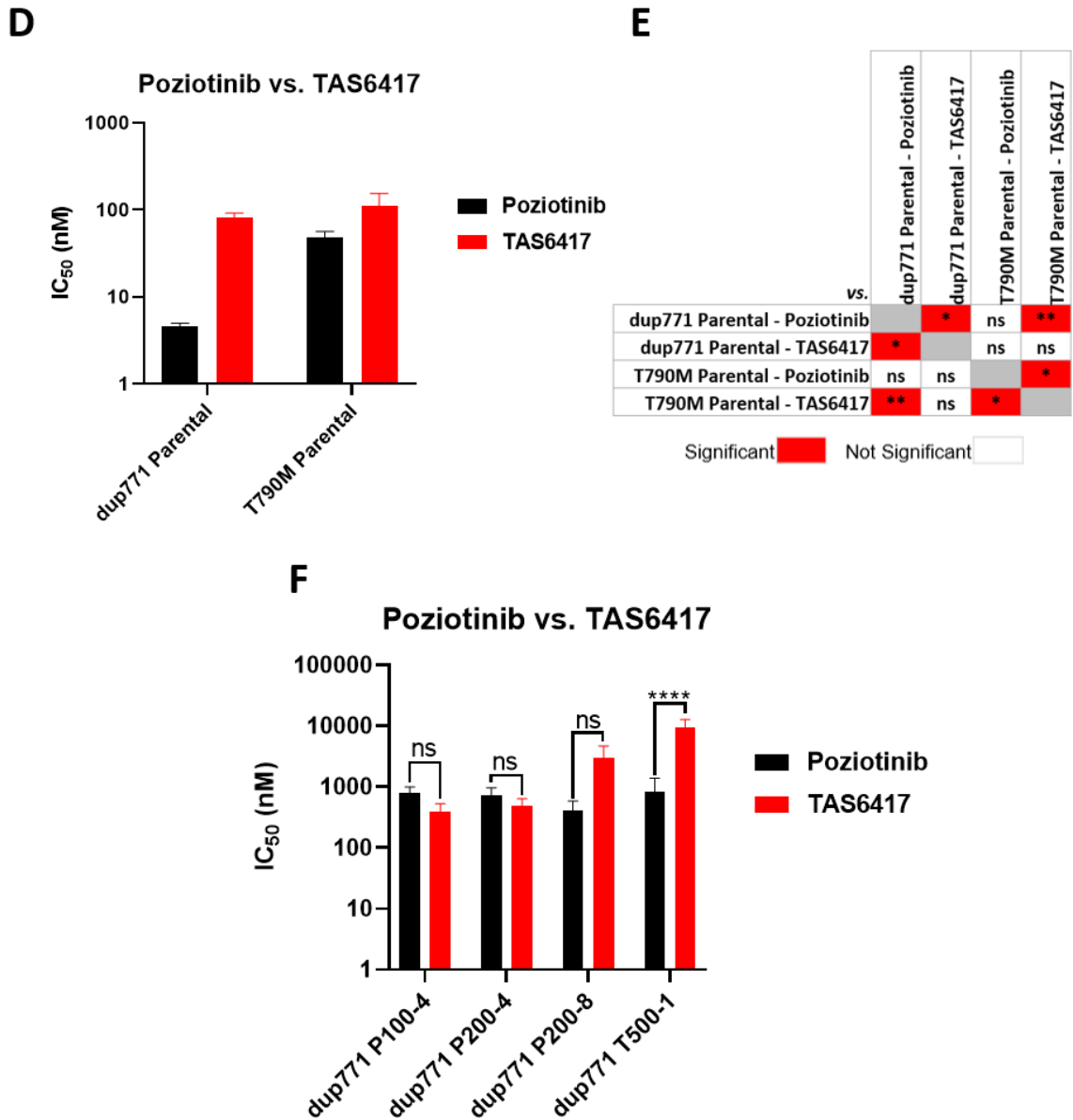


Figure 5.8 (cont.) – Resistant subpopulations isolated from the ENU mutagenesis screens are resistant to poziotinib and TAS6417 compared with parental cells. (D) Bar charts showing IC₅₀ values of dup771 Parental and T790M Parental cells upon treatment with poziotinib or TAS6417 calculated from A. IC₅₀ was calculated using four-parameter non-linear regression analysis performed on GraphPad Prism 8. (E) Statistical significance for the indicated pairwise comparisons of IC₅₀ values was calculated by 2-way ANOVA followed by Tukey's multiple comparisons test. * = p<0.05, ** = p<0.01, ns = not significant. (F) Bar charts showing the IC₅₀ values for the indicated resistant subpopulations upon treatment with TAS6417 or poziotinib calculated from A. IC₅₀ was calculated using four-parameter non-linear regression analysis performed on GraphPad Prism 8. Statistical significance for the indicated pairwise comparisons was calculated by 2-way ANOVA followed by Sidak's multiple comparisons test. **** = p<0.0001, ns = not significant. (A, B, D, F) Values represent mean ± standard deviation from n = 3 biological replicates.

To investigate whether the decreased sensitivity to poziotinib and TAS6417 observed in Figure 5.8 was due to reduced inhibition of EGFR following inhibitor treatment, resistant subpopulations were treated with poziotinib or TAS6417 for 6 h at the dose they were selected with following ENU mutagenesis: dup771 P100-4 was treated with 100 nM poziotinib; dup771 P200-4 and dup771 P200-8 were treated with 200 nM poziotinib; and dup771 T500-1 was treated with 500 nM TAS6417. EGFR phosphorylation was measured by western blot and compared to parental dup771 cells treated with the same conditions (Figure 5.9). This revealed that EGFR phosphorylation was potently inhibited in parental dup771 cells following treatment with 100 nM poziotinib, 200 nM poziotinib, or 500 nM TAS6417. By contrast, EGFR remained phosphorylated in all resistant subpopulations following treatment with poziotinib or TAS6417. These signalling data indicate that these cells are resistant to poziotinib or TAS6417 as they are able to maintain EGFR phosphorylation following poziotinib or TAS6417 treatment.

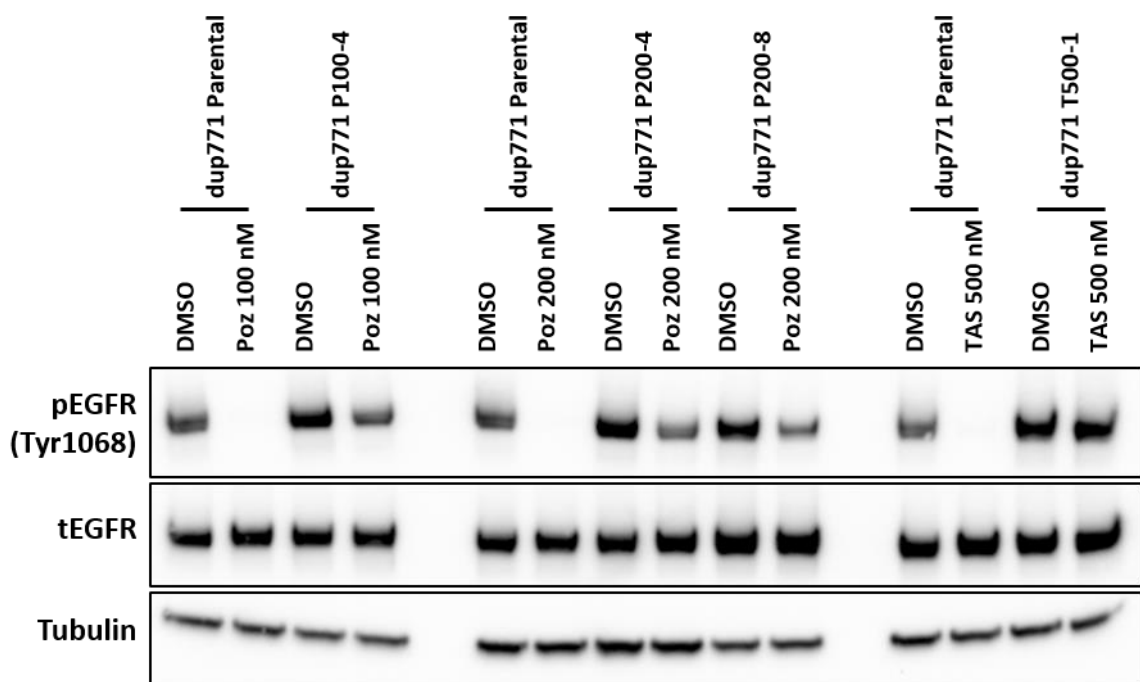


Figure 5.9 – Resistant subpopulations sustain EGFR phosphorylation following treatment with poziotinib or TAS6417. Western blot showing EGFR phosphorylation in the indicated resistant subpopulations or Ba/F3 cells expressing dup771 following 6 h treatment with poziotinib or TAS6417 at the indicated doses. Tubulin was used as a loading control. Blots shown are representative of $n = 2$ biological replicates.

Data presented in Figure 5.8 revealed that resistant subpopulations harbouring an additional C797S mutation were ~7 – 22-fold less sensitive to TAS6417 compared to those harbouring an additional T790M mutation. To examine the mechanism leading to this differential sensitivity, dup771 P100-4 (which harbours an additional T790M mutation) and dup771 T500-1 (which harbours an additional C797S mutation) were treated with TAS6417 at a range of doses for 6 h and EGFR phosphorylation was analysed by western blot (Figure 5.10). This revealed that EGFR phosphorylation was inhibited at lower TAS6417 doses in dup771 P100-4 compared to dup771 T500-1. In dup771 P100-4 EGFR phosphorylation was inhibited following treatment with 500 nM TAS6417, whereas in dup771 T500-1 there was no change in EGFR phosphorylation at the same dose compared to vehicle control (DMSO). Strikingly, in dup771 T500-1 there was no clear reduction in EGFR phosphorylation compared to vehicle control following 5 μ M TAS6417 treatment. Taken together with cell viability data presented in Figure 5.8, these data are consistent with an additional C797S mutation in dup771-harboured Ba/F3 cells conferring greater resistance to TAS6417 compared to an additional T790M mutation by preventing EGFR inhibition at higher doses of TAS6417.

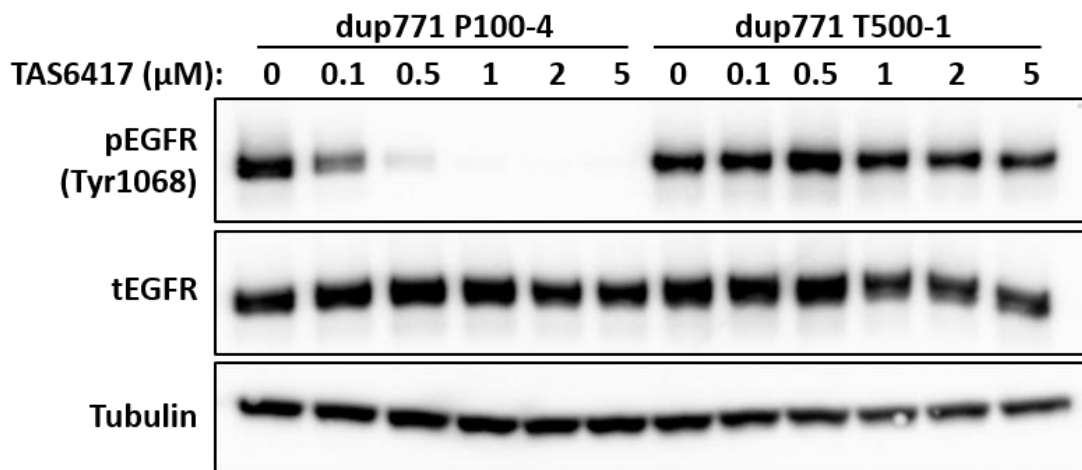


Figure 5.10 – C797S-harboured clone sustains EGFR phosphorylation at 10-fold higher TAS6417 doses compared to T790M-harboured clone. Western blot showing EGFR phosphorylation in dup771 P100-4 cells and dup771 T500-1 cells following 6 h treatment with TAS6417 at the indicated doses. Tubulin was used as a loading control. $n = 1$ biological replicate.

5.5 Ba/F3 cells expressing dup771 with an additional T790M or C797S mutation are sensitive to a Hsp90 inhibitor

To investigate potential salvage therapies to overcome T790M- or C797S-mediated resistance in the Ex20Ins setting, dup771 P100-4 and dup771 T500-1 as well as parental dup771 cells were subjected to the small molecule inhibitor screen used in chapter 4 (Figure 5.11 A). Interestingly, this screen demonstrated that both dup771 P100-4 cells and dup771 T500-1 were sensitive to the Hsp90 inhibitor luminespib (NVP-AUY922), indicated by a blue box on Figure 5.11 A. EV and parental dup771 cells were also sensitive to luminespib, indicating that the effect of luminespib is not specific to Ba/F3 cells harbouring EGFR mutants. Similar results have been reported in a study focusing on poziotinib resistance mechanisms in Ba/F3 cells expressing HER2 Ex20Ins mutants, which identified the Hsp90 inhibitors luminespib and ganetespib as being effective against resistant clones harbouring an additional C805S mutation (the HER2 homologue of the C797S mutation in EGFR) (Koga *et al.*, 2018). Dose-response experiments were performed to assess whether luminespib was effective against dup771 P100-4, dup771 T500-1, and parental dup771 cells (Figure 5.11 B). These revealed that parental dup771 cells were highly sensitive to luminespib and both dup771 P100-4 and dup771 T500-1 were more sensitive to luminespib compared to either poziotinib or TAS6417 (IC₅₀ values for poziotinib, TAS6417, and luminespib were 4.59 nM, 81.61 nM, and 5.39 nM for parental dup771 cells, 797.60 nM, 389.56 nM, and 8.79 nM for dup771 P100-4, and 843.62 nM, 9.57 µM, and 3.29 nM for dup771 T500-1 respectively) (Figure 5.11 C). The sensitivity of dup771 P100-4, dup771 T500-1, and parental dup771 cells to luminespib is consistent with findings from a phase II clinical (NCT01854034) which found that luminespib treatment resulted in a 17% ORR in NSCLC patients harbouring Ex20Ins mutations in EGFR (Piotrowska *et al.*, 2018). Taken together, these data indicate that Hsp90 inhibition could be a potential salvage therapy to overcome T790M- or C797S-mediated resistance to poziotinib or TAS6417.

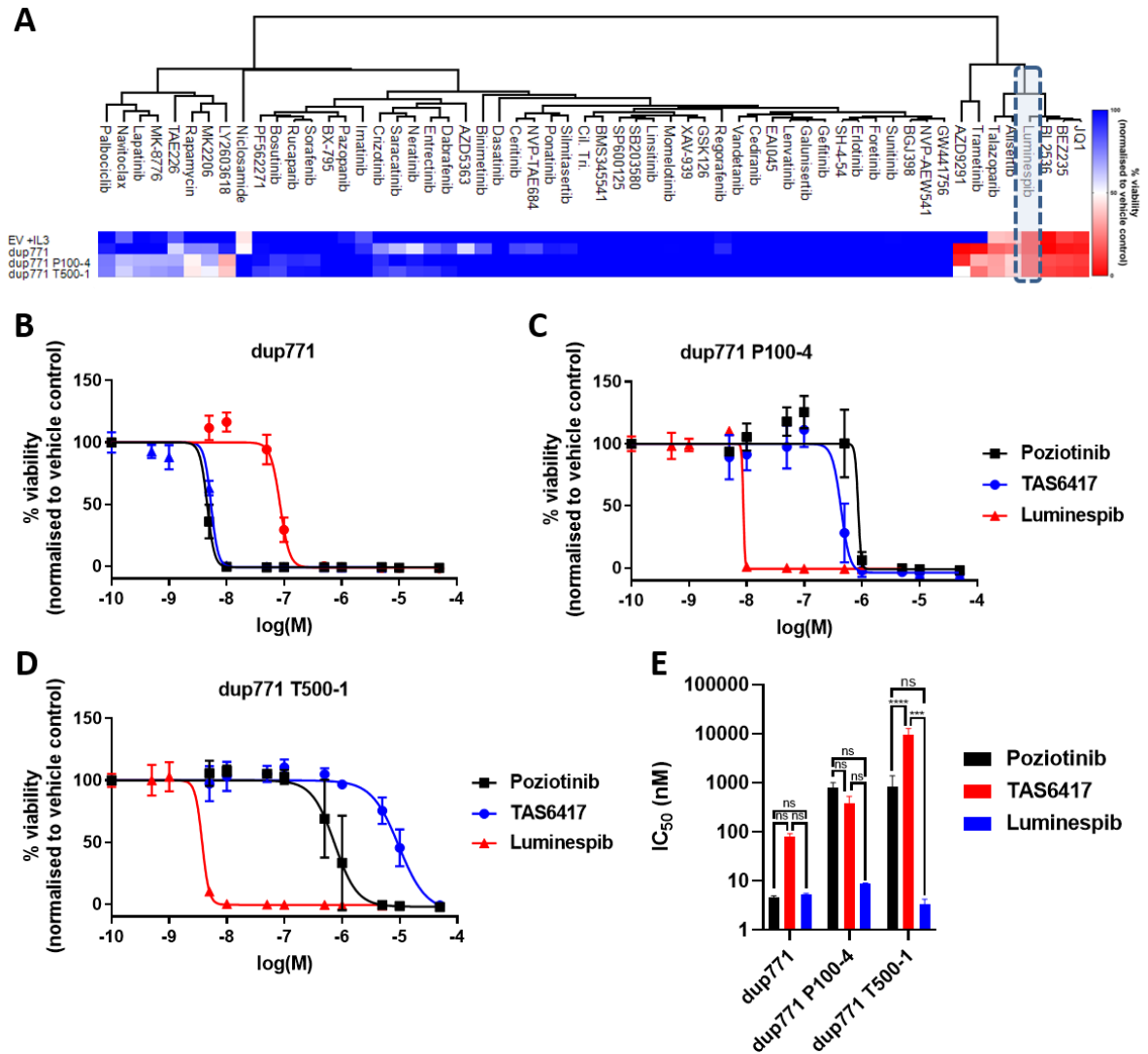


Figure 5.11 – Small molecule inhibitor screen reveals resistant subpopulations are sensitive to luminespib. (A) A heatmap showing cell viability of dup771 P100-4, dup771 T500-1, and parental dup771 cells upon treatment with 500 nM of the indicated inhibitors (or 50 nM luminespib). Cell viability was measured by Cell Titre Glo and normalised to vehicle control (DMSO). 1-way hierarchical clustering based on Euclidean distance was performed using Perseus software. Values shown for EV and dup771 are the mean of $n = 2$ biological replicates. Values shown for dup771 P100-4 and dup771 T500-1 are the mean of $n = 2$ technical replicates, $n = 1$ biological replicates. (B) Dose-response curves for parental dup771 cells upon treatment with poziotinib, TAS6417, or luminespib. Cell viability was measured by Cell Titre Glo and normalised to vehicle control (DMSO). (C) Dose-response curves for dup771 P100-4 cells upon treatment with poziotinib, TAS6417, or luminespib. Cell viability was measured by Cell Titre Glo and normalised to vehicle control (DMSO). (D) Dose-response curves for dup771 T500-1 upon treatment with poziotinib, TAS6417, or luminespib. Cell viability was measured by Cell Titre Glo and normalised to vehicle control (DMSO). (E) Bar charts showing the IC₅₀ values for dup771 P100-4, dup771 T500-1, and parental dup771 cells upon treatment with

poziotinib, TAS6417, or luminespib calculated from B. IC₅₀ was calculated using four-parameter non-linear regression analysis performed on GraphPad Prism 8. Statistical significance for the indicated pairwise comparisons was calculated by Tukey's multiple comparisons test. *** = p<0.001, **** = p<0.0001, ns = not significant. (B,C) Values shown for poziotinib and TAS6417 represent mean ± standard deviation from *n* = 3 biological replicates. Values shown for luminespib represent mean ± standard deviation from *n* = 3 technical replicates, *n* = 1 biological replicate.

5.6 Discussion

Recent advances in our ability to target Ex20Ins EGFR mutants has the potential to greatly improve therapeutic options for patients who harbour these mutations; the largest class of *EGFR* mutations for which there are currently no approved targeted therapies. However, experience with previous generations of EGFRi suggests that acquired resistance to these inhibitors is anticipated. Indeed, early clinical data has already shown that patients treated with poziotinib acquire resistance-causing secondary mutations in *EGFR* (Elamin *et al.*, 2019). It is therefore essential to model potential resistance mechanisms in preclinical studies and identify approaches to overcome these resistance mechanisms.

In this chapter, ENU mutagenesis screens were used to generate subpopulations from Ba/F3 cells expressing Ex20Ins mutant EGFR to poziotinib and TAS6417. Importantly, whilst both T790M and C797S were identified as potential resistance mechanisms to poziotinib, only C797S was identified as a potential resistance mechanism to TAS6417. A higher frequency of T790M and a lower frequency of C797S was identified in resistant subpopulations isolated from dup767 compared to resistant subpopulations isolated from dup768 and dup771, indicating that poziotinib resistance mechanisms may vary between individual Ex20Ins mutants. These differences could have the same structural basis as the variable sensitivity of individual Ex20Ins mutants to EGFRi discussed in chapter 1 (Yasuda *et al.*, 2013; Kosaka *et al.*, 2017; Floc'h *et al.*, 2018). To investigate this possibility, computational modelling techniques (such as those described in (Brown *et al.*, 2019a) to explain why a secondary G724S mutation in EGFR conferred osimertinib resistance in Ba/F3 cells expressing del746 but not L858R) could examine the structural

consequences of T790M or C797S in the context of specific Ex20Ins mutants to determine whether specific Ex20Ins mutants have a propensity for T790M or C797S.

A small molecule inhibitor screen of 58 compounds identified the Hsp90 inhibitor luminespib as a potential salvage therapy to overcome T790M- or C797S-mediated resistance to Ex20Ins-targeting EGFRi. Dose-response experiments demonstrated that Ba/F3 cells expressing Ex20Ins EGFR with secondary T790M or C797S were highly sensitive to luminespib at a level comparable to the sensitivity of parental dup771 cells to poziotinib. In chapter 4, luminespib was not investigated further following the small molecule inhibitor screen as it was potently active against all EGFR mutant expressing Ba/F3 cells as well as EV Ba/F3 cells. The aim of the small molecule inhibitor screen presented in this chapter differs to the aim of the small molecule inhibitor screen presented in chapter 4. In chapter 4, the small molecule inhibitor screen aimed to identify inhibitors capable of targeting EGFR signalling. As luminespib was potently active against all Ba/F3 cells included in the screen, and therefore displayed no EGFR-dependent effect, it was discounted from further investigation. In this chapter, the small molecule inhibitor screen aimed to identify inhibitors capable of overcoming resistance to poziotinib and TAS6417 in Ex20Ins-expressing Ba/F3 cells regardless of the inhibitor's effect on EGFR signalling. The small molecule inhibitor screen identified 4 inhibitors that were potently active against poziotinib- and TAS6417-resistant cells: JQ1, BEZ235, BI2536, and luminespib. Luminespib was selected for further investigation from these 4 inhibitors as a previous study demonstrated that luminespib was able to overcome poziotinib resistance in the context of HER2 Ex20Ins (Koga *et al.*, 2018). In this study, ENU mutagenesis screens identified C805S (the HER2 homologue of C797S) as a resistance mechanism to poziotinib. The authors went on to describe how resistant subpopulations harbouring additional C805S mutations were sensitive to the Hsp90 inhibitors luminespib and ganetespib. Additionally, a phase II clinical trial (NCT01854034) found that luminespib has shown efficacy in NSCLC patients whose tumours harbour Ex20Ins mutations in EGFR (Piotrowska *et al.*, 2018). Data presented in this chapter therefore adds to a body of evidence suggesting that Hsp90 inhibitors could be used to overcome acquired resistance to poziotinib. However, it is important to note that the effects of luminespib are not selective to

EGFR. Data presented in this chapter showed that EV cells are also sensitive to luminespib treatment, suggesting luminespib may be exerting general cell toxicity as opposed to exploiting a sensitivity specific to poziotinib- or TAS6417-resistant cells. However, considering that a phase II clinical trial reported the safe and effective use of luminespib in NSCLC patients with Ex20Ins mutation in EGFR (Piotrowska *et al.*, 2018), and considering that there are currently no alternative treatment options for patients who acquire resistance to these inhibitors, luminespib therapy could have important clinical application. Although there are no clinical data regarding the use of JQ1 and BEZ235 in NSCLC, a phase II clinical trial found that BI2536 had modest efficacy for the treatment of NSCLC (Sebastian *et al.*, 2010). Although this clinical trial did not assess EGFR mutation status, taken together with data presented in this chapter it indicates that BI2536 may be an effective treatment to overcome poziotinib- and TAS6417-resistance in NSCLC patients harbouring Ex20Ins mutations in EGFR.

Luminespib has been investigated for use in NSCLC patients harbouring Ex20Ins mutant EGFR in a phase II clinical trial of 29 patients which reported a 17% ORR and a median PFS of 2.9 months (Piotrowska *et al.*, 2018). Although this is a shorter median PFS compared to the Ex20Ins-targeting EGFRi poziotinib (4.2 months) (Le *et al.*, 2020) and mobocertinib (7.3 months) (Gonzalvez, 2020), this trial demonstrates the clinical activity of luminespib in NSCLC patients harbouring Ex20Ins mutant EGFR. However, there are significant challenges associated with the clinical use of Hsp90 inhibitors. Hsp90 is an ATP-dependent molecular chaperone that has an important role in the folding, maturation, and stabilisation of a wide range of “client proteins”, including signalling proteins involved in oncogenesis (Shimamura *et al.*, 2005; Trepel *et al.*, 2010; Barrott and Haystead, 2013). This has led to the hypothesis that Hsp90 inhibitors could be used as broad-spectrum “super-kinase” inhibitors (Harrison and Huang, 2018). Although Hsp90 inhibitors have shown activity in *in vitro* and *in vivo* studies (Xu *et al.*, 2007, 2012; Sawai *et al.*, 2008; Shimamura *et al.*, 2008; Courtin *et al.*, 2016), clinical trials have reported low response rates and high toxicity (Sequist *et al.*, 2010a; Socinski *et al.*, 2013; Johnson *et al.*, 2015). Notably, in a phase I/II study assessing the efficacy of luminespib in NSCLC patients 4 patients discontinued therapy owing to ocular

toxicity, 2 patients discontinued therapy owing to aspartate transaminase/alanine transaminase abnormalities, and 1 patient discontinued therapy owing to diarrhoea/colitis (Johnson *et al.*, 2015). Despite this, a phase II study (NCT01854034) demonstrated that luminespib is generally well tolerated in NSCLC patients harbouring Ex20Ins mutant EGFR; although a high proportion of patients experienced adverse events, only a minority of patients experienced grade 3 adverse events (grade 3 adverse events experienced were ocular toxicity ($n = 1/29$), hypertension ($n = 3/29$), and hypophosphataemia ($n = 2/29$)) all of which could be managed with dose reduction or treatment delays (Piotrowska *et al.*, 2018). There were no grade 4 adverse events. Although together these data indicate that luminespib may be a safe and effective treatment for NSCLC patients who harbour Ex20Ins mutant EGFR and have T790M- or C797S-mediated resistance to poziotinib, it should be noted that luminespib treatment in NSCLC patients harbouring Ex20Ins mutant EGFR led to a short median PFS (2.9 months) and median OS (13 months) and therefore is unlikely to lead to durable clinical responses for these patients.

The ENU mutagenesis screens presented in this chapter study focused on Ba/F3 cells expressing Ex20Ins mutants in order to investigate resistance mechanisms to poziotinib and TAS6417. This is because these inhibitors are under clinical investigation for use in patients with Ex20Ins mutations, which are a class of EGFR mutations that do not currently have any approved anti-EGFR therapy, and it will be important to understand potential resistance mechanisms to these inhibitors as they progress through clinical trials. It would have been possible to include Ba/F3 cells expressing WT-EGFR in the ENU mutagenesis screens, as Ba/F3 cells expressing WT-EGFR were shown in chapter 3 to grow in IL-3 independent conditions in media supplemented with EGF (Figure 3.8 B). It seems likely that C797S would emerge as the sole resistance-causing mutation to TAS6417 in Ba/F3 cells expressing WT-EGFR, as C797S was the only additional mutation to be detected in the screens using Ba/F3 cells expressing Ex20Ins EGFR presented in this chapter. Additionally, data presented in this chapter suggests that resistant subpopulations harbouring additional T790M mutations were less resistant to TAS6417 compared with resistant subpopulations harbouring additional C797S mutations, further indicating that C797S would likely be the only mutation to arise from these screens. The anticipated

results are less clear regarding potential resistance mechanisms to poziotinib in the context of WT-EGFR expressing Ba/F3 cells. T790M and C797S were the only 2 mutations detected in the poziotinib screens using Ba/F3 cells expressing Ex20Ins EGFR presented in this chapter, so it seems likely these mutations would also confer resistance in the context of WT-EGFR. However, data presented in this chapter showed that parental T790M cells were less resistant to poziotinib compared to resistant subpopulations of Ex20Ins expressing Ba/F3 cells that harboured additional T790M mutations, indicating that the combination of Ex20Ins and T790M confers greater resistance to poziotinib compared with T790M alone. This suggests that in the context of WT-EGFR expressing Ba/F3 cells T790M may not confer as pronounced a resistance phenotype compared with T790M occurring in the context of an Ex20Ins mutation. Therefore, it is possible that T790M would occur at a lower frequency in the context of WT-EGFR compared with Ex20Ins.

A potential shortcoming of this study is the use of ENU mutagenesis. ENU is a non-targeted mutagen that causes mutations throughout the whole genome and not only in *EGFR*. This means that it is possible that subpopulations which have acquired EGFRi resistance following ENU treatment may have acquired a mutation elsewhere in the genome outside of *EGFR* that confers an ability to grow in the presence of EGFRi. In this study, mutations elsewhere in the genome would not have been detected as only *EGFR* was sequenced. This event may have been observed in this study, as 1 of the subpopulations isolated in the 200 nM poziotinib ENU screen of Ba/F3 cells expressing dup771 did not have a mutation detected in the kinase domain of *EGFR*. It is possible that this clone had acquired a mutation elsewhere in the genome or elsewhere in *EGFR* outside of the kinase domain that enabled it to grow in the presence of 200 nM poziotinib. This type of mutational event that is extragenic to *EGFR* is observed in patients with resistance to first- and third-generation EGFRi, where ~35-50% and ~80-90% of resistance mechanisms, respectively, are extragenic to *EGFR* (Westover *et al.* 2018; Leonetti *et al.*, 2019). Another caveat to ENU mutagenesis is that multiple mutations can co-occur within the same cell. For example, a resistant subpopulation may have acquired a T790M mutation in *EGFR*, which was detected by sequencing the kinase domain of *EGFR*, but also acquired an activating mutation in *SRC*, which would not have been detected as *SRC* was not sequenced in this study. In this circumstance, it is possible

that it is the undetected mutation that causes resistance while the detected mutation is only a passenger mutation with no role in resistance. This challenge could be addressed by generating an expression vector encoding the original *EGFR* mutation present in the parental cells used in the ENU screen with an additional T790M mutation. Expression of this construct in Ba/F3 cells would facilitate dose-response experiments which would demonstrate whether addition of T790M to the original *EGFR* mutant conferred inhibitor resistance. Both the challenge of mutations occurring elsewhere in the genome other than *EGFR* and the challenge of multiple mutations co-occurring within the same cell can be addressed with “tiling” mutagenesis screens using clustered regularly interspaced short palindromic repeats (CRISPR)-Cas9 technology. CRISPR-Cas9 technology employs guide RNAs (gRNAs) that associate with the Cas9 nuclease to target Cas9 to gRNA binding sites that are found throughout the genome (called protospacer adjacent motifs, or PAMs). CRISPR-tiling mutagenesis techniques use a library of gRNAs that target Cas9 to every PAM within a gene. Once targeted to the different PAMs by the gRNAs, Cas9 causes double strand breaks which are then repaired by the cell. Errors in DNA repair can lead to the introduction of mutations at the cleavage sites. As the gRNA library is gene-specific and can be transduced into a population of cells so that each cell only receives 1 gRNA, this experiment ensures that mutations generated are only generated in the gene of interest and only 1 mutation is generated in each cell. This approach was utilised to study poly-ADP ribose polymerase (PARP) inhibitor resistance-causing mutations in poly-ADP ribose polymerase 1 (*PARP1*) across the full length of the gene (Pettitt *et al.*, 2018). However, this study used WT Cas9, which has a propensity for inducing insertion and deletion mutations, rather than the point mutations that are more commonly observed in patients. More recent iterations of CRISPR-tiling techniques utilise base editors; deactivated Cas9 (dCas9) proteins tethered to cytosine or adenosine deaminases (Gaudelli *et al.*, 2017; Hess *et al.*, 2017). Base editors cause nucleotide substitution without causing DNA cleavage, thus inducing point mutations whilst preventing insertion and deletion mutations. Tethering base editors to dCas9 enables the targeting of base editors to specific PAM sites using gRNAs. Combined approaches of a gRNA library covering a whole gene expressed in a population of cells so that each cell receives 1 gRNA, in tandem with dCas9-tethered base editors would facilitate the generation of a large number mutant clones harbouring single,

distinct point mutations in the gene of interest which can then be selected for using an inhibitor. As part of this project, I undertook preliminary work to establish this platform where a library of 626 gRNAs targeting every PAM across the full length of *EGFR* was transduced at multiplicity of infection (MOI) 0.3 into the human NSCLC cancer cell line CUTO17, which harbours an endogenous dup771 mutation. MOI 0.3 was used to ensure each cell within the transduced population received 1 gRNA. I also optimised conditions for the transfection of the base editors BE3, BE4, Target-AID (reviewed in Hess *et al.*, 2017), and ABE7.10 (described in Gaudelli *et al.*, 2017) into these cells. However, time constraints prevented mutagenesis screens from being performed using these tools. Despite the shortcomings of ENU mutagenesis as an approach to studying acquired resistance, it should be noted that mutations identified in ENU mutagenesis screens have subsequently been found in patients who have progressed on the same inhibitors (Kobayashi *et al.*, 2017). Additionally, the mutations identified in the ENU mutagenesis screens presented in this chapter (T790M and C797S) have both previously been shown in Ba/F3 cells to confer resistance to poziotinib in the context of an L858R primary mutation (Robichaux *et al.*, 2018) and have been identified in patients whose disease has progressed following first-generation EGFRi therapy (Yu *et al.*, 2013) and osimertinib respectively (Thress *et al.*, 2015). Together, these considerations suggest that the findings presented in this chapter should be good indicators of anticipated resistance mechanisms to poziotinib and TAS6417 in NSCLC patients harbouring Ex20Ins mutant EGFR.

In addition to EGFR-dependent resistance mechanisms such as those identified in this chapter, there is evidence that EGFR-independent mechanisms, such as those discussed in chapter 1, may also lead to resistance to Ex20Ins-targeting EGFRi. Analysis of patient biopsies from a phase II clinical trial of poziotinib in NSCLC patients harbouring Ex20Ins mutant EGFR (NCT03066206) identified a number of “bypass” resistance mechanisms in patients whose disease had progressed on poziotinib treatment (Elamin *et al.*, 2019). Mutations in *PIK3CA* and *MAPK2* were detected, as were amplifications in *MET* and *CDK6*. The same study also identified *KRAS*, *HER2*, and *HER4* mutations in genetically engineered mouse models harbouring Ex20Ins mutant EGFR following progression on poziotinib. Furthermore, unpublished data from our laboratory has identified elevated *FGFR1* expression in

CUTO17 cells with acquired poziotinib resistance following chronic exposure to escalating doses of poziotinib. Bypass signalling mediated by FGFR1 has previously been identified as an EGFRi resistance mechanism in NSCLC cell line models harbouring common EGFR mutants (Ware *et al.*, 2013b; Raof *et al.*, 2019) and unpublished data from our laboratory demonstrates that combined inhibition of FGFR1 and EGFR in poziotinib-resistant CUTO17 cells is more effective compared to either EGFR or FGFR1 inhibition alone, indicating that FGFR1 signalling may confer EGFR-independent resistance to poziotinib. Together, these data suggest that EGFRi resistance in patients harbouring Ex20Ins mutant EGFR will not be confined only to EGFR-dependent mechanisms but will also include EGFR-independent resistance mechanisms. It is therefore critical that preclinical studies focus on anticipating both EGFR-dependent and EGFR-independent mechanisms of resistance to Ex20Ins-targeting EGFRi and investigate strategies to overcome these resistance mechanisms. One approach to studying EGFR-independent resistance mechanisms is through genome-wide CRISPR screening. Genome-wide CRISPR screening techniques use a library of gRNAs that target Cas9 to genes across the whole genome, leading to the introduction of missense mutations or gene knockout. Genome-wide mutagenesis or gene knock-out screening using CRISPR-Cas9 techniques in combination with Ex20Ins-targeting EGFRi treatment could be leveraged to identify putative EGFR-independent resistance mechanisms to these EGFRi. These techniques have previously been utilised to identify PARP1-independent mechanisms of resistance to the PARP inhibitor talazoparib (Pettitt *et al.*, 2018).

As our ability to treat patients harbouring Ex20Ins mutant EGFR improves, it is essential to anticipate likely mechanisms of resistance to Ex20Ins-targeting EGFRi and identify salvage therapies to treat patients who develop resistant disease. Data presented in this chapter has identified on-target mutations capable of conferring resistance to poziotinib and TAS6417 in Ba/F3 cells expressing Ex20Ins mutant EGFR and has identified potential therapeutic strategies to overcome resistance to these inhibitors. Additionally, data presented in this chapter has shown variations in the frequency of resistance-associated mutations occurring in cell lines expressing different Ex20Ins and has shown that C797S confers greater resistance to TAS6417 compared to T790M. Future studies should focus on understanding the basis for the

variable frequency of resistance-associated mutations observed between individual Ex20Ins mutants and investigate whether TAS6417 can be used to overcome T790M-mediated poziotinib resistance. Furthermore, future studies should aim to elucidate EGFR-independent mechanisms of resistance to Ex20Ins-targeting EGFRi. A detailed understanding of potential resistance mechanisms to Ex20Ins-targeting EGFRi and strategies to overcome these mechanisms will be essential for providing the best therapeutic options for patients harbouring Ex20Ins mutant EGFR who acquire resistance to the Ex20Ins-targeting inhibitors currently under clinical investigation.

Chapter 6

Discussion

6.1 Introduction

Since the discovery of *EGFR* mutations that confer sensitivity to EGFRi, our ability to treat patients whose tumours harbour these mutations has improved dramatically. In particular, recent years have seen significant advances in the treatment of NSCLC patients with common *EGFR* mutations who have developed resistance to first-generation EGFRi and NSCLC patients with Ex20Ins mutations. Despite these successes, acquired resistance to anti-EGFR therapy remains inevitable for the majority of NSCLC patients with *EGFR* mutations. Additionally, outcomes for GBM patients whose tumours bear *EGFR* mutations have improved little despite advances in our understanding of EGFR biology. Several areas of active research hold promise for maximising therapeutic response in patients. In this chapter, I discuss some of the outstanding challenges for the treatment of EGFR-mutant cancers as well as some of the emerging opportunities.

6.2 Outstanding challenges for studying EGFR-mutant cancers

6.2.1 Overreliance on model systems

One caveat to the data presented in this thesis is its reliance on the Ba/F3 model system. Ba/F3 cells are murine pro-B cells which have been engineered lose their growth dependence on IL-3 in place of a growth dependence on exogenously expressed *EGFR* mutants. These factors represent a significant departure from the physiological setting that is being modelled by these cells. Use of human cancer cell lines with endogenous mutant *EGFR* would provide a cellular context that is more physiologically relevant, however for many of the less common *EGFR* mutants no such human cancer cell lines exist. Reliance on model systems such as Ba/F3 cells means that it may not be possible to detect variations between different EGFR mutants that are only observed in their physiological context: for example, specific EGFR mutants have distinct interactomes that cannot be observed when expressed exogenously in a model system such as Ba/F3 cells. This caveat is not restricted to

data presented in this thesis, but is prevalent in the study of rare *EGFR* mutants (Kobayashi *et al.*, 2015; Kohsaka *et al.*, 2017; Kosaka *et al.*, 2017; Robichaux *et al.*, 2018). Development of human cancer cell lines that endogenously harbour rare *EGFR* mutants is therefore urgently needed to improve our ability to study these mutants. Recent studies have described patient-derived NSCLC cell lines which endogenously express Ex20Ins mutants (Estrada-Bernal *et al.*, 2018; Jang *et al.*, 2018). Cell lines such as these have facilitated the development of EGFRi capable of targeting Ex20Ins mutant EGFR that are currently undergoing clinical investigation. More patient-derived cell lines harbouring other rare *EGFR* mutants could facilitate similar advances in therapies for these mutants. In the absence of human cell lines with endogenous rare *EGFR* mutants, efforts should be made to engineer physiologically relevant model cell lines to express these mutants. Recently, a number of studies have employed elegant techniques to engineer Ex20Ins mutants into human NSCLC cell lines. Hasako *et al.* used TALEN mutagenesis to introduce D770_N771insSVD into the human NSCLC cell line H1975, which has endogenous L858R and T790M mutations in *EGFR* (Hasako *et al.*, 2018). A subsequent round of TALEN mutagenesis removed the original L858R and T790M mutations. The result is a human NSCLC cell line with an Ex20Ins mutation in *EGFR* encoded in the endogenous allele. Similarly, Floc'h *et al.* used CRISPR-Cas9 technology to introduce Ex20Ins mutants into the human NSCLC cell line H2073, which endogenously expresses WT-EGFR (Floc'h *et al.*, 2018). In addition to providing a more physiologically relevant cellular context, engineered cell line models such as these have the additional advantage of being heterozygous with both mutant and WT-EGFR alleles. Although the Ba/F3 model system has been used to study compound mutations in *EGFR* that occur in *trans* (Kohsaka *et al.*, 2017), studies utilising Ba/F3 cells express only the mutant form of *EGFR*. This is not consistent with the clinical scenario, where *EGFR* mutations are heterozygous with WT-EGFR (Lynch *et al.*, 2004). These techniques could be used to introduce a panel of *EGFR* mutants, such as those described in this thesis, into human cancer cell lines relevant to the disease type the mutants are identified in. Such a panel of cell lines would provide a valuable resource for preclinical studies of rare *EGFR* mutations and may lead to advances in treatment options, such as has been observed for Ex20Ins mutant *EGFR*.

In addition to the challenges of studying rare *EGFR* mutations in the preclinical setting, there are also significant barriers to investigating these mutations in the clinic. Many clinical trials focus on the common *EGFR* mutations L858R and Ex19Del (Rosell *et al.*, 2012; Park *et al.*, 2016; Paz-Ares *et al.*, 2017; Wu *et al.*, 2017; Soria *et al.*, 2018). There are several reasons for the exclusion of rare *EGFR* mutations from large clinical trials. As these mutations are rare, it may be challenging to recruit sufficient patients for large phase III studies. Furthermore, the small patient population may mean that large clinical trials required for clinical approval are a poor investment for the manufacturer of the drug. Additionally, certain trials intentionally exclude rare *EGFR* mutations in order to address their hypothesis. For example, the FLAURA trial excludes rare *EGFR* mutations as it aims to compare osimertinib with approved EGFRi in the first-line setting specifically in patients with Ex19Del or L858R (Soria *et al.*, 2018). Lack of clinical data is a major obstacle to progress in the treatment of rare *EGFR* mutations as it limits our ability to translate preclinical findings into clinical practice. Therefore, future clinical trials should study the efficacy of EGFRi in patients harbouring rare *EGFR* mutants. In the absence of clinical trials focusing specifically on rare *EGFR* mutants, it is essential that clinical trials provide detailed information on the individual *EGFR* mutants detected in patients enrolled in the trial and their response to therapy (Yang *et al.*, 2012; Sequist *et al.*, 2013; Wu *et al.*, 2014; Goss *et al.*, 2016). This information enables post-hoc, pooled studies to evaluate the efficacy of EGFRi treatment in patients with rare *EGFR* mutants and has previously led to the approval of new EGFRi therapy for patients harbouring rare *EGFR* mutants (Yang *et al.*, 2015a). In addition to limited clinical data pertaining to rare *EGFR* mutants, certain rare *EGFR* mutations (such as E709X mutants and less common Ex19Del variants) are not detected by currently available diagnostic kits, such as the PCR-based cobas® *EGFR* Mutation Test v2 platform (Roche) (Wu and Shih, 2016; Malapelle *et al.*, 2017; Oskina *et al.*, 2017; Russo *et al.*, 2019). Increased use of NGS in diagnostics would improve our ability to identify these mutations in patients and subsequently facilitate better treatment outcomes.

6.2.2 Tumour heterogeneity and residual disease

Cancer is an example of a Darwinian evolutionary system (Greaves and Maley, 2012). In recent years it has become well-appreciated that population-level evolutionary mechanisms are a key driver of drug resistance in patients (Andre *et al.*, 2014; Alizadeh *et al.*, 2015). During tumour initiation, “driver” mutations occur that confer a growth advantage to the tumour cell. As driver mutations occur early in tumorigenesis, they are present in all cells within the tumour (known as “clonal” mutations) and can therefore represent good therapeutic targets (Govindan *et al.*, 2012; McGranahan *et al.*, 2015). However, as a tumour develops additional mutations are acquired in individual cells leading to the formation of genetically distinct “subclones” (Greaves and Maley, 2012). Such evolutionary divergence leads to tumour heterogeneity in patients and can have significant implications for therapeutic outcomes, as application of a selective pressure such as drug intervention can lead to the outgrowth of a particular subclone. For example, in NSCLC an activating, EGFRi-sensitising mutation in *EGFR* such as L858R may be clonal throughout the whole tumour. However, as the tumour develops a subclone might emerge that has acquired an additional T790M mutation in *EGFR*. Treatment of the tumour with first-generation EGFRi would kill the cells harbouring only the clonal L858R mutation but would allow the outgrowth of the subclone with an additional T790M mutation, ultimately leading to first-generation EGFRi-resistant disease. This has been observed in preclinical studies of PC9 cells (which have a del746 mutation in *EGFR*), where chronic treatment with first-generation EGFRi leads to the outgrowth of pre-existing clones bearing additional T790M mutations (Hata *et al.*, 2016). Tumour heterogeneity has also been observed in NSCLC patients. The ongoing large-scale, longitudinal TRACERx clinical trial (NCT01888601) that studies cancer evolution in patients throughout therapy identified subclonal mutations in 75% of NSCLC patients who had clonal alterations in *EGFR*, *MET*, or *BRAF* (Jamal-Hanjani *et al.*, 2017). Furthermore, whole-exome sequencing of a primary tumour and 7 metastatic sites from the same patient demonstrated that subclonal mutations also arise independently in metastatic lesions (Blakely *et al.*, 2017).

In addition to the selection of pre-existing resistant populations within a heterogeneous tumour, resistant disease can also arise from cells that do not harbour any pre-existing resistance-causing mutations but survive initial treatment by entering a “drug-tolerant” state (Bivona and Doebele, 2016). These drug-tolerant “persister” cells act as a reservoir of residual disease from which resistant tumour cells can emerge. This has been observed preclinically in studies of acquired resistance to first-generation EGFRi in PC9 cells (Hata *et al.*, 2016; Ramirez *et al.*, 2016). Both Hata *et al.* and Ramirez *et al.* describe a small population of slow-growing cells that survive EGFRi treatment from which fully-resistant clones eventually emerge following continued EGFRi treatment. Notably, Ramirez *et al.* identified resistant clones which arose from a drug-tolerant state that displayed diverse mechanisms of resistance, highlighting that residual disease could be a source of tumour heterogeneity (Ramirez *et al.*, 2016). A deep understanding of residual disease and drug-tolerant persister cells will enhance our ability to achieve durable therapeutic responses in patients. Crucially, future work must focus on identifying and therapeutically targeting drug-tolerant persister cells in the clinic. Interestingly, preclinical studies have shown that the drug-tolerant state is reversible (Sharma *et al.*, 2010), which may explain good responses observed in NSCLC patients who have developed resistant disease and are rechallenged with the same EGFRi after a period of time not receiving the EGFRi (Kurata *et al.*, 2004; Oh *et al.*, 2012). *In vitro* studies have also identified essential epigenetic alterations and signalling pathways in drug-tolerant persister cells (Roesch *et al.*, 2010; Sharma *et al.*, 2010; Rusan *et al.*, 2018; Terai *et al.*, 2018). Future work focused on assessing the safety and efficacy of exploiting these dependencies *in vivo* is essential for advancing our ability to target drug-tolerant persister cells in patients.

6.2.3 Targeting EGFR mutations in GBM

Despite *EGFR* being among the most commonly altered genes in GBM (Brennan *et al.*, 2013) no anti-EGFR therapies are currently approved for GBM patients. There are significant obstacles to targeting EGFR in GBM, including high levels of tumour heterogeneity (Patel *et al.*, 2014), presence of compensatory signalling pathways

driving tumour cell growth (Hegi *et al.*, 2011), and a paucity of drugs capable of penetrating the blood-brain barrier (Sarkaria *et al.*, 2018). Notably, the spectrum of *EGFR* mutations occurring in GBM and NSCLC are largely non-overlapping, with the majority of GBM mutations occurring in the extracellular domain and the majority of NSCLC mutations occurring in the intracellular domain (Zandi *et al.*, 2007). There are currently no data investigating the reason for the mutually exclusive distribution of *EGFR* mutations observed between GBM and NSCLC. However, considering the differences in the mechanisms by which these mutations activate EGFR, the availability of ligand at the anatomical site may be an important factor. For example, extracellular domain mutations have been shown to reduce the need for ligand binding to activate the receptor: EGFR-vIII cannot bind a ligand, but promotes constitutive dimerisation (Su Huang *et al.*, 1997); A289V and R108K have been shown to either facilitate ligand-independent activation of EGFR (Lee *et al.*, 2006) or greatly increase the receptor's affinity for EGF (Bessman *et al.*, 2014). By contrast, intracellular domain mutations such as L858R have been shown to stabilise the active conformation of the kinase domain following dimerization (Yun *et al.*, 2007; Shan *et al.*, 2012). Possibly, variation in the availability of ligand within the brain or within the lung applies distinct evolutionary pressures that enriches for extracellular or intracellular domain mutations in these different anatomical sites.

The large extracellular domain deletion EGFR-vIII, which was not studied in this thesis, is the most common and well-studied *EGFR* mutation in GBM (Jeuken *et al.*, 2009). EGFRi that have been successfully used to treat *EGFR*-mutant NSCLC have also been investigated in the context of EGFR-vIII and GBM. *In vitro* experiments have shown that gefitinib is less active against EGFR-vIII compared to WT-EGFR (Pedersen *et al.*, 2005) and clinical studies focusing on GBM patients have shown that first-generation EGFRi poorly inhibit EGFR signalling in tumour tissue (Lassman *et al.*, 2005; Hegi *et al.*, 2011). The second generation EGFRi neratinib and afatinib have been shown to inhibit EGFR-vIII *in vitro* (Ji *et al.*, 2006b; Vengoji *et al.*, 2019). *In vivo* experiments revealed that neratinib was able to reduce the volume of tumours bearing EGFR-vIII in mice (Ji *et al.*, 2006b). Although it should be noted that the tumours described by Ji *et al.* were pulmonary tumours, there is preclinical and clinical evidence to suggest that neratinib is active within the brain (Duchnowska *et al.*, 2018; Nagpal *et al.*, 2019). A phase II clinical trial assessing the use of

neratinib in GBM is currently ongoing (NCT02977780). *In vivo* experiments also found that combination treatment of afatinib and temozolomide, an alkylating agent commonly used to treat GBM, significantly reduced the growth of xenografts bearing EGFR-vIII compared to either single agent alone. Notably, afatinib has been shown to penetrate the blood-brain barrier (Hoffknecht *et al.*, 2015). Despite this, a phase I/II trial found limited single agent activity of afatinib in non-selected GBM (Reardon *et al.*, 2014), indicating that afatinib may only be effective in *EGFR*-mutant GBM or in combination with temozolomide. The third-generation EGFRi osimertinib has also been shown to be highly brain penetrant (Cross *et al.*, 2014). Preclinical studies have shown that osimertinib can inhibit EGFR-vIII and provides a 47% increase in OS in mice intracranially implanted with cells harbouring EGFR-vIII compared to vehicle control (Kwatra *et al.*, 2017). A phase I/II trial is currently ongoing assessing the use of osimertinib in GBM (NCATS 1-UH2-TR001370-01). Although lapatinib has been shown to be more effective against EGFR-vIII and other GBM-associated extracellular domain *EGFR* mutants (A289D, A289V, and G598V) compared to erlotinib (Vivanco *et al.*, 2012), a multicentre trial of 44 GBM patients conducted by Vivanco *et al.* found that lapatinib did not achieve sufficient intratumoural concentration to inhibit EGFR. Together, these studies indicate that neratinib, afatinib, and osimertinib are effective against EGFR-vIII and are capable of passing the blood-brain barrier, suggesting that they may be viable treatment strategies for GBM patients with EGFR-vIII.

Data presented in this thesis indicates that neratinib is also active against a number of GBM-associated EGFR mutants (L62R, R108G, A289D/T/V, G598V) (Figure 4.2, Figure 4.3 C), suggesting that neratinib may be an effective treatment option for GBM patients with these mutants. Additionally, data presented in this thesis (Figure 4.2, Figure 4.3 C, and Figure 4.3 D) and elsewhere (Kohsaka *et al.*, 2017) has shown that these GBM-associated EGFR mutants are also sensitive to afatinib and osimertinib treatment, suggesting that afatinib and osimertinib may also be effective for treating GBM patients whose tumours bear these mutants. Notably, data presented in this thesis has demonstrated for the first time that the Ex20Ins-targeting EGFRi poziotinib and TAS6417 are active against GBM-associated EGFR mutants (L62R, R108G, A289D/T/V, G598V) (Figure 4.2, Figure 4.3 F). Future work

assessing the efficacy of these EGFRi in *in vivo* models of GBM are urgently needed to establish their utility as candidate anti-EGFR therapies in GBM.

Therapies based on the mAb806 monoclonal antibody are another promising experimental treatment strategy for GBM patients harbouring *EGFR* mutations. mAb806 binds to a short cysteine-loop on EGFR between C287-C302 that is buried in WT-EGFR but exposed in EGFR-vIII (Johns *et al.*, 2004). *In vitro* experiments found that mAb806 is also able to bind A289V significantly better than WT-EGFR (Binder *et al.*, 2018), and *in silico* modelling suggests that mAb806 will also be able to bind to R108K and G598V mutant EGFR (Orellana *et al.*, 2019). *In vivo* studies demonstrated that mAb806 reduces tumour volume in mice bearing EGFR-vIII or A289V (Binder *et al.*, 2018). Together these data indicate that mAb806 may be an effective treatment option for GBM patients with these EGFR mutants. An antibody-drug conjugate of mAb806 and the toxin monomethyl auristatin F (MMAF), which inhibits tubulin assembly (Phillips *et al.*, 2016), called ABT-414 was shown to bind to EGFR in intracranial tumours in a phase I trial (Gan *et al.*, 2013) and is now under clinical investigation for the treatment of GBM in a phase II (NCT02343406) and a phase II/III (NCT02573324).

Together, these data suggest that there are viable therapeutic approaches for treating *EGFR*-mutant GBM and that approved anti-EGFR therapies for GBM may soon reach the clinic. However, additional *in vivo* and clinical studies are urgently required to build on the *in vitro* evidence discussed in this chapter and in chapter 1. Furthermore, it should be anticipated that challenges associated with tumour heterogeneity and compensatory signalling pathways, both of which are prevalent in GBM, will need to be overcome to achieve long term therapeutic responses in patients.

6.3 Emerging opportunities for the treatment of EGFR-mutant cancers

6.3.1 Adaptive therapies and polypharmacology

Attempts have been made to devise adaptive treatment strategies to target multiple distinct subclonal populations within a tumour. Studies of acquired EGFRi resistance in the PC9 cell line demonstrated that cells with T790M-mediated acquired EGFRi resistance were slower growing compared to parental PC9 cells (Chmielecki *et al.*, 2011). Under the hypothesis that tumours with acquired resistance likely comprise mixed populations of drug-sensitive and drug-resistant cells, mathematical modelling predicted that continuous administration of low-dose erlotinib, to target the parental population, combined with intermittent high-dose afatinib, to target the T790M-positive erlotinib-resistant population, would delay the emergence of T790M-mediated resistance. *In vitro* experiments demonstrated that this adaptive strategy doubled the time to acquired resistance compared to continuous dosing. Intermittent dosing schedules have also been used to exploit the phenomenon of drug addiction. Preclinical studies of melanoma driven by a *BRAF* V600E mutation identified signalling alterations in melanoma cells with acquired resistance to combined BRAF and MEK inhibition that cause the cells to become sensitive to the withdrawal of the inhibitors (das Thakur *et al.*, 2013; Moriceau *et al.*, 2015). Exploiting this sensitivity by employing intermittent dosing schedules delayed acquired resistance in xenograft models of melanoma compared to continuous dosing (das Thakur *et al.*, 2013). Similar drug addiction to EGFRi has been reported in cell line models of *EGFR*-mutant NSCLC (Suda *et al.*, 2012). Despite the promising preclinical evidence described by Das Thakur *et al.* and Moriceau *et al.*, a recent phase II clinical trial assessing the use of intermittent BRAF and MEK inhibition found no PFS or OS benefit for intermittent dosing compared to continuous dosing (Algazi *et al.*, 2020). Algazi *et al.* suggest that the relatively long half-life of the BRAF inhibitor vemurafenib and the MEK inhibitor trametinib in patients prevents sufficient decreases in systemic drug levels necessary to exploit drug addiction. Taken together, these data suggest that in addition to identifying the optimal EGFRi for distinct EGFR mutants, an understanding of the optimal dosing schedule is crucial to maximising patient response to anti-EGFR therapy. Adaptive therapies

have also been described that target compensatory signalling pathways activated in subclonal populations. Jonsson *et al.* describe a NSCLC patient who developed resistant disease following 4 months' erlotinib treatment (Jonsson *et al.*, 2017). In addition to the L858R mutation in *EGFR* that was detected at initial diagnosis, exome sequencing revealed that the patient also harboured a mutant allele-specific focal amplification of *EGFR*-L858R, a *BRAF* V600E mutation, *MET* amplification, and a low frequency T790M mutation in *EGFR*. The authors used computational modelling to determine optimal strategy to target the various subclones and found that maximal control of tumour growth was achieved by alternating between different combination therapies; targeting specific subclones whilst allowing others to grow out, before switching therapies to target the subclones which had grown out. More recently a preclinical study used a similar adaptive treatment strategy in order to exploit "evolutionary steering" (Acar *et al.*, 2020). Evolutionary steering aims to identify a sequence of treatments that exploits collateral sensitivities acquired by resistant subclones in order to control tumour evolution and maximise therapeutic response. By using large-scale cell barcoding experiments to study subclonal evolution in the HCC827 NSCLC cell line (which has a del746 mutation in *EGFR*) following high-dose gefitinib treatment, Acar *et al.* identified three functional subgroups in resistant cells. Notably, the authors were able to show that these subclones were also present in the pre-treatment population. Two of the subgroups harboured *MET* amplifications and one showed markers of EMT. The authors demonstrated that clones isolated from the *MET*-amplified subgroups were more sensitive to the *MET* inhibitor capatinib compared to the parental population, suggesting that an adaptive treatment strategy alternating between gefitinib and capatinib may be an effective approach to control the outgrowth of gefitinib resistant subclones. This approach of disease control rather than cure described by Jonsson *et al.* and Acar *et al.* is well established in other fields, such as HIV (Ghosn *et al.*, 2018) and antibiotics (Nichol *et al.*, 2015). Future work should assess the efficacy of alternating therapies in *in vivo* models that recapitulate the tumour heterogeneity observed in patients. Furthermore, it will be essential to establish that the proposed adaptive therapies are safe in patients and do not incur any novel toxicities that are not observed when the therapies are administered as single agents (Park *et al.*, 2013).

An alternative approach to targeting multiple subclones is to exploit polypharmacology: utilising a single drug to target multiple signalling pathways (Antolin *et al.*, 2016). Due to the highly conserved structure of the ATP-binding site in kinases, many inhibitors bind to and inhibit multiple different kinases (Roth *et al.*, 2004; Fabian *et al.*, 2005). Although this is often seen negatively as a potential catalyst for off-target effects and adverse events, targeting multiple signalling pathways could have utility in overcoming, delaying, or even preventing drug resistance that is driven by compensatory signalling mechanisms, such as those identified by Jonsson *et al.* (Jonsson *et al.*, 2017). This approach was used in a preclinical study to overcome PDGFR α inhibitor resistance in malignant rhabdoid tumour (MRT) cell lines (Wong *et al.*, 2016). Molecular profiling identified elevated FGFR1 phosphorylation in MRT cell lines that had acquired resistance to PDGFR α inhibitors. Combined treatment of cells with PDGFR α and FGFR1 inhibitors increased apoptosis compared to either inhibitor alone. Wong *et al.* therefore investigated the use of ponatinib, which inhibits both PDGFR α and FGFR1 with equal potency. The authors found that the single agent ponatinib overcame the MRT cells' resistance to PDGFR α inhibition and induced comparable levels of apoptosis compared to the combination of PDGFR α and FGFR1 inhibitors. Use of a single, multi-target inhibitor in this way may be advantageous compared to combination-based therapies as single agents may have more predictable toxicities, pharmacodynamics, and pharmacokinetics compared to combination therapies. Furthermore, polypharmacology may further delay resistant disease by targeting tumour cell extrinsic factors, such as angiogenesis. Although only two inhibitors have received FDA approval for inhibiting multiple approved targets (Imatinib, which was originally developed to target BCR-ABL but is now also approved to target KIT and PDGFR β , and crizotinib, which was originally designed to target MET but is now also approved to target ALK and ROS1), clinical studies are now investigating the use of a further 8 multi-target inhibitors (Table 6.1) indicating that the use of polypharmacology may increase in the near future (Antolin *et al.*, 2016). In this thesis, 6 multi-target, broad-spectrum kinase inhibitors (dasatinib, saracatinib, bosutinib, cediranib, vandetanib, and ponatinib) were identified that selectively target NSCLC-associated EGFR kinase domain mutations (del746, del747, and L858R) (Figure 4.4). Notably, dasatinib, bosutinib, and ponatinib all caused reduction in both EGFR and SRC phosphorylation (Figure 4.8). Preclinical studies

have shown that SRC is active in NSCLC cell lines with Ex19Del or L858R mutations and have demonstrated that combined inhibition of EGFR and SRC is synergistic (Song *et al.*, 2006; Zhang *et al.*, 2007). Furthermore, SRC signalling that is independent of EGFR has been observed in PC9 cells with acquired resistance to gefitinib (Yoshida *et al.*, 2014) and osimertinib (Ichihara *et al.*, 2017). Taken together, these data indicate that use of an inhibitor capable of inhibiting both EGFR and SRC, such as those identified in this study, may increase therapeutic potency in the first line setting and delay or overcome resistance mediated by SRC signalling.

Drug	Target	IC50	Dose	Indication	Approval	Biomarker	References	Population
Imatinib	ABL1	61 nM	400-600mg/day	CML, ALL	2001	BCR-ABL translocation	FDA label	100%, N/A
	KIT	100 nM	100-400mg/day	GIST, ASM	2002	KIT +, without D816V	FDA label	85%, N/A
	PDGFRA	50 nM	400mg/day	MDS/MPD	2006	PDGFR rearrangements	FDA label	N/A
	PDGFRB	50 nM						
Crizotinib	ALK	183 nM	200-250 mg BID	NSCLC	2011	ALK positive	FDA label	3-7%
	ROS1	4.1 nM	250 mg BID	NSCLC	2016	ROS1 positive	NCT02499614	2%
	MET	2.25 nM	250 mg BID	NSCLC	Phase 2	MET-aplications	NCT02499614, etc.	2-4%
Afatinib	EGFR	0.22 nM	40 mg/day	NSCLC	2013	EGFR ex.19 del. or ex.21 L858R	FDA label	5-17%
	HER2	5 nM	40 mg/day	NSCLC, etc.	Phase 2	HER2 positive /overexpression	NCT02274012, etc	N/A
Ceritinib	ALK	14.1 nM	750 mg/day	NSCLC	2014	ALK positive	FDA label	3-7%
	ROS1	141.8 nM	750 mg/day	several	Phase 2	ROS1 mutation	NCT02186821	2%
Dasatinib	ABL1	0.71 nM	140 mg/day	CML, ALL	2006	BCR-ABL translocation	FDA label	100%, N/A
	DDR2	3.2 nM	140 mg/day	NSCLC	Phase 2	DDR2 mutation	NCT01514864	2.5-4%
	SRC	0.6 nM	100 mg/day	HNSCC, NSCLC	Phase 1	SRC modulation	NCT00779389	N/A, N/A
Erlotinib	EGFR	19.3 nM	100-150 mg/day	NSCLC, PACA	2004	EGFR ex.19 del. or ex.21 L858R	FDA label	5-17%
	JAK2(V617F)	N/A	150 mg/day	PV	Phase 2	JAK2 V617F	NCT01038856	N/A
	HER2	360 nM	100-150 mg/day	PACA	Phase 2	HER2 expression	NCT00674973	N/A
	HER3	1100 nM	N/A (100-150 mg/day)	PACA	Phase 2	HER3 expression	NCT00674973	N/A
Nilotinib	ABL1	18 nM	300-400 mg BID	CML	2007	BCR-ABL translocation	FDA label	100%
	KIT	98 nM	400 mg BID	SKCM	Phase 2	KIT aberration	NCT01099514	2-8%
Ponatinib	ABL1	1.7 nM	45 mg/day	CML, ALL	2012	BCR-ABL translocation	FDA label	100%, N/A
	FLT3	0.3 nM	45 mg/day	AML	Phase 2	FLT3-ITD mutant	NCT02428543	24.30%
	FGFR2	N/A	N/A	BDC	Phase 2	FGFR2 fusion	NCT02265341	N/A
	RET	N/A	30 mg/day	NSCLC	Phase 2	RET translocation	NCT01813734	1.30%

Table 6.1 – Current clinical use or clinical investigation of polypharmacology. Multi-target inhibitors that are either currently approved for multiple targets (imatinib and crizotinib) or are under investigation for use against multiple targets (afatinib, ceritinib, dasatinib, erlotinib, nilotinib, ponatinib). (Adapted from Antolin *et al.*, 2016).

Another approach to addressing tumour heterogeneity is through Hsp90 inhibition. In addition to its function in the folding, maturation, and stabilisation of client proteins (Barrott and Haystead, 2013), Hsp90 plays a key role in the accumulation of genetic variance within a population of cells whilst maintaining phenotypic invariance (Flatt,

2005). Under basal conditions, regulation by Hsp90 can maintain the ability of mutant proteins to perform wild-type biochemical functions (Jarosz *et al.*, 2010) leading to the accumulation of genetic diversity within a population (Jarosz and Lindquist, 2010). This buffering activity can be overcome by the application of a selective pressure, such as drug intervention, which can lead to the outgrowth of the most resistant clones from a pool of genetically diverse cells. A preclinical study of oestrogen-receptor (ER) positive breast cancer demonstrated that Hsp90 inhibition can delay the emergence of resistant disease (Whitesell *et al.*, 2014). Exposure of MCF-7 cells to low doses of the Hsp90 inhibitor ganetespib in combination with the selective ER modulator tamoxifen significantly delayed emergence of tamoxifen resistance. Data presented in this thesis (Figure 5.11) and elsewhere (Koga *et al.*, 2018) has shown the ability of Hsp90 inhibitors to overcome resistance to Ex20Ins-targeting EGFRi. Together with evidence that use of low-dose Hsp90 inhibition can delay the emergence of resistant disease, there is a clear case for investigating the use of Hsp90 inhibitors in the treatment of patients harbouring Ex20Ins mutations, both in combination with Ex20Ins-targeting EGFRi to delay the emergence of resistant disease in the first-line setting and as a salvage therapy.

6.3.2 Immunotherapy

Clinical studies of immunotherapies in NSCLC have demonstrated significant benefits for patients compared to chemotherapy. Antibodies that target the PD1/PD-L1 immune checkpoint (such as pembrolizumab, nivolumab, durvalumab, and atezolizumab) have been shown to provide improvements in median PFS and OS compared to chemotherapy in ~20% of advanced NSCLC patients (Borghaei *et al.*, 2015; Fehrenbacher *et al.*, 2016; Reck *et al.*, 2016; Rittmeyer *et al.*, 2017; Antonia *et al.*, 2018). Despite this success, a meta-analysis assessing the use of *EGFR* mutation status as a predictive OS biomarker for immune checkpoint inhibition in NSCLC found that patients with *EGFR* mutants did not have an OS benefit following immune checkpoint inhibitor therapy compared to docetaxel (Lee *et al.*, 2017a). However, this study did not delineate the response of patients harbouring different *EGFR* mutants to immunotherapy. Although it is widely accepted that

immunotherapies are ineffective in NSCLC patients with common *EGFR* mutants, there is evidence to suggest that these therapies might be effective in patients with rare *EGFR* mutants. A recent retrospective analysis of 27 NSCLC patients with *EGFR* mutants treated with pembrolizumab or nivolumab identified patients harbouring G719X and Ex20Ins mutants as having longer median PFS compared to patients with common *EGFR* mutants (8.4 vs 1.6 months) (Yamada *et al.*, 2019). This observation is consistent with a previous study of 24 NSCLC patients that also identified uncommon *EGFR* mutants as being associated with longer median PFS following treatment with nivolumab (Yoshida *et al.*, 2018), follow-up data from a phase I trial of nivolumab in NSCLC patients which reported 2 patients with uncommon *EGFR* mutants (G719A and an Ex20Ins mutation) who survived for over 5-years following nivolumab treatment (Gettinger *et al.*, 2018), and a case series of 4 patients showing that 3 patients harbouring G719X mutants responded to pembrolizumab therapy (Taniguchi *et al.*, 2018a). These small clinical studies provide preliminary evidence indicating that immunotherapy may be an effective treatment option for NSCLC patients with rare *EGFR* mutants. However, larger clinical studies will be necessary to establish this. Furthermore, head-to-head trials comparing the efficacy of EGFRi vs immunotherapies in patients harbouring rare *EGFR* mutants will be essential to identify the most effective treatment strategy for this patient population. For example, although Yamada *et al.* demonstrated that patients with G719X have a longer median PFS compared to patients with common *EGFR* mutants (8.4 vs 1.6 months) (Yamada *et al.*, 2019), patients with G719X mutants have previously been reported to achieve longer median PFS following afatinib treatment (13.8 months) (Yang *et al.*, 2015a). This highlights the importance of clinical trials that focus on patients with rare *EGFR* mutations in order to clarify the most effective treatment strategies for these patients.

Variation in PD-L1 expression may account for the differences in response to immunotherapy observed between NSCLC harbouring common *EGFR* mutants and NSCLC harbouring rare *EGFR* mutants. Although PD-L1 expression has been shown to be predictive of response to immunotherapies in NSCLC, subgroup analyses have found that median OS does not significantly differ with PD-L1 expression for NSCLC patients with *EGFR* mutants (Borghaei *et al.*, 2015; Fehrenbacher *et al.*, 2016). Furthermore, *EGFR*-mutant NSCLC has been shown to

be associated with low PD-L1 expression levels which may account for the low response rates to PD1/PD-L1 blocking therapies (Gainor *et al.*, 2016b). By contrast, there is evidence to suggest that patients with rare *EGFR* mutations have higher expression levels of PD-L1. Analysis of PD-L1 expression in biopsy or surgical resection samples from 411 NSCLC patients found that 56.6% of patients harbouring uncommon *EGFR* mutants ($n = 29$) had a PD-L1 tumour proportion score (TPS) of $\geq 50\%$, whereas only 35.5% of patients harbouring common *EGFR* mutants ($n = 78$) had a PD-L1 TPS of $\geq 50\%$ ($p=0.002$) (Taniguchi *et al.*, 2018b). However, the predictive value of PD-L1 expression for response to immunotherapy in NSCLC patients with rare *EGFR* mutants is controversial. In a case series of 4 patients, 3 patients with G719X mutations in *EGFR* responded to pembrolizumab treatment whereas the fourth patient, who harboured a rare Ex19Del variant with an additional T790M mutation, did not respond to pembrolizumab despite all 4 patients having PD-L1 expression of $\geq 50\%$ (Taniguchi *et al.*, 2018a). Conversely, the 2 patients with uncommon *EGFR* mutants (G719A and an Ex20Ins mutation) who achieved ≥ 5 -year survival following nivolumab therapy had low PD-L1 expression ($< 1\%$) (Gettinger *et al.*, 2018). Future clinical studies assessing the efficacy of immunotherapies in patients harbouring rare *EGFR* mutations should also measure PD-L1 expression levels to clarify its value as a predictive biomarker for response in this patient population.

Despite encouraging results for NSCLC patients with rare *EGFR* mutants, clinical investigation of immunotherapies in GBM has thus far yielded disappointing results largely due to low immunogenicity and an immunosuppressive microenvironment (Weenink *et al.*, 2020). However, a recent preclinical study has shown that combination of immune checkpoint inhibitor therapy with the immunotoxin D2C7-IT was able to suppress tumour growth in intracranial *in vivo* models bearing *EGFR*-VIII (Chandramohan *et al.*, 2019). Chandramohan *et al.* demonstrated that in addition to targeting tumour cells, D2C7-IT induced a T-cell response that enhanced the activity of immunotherapies that target the immune checkpoint indicating that such combination therapies may be effective treatment strategies for GBM patients.

Interestingly, combining immunotherapy with *EGFR*i therapy appears to be more effective compared with either therapy alone. *In vitro* studies have shown that short-term exposure to low doses of erlotinib increases the sensitivity of NSCLC cell lines

to immune-mediated cytotoxicity via an upregulation of caspase-mediated apoptosis (Dominguez *et al.*, 2016). Combinations of immunotherapy and EGFRi therapy are currently under investigation for both treatment-naïve and EGFRi-resistant NSCLC, and preliminary data indicates marginal benefits for combination treatment compared to EGFRi therapy alone (Ahn *et al.*, 2017; Moya-Horno *et al.*, 2018). Whilst combining immunotherapy with EGFRi could improve patient responses or delay the onset of EGFRi resistance, combination therapies are associated with high incidence of grade 3 and 4 toxicities. Further work to establish both the therapeutic benefit conferred by combination therapies as well as the optimal drug scheduling strategy will therefore be essential to advance these therapies into the clinic.

6.3.3 PROTAC degraders

Proteolysis targeting chimeras (PROTACs) exploit the ubiquitin-proteasome system (UPS) to facilitate the targeted degradation of proteins within a cell. The UPS is the mechanism by which cells destroy damaged or unrequired proteins (Amm *et al.*, 2014). A crucial step in the UPS is the ligation of activated ubiquitin, which signals a protein for destruction by the proteasome (Grice and Nathan, 2016), onto the target protein by an E3 ubiquitin ligase. It is this step that PROTACs exploit to enable degradation of specific target proteins. PROTAC technology utilises a bifunctional molecule consisting of E3 ubiquitin ligase ligands coupled to a targeting element for the protein of interest by a flexible chemical linker (Burslem and Crews, 2020). A recent study described the development of a PROTAC that is able to degrade EGFR by coupling the E3 ubiquitin ligase von Hippel-Lindau (VHL) to the dual EGFR-HER2 inhibitor lapatinib (which served as the targeting element for EGFR) (Burslem *et al.*, 2018). This PROTAC was able to degrade WT-EGFR in the ovarian cancer cell line OVCAR8 at low-nanomolar concentrations. Strikingly, this PROTAC was also able to induce degradation of dup767 EGFR expressed in HeLa cells. Furthermore, the authors demonstrated that altering the EGFR targeting element from lapatinib to gefitinib enabled targeting of L858R or Ex19Del EGFR whilst sparing WT-EGFR, and altering the EGFR targeting element to afatinib enabled the degradation of L858R+T790M. PROTACs' mechanism of action makes them more potent

compared to traditional small molecule inhibitors. As PROTACs initiate the degradation of the target protein, they do not need to continually occupy the target protein (Bondeson *et al.*, 2015). This means that one PROTAC molecule can initiate the degradation of multiple target proteins, whereas kinase inhibitors must continually occupy the target kinase to cause inhibition. This has been shown to lead to an increased potency of PROTACs compared to small molecule inhibitors in *in vitro* experiments focusing on the HER2-driven breast cancer cell line SKBr3 (Burslem *et al.*, 2018). Dose-response experiments demonstrated that SKBr3 cells were more sensitive to treatment with a lapatinib-based PROTAC which targeted HER2 compared to HER2 inhibition by a lapatinib-based control molecule that does not result in HER2 degradation. Similarly, PROTAC treatment also resulted in sustained suppression of downstream signalling pathways compared to HER2 inhibition by the lapatinib-based control molecule. In addition to increased potency compared to small molecule inhibitors, recent studies have achieved tumour-specific degradation of a target protein by exploiting E3 ligases that are selectively expressed in tumours (Khan *et al.*, 2019; Schapira *et al.*, 2019). Despite these advantages, there are safety concerns associated with the use of PROTACs in patients. As PROTACs cause near-complete depletion of their targets, on-target toxicities can occur if the target protein has scaffold function as well as kinase activity. Off-target toxicities can also occur as PROTACs can result in the degradation of proteins other than their targets, for example proteins that are in complex with the target protein can also be degraded (Hsu *et al.*, 2020). Two PROTACs are currently under clinical investigation. ARV-110 is an androgen receptor-targeting PROTAC that is currently being studied in a phase I/II trial of metastatic castrate-resistant prostate cancer (NCT03888612). Preliminary data from this study indicated that ARV-110 was safe demonstrated antitumour activity (Petrylak *et al.*, 2020). ARV-471 is an ER-targeting PROTAC currently under investigation in a phase I/II clinical trial of ER-positive/HER-negative locally advanced or metastatic breast cancer (NCT04072952). Although no data has been reported from this trial yet, preclinical data showed that ARV-471 is able to degrade ER at low-nanomolar concentrations (half-maximal degradation concentration (DC₅₀) ~2 nM) and caused significant tumour shrinkage in multiple xenograft models (Flanagan *et al.*, 2019). To progress PROTAC-based therapy into the clinic for patients harbouring EGFR mutations, future *in vivo* studies will be required to

establish their efficacy in EGFR-mutant cancers. Considering that EGFRi are used in PROTACs to target the E3 ubiquitin ligase to EGFR, it will be important to establish whether rare *EGFR* mutants that do not respond to EGFRi therapy can be targeted with PROTACs. Another important question to address is whether EGFR PROTACs based on EGFRi that bind to WT-EGFR as well as mutant EGFR, such as afatinib, will suffer from the same toxicities associated with the targeting of WT-EGFR that are observed in the clinical use of the EGFRi.

6.4 Concluding remarks

Activating mutations in *EGFR* are a major oncogenic driver in a number of cancers (Cerami et al., 2012; Gao et al., 2013), in particular GBM and NSCLC (Brennan et al., 2013; Siegelin and Borczuk, 2014). Despite significant advances in our ability to target EGFR therapeutically, improvements can still be made through optimising the use of available inhibitors for distinct EGFR mutants. Furthermore, it has become increasingly clear that targeting EGFR alone has limited therapeutic benefit for the reasons discussed in this chapter. It is therefore crucial that future work takes advantage of novel treatment paradigms in order to optimise tumour control and maximise clinical response in patients.

Data presented in this thesis makes a number of significant contributions to our understanding of EGFR mutant cancers and how to treat them. First, the sensitivity of 18 EGFR mutants to 9 EGFRi was assessed including the first examination of poziotinib and TAS6417 against a large number of non-Ex20Ins mutants. Importantly, this thesis identified a number of inhibitors that showed activity against extracellular domain mutants associated with GBM: neratinib, afatinib, osimertinib, poziotinib, and TAS6417. The activity of afatinib and osimertinib against extracellular domain mutants has been reported elsewhere (Kohsaka et al., 2017), but the activity of neratinib, poziotinib, and TAS6417 is reported for the first time in this thesis. Although neratinib, afatinib, and osimertinib have been shown to penetrate the blood-brain barrier (Cross et al., 2014; Hoffknecht et al., 2015; Duchnowska et al., 2018; Nagpal et al., 2019), there is no data regarding the CNS activity of poziotinib and TAS6417. Furthermore, there is very little data regarding

the activity of any of these inhibitors against GBM-associated extracellular domain EGFR mutants *in vitro* or *in vivo*. The paucity of cell line models harbouring extracellular domain mutants means that new models will need to be developed in order to advanced the findings presented in this thesis. New cell line models could either be derived from patients whose tumours harbour the mutations of interest or engineered using techniques such as those described by Hasako *et al.* from a cell line such as SF268, a human GBM cell line which harbours an A289V mutation, in order to derive human GBM cell lines that harbour the EGFR mutations of interest (Hasako *et al.*, 2018; Vivanco *et al.* 2012). Cell lines such as this should be used to build on the data from Ba/F3 models presented here and elsewhere (Kohsaka *et al.*, 2017), demonstrating that these inhibitors work in the context of human GBM cell lines. Subsequently, experiments using *in vivo* intracranial models would be essential to demonstrate that these inhibitors are active within the brain and provide the evidential basis for phase I clinical trials.

Second, 6 broad-spectrum TKI were identified that inhibit specific EGFR mutants. Although these mutants respond to clinically approved EGFRi, the broad-spectrum TKI identified in this thesis may have some clinical utility. As these inhibitors target multiple kinases, they may be able to delay acquired resistance by blocking bypass signalling pathways. In order to examine this, future *in vitro* experiments should compare the time taken for NSCLC cell lines to acquire resistance to the inhibitors identified in this thesis with approved EGFRi. Furthermore, cediranib, ponatinib, and vandetanib also inhibit VEGF signalling in addition to the EGFR mutants identified in this thesis. The ability of these inhibitors to block both oncogenic EGFR signalling and angiogenesis could enhance their antitumour activity. To investigate this, experiments using PDX models could analyse the effect that these inhibitors have on both tumour growth and angiogenesis (Harrison and Huang, 2018). Additionally, these inhibitors may have clinical utility for patients who have an unknown resistance mechanism to EGFRi. Around 10% and 30-50% of acquired resistance to first- and third-generation EGFRi, respectively, occurs via an unknown mechanism (Westover *et al.* 2018; Leonetti *et al.*, 2019). A phase I clinical trial of patients whose disease has progressed following first- or third-generation EGFRi via an unknown mechanism would provide valuable information on the efficacy of these inhibitors for this patient population. As dasatinib has been the most

extensively studied inhibitor identified in this thesis in NSCLC, and the toxicities associated with dasatinib treatment are well understood and manageable, clinical investigation should begin with dasatinib.

Finally, data presented in this thesis identified potential resistance mechanisms to poziotinib and TAS6417 treatment in the context of Ex20Ins mutant EGFR and identified luminespib as a potential salvage therapy to overcome resistance to these inhibitors. These are the first data regarding possible resistance mechanisms to poziotinib and TAS6417 in the context of Ex20Ins mutant EGFR and could provide important information regarding the treatment of patients whose tumors harbour Ex20Ins mutant EGFR and progress following poziotinib or TAS6417 treatment. These results are particularly relevant at this time as both poziotinib and TAS6417 are currently under clinical investigation for NSCLC harbouring Ex20Ins mutations in EGFR; an indication that currently has no approved anti-EGFR therapy. In order to translate these findings, *in vivo* models of T790M- or C797S-mediated resistance to Ex20Ins-targeting EGFRi should be generated and luminespib tested for efficacy in these models. Subsequently, clinical trials assessing the use of poziotinib and TAS6417 should test patients for the presence of T790M or C797S before treatment initiation and following disease progression. Patients who develop resistant disease that harbours T790M or C797S following poziotinib or TAS6417 treatment should be enrolled in a phase I clinical trial assessing the use of luminespib for this indication, and particular attention should be paid to the safety of luminespib in these patients.

Despite the success of treating NSCLC patients with common *EGFR* mutants, there remains limited or no therapeutic options for patients who harbour other *EGFR* mutants. It is therefore essential that future *in vivo* and clinical studies build on the data presented in this thesis and elsewhere (Duong-Ly *et al.*, 2016; Kohsaka *et al.*, 2017) to identify the most effective inhibitor for distinct *EGFR* mutants. As Ex20Ins-targeting EGFRi progress through clinical trials, it is critical that acquired resistance to these inhibitors is anticipated and approaches to overcome acquired resistance are investigated. Interestingly, data presented in this thesis indicates that poziotinib treatment preferentially selects for resistance mediated by the T790M mutation, whereas TAS6417 preferentially selects for resistance mediated by C797S and is relatively effective against cells with additional T790M mutations. This raises the

possibility of designing an adaptive treatment strategy exploiting the concept of evolutionary steering that begins with poziotinib treatment and switches to TAS6417 treatment upon emergence of T790M-mediated poziotinib resistance. To investigate the efficacy of such an approach, future *in vivo* studies could compare the proposed adaptive therapy with single agent poziotinib or TAS6417. Furthermore, inhibition of Hsp90 appears to be an effective salvage therapy to overcome resistance to Ex20Ins-targeting EGFRi. Taken together with evidence that Hsp90 inhibition can delay the onset of acquired resistance (Whitesell *et al.*, 2014), there is a clear case for investigating the use of Hsp90 inhibitors either in combination with EGFRi in the first line setting or in the resistant disease setting. Ultimately, considering the prevalence of acquired resistance to anti-EGFR therapies, it is likely that it will be necessary to move beyond traditional EGFRi therapy and exploit novel treatment strategies, such as those discussed in this chapter, to optimise therapeutic response and achieve durable tumour control in patients.

Chapter 7
Appendix

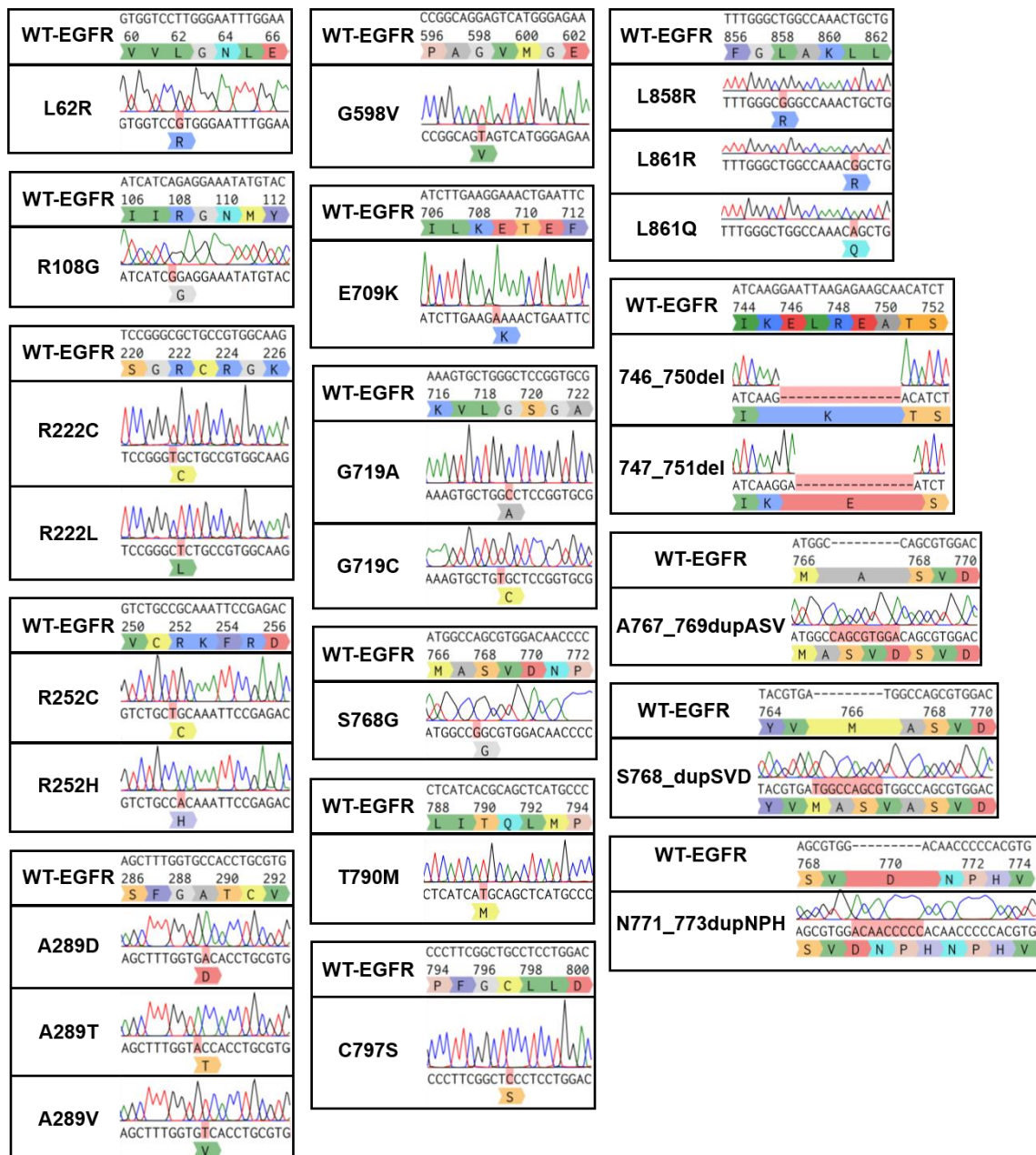


Figure 7.1 – Sanger sequencing of EGFR mutants. Sanger sequencing was used to confirm the presence of mutations in pFB-EGFR mutant constructs. The whole EGFR gene was sequenced to confirm no additional unintended mutations were present (not shown). Sequences were aligned to WT-EGFR using the online tool Benchling (<https://benchling.com/>). Altered nucleotides are highlighted in red and altered amino acids are displayed immediately below. The corresponding amino acid position is shown in the WT-EGFR row.

Bibliography

- Abounader, R. and Laterra, J. (2005) "Scatter factor/hepatocyte growth factor in brain tumor growth and angiogenesis," *Neuro-Oncology*, **7(4)**, pp. 436–451.
- Acar, A. *et al.* (2020) "Exploiting evolutionary steering to induce collateral drug sensitivity in cancer.," *Nature Communications*, **11(1)**, p. 1923.
- Addeo, A. (2018) "Dacomitinib in NSCLC: a positive trial with little clinical impact," *The Lancet Oncology*, p. e4.
- Ahn, M. *et al.* (2019) "Osimertinib in patients with T790M mutation-positive, advanced non-small cell lung cancer: Long-term follow-up from a pooled analysis of 2 phase 2 studies," *Cancer*, **125(6)**, pp. 892–901.
- Ahn, M.-J. *et al.* (2017) "EGFR TKI combination with immunotherapy in non-small cell lung cancer," *Expert Opinion on Drug Safety*, **16(4)**, pp. 465–469.
- Ahn, M.-J. *et al.* (2018a) "An open-label, multicenter, phase II single arm trial of osimertinib in non-small cell lung cancer patients with uncommon EGFR mutation (KCSG-LU15-09).," *Journal of Clinical Oncology*, **36(15_suppl)**, pp. 9050–9050.
- Ahn, M.-J. *et al.* (2018b) "An open-label, multicenter, phase II single arm trial of osimertinib in non-small cell lung cancer patients with uncommon EGFR mutation (KCSG-LU15-09).," *Journal of Clinical Oncology*, **36(15_suppl)**, pp. 9050–9050.
- Akahane, K. *et al.* (2016) "HSP90 inhibition leads to degradation of the TYK2 kinase and apoptotic cell death in T-cell acute lymphoblastic leukemia," *Leukemia*, **30(1)**, pp. 219–228.
- Alessi, D. R. *et al.* (1997) "Characterization of a 3-phosphoinositide-dependent protein kinase which phosphorylates and activates protein kinase B α ," *Current Biology*, **7(4)**, pp. 261–269.
- Algazi, A. P. *et al.* (2020) "Continuous versus intermittent BRAF and MEK inhibition in patients with BRAF-mutated melanoma: a randomized phase 2 trial," *Nature Medicine*, **26(10)**, pp. 1564–1568.
- Alizadeh, A. A. *et al.* (2015) "Toward understanding and exploiting tumor heterogeneity.," *Nature Medicine*, **21(8)**, pp. 846–53.
- Amm, I., Sommer, T. and Wolf, D. H. (2014) "Protein quality control and elimination of protein waste: The role of the ubiquitin-proteasome system," *Biochimica et Biophysica Acta - Molecular Cell Research*, pp. 182–196.
- Anastassiadis, T. *et al.* (2011) "Comprehensive assay of kinase catalytic activity reveals features of kinase inhibitor selectivity," *Nature Biotechnology*, **29(11)**, pp. 1039–1045.

- Andre, F. *et al.* (2014) "Prioritizing targets for precision cancer medicine," *Annals of Oncology*, **25(12)**, pp. 2295–2303.
- Antolin, A. A. *et al.* (2016) "Polypharmacology in Precision Oncology: Current Applications and Future Prospects.," *Current pharmaceutical design*, **22(46)**, pp. 6935–6945.
- Antonia, S. J. *et al.* (2018) "Overall survival with durvalumab after chemoradiotherapy in stage III NSCLC," *New England Journal of Medicine*, **379(24)**, pp. 2342–2350.
- Apperley, J. F. *et al.* (2002) "Response to imatinib mesylate in patients with chronic myeloproliferative diseases with rearrangements of the platelet-derived growth factor receptor beta," *New England Journal of Medicine*, **347(7)**, pp. 481–487.
- Apsel, B. *et al.* (2008) "Targeted polypharmacology: Discovery of dual inhibitors of tyrosine and phosphoinositide kinases," *Nature Chemical Biology*, **4(11)**, pp. 691–699.
- Arcila, M. E. *et al.* (2013) "EGFR exon 20 insertion mutations in lung adenocarcinomas: prevalence, molecular heterogeneity, and clinicopathologic characteristics.," *Molecular Cancer Therapeutics*, **12(2)**, pp. 220–9.
- Arteaga, C. (2003) "ErbB-targeted therapeutic approaches in human cancer," *Experimental Cell Research*, **284(1)**, pp. 122–130.
- Asahina, H. *et al.* (2006) "Non-responsiveness to gefitinib in a patient with lung adenocarcinoma having rare EGFR mutations S768I and V769L," *Lung Cancer*, **54(3)**, pp. 419–422.
- Avizienyte, E., Ward, R. A. and Garner, A. P. (2008) "Comparison of the EGFR resistance mutation profiles generated by EGFR-targeted tyrosine kinase inhibitors and the impact of drug combinations.," *The Biochemical journal*, **415(2)**, pp. 197–206.
- Avraham, R. and Yarden, Y. (2011) "Feedback regulation of EGFR signalling: Decision making by early and delayed loops," *Nature Reviews Molecular Cell Biology*, pp. 104–117.
- Baek, J. H. *et al.* (2015) "Efficacy of EGFR tyrosine kinase inhibitors in patients with EGFR-mutated non-small cell lung cancer except both exon 19 deletion and exon 21 L858R: A retrospective analysis in Korea," *Lung Cancer*.
- Bajaj, M. *et al.* (1987) "On the tertiary structure of the extracellular domains of the epidermal growth factor and insulin receptors," *Biochimica et Biophysica Acta (BBA)/Protein Structure and Molecular*, **916(2)**, pp. 220–226.

- Balak, M. N. *et al.* (2006) "Novel D761Y and Common Secondary T790M Mutations in Epidermal Growth Factor Receptor-Mutant Lung Adenocarcinomas with Acquired Resistance to Kinase Inhibitors," *Clinical Cancer Research*, **12(21)**, pp. 6494–6501.
- Banno, E. *et al.* (2016) "Sensitivities to various epidermal growth factor receptor-tyrosine kinase inhibitors of uncommon *epidermal growth factor receptor* mutations L861Q and S768I: What is the optimal epidermal growth factor receptor-tyrosine kinase inhibitor?," *Cancer Science*, **107(8)**, pp. 1134–1140.
- Bao, J., Gur, G. and Yarden, Y. (2003) "Src promotes destruction of c-Cbl: Implications for oncogenic synergy between Src and growth factor receptors," *Proceedings of the National Academy of Sciences of the United States of America*, **100(5)**, pp. 2438–2443.
- Barkovich, K. J. *et al.* (2012) "Kinetics of inhibitor cycling underlie therapeutic disparities between EGFR-driven lung and brain cancers," *Cancer Discovery*, **2(5)**, pp. 450–457.
- Barone, M. V. and Courtneidge, S. A. (1995) "Myc but not Fos rescue of PDGF signalling block caused by kinase-inactive Src," *Nature*, **378(6556)**, pp. 509–512.
- Barrott, J. J. and Haystead, T. A. (2013) "Hsp90, an unlikely ally in the war on cancer," *FEBS J.* 2013/01/30, **280(6)**, pp. 1381–1396.
- Batzer, A. G. *et al.* (1994) "Hierarchy of binding sites for Grb2 and Shc on the epidermal growth factor receptor.," *Molecular and Cellular Biology*, **14(8)**, pp. 5192–5201.
- Bean, J. *et al.* (2008) "Acquired resistance to epidermal growth factor receptor kinase inhibitors associated with a novel T854A mutation in a patient with EGFR-mutant lung adenocarcinoma," *Clinical Cancer Research*, **14(22)**, pp. 7519–7525.
- Beau-Faller, M. *et al.* (2013) "Rare EGFR exon 18 and exon 20 mutations in non-small-cell lung cancer on 10 117 patients: a multicentre observational study by the French ERMETIC-IFCT network," *Annals of Oncology*, **25(1)**, pp. 126–131.
- Bersanelli, M. *et al.* (2016) "L718Q Mutation as New Mechanism of Acquired Resistance to AZD9291 in EGFR-Mutated NSCLC," *Journal of Thoracic Oncology*, **11(10)**, pp. e121–e123.
- Bessette, D. C. *et al.* (2015) "Using the MCF10A/MCF10CA1a Breast Cancer Progression Cell Line Model to Investigate the Effect of Active, Mutant Forms of EGFR in Breast Cancer Development and Treatment Using Gefitinib.," *PloS one*, **10(5)**, p. e0125232.

- Bessman, N. J. *et al.* (2014) “Complex Relationship between Ligand Binding and Dimerization in the Epidermal Growth Factor Receptor,” *Cell Reports*, **9(4)**, pp. 1306–1317.
- Binder, Z. A. *et al.* (2018) “Epidermal Growth Factor Receptor Extracellular Domain Mutations in Glioblastoma Present Opportunities for Clinical Imaging and Therapeutic Development,” *Cancer Cell*, **34(1)**, pp. 163-177.e7.
- Bivona, T. G. and Doebele, R. C. (2016) “A framework for understanding and targeting residual disease in oncogene-driven solid cancers,” *Nature Medicine*, **22(5)**, pp. 472–478.
- Blakely, C. M. *et al.* (2017) “Evolution and clinical impact of co-occurring genetic alterations in advanced-stage EGFR-mutant lung cancers,” *Nature Genetics*, **49(12)**, pp. 1693–1704.
- Bondeson, D. P. *et al.* (2015) “Catalytic in vivo protein knockdown by small-molecule PROTACs,” *Nature Chemical Biology*, **11(8)**, pp. 611–617.
- Borghaei, H. *et al.* (2015) “Nivolumab versus Docetaxel in Advanced Nonsquamous Non–Small-Cell Lung Cancer,” *New England Journal of Medicine*, **373(17)**, pp. 1627–1639.
- Borisov, N. *et al.* (2009) “Systems-level interactions between insulin-EGF networks amplify mitogenic signaling,” *Molecular Systems Biology*, **5**, p. 256.
- Bos, J. L. (1989) “ras Oncogenes in human cancer: A review,” *Cancer Research*, **49(17)**, pp. 4682–4689.
- Brennan, C. W. *et al.* (2013) “The somatic genomic landscape of glioblastoma,” *Cell*, **155(2)**, p. 462.
- Brewer, M. R. *et al.* (2013) “Mechanism for activation of mutated epidermal growth factor receptors in lung cancer,” *Proceedings of the National Academy of Sciences of the United States of America*, **110(38)**, p. E3595.
- Brixey, A. G. and Light, R. W. (2010) “Pleural effusions due to dasatinib,” *Current opinion in pulmonary medicine*, **16(4)**, pp. 351–356.
- Brown, B. P. *et al.* (2019a) “On-target Resistance to the Mutant-Selective EGFR Inhibitor Osimertinib Can Develop in an Allele-Specific Manner Dependent on the Original EGFR-Activating Mutation.,” *Clinical Cancer Research*, p. clincanres.3829.2018.
- Brown, B. P. *et al.* (2019b) “On-target resistance to the mutant-selective EGFR inhibitor osimertinib can develop in an allele-specific manner dependent on the original EGFR-activating mutation,” *Clinical Cancer Research*, **25(11)**, pp. 3341–3351.

- Brown, M. T. and Cooper, J. A. (1996) "Regulation, substrates and functions of src," *Biochimica et Biophysica Acta - Reviews on Cancer*, pp. 121–149.
- Brown, T. *et al.* (2010) "Gefitinib for the first-line treatment of locally advanced or metastatic non-small cell lung cancer.," *Health technology assessment (Winchester, England)*, pp. 71–79.
- de Bruin, E. C. *et al.* (2014) "Reduced NF1 expression confers resistance to EGFR inhibition in lung cancer," *Cancer Discovery*, **4(5)**, pp. 606–619.
- Buday, L., Warne, P. H. and Downward, J. (1995) "Downregulation of the Ras activation pathway by MAP kinase phosphorylation of Sos," *Oncogene*, **11(7)**, pp. 1327–1331.
- Burch, P. M. *et al.* (2004) "An Extracellular Signal-Regulated Kinase 1- and 2-Dependent Program of Chromatin Trafficking of c-Fos and Fra-1 Is Required for Cyclin D1 Expression during Cell Cycle Reentry," *Molecular and Cellular Biology*, **24(11)**, pp. 4696–4709.
- Burgess, A. W. *et al.* (2003) "An Open-and-Shut Case? Recent Insights into the Activation of EGF/ErbB Receptors," *Molecular Cell*, **12(3)**, pp. 541–552.
- Burslem, G. M. *et al.* (2018) "The Advantages of Targeted Protein Degradation Over Inhibition: An RTK Case Study," *Cell Chemical Biology*, **25(1)**, pp. 67-77.e3.
- Burslem, G. M. and Crews, C. M. (2020) "Proteolysis-Targeting Chimeras as Therapeutics and Tools for Biological Discovery," *Cell*, pp. 102–114.
- Burstein, H. J. (2005) "The Distinctive Nature of HER2-Positive Breast Cancers," *New England Journal of Medicine*, **353(16)**, pp. 1652–1654.
- Callegari, D. *et al.* (2018) "L718Q mutant EGFR escapes covalent inhibition by stabilizing a non-reactive conformation of the lung cancer drug osimertinib.," *Chemical science*, **9(10)**, pp. 2740–2749.
- Calò, V. *et al.* (2003) "STAT proteins: From normal control of cellular events to tumorigenesis," *Journal of Cellular Physiology*, **197(2)**, pp. 157–168.
- Capoferri, L. *et al.* (2015) "Quantum Mechanics/Molecular Mechanics Modeling of Covalent Addition between EGFR–Cysteine 797 and *N*-(4-Anilinoquinazolin-6-yl) Acrylamide," *Journal of Chemical Information and Modeling*, **55(3)**, pp. 589–599.
- Cardone, M. H. *et al.* (1998) "Regulation of cell death protease caspase-9 by phosphorylation," *Science*, **282(5392)**, pp. 1318–1321.
- Carey, K. D. *et al.* (2006) "Kinetic Analysis of Epidermal Growth Factor Receptor Somatic Mutant Proteins Shows Increased Sensitivity to the Epidermal Growth

Factor Receptor Tyrosine Kinase Inhibitor, Erlotinib,” *Cancer Research*, **66(16)**, pp. 8163–8171.

Carragher, N. O. *et al.* (2003) “A novel role for FAK as a protease-targeting adaptor protein: Regulation by p42 ERK and Src,” *Current Biology*, **13(16)**, pp. 1442–1450.

Carragher, N. O. and Frame, M. C. (2002) “Calpain: A role in cell transformation and migration,” *International Journal of Biochemistry and Cell Biology*, pp. 1539–1543.

Carraway, K. L. and Sweeney, C. (2002) “EGF receptor activation by heterologous mechanisms,” *Cancer Cell*, pp. 405–406.

Cerami, E. *et al.* (2012) “The cBio Cancer Genomics Portal: An Open Platform for Exploring Multidimensional Cancer Genomics Data,” *Cancer Discovery*, **2(5)**, pp. 401–4.

Cha, M. Y. *et al.* (2012) “Antitumor activity of HM781-36B, a highly effective pan-HER inhibitor in erlotinib-resistant NSCLC and other EGFR-dependent cancer models,” *International Journal of Cancer*, **130(10)**, pp. 2445–2454.

Chabon, J. J. *et al.* (2016) “Circulating tumour DNA profiling reveals heterogeneity of EGFR inhibitor resistance mechanisms in lung cancer patients,” *Nature Communications*, **7**.

Chalhoub, N. and Baker, S. J. (2009) “PTEN and the PI3-Kinase Pathway in Cancer,” *Annual Review of Pathology: Mechanisms of Disease*, **4(1)**, pp. 127–150.

Chambard, J. C. *et al.* (2007) “ERK implication in cell cycle regulation,” *Biochimica et Biophysica Acta - Molecular Cell Research*, pp. 1299–1310.

Chandramohan, V. *et al.* (2019) “Improved efficacy against malignant brain tumors with EGFRwt/EGFRvIII targeting immunotoxin and checkpoint inhibitor combinations,” *Journal for ImmunoTherapy of Cancer*, **7(1)**, p. 142.

Chattopadhyay, A. *et al.* (1999) “The role of individual SH2 domains in mediating association of phospholipase C- γ 1 with the activated EGF receptor,” *Journal of Biological Chemistry*, **274(37)**, pp. 26091–26097.

Chen, K. *et al.* (2017) “Novel Mutations on EGFR Leu792 Potentially Correlate to Acquired Resistance to Osimertinib in Advanced NSCLC,” *Journal of Thoracic Oncology*, **12(6)**, pp. e65–e68.

Chen, W., Li, Y. and Wang, Z. (2018) “Evolution of oncogenic signatures of mutation hotspots in tyrosine kinases supports the atavistic hypothesis of cancer,” *Scientific Reports*, **8(1)**, p. 8256.

- Cheng, C. *et al.* (2015) "EGFR Exon 18 Mutations in East Asian Patients with Lung Adenocarcinomas: A Comprehensive Investigation of Prevalence, Clinicopathologic Characteristics and Prognosis," *Scientific Reports*, **5(1)**, p. 13959.
- Chiba, M. *et al.* (2017) "Efficacy of irreversible EGFR-TKIs for the uncommon secondary resistant EGFR mutations L747S, D761Y, and T854A.," *BMC cancer*, **17(1)**, p. 281.
- Chiu, C.-H. *et al.* (2015) "Epidermal Growth Factor Receptor Tyrosine Kinase Inhibitor Treatment Response in Advanced Lung Adenocarcinomas with G719X/L861Q/S768I Mutations," *Journal of Thoracic Oncology*, **10(5)**, pp. 793–799.
- Chmielecki, J. *et al.* (2011) "Optimization of dosing for EGFR-mutant non-small cell lung cancer with evolutionary cancer modeling," *Science Translational Medicine*, **3(90)**, pp. 90ra59-90ra59.
- Cho, J. *et al.* (2013) "Cetuximab response of lung cancer-derived EGF receptor mutants is associated with asymmetric dimerization," *Cancer Research*, **73(22)**, pp. 6770–6779.
- Chung, K. P. *et al.* (2012) "Clinical outcomes in non-small cell lung cancers harboring different exon 19 deletions in EGFR," *Clinical Cancer Research*, **18(12)**, pp. 3470–3477.
- Coghill, E. L. *et al.* (2002) "A gene-driven approach to the identification of ENU mutants in the mouse," *Nature Genetics*, **30(3)**, pp. 255–256.
- Collisson, E. A., Campbell, J. D., Brooks, A. N., Berger, A. H., Lee, W. *et al.* (2014) "Comprehensive molecular profiling of lung adenocarcinoma," *Nature*, **511(7511)**, pp. 543–550.
- Cortes, J. E. *et al.* (2017) "Pleural Effusion in Dasatinib-Treated Patients With Chronic Myeloid Leukemia in Chronic Phase: Identification and Management.," *Clinical lymphoma, myeloma & leukemia*, **17(2)**, pp. 78–82.
- Cortot, A. B. *et al.* (2013) "Resistance to irreversible EGF receptor tyrosine kinase inhibitors through a multistep mechanism involving the IGF1R pathway," *Cancer Research*, **73(2)**, pp. 834–843.
- Costa, D. B. *et al.* (2007) "BIM Mediates EGFR Tyrosine Kinase Inhibitor-Induced Apoptosis in Lung Cancers with Oncogenic EGFR Mutations," *PLoS Medicine*. Edited by I. K. Mellinghoff, **4(10)**, p. e315.
- Courtin, A. *et al.* (2016) "Emergence of resistance to tyrosine kinase inhibitors in non-small-cell lung cancer can be delayed by an upfront combination with the

HSP90 inhibitor onalespib,” *British Journal of Cancer*. 2016/10/26, **115(9)**, pp. 1069–1077.

Creelan, B. C. *et al.* (2019) “Phase 1 trial of dasatinib combined with afatinib for epidermal growth factor receptor- (EGFR-) mutated lung cancer with acquired tyrosine kinase inhibitor (TKI) resistance.,” *British journal of cancer*, **120(8)**, pp. 791–796.

Cross, D. A. E. *et al.* (2014) “AZD9291, an irreversible EGFR TKI, overcomes T790M-mediated resistance to EGFR inhibitors in lung cancer.,” *Cancer Discovery*, **4(9)**, pp. 1046–61.

Cruz, A. L. S. *et al.* (2019) “Cell Cycle Progression Regulates Biogenesis and Cellular Localization of Lipid Droplets,” *Molecular and cellular biology*, **39(9)**, pp. e00374-18.

Crystal, A. S. *et al.* (2014) “Patient-derived models of acquired resistance can identify effective drug combinations for cancer,” *Science*, **346(6216)**, pp. 1480–1486.

Daksis, J. I. *et al.* (1994) “Myc induces cyclin D1 expression in the absence of de novo protein synthesis and links mitogen-stimulated signal transduction to the cell cycle.,” *Oncogene*, **9(12)**, pp. 3635–3645.

D’Angelo, S. P. *et al.* (2011) “Incidence of EGFR exon 19 deletions and L858R in tumor specimens from men and cigarette smokers with lung adenocarcinomas.,” *Journal of Clinical Oncology*, **29(15)**, pp. 2066–70.

Dar, A. C. *et al.* (2012) “Chemical genetic discovery of targets and anti-targets for cancer polypharmacology,” *Nature*, **486(7401)**, pp. 80–84.

Datta, S. R. *et al.* (1997) “Akt phosphorylation of BAD couples survival signals to the cell- intrinsic death machinery,” *Cell*, **91(2)**, pp. 231–241.

Daud, A. I. *et al.* (2012) “Phase I Study of Bosutinib, a Src/Abl Tyrosine Kinase Inhibitor, Administered to Patients with Advanced Solid Tumors,” *Clinical Cancer Research*, **18(4)**, pp. 1092 LP – 1100.

David, M. *et al.* (1996) “STAT activation by epidermal growth factor (EGF) and amphiregulin: Requirement for the EGF receptor kinase but not for tyrosine phosphorylation sites or JAK1,” *Journal of Biological Chemistry*, **271(16)**, pp. 9185–9188.

Davies, H. *et al.* (2002) “Mutations of the BRAF gene in human cancer,” *Nature*, **417(6892)**, pp. 949–954.

Davis, M. I. *et al.* (2011) “Comprehensive analysis of kinase inhibitor selectivity,” *Nature Biotechnology*, **29(11)**, pp. 1046–1051.

- Deeks, E. D. and Keating, G. M. (2018) "Afatinib in advanced NSCLC: a profile of its use," *Drugs and Therapy Perspectives*, **34(3)**, pp. 89–98.
- Demetri, G. D. *et al.* (2002) "Efficacy and safety of imatinib mesylate in advanced gastrointestinal stromal tumors," *New England Journal of Medicine*, **347(7)**, pp. 472–480.
- Dhingra, K. (2016) "Rociletinib: has the TIGER lost a few of its stripes?," *Annals of Oncology*, **27(6)**, pp. 1161–1164.
- Diehl, J. A. *et al.* (1998) "Glycogen synthase kinase-3 β regulates cyclin D1 proteolysis and subcellular localization," *Genes and Development*, **12(22)**, pp. 3499–3511.
- Ding, H. *et al.* (2001) "Astrocyte-specific expression of activated p21-ras results in malignant astrocytoma formation in a transgenic mouse model of human gliomas," *Cancer Research*, **61(9)**, pp. 3826–3836.
- Doebbele, R. C. *et al.* (2018) "First report of safety, PK, and preliminary antitumor activity of the oral EGFR/HER2 exon 20 inhibitor TAK-788 (AP32788) in non-small cell lung cancer (NSCLC).," *Journal of Clinical Oncology*, **36(15_suppl)**, pp. 9015–9015.
- Dominguez, C., Tsang, K.-Y. and Palena, C. (2016) "Short-term EGFR blockade enhances immune-mediated cytotoxicity of EGFR mutant lung cancer cells: rationale for combination therapies.," *Cell death & disease*, **7(9)**, p. e2380.
- Druker, B. J. *et al.* (1996) "Effects of a selective inhibitor of the Abl tyrosine kinase on the growth of Bcr-Abl positive cells," *Nature Medicine*, **2(5)**, pp. 561–566.
- Du, Z. and Lovly, C. M. (2018) "Mechanisms of receptor tyrosine kinase activation in cancer," *Molecular Cancer*, **17(1)**, pp. 1–13.
- Duchnowska, R., Loibl, S. and Jassem, J. (2018) "Tyrosine kinase inhibitors for brain metastases in HER2-positive breast cancer," *Cancer Treatment Reviews*, **67**, pp. 71–77.
- Duong-Ly, K. C. *et al.* (2016) "Kinase Inhibitor Profiling Reveals Unexpected Opportunities to Inhibit Disease-Associated Mutant Kinases," *Cell Reports*, **14(4)**, pp. 772–781.
- Eck, M. J. and Yun, C.-H. (2010) "Structural and mechanistic underpinnings of the differential drug sensitivity of EGFR mutations in non-small cell lung cancer.," *Biochimica et Biophysica Acta*, **1804(3)**, pp. 559–66.
- Elamin, Y. *et al.* (2019) "MA09.03 Identification of Mechanisms of Acquired Resistance to Poziotinib in EGFR Exon 20 Mutant Non-Small Cell Lung Cancer (NSCLC)," *Journal of Thoracic Oncology*, **14(10)**, pp. S282–S283.

- Ellis, P. M. *et al.* (2014) “NCIC CTG BR.26: A phase III randomized, double blind, placebo controlled trial of dacomitinib versus placebo in patients with advanced/metastatic non-small cell lung cancer (NSCLC) who received prior chemotherapy and an EGFR TKI.,” *Journal of Clinical Oncology*, **32(15_suppl)**, pp. 8036–8036.
- Engelman, J. A. *et al.* (2007a) “MET amplification leads to gefitinib resistance in lung cancer by activating ERBB3 signaling,” *Science*, **316(5827)**, pp. 1039–1043.
- Engelman, J. A. *et al.* (2007b) “PF00299804, an irreversible pan-ERBB inhibitor, is effective in lung cancer models with EGFR and ERBB2 mutations that are resistant to gefitinib,” *Cancer Research*, **67(24)**, pp. 11924–11932.
- Ercan, D. *et al.* (2015) “EGFR Mutations and Resistance to Irreversible Pyrimidine-Based EGFR Inhibitors.,” *Clinical Cancer Research*, **21(17)**, pp. 3913–23.
- Estrada-Bernal, A. *et al.* (2018) “Abstract A157: Antitumor activity of tarloxotinib, a hypoxia-activated EGFR TKI, in patient-derived lung cancer cell lines harboring EGFR exon 20 insertions,” in, pp. A157–A157.
- Fabian, M. A. *et al.* (2005) “A small molecule–kinase interaction map for clinical kinase inhibitors,” *Nature Biotechnology*, **23(3)**, pp. 329–336.
- Fairclough, S. R. *et al.* (2019) “Identification of osimertinib-resistant EGFR L792 mutations by cfDNA sequencing: Oncogenic activity assessment and prevalence in large cfDNA cohort,” *Experimental Hematology and Oncology*, **8(1)**.
- Fans, Z. *et al.* (1994) “Antibody-induced Epidermal Growth Factor Receptor Dimerization Mediates Inhibition of Autocrine Proliferation of A431 Squamous Carcinoma Cells*,” *Journal of Biological Chemistry*, **269(44)**, pp. 27595–27602.
- Fassunke, J. *et al.* (2018) “Overcoming EGFRG724S-mediated osimertinib resistance through unique binding characteristics of second-generation EGFR inhibitors,” *Nature Communications*, **9(1)**, p. 4655.
- FDA (2017) *Osimertinib (TAGRISSO) | FDA.*
- FDA (2018a) *FDA approves dacomitinib for metastatic non-small cell lung cancer | FDA.*
- FDA (2018b) *FDA approves osimertinib for first-line treatment of metastatic NSCLC with most common EGFR mutations | FDA.*
- FDA (2018c) *FDA broadens afatinib indication to previously untreated, metastatic NSCLC with other non-resistant EGFR mutations, FDA.*

- Fehrenbacher, L. *et al.* (2016) “Atezolizumab versus docetaxel for patients with previously treated non-small-cell lung cancer (POPLAR): a multicentre, open-label, phase 2 randomised controlled trial,” *The Lancet*, **387(10030)**, pp. 1837–1846.
- Flanagan, J. J. *et al.* (2019) “Abstract P5-04-18: ARV-471, an oral estrogen receptor PROTAC degrader for breast cancer,” *Cancer Research*, **79(4 Supplement)**, pp. P5-04-18 LP-P5-04–18.
- Flatt, T. (2005) “The evolutionary genetics of canalization,” *Q Rev Biol*, **80(3)**, pp. 287–316.
- Floc’h, N. *et al.* (2018) “Anti-tumor activity of osimertinib, an irreversible mutant-selective EGFR tyrosine kinase inhibitor, in NSCLC harboring EGFR Exon 20 Insertions,” *Molecular Cancer Therapeutics*, p. molcanther.0758.2017.
- Formisano, L. *et al.* (2015) “Src inhibitors act through different mechanisms in Non-Small Cell Lung Cancer models depending on EGFR and RAS mutational status.,” *Oncotarget*, **6(28)**, pp. 26090–103.
- Frederick, L. *et al.* (2000) *Diversity and Frequency of Epidermal Growth Factor Receptor Mutations in Human Glioblastomas*, *Cancer Research*.
- Friboulet, L. *et al.* (2014) “The ALK inhibitor ceritinib overcomes crizotinib resistance in non-small cell lung cancer.,” *Cancer Discovery*, **4(6)**, pp. 662–673.
- Froudarakis, M. E. (2012) “Pleural effusion in lung cancer: more questions than answers.,” *Respiration; international review of thoracic diseases*, **83(5)**, pp. 367–376.
- Fujita, Y. *et al.* (2002) “Hakai, a c-Cbl-like protein, ubiquitinates and induces endocytosis of the E-cadherin complex,” *Nature Cell Biology*, **4(3)**, pp. 222–231.
- Fukuoka, M. *et al.* (2003) “Multi-institutional randomized phase II trial of gefitinib for previously treated patients with advanced non-small-cell lung cancer,” *Journal of Clinical Oncology*, **21(12)**, pp. 2237–2246.
- Gainor, J. F. *et al.* (2016a) “Dramatic response to combination erlotinib and crizotinib in a patient with advanced, EGFR-mutant lung cancer harboring de Novo MET amplification,” *Journal of Thoracic Oncology*, **11(7)**, pp. e83–e85.
- Gainor, J. F. *et al.* (2016b) “EGFR mutations and ALK rearrangements are associated with low response rates to PD-1 pathway blockade in non-small cell lung cancer: A retrospective analysis,” *Clinical Cancer Research*, **22(18)**, pp. 4585–4593.
- Gainor, J. F. *et al.* (2020) “A Phase II Study of the Multikinase Inhibitor Ponatinib in Patients With Advanced, RET-Rearranged NSCLC,” *JTO Clinical and Research Reports*, **1(3)**, p. 100045.

- Gan, H. K. *et al.* (2012) “Targeting of a conformationally exposed, tumor-specific epitope of EGFR as a strategy for cancer therapy,” *Cancer Research*, pp. 2924–2930.
- Gan, H. K. *et al.* (2013) “ A phase I and biodistribution study of ABT-806i, an 111 indium-labeled conjugate of the tumor-specific anti-EGFR antibody ABT-806. ,” *Journal of Clinical Oncology*, **31(15_suppl)**, pp. 2520–2520.
- Gao, J. *et al.* (2013) “Integrative analysis of complex cancer genomics and clinical profiles using the cBioPortal.,” *Science signaling*, **6(269)**, p. p11.
- Gao, Y., Vallentgoed, W. R. and French, P. J. (2018) “Finding the right way to target EGFR in glioblastomas; Lessons from lung adenocarcinomas,” *Cancers*, **10(12)**.
- Garrett, T. P. J. *et al.* (2002) “Crystal structure of a truncated epidermal growth factor receptor extracellular domain bound to transforming growth factor α ,” *Cell*, **110(6)**, pp. 763–773.
- Gaudelli, N. M. *et al.* (2017) “Programmable base editing of T to G C in genomic DNA without DNA cleavage,” *Nature*, **551(7681)**, pp. 464–471.
- Gazdar, A. F. (2009) “Activating and resistance mutations of EGFR in non-small-cell lung cancer: role in clinical response to EGFR tyrosine kinase inhibitors.,” *Oncogene*, **28 Suppl 1(Suppl 1)**, pp. S24-31.
- Ge, H., Gong, X. and Tang, C. K. (2002) “Evidence of high incidence of EGFRvIII expression and coexpression with EGFR in human invasive breast cancer by laser capture microdissection and immunohistochemical analysis,” *International Journal of Cancer*, **98(3)**, pp. 357–361.
- Gettinger, S. *et al.* (2018) “Five-Year Follow-Up of Nivolumab in Previously Treated Advanced Non-Small-Cell Lung Cancer: Results From the CA209-003 Study.,” *Journal of Clinical Oncology*, **36(17)**, pp. 1675–1684.
- Gettinger, S. N. *et al.* (2016) “Activity and safety of brigatinib in ALK-rearranged non-small-cell lung cancer and other malignancies: a single-arm, open-label, phase 1/2 trial,” *The Lancet Oncology*, **17(12)**, pp. 1683–1696.
- Ghosn, J. *et al.* (2018) “HIV,” *The Lancet*, **392(10148)**, pp. 685–697.
- Giaccone, G. *et al.* (2004) “Gefitinib in combination with gemcitabine and cisplatin in advanced non-small-cell lung cancer: A phase III trial - INTACT 1,” *Journal of Clinical Oncology*, **22(5)**, pp. 777–784.
- Godin-Heymann, N. *et al.* (2007) “Oncogenic activity of epidermal growth factor receptor kinase mutant alleles is enhanced by the T790M drug resistance mutation,” *Cancer Research*, **67(15)**, pp. 7319–7326.

- Goldberg, S. B. *et al.* (2013) “Chemotherapy With Erlotinib or Chemotherapy Alone in Advanced Non-Small Cell Lung Cancer With Acquired Resistance to EGFR Tyrosine Kinase Inhibitors,” *The Oncologist*, **18(11)**, pp. 1214–1220.
- Goldstein, N. I. *et al.* (1995) “Biological Efficacy of a Chimeric Antibody to the Epidermal Growth Factor Receptor in a Human Tumor Xenograft Model,” *Clinical Cancer Research*, **1(11)**, pp. 1311–1318.
- Gonzalvez, F. *et al.* (2016) “Abstract 2644: AP32788, a potent, selective inhibitor of EGFR and HER2 oncogenic mutants, including exon 20 insertions, in preclinical models,” *Cancer Research*, **76(14 Supplement)**, pp. 2644–2644.
- Gonzalvez, F. (2020) *TAK-788: An EGFR inhibitor, currently in Phase II clinical trials, targeting lung cancers with Exon20 insertion mutations*, AACR 2020.
- Goss, G. *et al.* (2016) “Osimertinib for pretreated EGFR Thr790Met-positive advanced non-small-cell lung cancer (AURA2): a multicentre, open-label, single-arm, phase 2 study,” *The Lancet Oncology*, **17**, pp. 1643–52.
- Govindan, R. *et al.* (2012) “Genomic landscape of non-small cell lung cancer in smokers and never-smokers,” *Cell*, **150(6)**, pp. 1121–1134.
- Grandal, M. v *et al.* (2007) “EGFRvIII escapes down-regulation due to impaired internalization and sorting to lysosomes,” *Carcinogenesis*, **28(7)**, pp. 1408–1417.
- Greaves, M. and Maley, C. C. (2012) “Clonal evolution in cancer,” *Nature*, pp. 306–313.
- Greulich, H. *et al.* (2005) “Oncogenic transformation by inhibitor-sensitive and -resistant EGFR mutants.,” *PLoS medicine*, **2(11)**, p. e313.
- Greulich, H. *et al.* (2012) “Functional analysis of receptor tyrosine kinase mutations in lung cancer identifies oncogenic extracellular domain mutations of ERBB2.,” *Proceedings of the National Academy of Sciences of the United States of America*, **109(36)**, pp. 14476–81.
- Grice, G. L. and Nathan, J. A. (2016) “The recognition of ubiquitinated proteins by the proteasome,” *Cellular and Molecular Life Sciences*, pp. 3497–3506.
- Gu, H. and Neel, B. G. (2003) “The ‘Gab’ in signal transduction,” *Trends in Cell Biology*, pp. 122–130.
- de Gunst, M. M. *et al.* (2007) “Functional analysis of cancer-associated EGFR mutants using a cellular assay with YFP-tagged EGFR intracellular domain,” *Molecular Cancer*, **6**, p. 56.

Guo, A. *et al.* (2008) "Signaling networks assembled by oncogenic EGFR and c-Met," *Proceedings of the National Academy of Sciences of the United States of America*, **105(2)**, pp. 692–697.

Guo, L. *et al.* (2003) "Studies of ligand-induced site-specific phosphorylation of epidermal growth factor receptor," *Journal of the American Society for Mass Spectrometry*, **14(9)**, pp. 1022–1031.

Ham, J. S. *et al.* (2016) "Two cases of small cell lung cancer transformation from EGFR mutant adenocarcinoma during AZD9291 treatment," *Journal of Thoracic Oncology*, **11(1)**, pp. e1–e4.

Han, J. Y. *et al.* (2017) "A phase II study of poziotinib in patients with epidermal growth factor receptor (EGFR)-mutant lung adenocarcinoma who have acquired resistance to EGFR-tyrosine kinase inhibitors," *Cancer Research and Treatment*, **49(1)**, pp. 10–19.

Harrison, P. T. and Huang, P. H. (2018) "Exploiting vulnerabilities in cancer signalling networks to combat targeted therapy resistance.," *Essays in biochemistry*, p. EBC20180016.

Harrison, P. T., Vyse, S. and Huang, P. H. (2019) "Rare epidermal growth factor receptor (EGFR) mutations in non-small cell lung cancer," *Seminars in Cancer Biology*.

Hasako, S. *et al.* (2018) "TAS6417, A Novel EGFR Inhibitor Targeting Exon 20 Insertion Mutations," *Molecular Cancer Therapeutics*, **17(8)**, pp. 1648–1658.

Hata, A. *et al.* (2010) "Complex mutations in the epidermal growth factor receptor gene in non-small cell lung cancer," *Journal of Thoracic Oncology*, **5(10)**, pp. 1524–1528.

Hata, A. N. *et al.* (2016) "Tumor cells can follow distinct evolutionary paths to become resistant to epidermal growth factor receptor inhibition," *Nature Medicine*, **22(3)**, pp. 262–269.

Haura, E. B. *et al.* (2010) "Phase I/II study of the Src inhibitor dasatinib in combination with erlotinib in advanced non-small-cell lung cancer.," *Journal of clinical oncology : official journal of the American Society of Clinical Oncology*, **28(8)**, pp. 1387–1394.

He, M. *et al.* (2012a) "EGFR exon 19 insertions: a new family of sensitizing EGFR mutations in lung adenocarcinoma.," *Clinical cancer research : an official journal of the American Association for Cancer Research*, **18(6)**, pp. 1790–7.

He, M. *et al.* (2012b) "EGFR exon 19 insertions: a new family of sensitizing EGFR mutations in lung adenocarcinoma.," *Clinical cancer research : an official journal of the American Association for Cancer Research*, **18(6)**, pp. 1790–7.

- Hegi, M. E. *et al.* (2011) "Pathway analysis of glioblastoma tissue after preoperative treatment with the EGFR tyrosine kinase inhibitor gefitinib - A phase II trial," *Molecular Cancer Therapeutics*, **10(6)**, pp. 1102–1112.
- Heigener, D. F. *et al.* (2015) "Afatinib in Non-Small Cell Lung Cancer Harboring Uncommon EGFR Mutations Pretreated With Reversible EGFR Inhibitors.," *The oncologist*, **20(10)**, pp. 1167–74.
- Heinrich, M. C. *et al.* (2003) "Kinase mutations and imatinib response in patients with metastatic gastrointestinal stromal tumor," *Journal of Clinical Oncology*, **21(23)**, pp. 4342–4349.
- Heldin, C.-H. (1995) "Dimerization of Cell Surface Receptors in Signal Transduction Review," *Cell*, **80**, pp. 213–223.
- Hellmann, M. D. *et al.* (2014) "Clinical and in vivo Evidence that EGFR S768I Mutant Lung Adenocarcinomas Are Sensitive to Erlotinib," *Journal of Thoracic Oncology*, **9(10)**, pp. e73–e74.
- Herbst, R. S. *et al.* (2004) "Gefitinib in combination with paclitaxel and carboplatin in advanced non-small-cell lung cancer: A phase III trial - INTACT 2," *Journal of Clinical Oncology*, **22(5)**, pp. 785–794.
- Hess, G. T. *et al.* (2017) "Methods and applications of CRISPR-mediated base editing in eukaryotic genomes," *Mol Cell*, **68**, pp. 26–43.
- Heymach, J. v *et al.* (2014) "EGFR biomarkers predict benefit from vandetanib in combination with docetaxel in a randomized phase III study of second-line treatment of patients with advanced non-small cell lung cancer," *Annals of Oncology*, **25(10)**, pp. 1941–1948.
- Hirschhaeuser, F. *et al.* (2010) "Multicellular tumor spheroids: An underestimated tool is catching up again," *Journal of Biotechnology*, **148(1)**, pp. 3–15.
- Hoffknecht, P. *et al.* (2015) "Efficacy of the irreversible ErbB family blocker afatinib in epidermal growth factor receptor (EGFR) tyrosine kinase inhibitor (TKI)-pretreated non-small-cell lung cancer patients with brain metastases or leptomeningeal disease," *Journal of Thoracic Oncology*, **10(1)**, pp. 156–163.
- Hsu, J. H.-R. *et al.* (2020) "EED-Targeted PROTACs Degrade EED, EZH2, and SUZ12 in the PRC2 Complex.," *Cell Chemical Biology*, **27(1)**, pp. 41-46.e17.
- Huang, P. H. *et al.* (2007) "Quantitative analysis of EGFRvIII cellular signaling networks reveals a combinatorial therapeutic strategy for glioblastoma.," *Proceedings of the National Academy of Sciences of the United States of America*, **104(31)**, pp. 12867–72.

- Huang, P. H. *et al.* (2010) "Phosphotyrosine signaling analysis of site-specific mutations on EGFRvIII identifies determinants governing glioblastoma cell growth," *Molecular BioSystems*, **6(7)**, pp. 1227–1237.
- Hubbard, S. R. (1999) "Structural analysis of receptor tyrosine kinases," *Progress in Biophysics and Molecular Biology*, **71(3–4)**, pp. 343–358.
- Humphrey, P. A. *et al.* (1991) "Deletion-mutant epidermal growth factor receptor in human gliomas: Effect of type II mutation on receptor function," *Biochemical and Biophysical Research Communications*, **178(3)**, pp. 1413–1420.
- Ichihara, E. *et al.* (2017) "SFK/FAK Signaling Attenuates Osimertinib Efficacy in Both Drug-Sensitive and Drug-Resistant Models of EGFR-Mutant Lung Cancer," *Cancer Research*, **77(11)**, pp. 2990–3000.
- Iuchi, T. *et al.* (2015) "Frequency of brain metastases in non-small-cell lung cancer, and their association with epidermal growth factor receptor mutations," *International Journal of Clinical Oncology*, **20(4)**, pp. 674–679.
- Iyevleva, A. G. *et al.* (2014) "Lung carcinomas with EGFR exon 19 insertions are sensitive to gefitinib treatment," *Journal of Thoracic Oncology*, pp. e31–e33.
- Jackman, D. M. *et al.* (2006) "Exon 19 deletion mutations of epidermal growth factor receptor are associated with prolonged survival in non-small cell lung cancer patients treated with gefitinib or erlotinib.," *Clinical Cancer Research*, **12(13)**, pp. 3908–14.
- Jallal, B., Schlessinger, J. and Ullrich, A. (1992) "Tyrosine phosphatase inhibition permits analysis of signal transduction complexes in p185HER2/neu-overexpressing human tumor cells.," *The Journal of Biological Chemistry*, **267(7)**, pp. 4357–4363.
- Jamal-Hanjani, M. *et al.* (2017) "Tracking the Evolution of Non-Small-Cell Lung Cancer," *New England Journal of Medicine*, **376(22)**, pp. 2109–2121.
- Jamora, C. and Fuchs, E. (2002) "Intercellular adhesion, signalling and the cytoskeleton," *Nature Cell Biology*, pp. E101–E108.
- Jang, J. *et al.* (2018) "Discovery of a Highly Potent and Broadly Effective EGFR and HER2 Exon 20 Insertion Mutant Inhibitor," *Angewandte Chemie International Edition*, **02115**, pp. 11629–11633.
- Janjigian, Y. Y. *et al.* (2014) "Dual inhibition of EGFR with afatinib and cetuximab in kinase inhibitor-resistant EGFR-mutant lung cancer with and without T790M mutations," *Cancer Discovery*, **4(9)**, pp. 1036–1045.

- Jänne, P. A. *et al.* (2004) "Outcomes of patients with advanced non-small cell lung cancer treated with gefitinib (ZD1839, 'Iressa') on an expanded access study," *Lung Cancer*, **44(2)**, pp. 221–230.
- Jänne, P. A. *et al.* (2011) "Phase I dose-escalation study of the pan-HER inhibitor, PF299804, in patients with advanced malignant solid tumors," *Clinical Cancer Research*, **17(5)**, pp. 1131–1139.
- Jänne, P. A. *et al.* (2014) "Dacomitinib as first-line treatment in patients with clinically or molecularly selected advanced non-small-cell lung cancer: a multicentre, open-label, phase 2 trial," *The Lancet Oncology*, **15(13)**, pp. 1433–1441.
- Jarosz, D. F. and Lindquist, S. (2010) "Hsp90 and environmental stress transform the adaptive value of natural genetic variation," *Science*, **330(6012)**, pp. 1820–1824.
- Jarosz, D. F., Taipale, M. and Lindquist, S. (2010) "Protein homeostasis and the phenotypic manifestation of genetic diversity: principles and mechanisms," *Annu Rev Genet.* 2010/11/05, **44**, pp. 189–216.
- Jeuken, J. *et al.* (2009) "Robust detection of EGFR copy number changes and EGFR variant III: technical aspects and relevance for glioma diagnostics.," *Brain pathology (Zurich, Switzerland)*, **19(4)**, pp. 661–71.
- Ji, H. *et al.* (2006a) "Epidermal growth factor receptor variant III mutations in lung tumorigenesis and sensitivity to tyrosine kinase inhibitors," *Proceedings of the National Academy of Sciences of the United States of America*, **103(20)**, pp. 7817–7822.
- Ji, H. *et al.* (2006b) "Epidermal growth factor receptor variant III mutations in lung tumorigenesis and sensitivity to tyrosine kinase inhibitors," *Proceedings of the National Academy of Sciences of the United States of America*, **103(20)**, pp. 7817–7822.
- Jia, Y. *et al.* (2016) "Overcoming EGFR(T790M) and EGFR(C797S) resistance with mutant-selective allosteric inhibitors," *Nature*, **534(7605)**, pp. 129–132.
- Johns, T. G. *et al.* (2004) "Identification of the epitope for the epidermal growth factor receptor-specific monoclonal antibody 806 reveals that it preferentially recognizes an untethered form of the receptor," *Journal of Biological Chemistry*, **279(29)**, pp. 30375–30384.
- Johnson, F. M. *et al.* (2010) "Phase II study of dasatinib in patients with advanced non-small-cell lung cancer.," *Journal of clinical oncology : official journal of the American Society of Clinical Oncology*, **28(30)**, pp. 4609–4615.

- Johnson, M. L. *et al.* (2011) “Phase II trial of dasatinib for patients with acquired resistance to treatment with the epidermal growth factor receptor tyrosine kinase inhibitors erlotinib or gefitinib.,” *Journal of thoracic oncology : official publication of the International Association for the Study of Lung Cancer*, **6(6)**, pp. 1128–1131.
- Johnson, M. L. *et al.* (2015) “Phase I/II Study of HSP90 Inhibitor AUY922 and Erlotinib for EGFR-Mutant Lung Cancer With Acquired Resistance to Epidermal Growth Factor Receptor Tyrosine Kinase Inhibitors,” *Journal of Clinical Oncology*, **33(15)**, pp. 1666–1673.
- Jonsson, V. D. *et al.* (2017) “Novel computational method for predicting polytherapy switching strategies to overcome tumor heterogeneity and evolution,” *Scientific Reports*, **7**, p. 44206.
- Jorge, S. E. *et al.* (2018) “EGFR Exon 20 Insertion Mutations Display Sensitivity to Hsp90 Inhibition in Preclinical Models and Lung Adenocarcinomas,” *Clinical Cancer Research*, **24(24)**, pp. 6548 LP – 6555.
- Jura, N. *et al.* (2009) “Mechanism for Activation of the EGF Receptor Catalytic Domain by the Juxtamembrane Segment,” *Cell*, **137(7)**, pp. 1293–1307.
- Jura, N. *et al.* (2011) “Catalytic Control in the EGF Receptor and Its Connection to General Kinase Regulatory Mechanisms,” *Molecular Cell*, pp. 9–22.
- Kaneda, T. *et al.* (2014) “Possible differential EGFR-TKI efficacy among exon 19 deletional locations in EGFR-mutant non-small cell lung cancer,” *Lung Cancer*, **86(2)**, pp. 213–218.
- Kantarjian, H. *et al.* (2006) “Dasatinib,” *Nature Reviews Drug Discovery 2006* **5:9**, **5(9)**, pp. 717–718.
- Karaman, M. W. *et al.* (2008) “A quantitative analysis of kinase inhibitor selectivity,” *Nature Biotechnology*, **26(1)**, pp. 127–132.
- Katakami, N. *et al.* (2013) “LUX-Lung 4: a phase II trial of afatinib in patients with advanced non-small-cell lung cancer who progressed during prior treatment with erlotinib, gefitinib, or both.,” *Journal of Clinical Oncology*, **31(27)**, pp. 3335–41.
- Katayama, R. *et al.* (2015) “Cabozantinib overcomes crizotinib resistance in ROS1 fusion-positive cancer.,” *Clinical Cancer Research*, **21(1)**, pp. 166–174.
- Kentsis, A. *et al.* (2012) “Autocrine activation of the MET receptor tyrosine kinase in acute myeloid leukemia,” *Nature Medicine*, **18(7)**, pp. 1118–1122.
- Khan, S. *et al.* (2019) “A selective BCL-X(L) PROTAC degrader achieves safe and potent antitumor activity.,” *Nature Medicine*, **25(12)**, pp. 1938–1947.

- Kim, J. Y., Cho, C. H. and Song, H. S. (2017) "Targeted therapy of ovarian cancer including immune check point inhibitor," *Korean Journal of Internal Medicine*, pp. 798–804.
- Kim, N. *et al.* (2020) "Colorectal adenocarcinoma-derived EGFR mutants are oncogenic and sensitive to EGFR-targeted monoclonal antibodies, cetuximab and panitumumab," *International Journal of Cancer*, **146(8)**, pp. 2194–2200.
- Kisseleva, T. *et al.* (2002) "Signaling through the JAK/STAT pathway, recent advances and future challenges," *Gene*, pp. 1–24.
- Kobayashi, S. *et al.* (2005) "EGFR Mutation and Resistance of Non–Small-Cell Lung Cancer to Gefitinib," *New England Journal of Medicine*, **352(8)**, pp. 786–792.
- Kobayashi, S. *et al.* (2013) "Compound EGFR mutations and response to EGFR tyrosine kinase inhibitors.," *Journal of thoracic oncology : official publication of the International Association for the Study of Lung Cancer*, **8(1)**, pp. 45–51.
- Kobayashi, Y. *et al.* (2015) "EGFR Exon 18 Mutations in Lung Cancer: Molecular Predictors of Augmented Sensitivity to Afatinib or Neratinib as Compared with First- or Third-Generation TKIs," *Clinical Cancer Research*, **21(23)**, pp. 5305–5313.
- Kobayashi, Y. *et al.* (2017) "Characterization of EGFR T790M, L792F, and C797S Mutations as Mechanisms of Acquired Resistance to Afatinib in Lung Cancer.," *Molecular cancer therapeutics*, **16(2)**, pp. 357–364.
- Kobayashi, Y. *et al.* (2018) "EGFR T790M and C797S Mutations as Mechanisms of Acquired Resistance to Dacomitinib," *Journal of Thoracic Oncology*, **13(5)**, pp. 727–731.
- Kobayashi, Y. and Mitsudomi, T. (2016) "Not all epidermal growth factor receptor mutations in lung cancer are created equal: Perspectives for individualized treatment strategy," *Cancer Science*, **107**, pp. 1179–1186.
- Koga, T. *et al.* (2018) "Activity of a novel HER2 inhibitor, poziotinib, for HER2 exon 20 mutations in lung cancer and mechanism of acquired resistance: An in vitro study," *Lung Cancer*, **126**, pp. 72–79.
- Kohsaka, S. *et al.* (2017) "A method of high-Throughput functional evaluation of EGFR gene variants of unknown significance in cancer," *Science Translational Medicine*, **9(416)**, p. eaan6566.
- Konduri, K. *et al.* (2016) "EGFR fusions as novel therapeutic targets in lung cancer," *Cancer Discovery*, **6(6)**, pp. 601–611.

- Kosaka, T. *et al.* (2004) "Mutations of the epidermal growth factor receptor gene in lung cancer: Biological and clinical implications," *Cancer Research*, **64(24)**, pp. 8919–8923.
- Kosaka, T. *et al.* (2006) "Analysis of Epidermal Growth Factor Receptor Gene Mutation in Patients with Non–Small Cell Lung Cancer and Acquired Resistance to Gefitinib," *Clinical Cancer Research*, **12(19)**, pp. 5764–5769.
- Kosaka, T. *et al.* (2017) "Response heterogeneity of EGFR and HER2 exon 20 insertions to covalent EGFR and HER2 inhibitors," *Cancer Research*, **77(10)**, pp. 2712–2721.
- Kris, M. G. *et al.* (2003) "Efficacy of Gefitinib, an Inhibitor of the Epidermal Growth Factor Receptor Tyrosine Kinase, in Symptomatic Patients with Non-Small Cell Lung Cancer: A Randomized Trial," *Journal of the American Medical Association*, **290(16)**, pp. 2149–2158.
- Kruser, T. J., Traynor, A. M. and Wheeler, D. L. (2011) "The use of single-agent dasatinib in molecularly unselected non-small-cell lung cancer patients.," *Expert opinion on investigational drugs*, **20(2)**, pp. 305–307.
- Kurata, T. *et al.* (2004) "Effect of re-treatment with gefitinib ('Iressa', ZD1839) after acquisition of resistance," *Annals of Oncology*, **15(1)**, p. 173.
- Kwak, E. L. *et al.* (2005) "Irreversible inhibitors of the EGF receptor may circumvent acquired resistance to gefitinib," *Proceedings of the National Academy of Sciences of the United States of America*, **102(21)**, pp. 7665–7670.
- Kwatra, M. *et al.* (2017) "EXTH-46. A precision medicine approach to target EGFRvIII in GBM: Osimertinib (AZD9291) inhibits the growth of EGFRvIII-positive glioblastoma stem cells and increases survival of mice bearing intracranial EGFRvIII-positive GBM," *Neuro-Oncology*. 2017/11/06, **19(Suppl 6)**, pp. vi82–vi82.
- Lamont, F. R. *et al.* (2011) "Small molecule FGF receptor inhibitors block FGFR-dependent urothelial carcinoma growth in vitro and in vivo," *British Journal of Cancer*, **104(1)**, pp. 75–82.
- Lassman, A. B. *et al.* (2005) "Molecular study of malignant gliomas treated with epidermal growth factor receptor inhibitors: Tissue analysis from North American Brain Tumor Consortium trials 01-03 and 00-01," *Clinical Cancer Research*, **11(21)**, pp. 7841–7850.
- Laurie, S. A. *et al.* (2014) "A Phase II Trial of Saracatinib, an Inhibitor of src Kinases, in Previously-Treated Advanced Non–Small-Cell Lung Cancer: The Princess Margaret Hospital Phase II Consortium," *Clinical Lung Cancer*, **15(1)**, pp. 52–57.

- Le, X. *et al.* (2018) "Landscape of EGFR-dependent and -independent resistance mechanisms to osimertinib and continuation therapy beyond progression in EGFR-mutant NSCLC," *Clinical Cancer Research*, **24(24)**, pp. 6195–6203.
- Le, X. *et al.* (2020) "Poziotinib shows activity and durability of responses in subgroups of previously treated EGFR exon 20 NSCLC patients.," *Journal of Clinical Oncology*, **38(15_suppl)**, p. 9514.
- Lee, C. K. *et al.* (2015) "Impact of specific Epidermal Growth Factor Receptor (EGFR) mutations and clinical characteristics on outcomes after treatment with EGFR tyrosine kinase inhibitors versus chemotherapy in EGFR-mutant lung cancer: A meta-analysis," *Journal of Clinical Oncology*, **33(17)**, pp. 1958–1965.
- Lee, C. K. *et al.* (2017a) "Checkpoint Inhibitors in Metastatic EGFR-Mutated Non-Small Cell Lung Cancer—A Meta-Analysis," *Journal of Thoracic Oncology*, **12(2)**, pp. 403–407.
- Lee, J. C. *et al.* (2006) "Epidermal growth factor receptor activation in glioblastoma through novel missense mutations in the extracellular domain.," *PLoS medicine*, **3(12)**, p. e485.
- Lee, S.-H. *et al.* (2017b) "Vandetanib in pretreated patients with advanced non-small cell lung cancer-harboring RET rearrangement: a phase II clinical trial.," *Annals of oncology : official journal of the European Society for Medical Oncology*, **28(2)**, pp. 292–297.
- Lee, V. H. F. *et al.* (2013) "Association of exon 19 and 21 EGFR mutation patterns with treatment outcome after first-line tyrosine kinase inhibitor in metastatic non-small-cell lung cancer," *Journal of Thoracic Oncology*, **8(9)**, pp. 1148–1155.
- Lemmon, M. A. and Schlessinger, J. (2010) "Cell signaling by receptor tyrosine kinases.," *Cell*, **141(7)**, pp. 1117–34.
- Leonetti, A. *et al.* (2019a) "Resistance mechanisms to osimertinib in EGFR-mutated non-small cell lung cancer," *British Journal of Cancer*, pp. 725–737.
- Leonetti, A. *et al.* (2019b) "Resistance mechanisms to osimertinib in EGFR-mutated non-small cell lung cancer," *British Journal of Cancer*, pp. 725–737.
- Leventakos, K. *et al.* (2016) "S768I Mutation in EGFR in Patients with Lung Cancer," *Journal of Thoracic Oncology*, **11(10)**, pp. 1798–1801.
- Li, B. *et al.* (2004) "Mutant epidermal growth factor receptor displays increased signaling through the phosphatidylinositol-3 kinase/AKT pathway and promotes radioresistance in cells of astrocytic origin," *Oncogene*, **23(26)**, pp. 4594–4602.
- Li, D. *et al.* (2008) "BIBW2992, an irreversible EGFR/HER2 inhibitor highly effective in preclinical lung cancer models," *Oncogene*, **27(34)**, pp. 4702–4711.

- Lim, S. H. *et al.* (2014) "Comparison of clinical outcomes following gefitinib and erlotinib treatment in non-small-cell lung cancer patients harboring an epidermal growth factor receptor mutation in either exon 19 or 21," *Journal of Thoracic Oncology*, **9(4)**, pp. 506–511.
- Liu, Y. *et al.* (2013) "Screening for EGFR and KRAS mutations in non-small cell lung carcinomas using DNA extraction by hydrothermal pressure coupled with PCR-based direct sequencing.," *International journal of clinical and experimental pathology*, **6(9)**, pp. 1880–9.
- Lowenstein, E. J. *et al.* (1992) "The SH2 and SH3 Domain-Containing Protein GRB2 Links Receptor Tyrosine Kinases to ras Signaling," *Cell*, **70**, pp. 431–442.
- Lynch, T. J. *et al.* (2004) "Activating Mutations in the Epidermal Growth Factor Receptor Underlying Responsiveness of Non–Small-Cell Lung Cancer to Gefitinib," *New England Journal of Medicine*, **350(21)**, pp. 2129–2139.
- Maa, M. C. *et al.* (1995) "Potentiation of epidermal growth factor receptor-mediated oncogenesis by c-Src: Implications for the etiology of multiple human cancers," *Proceedings of the National Academy of Sciences of the United States of America*, **92(15)**, pp. 6981–6985.
- MacConaill, L. E. *et al.* (2009) "Profiling critical cancer gene mutations in clinical tumor samples," *PLoS ONE*, **4(11)**, p. e7887.
- Maemondo, M. *et al.* (2010) "Gefitinib or Chemotherapy for Non–Small-Cell Lung Cancer with Mutated EGFR," *New England Journal of Medicine*, **362(25)**, pp. 2380–2388.
- Makhlin, I. *et al.* (2019) "Clinical activity of the EGFR tyrosine kinase inhibitor osimertinib in EGFR -mutant glioblastoma ," *CNS Oncology*, **8(3)**, p. CNS43.
- Malapelle, U. *et al.* (2017) "Profile of the Roche cobas® EGFR mutation test v2 for non-small cell lung cancer," *Expert Review of Molecular Diagnostics*, **17(3)**, pp. 209–215.
- Mandal, M. *et al.* (1998) "Nuclear targeting of Bax during apoptosis in human colorectal cancer cells," *Oncogene*, **17(8)**, pp. 999–1007.
- Marcoux, N. *et al.* (2019) "EGFR-mutant adenocarcinomas that transform to small-cell lung cancer and other neuroendocrine carcinomas: Clinical outcomes," *Journal of Clinical Oncology*, **37(4)**, pp. 278–285.
- Marshall, C. J. (1995) "Specificity of Receptor Tyrosine Kinase Signaling: Transient versus Sustained Extracellular Signal-Regulated Kinase Activation Review," *Cell*, **80**, pp. 179–185.

- Masago, K. *et al.* (2010) “Good Clinical Response to Gefitinib in a Non-small Cell Lung Cancer Patient Harboring a Rare Somatic Epidermal Growth Factor Gene Point Mutation; Codon 768 AGC > ATC in Exon 20 (S768I),” *Japanese Journal of Clinical Oncology*, **40(11)**, pp. 1105–1109.
- Masaki, T. *et al.* (2003) “pp60c-src activation in lung adenocarcinoma.,” *European Journal of Cancer*, **39(10)**, pp. 1447–1455.
- Mayo, L. D. and Donner, D. B. (2001) “A phosphatidylinositol 3-kinase/Akt pathway promotes translocation of Mdm2 from the cytoplasm to the nucleus,” *Proceedings of the National Academy of Sciences of the United States of America*, **98(20)**, pp. 11598–11603.
- McClellan, M. *et al.* (1999) “Regulation of proliferation and apoptosis by epidermal growth factor and protein kinase C in human ovarian surface epithelial cells,” *Experimental Cell Research*, **246(2)**, pp. 471–479.
- McGranahan, N. *et al.* (2015) “Clonal status of actionable driver events and the timing of mutational processes in cancer evolution,” *Science Translational Medicine*, **7(283)**, pp. 283ra54-283ra54.
- McTigue, M. *et al.* (2012) “Molecular conformations, interactions, and properties associated with drug efficiency and clinical performance among VEGFR TK inhibitors,” *Proceedings of the National Academy of Sciences of the United States of America*, **109(45)**, pp. 18281–18289.
- Merid, S. K., Goranskaya, D. and Alexeyenko, A. (2014) “Distinguishing between driver and passenger mutations in individual cancer genomes by network enrichment analysis,” *BMC Bioinformatics*, **15(1)**, p. 308.
- Metz, J. T. *et al.* (2011) “Navigating the kinome,” *Nature Chemical Biology*, **7(4)**, pp. 200–202.
- Milenic, D. E., Brady, E. D. and Brechbiel, M. W. (2004) “Antibody-targeted radiation cancer therapy,” *Nature Reviews Drug Discovery*, pp. 488–498.
- Miller, V. A. *et al.* (2004) “Bronchioloalveolar pathologic subtype and smoking history predict sensitivity to gefitinib in advanced non-small-cell lung cancer.,” *Journal of clinical oncology : official journal of the American Society of Clinical Oncology*, **22(6)**, pp. 1103–9.
- Miller, V. A. *et al.* (2012) “Afatinib versus placebo for patients with advanced, metastatic non-small-cell lung cancer after failure of erlotinib, gefitinib, or both, and one or two lines of chemotherapy (LUX-Lung 1): a phase 2b/3 randomised trial,” *The Lancet Oncology*, **13(5)**, pp. 528–538.
- Mitsudomi, T. *et al.* (2010) “Gefitinib versus cisplatin plus docetaxel in patients with non-small-cell lung cancer harbouring mutations of the epidermal growth factor

receptor (WJTOG3405): an open label, randomised phase 3 trial," *The Lancet Oncology*, **11(2)**, pp. 121–128.

Mok, T. S. *et al.* (2009) "Gefitinib or Carboplatin–Paclitaxel in Pulmonary Adenocarcinoma," *New England Journal of Medicine*, **361(10)**, pp. 947–957.

Mok, T. S. *et al.* (2017a) "Osimertinib or Platinum–Pemetrexed in *EGFR* T790M–Positive Lung Cancer," *New England Journal of Medicine*, **376(7)**, pp. 629–640.

Mok, T. S. *et al.* (2018) "Improvement in overall survival in a randomized study that compared dacomitinib with gefitinib in patients with advanced non–small-cell lung cancer and *EGFR*-activating mutations," *Journal of Clinical Oncology*.

Mok, T. S. K. *et al.* (2017b) "Gefitinib Plus Chemotherapy Versus Chemotherapy in Epidermal Growth Factor Receptor Mutation–Positive Non–Small-Cell Lung Cancer Resistant to First-Line Gefitinib (IMPRESS): Overall Survival and Biomarker Analyses," *Journal of Clinical Oncology*, **35(36)**, pp. 4027–4034.

Molina, J. R. and Adjei, A. A. (2006) "The Ras/Raf/MAPK Pathway," *Journal of Thoracic Oncology*, **1(1)**, pp. 7–9.

Moriceau, G. *et al.* (2015) "Tunable-Combinatorial Mechanisms of Acquired Resistance Limit the Efficacy of BRAF/MEK Cotargeting but Result in Melanoma Drug Addiction," *Cancer Cell*, **27(2)**, pp. 240–256.

Moriguchi, H., Kim, T. Y. and Sato, C. (2006) "Gefitinib for refractory advanced non-small-cell lung cancer," *Lancet*, pp. 299–300.

Moscatoello, D. K. *et al.* (1998) "Constitutive Activation of Phosphatidylinositol 3-Kinase by a Naturally Occurring Mutant Epidermal Growth Factor Receptor," *Journal of Biological Chemistry*, **273(1)**, pp. 200–206.

Moya-Horno, I. *et al.* (2018) "Combination of immunotherapy with targeted therapies in advanced non-small cell lung cancer (NSCLC).," *Therapeutic advances in medical oncology*, **10**, p. 1758834017745012.

Mukohara, T. *et al.* (2005) "Differential Effects of Gefitinib and Cetuximab on Non-small-cell Lung Cancers Bearing Epidermal Growth Factor Receptor Mutations," *Journal of the National Cancer Institute*, **97(16)**.

Murakami, H. *et al.* (2012) "Phase I study of continuous afatinib (BIBW 2992) in patients with advanced non-small cell lung cancer after prior chemotherapy/erlotinib/gefitinib (LUX-Lung 4)," *Cancer Chemotherapy and Pharmacology*, **69(4)**, pp. 891–899.

Murphy, L. O. *et al.* (2002) "Molecular interpretation of ERK signal duration by immediate early gene products," *Nature Cell Biology*, **4(8)**, pp. 556–564.

- Murphy, L. O. and Blenis, J. (2006) "MAPK signal specificity: the right place at the right time," *Trends in Biochemical Sciences*, pp. 268–275.
- Nagar, B. *et al.* (2003) "Structural basis for the autoinhibition of c-Abl tyrosine kinase," *Cell*, **112(6)**, pp. 859–871.
- Nagpal, A. *et al.* (2019) "Neoadjuvant neratinib promotes ferroptosis and inhibits brain metastasis in a novel syngeneic model of spontaneous HER2+ve breast cancer metastasis," *Breast Cancer Research*, **21(1)**, p. 94.
- Naidoo, J. *et al.* (2015) "Epidermal growth factor receptor exon 20 insertions in advanced lung adenocarcinomas: Clinical outcomes and response to erlotinib," *Cancer*, **121(18)**, pp. 3212–3220.
- Navé, B. T. *et al.* (1999) "Mammalian target of rapamycin is a direct target for protein kinase B: Identification of a convergence point for opposing effects of insulin and amino-acid deficiency on protein translation," *Biochemical Journal*, **344(2)**, pp. 427–431.
- News, P. O. (2019) *Spectrum's Poziotinib Failed to Meet Primary Phase II Trial Endpoint | Precision Oncology News*.
- NICE (2020) "1 Recommendations | Osimertinib for untreated EGFR mutation-positive non-small-cell lung cancer | Guidance | NICE."
- Nichol, D. *et al.* (2015) "Steering Evolution with Sequential Therapy to Prevent the Emergence of Bacterial Antibiotic Resistance.," *PLoS computational biology*, **11(9)**, p. e1004493.
- Niederst, M. J. *et al.* (2015) "RB loss in resistant EGFR mutant lung adenocarcinomas that transform to small-cell lung cancer," *Nature Communications*, **6**, p. 6377.
- Noble, M. E. M., Endicott, J. A. and Johnson, L. N. (2004) "Protein Kinase Inhibitors: Insights into Drug Design from Structure," *Science*, **303(5665)**, pp. 1800–1805.
- Nolan, P. M., Hugill, A. and Cox, R. D. (2002) "ENU mutagenesis in the mouse: Application to human genetic disease," *Briefings in Functional Genomics and Proteomics*, **1(3)**, pp. 278–289.
- Nolen, B., Taylor, S. and Ghosh, G. (2004) "Regulation of protein kinases: Controlling activity through activation segment conformation," *Molecular Cell*, **15(5)**, pp. 661–675.
- Ogiso, H. *et al.* (2002) "Crystal structure of the complex of human epidermal growth factor and receptor extracellular domains," *Cell*, **110(6)**, pp. 775–787.

- Oh, I. J. *et al.* (2012) "Retreatment of gefitinib in patients with non-small-cell lung cancer who previously controlled to gefitinib: A single-arm, open-label, phase II study," *Lung Cancer*, **77(1)**, pp. 121–127.
- O'Hare, T. *et al.* (2009) "AP24534, a Pan-BCR-ABL Inhibitor for Chronic Myeloid Leukemia, Potently Inhibits the T315I Mutant and Overcomes Mutation-Based Resistance," *Cancer Cell*, **16(5)**, pp. 401–412.
- Ohashi, K. *et al.* (2012) "Lung cancers with acquired resistance to EGFR inhibitors occasionally harbor BRAF gene mutations but lack mutations in KRAS, NRAS, or MEK1," *Proceedings of the National Academy of Sciences of the United States of America*, **109(31)**, pp. E2127–E2133.
- Okamoto, I. *et al.* (2003) "Expression of constitutively activated EGFRvIII in non-small cell lung cancer," *Cancer Science*, **94(1)**, pp. 50–56.
- Olapade-Olaopa, E. O. *et al.* (2000) "Evidence for the differential expression of a variant EGF receptor protein in human prostate cancer," *British Journal of Cancer*, **82(1)**, pp. 186–194.
- Ono, M. *et al.* (2004) "Sensitivity to gefitinib (Iressa, ZD1839) in non-small cell lung cancer cell lines correlates with dependence on the epidermal growth factor (EGF) receptor/extracellular signal-regulated kinase 1/2 and EGF receptor/Akt pathway for proliferation.," *Molecular cancer therapeutics*, **3(4)**, pp. 465–472.
- Orellana, L. *et al.* (2019) "Oncogenic mutations at the EGFR ectodomain structurally converge to remove a steric hindrance on a kinase-coupled cryptic epitope," *Proceedings of the National Academy of Sciences of the United States of America*, **116(20)**, pp. 10009–10018.
- Ortiz-Cuaran, S. *et al.* (2016) "Heterogeneous mechanisms of primary and acquired resistance to third-generation EGFR inhibitors," *Clinical Cancer Research*, **22(19)**, pp. 4837–4847.
- Oskina, N. *et al.* (2017) "Highly Sensitive and Reliable Detection of EGFR Exon 19 Deletions by Droplet Digital Polymerase Chain Reaction.," *Molecular diagnosis & therapy*, **21(5)**, pp. 555–562.
- Ou, S.-H. I. *et al.* (2017) "Emergence of novel and dominant acquired EGFR solvent-front mutations at Gly796 (G796S/R) together with C797S/R and L792F/H mutations in one EGFR (L858R/T790M) NSCLC patient who progressed on osimertinib," *Lung Cancer*, **108**, pp. 228–231.
- Oude Weernink, P. A. *et al.* (1994) "Functional interaction between the epidermal growth factor receptor and c-Src kinase activity," *FEBS Letters*, **352(3)**, pp. 296–300.

- Oxnard, G. R. *et al.* (2011) "Acquired resistance to EGFR tyrosine kinase inhibitors in EGFR-mutant lung cancer: Distinct natural history of patients with tumors harboring the T790M mutation," *Clinical Cancer Research*, **17(6)**, pp. 1616–1622.
- Oxnard, G. R. *et al.* (2013) "Natural history and molecular characteristics of lung cancers harboring EGFR exon 20 insertions.," *Journal of Thoracic Oncology*, **8(2)**, pp. 179–84.
- Oxnard, G. R. *et al.* (2018) "Assessment of Resistance Mechanisms and Clinical Implications in Patients with EGFR T790M-Positive Lung Cancer and Acquired Resistance to Osimertinib," *JAMA Oncology*, **4(11)**, pp. 1527–1534.
- Oztan, A. *et al.* (2017) "Emergence of EGFR G724S mutation in EGFR-mutant lung adenocarcinoma post progression on osimertinib.," *Lung Cancer*, **111**, pp. 84–87.
- Paasche, A. *et al.* (2010) "Mechanistic Study of the Reaction of Thiol-Containing Enzymes with α,β -Unsaturated Carbonyl Substrates by Computation and Chemoassays," *ChemMedChem*, **5(6)**, pp. 869–880.
- Paez, J. G. *et al.* (2004) "EGFR Mutations in Lung Cancer: Correlation with Clinical Response to Gefitinib Therapy," *Science*, **304(5621)**, pp. 1497–1500.
- Pallan, L., Taniere, P. and Koh, P. (2014) "Rare EGFR exon 20 S768I mutation predicts resistance to targeted therapy: a report of two cases.," *Journal of Thoracic Oncology*, **9(10)**, p. e75.
- Pao, W. *et al.* (2005) "Acquired resistance of lung adenocarcinomas to gefitinib or erlotinib is associated with a second mutation in the EGFR kinase domain," *PLoS Medicine*, **2**, pp. 0225–0235.
- Papadimitrakopoulou, V. A. *et al.* (2018) "LBA51 Analysis of resistance mechanisms to osimertinib in patients with EGFR T790M advanced NSCLC from the AURA3 study," *Annals of Oncology*, **29**, p. Suppl_8.
- Park, J. *et al.* (2014) "EGFR Exon 19 insertions show good response to Gefitinib, but short time to progression in Japanese patients," *Journal of Thoracic Oncology*, **9(2)**, pp. e10-11.
- Park, K. *et al.* (2016) "Afatinib versus gefitinib as first-line treatment of patients with EGFR mutation-positive non-small-cell lung cancer (LUX-Lung 7): A phase 2B, open-label, randomised controlled trial," *The Lancet Oncology*, **17(5)**, pp. 577–589.
- Park, S. R. *et al.* (2013) "Safety and feasibility of targeted agent combinations in solid tumours," *Nature Reviews Clinical Oncology*, **10(3)**, pp. 154–168.

- Patel, A. P. *et al.* (2014) "Single-cell RNA-seq highlights intratumoral heterogeneity in primary glioblastoma," *Science*, **344(6190)**, pp. 1396–1401.
- Paz-Ares, L. *et al.* (2017) "Afatinib versus gefitinib in patients with EGFR mutation-positive advanced non-small-cell lung cancer: overall survival data from the phase IIb LUX-Lung 7 trial," *Annals of Oncology*, **28**, pp. 270–277.
- Pearson, A. *et al.* (2016) "High-level clonal FGFR amplification and response to FGFR inhibition in a translational clinical trial," *Cancer Discovery*, **6(8)**, pp. 838–851.
- Pedersen, M. W. *et al.* (2005) "Differential response to gefitinib of cells expressing normal EGFR and the mutant EGFRvIII," *British Journal of Cancer*, **93(8)**, pp. 915–923.
- Peled, N. *et al.* (2017) "Subclonal Therapy by Two EGFR TKIs Guided by Sequential Plasma Cell-free DNA in EGFR-Mutated Lung Cancer," *Journal of Thoracic Oncology*, **12(7)**, pp. e81–e84.
- Peng, L., Song, Z.-G. and Jiao, S.-C. (2015) "Efficacy analysis of tyrosine kinase inhibitors on rare non-small cell lung cancer patients harboring complex EGFR mutations," *Scientific Reports*, **4(1)**, p. 6104.
- Petrylak, D. P. *et al.* (2020) "First-in-human phase I study of ARV-110, an androgen receptor (AR) PROTAC degrader in patients (pts) with metastatic castrate-resistant prostate cancer (mCRPC) following enzalutamide (ENZ) and/or abiraterone (ABI).," *Journal of Clinical Oncology*, **38(15_suppl)**, p. 3500.
- Pettitt, S. J. *et al.* (2018) "Genome-wide and high-density CRISPR-Cas9 screens identify point mutations in PARP1 causing PARP inhibitor resistance," *Nature Communications*, **9(1)**, p. 1849.
- Phillips, A. C. *et al.* (2016) "ABT-414, an antibody-drug conjugate targeting a tumor-selective EGFR epitope," *Molecular Cancer Therapeutics*, **15(4)**, pp. 661–669.
- Pines, G. *et al.* (2010) "EGFRvIV: a previously uncharacterized oncogenic mutant reveals a kinase autoinhibitory mechanism.," *Oncogene*, **29(43)**, pp. 5850–5860.
- Piotrowska, Z. *et al.* (2018) "Activity of the Hsp90 inhibitor luminespib among non-small-cell lung cancers harboring EGFR exon 20 insertions," *Annals of Oncology*, **29(10)**, pp. 2092–2097.
- Prigent, S. A. *et al.* (1996) "Enhanced tumorigenic behavior of glioblastoma cells expressing a truncated epidermal growth factor receptor is mediated through the Ras-Shc-Grb2 pathway.," *The Journal of biological chemistry*, **271(41)**, pp. 25639–25645.

- Ramalingam, S. S. *et al.* (2018a) "Mechanisms of acquired resistance to first-line osimertinib: Preliminary data from the phase III FLAURA study," *Annals of Oncology*, **29**, p. viii740.
- Ramalingam, S. S. *et al.* (2018b) "Osimertinib as first-line treatment of EGFR mutation-positive advanced non-small-cell lung cancer," *Journal of Clinical Oncology*, **36(9)**, pp. 841–849.
- Ramalingam, S. S. *et al.* (2020) "Overall Survival with Osimertinib in Untreated, EGFR -Mutated Advanced NSCLC," *New England Journal of Medicine*, **382(1)**, pp. 41–50.
- Ramirez, M. *et al.* (2016) "Diverse drug-resistance mechanisms can emerge from drug-tolerant cancer persister cells.," *Nature Communications*, **7**, p. 10690.
- Raof, S. *et al.* (2019) "Targeting FGFR overcomes EMT-mediated resistance in EGFR mutant non-small cell lung cancer," *Oncogene*, **38(37)**, pp. 6399–6413.
- Reardon, D. A. *et al.* (2014) "Phase I/randomized phase II study of afatinib, an irreversible ErbB family blocker, with or without protracted temozolomide in adults with recurrent glioblastoma," *Neuro-Oncology*, **17(3)**, pp. 430–439.
- Reck, M. *et al.* (2016) "Pembrolizumab versus Chemotherapy for PD-L1-Positive Non-Small-Cell Lung Cancer," *New England Journal of Medicine*, **375(19)**, pp. 1823–1833.
- Reichert, J. M. and Valge-Archer, V. E. (2007) "Development trends for monoclonal antibody cancer therapeutics," *Nature Reviews Drug Discovery*, **6(5)**, pp. 349–356.
- Remington, L. L. *et al.* (2009) "Global target profile of the kinase inhibitor bosutinib in primary chronic myeloid leukemia cells," *Leukemia*, **23(3)**, pp. 477–485.
- Ren, X. D. *et al.* (2000) "Focal adhesion kinase suppresses Rho activity to promote focal adhesion turnover.," *Journal of cell science*, **113 (Pt 2)**, pp. 3673–3678.
- Rich, J. N. *et al.* (2004) "Phase II trial of gefitinib in recurrent glioblastoma," *Journal of Clinical Oncology*, **22(1)**, pp. 133–142.
- Riely, G. J. *et al.* (2006) "Clinical course of patients with non-small cell lung cancer and epidermal growth factor receptor exon 19 and exon 21 mutations treated with gefitinib or erlotinib," *Clinical Cancer Research*, **12(3 I)**, pp. 839–844.
- Rittmeyer, A. *et al.* (2017) "Atezolizumab versus docetaxel in patients with previously treated non-small-cell lung cancer (OAK): a phase 3, open-label, multicentre randomised controlled trial," *The Lancet*, **389(10066)**, pp. 255–265.

- Robertson, S. C. *et al.* (1998) “Activating mutations in the extracellular domain of the fibroblast growth factor receptor 2 function by disruption of the disulfide bond in the third immunoglobulin-like domain,” *Proceedings of the National Academy of Sciences of the United States of America*, **95(8)**, pp. 4567–4572.
- Robichaux, J. P. *et al.* (2018) “Mechanisms and clinical activity of an EGFR and HER2 exon 20-selective kinase inhibitor in non-small cell lung cancer,” *Nature Medicine*, **24(5)**, pp. 638–646.
- Robinson, D. R., Wu, Y. M. and Lin, S. F. (2000) “The protein tyrosine kinase family of the human genome,” *Oncogene*, **19(49)**, pp. 5548–5557.
- Roengvoraphoj, M. *et al.* (2013) “Epidermal growth factor receptor tyrosine kinase inhibitors as initial therapy for non-small cell lung cancer: Focus on epidermal growth factor receptor mutation testing and mutation-positive patients,” *Cancer Treatment Reviews*, **39(8)**, pp. 839–850.
- Roesch, A. *et al.* (2010) “A Temporarily Distinct Subpopulation of Slow-Cycling Melanoma Cells Is Required for Continuous Tumor Growth,” *Cell*, **141(4)**, pp. 583–594.
- Rosell, R. *et al.* (2009) “Screening for Epidermal Growth Factor Receptor Mutations in Lung Cancer,” *New England Journal of Medicine*, **361(10)**, pp. 958–967.
- Rosell, R. *et al.* (2012) “Erlotinib versus standard chemotherapy as first-line treatment for European patients with advanced EGFR mutation-positive non-small-cell lung cancer (EURTAC): A multicentre, open-label, randomised phase 3 trial,” *The Lancet Oncology*, **13(3)**, pp. 239–246.
- Roskoski, R. (2012) “ERK1/2 MAP kinases: Structure, function, and regulation,” *Pharmacological Research*, pp. 105–143.
- Roskoski, R. (2015) “Src protein-tyrosine kinase structure, mechanism, and small molecule inhibitors This paper is dedicated to the memory of Prof. Donald F. Steiner (1930-2014) - Advisor, mentor, and discoverer of proinsulin.,” *Pharmacological Research*, pp. 9–25.
- Roth, B. L., Sheffler, D. J. and Kroeze, W. K. (2004) “Magic shotguns versus magic bullets: selectively non-selective drugs for mood disorders and schizophrenia,” *Nature Reviews Drug Discovery*, **3(4)**, pp. 353–359.
- Rusan, M. *et al.* (2018) “Suppression of adaptive responses to targeted cancer therapy by transcriptional repression,” *Cancer Discovery*, **8(1)**, pp. 59–73.
- Russo, A. *et al.* (2019) “Heterogeneous Responses to Epidermal Growth Factor Receptor (EGFR) Tyrosine Kinase Inhibitors (TKIs) in Patients with Uncommon

EGFR Mutations: New Insights and Future Perspectives in this Complex Clinical Scenario,” *International Journal of Molecular Sciences*, **20(6)**, p. 1431.

Sarkaria, J. N. *et al.* (2018) “Is the blood-brain barrier really disrupted in all glioblastomas? A critical assessment of existing clinical data,” *Neuro-Oncology*, **20(2)**, pp. 184–191.

Sasaki, H. *et al.* (2006) “L858R EGFR mutation status correlated with clinicopathological features of Japanese lung cancer,” *Lung Cancer*, **54(1)**, pp. 103–108.

Sastry, S. K. and Burridge, K. (2000) “Focal adhesions: A nexus for intracellular signaling and cytoskeletal dynamics,” *Experimental Cell Research*, **261(1)**, pp. 25–36.

Sato, J. D. *et al.* (1983) “Biological effects in vitro of monoclonal antibodies to human epidermal growth factor receptors,” *Molecular biology & medicine*, **1(5)**, pp. 511–529.

Sato, K. I. *et al.* (1995) “c-SRC phosphorylates epidermal growth factor receptor on tyrosine 845,” *Biochemical and Biophysical Research Communications*, **215(3)**, pp. 1078–1087.

Sato, K. Ichi (2013) “Cellular functions regulated by phosphorylation of EGFR on TYR845,” *International Journal of Molecular Sciences*, **14(6)**, pp. 10761–10790.

Sawai, A. *et al.* (2008) “Inhibition of Hsp90 down-regulates mutant epidermal growth factor receptor (EGFR) expression and sensitizes EGFR mutant tumors to paclitaxel,” *Cancer Res.* 2008/01/18, **68(2)**, pp. 589–596.

Schapira, M. *et al.* (2019) “Targeted protein degradation: expanding the toolbox,” *Nature reviews. Drug discovery*, **18(12)**, pp. 949–963.

Schlessinger, J. (2000) “Cell signaling by receptor tyrosine kinases,” *Cell*, **103(2)**, pp. 211–225.

Schlessinger, J. (2004) “Common and distinct elements in cellular signaling via EGF and FGF receptor,” *Science*, **306(5701)**, pp. 1506–1507.

Schlessinger, J. and Lemmon, M. A. (2003) “SH2 and PTB domains in tyrosine kinase signaling,” *Science’s STKE : signal transduction knowledge environment*, pp. re12–re12.

Schneider, M. R. and Wolf, E. (2009) “The epidermal growth factor receptor ligands at a glance,” *Journal of Cellular Physiology*, **218(3)**, pp. 460–466.

Schönwasser, D. C. *et al.* (1998) “Activation of the Mitogen-Activated Protein Kinase/Extracellular Signal-Regulated Kinase Pathway by Conventional, Novel,

and Atypical Protein Kinase C Isozymes,” *Molecular and Cellular Biology*, **18(2)**, pp. 790–798.

Schulze, W. X., Deng, L. and Mann, M. (2005) “Phosphotyrosine interactome of the ErbB-receptor kinase family.” *Molecular Systems Biology*, **1**, p. 2005.0008.

Sebastian, M. *et al.* (2010) “The Efficacy and Safety of BI 2536, a Novel PI3K-1 Inhibitor, in Patients with Stage IIIB/IV Non-small Cell Lung Cancer Who Had Relapsed after, or Failed, Chemotherapy: Results from an Open-Label, Randomized Phase II Clinical Trial,” *Journal of Thoracic Oncology*, **5(7)**, pp. 1060–1067.

Selvaggi, G. *et al.* (2004) “Epidermal growth factor receptor overexpression correlates with a poor prognosis in completely resected non-small-cell lung cancer,” *Annals of Oncology*, **15(1)**, pp. 28–32.

Sequist, L. V. *et al.* (2010a) “Activity of IPI-504, a novel heat-shock protein 90 inhibitor, in patients with molecularly defined non-small-cell lung cancer,” *Journal of Clinical Oncology*, **28(33)**, pp. 4953–4960.

Sequist, L. V. *et al.* (2010b) “Neratinib, an irreversible pan-ErbB receptor tyrosine kinase inhibitor: Results of a phase II trial in patients with advanced non-small-cell lung cancer,” *Journal of Clinical Oncology*, **28(18)**, pp. 3076–3083.

Sequist, L. V. *et al.* (2011) “Genotypic and histological evolution of lung cancers acquiring resistance to EGFR inhibitors,” *Science Translational Medicine*, **3(75)**, p. 75ra25.

Sequist, L. V. *et al.* (2013) “Phase III Study of Afatinib or Cisplatin Plus Pemetrexed in Patients With Metastatic Lung Adenocarcinoma With EGFR Mutations,” *Journal of Clinical Oncology*, **31(27)**, pp. 3327–3334.

Sequist, L. V. *et al.* (2015a) “Efficacy of rociletinib (CO-1686) in plasma-genotyped T790M-positive non-small cell lung cancer (NSCLC) patients (pts).,” *Journal of Clinical Oncology*, **33(15_suppl)**, pp. 8001–8001.

Sequist, L. V. *et al.* (2015b) “Rociletinib in EGFR -Mutated Non-Small-Cell Lung Cancer,” *New England Journal of Medicine*.

Sequist, L. V., Soria, J.-C. and Camidge, D. R. (2016) “Update to Rociletinib Data with the RECIST Confirmed Response Rate,” *New England Journal of Medicine*, **374(23)**, pp. 2296–2297.

Seth, A. *et al.* (1991) “A phosphorylation site located in the NH₂-terminal domain of c-Myc increases transactivation of gene expression,” *Journal of Biological Chemistry*, **266(35)**, pp. 23521–23524.

- Shan, Y. *et al.* (2012) "Oncogenic Mutations Counteract Intrinsic Disorder in the EGFR Kinase and Promote Receptor Dimerization," *Cell*, **149**, pp. 860–870.
- Sharma, S. v. *et al.* (2010) "A Chromatin-Mediated Reversible Drug-Tolerant State in Cancer Cell Subpopulations," *Cell*, **141(1)**, pp. 69–80.
- Shawver, L. K., Slamon, D. and Ullrich, A. (2002) "Smart drugs: Tyrosine kinase inhibitors in cancer therapy," *Cancer Cell*, pp. 117–123.
- Shepherd, F. A. *et al.* (2005) "Erlotinib in Previously Treated Non–Small-Cell Lung Cancer," *New England Journal of Medicine*, **353(2)**, pp. 123–132.
- Shi, Y. *et al.* (2014) "A Prospective, Molecular Epidemiology Study of EGFR Mutations in Asian Patients with Advanced Non–Small-Cell Lung Cancer of Adenocarcinoma Histology (PIONEER)," *Journal of Thoracic Oncology*, **9(2)**, pp. 154–162.
- Shimamura, T. *et al.* (2005) "Epidermal growth factor receptors harboring kinase domain mutations associate with the heat shock protein 90 chaperone and are destabilized following exposure to geldanamycins," *Cancer Research*, **65(14)**, pp. 6401–6408.
- Shimamura, T. *et al.* (2008) "Hsp90 inhibition suppresses mutant EGFR-T790M signaling and overcomes kinase inhibitor resistance," *Cancer Research*, **68(14)**, pp. 5827–5838.
- Siegelin, M. D. and Borczuk, A. C. (2014) "Epidermal growth factor receptor mutations in lung adenocarcinoma," *Laboratory Investigation*, **94(2)**, pp. 129–137.
- Silva, C. M. (2004) "Role of STATs as downstream signal transducers in Src family kinase-mediated tumorigenesis," *Oncogene*, **23(7)**, pp. 8017–8023.
- Simmons, A. D. *et al.* (2015) "Abstract 793: Insulin-like growth factor 1 (IGF1R)/insulin receptor (INSR) inhibitory activity of rociletinib (CO-1686) and its metabolites in nonclinical models," *Cancer Research*, **75(15 Supplement)**, pp. 793–793.
- Socinski, M. A. *et al.* (2013) "A multicenter phase II study of ganetespib monotherapy in patients with genotypically defined advanced non-small cell lung cancer," *Clin Cancer Res.* 2013/04/05, **19(11)**, pp. 3068–3077.
- Soda, M. *et al.* (2007) "Identification of the transforming EML4-ALK fusion gene in non-small-cell lung cancer," *Nature*, **448(7153)**, pp. 561–566.
- Sok, J. C. *et al.* (2006) "Mutant epidermal growth factor receptor (EGFRvIII) contributes to head and neck cancer growth and resistance to EGFR targeting," *Clinical Cancer Research*, **12(17)**, pp. 5064–5073.

- Solca, F. *et al.* (2012) "Target binding properties and cellular activity of afatinib (BIBW 2992), an irreversible ErbB family blocker.," *The Journal of pharmacology and experimental therapeutics*, **343(2)**, pp. 342–50.
- Song, L. *et al.* (2006) "Dasatinib (BMS-354825) Selectively Induces Apoptosis in Lung Cancer Cells Dependent on Epidermal Growth Factor Receptor Signaling for Survival," *Cancer Research*, **66(11)**, pp. 5542–5548.
- Sörby, M. and Östman, A. (1996) "Protein-tyrosine phosphatase-mediated decrease of epidermal growth factor and platelet-derived growth factor receptor tyrosine phosphorylation in high cell density cultures," *Journal of Biological Chemistry*, **271(18)**, pp. 10963–10966.
- Soria, J.-C. *et al.* (2018) "Osimertinib in Untreated *EGFR* -Mutated Advanced Non–Small-Cell Lung Cancer," *New England Journal of Medicine*, **378(2)**, pp. 113–125.
- Sorkin, A. and Goh, L. K. (2009) "Endocytosis and intracellular trafficking of ErbBs," *Experimental Cell Research*, **315(4)**, pp. 683–696.
- Sos, M. L. *et al.* (2009) "PTEN loss contributes to erlotinib resistance in *EGFR*-mutant lung cancer by activation of akt and *EGFR*," *Cancer Research*, **69(8)**, pp. 3256–3261.
- Stamos, J., Sliwkowski, M. X. and Eigenbrot, C. (2002) "Structure of the epidermal growth factor receptor kinase domain alone and in complex with a 4-anilinoquinazoline inhibitor," *Journal of Biological Chemistry*, **277(48)**, pp. 46265–46272.
- van der Steen, N. *et al.* (2016) "New developments in the management of non-small-cell lung cancer, focus on rociletinib: What went wrong?," *OncoTargets and Therapy*, **9**, pp. 6065–6074.
- Stewart, S. A. *et al.* (2003) "Lentivirus-delivered stable gene silencing by RNAi in primary cells.," *RNA*, **9(4)**, pp. 493–501.
- Su Huang, H. J. *et al.* (1997) "The enhanced tumorigenic activity of a mutant epidermal growth factor receptor common in human cancers is mediated by threshold levels of constitutive tyrosine phosphorylation and unattenuated signaling," *Journal of Biological Chemistry*, **272(5)**, pp. 2927–2935.
- Su, J. *et al.* (2017) "Molecular characteristics and clinical outcomes of *EGFR* exon 19 indel subtypes to *EGFR* TKIs in NSCLC patients.," *Oncotarget*, **8(67)**, pp. 111246–111257.
- Suda, K. *et al.* (2012) "Conversion from the 'oncogene addiction' to 'drug addiction' by intensive inhibition of the *EGFR* and *MET* in lung cancer with activating *EGFR* mutation," *Lung Cancer*, **76(3)**, pp. 292–299.

Sugio, K. *et al.* (2006) “Mutations within the tyrosine kinase domain of EGFR gene specifically occur in lung adenocarcinoma patients with a low exposure of tobacco smoking,” *British Journal of Cancer*, **94(6)**, pp. 896–903.

Takeda (2020) *Takeda Announces U.S. FDA Breakthrough Therapy Designation for Mobocertinib (TAK-788) for the Treatment of NSCLC Patients with EGFR Exon 20 Insertion Mutations.*

Takezawa, K. *et al.* (2012) “HER2 amplification: A potential mechanism of acquired resistance to egfr inhibition in EGFR -mutant lung cancers that lack the second-site EGFR T790M mutation,” *Cancer Discovery*, **2(10)**, pp. 922–933.

Talpaz, M. *et al.* (2006) “Dasatinib in Imatinib-Resistant Philadelphia Chromosome–Positive Leukemias,” *New England Journal of Medicine*, **354(24)**, pp. 2531–2541.

Tamirat, M. Z. *et al.* (2019) “Structural characterization of EGFR exon 19 deletion mutation using molecular dynamics simulation,” *PLoS ONE*, **14(9)**, p. e0222814.

Taniguchi, Y. *et al.* (2018a) “Effect of pembrolizumab on patients harboring uncommon epidermal growth factor receptor mutations,” *Annals of Oncology*, **29(5)**, pp. 1331–1333.

Taniguchi, Y. *et al.* (2018b) “Programmed death-ligand 1 expression in uncommon epidermal growth factor receptor mutation-positive non-small-cell lung cancer,” *Annals of Oncology*, **29(11)**, pp. 2262–2263.

Tate, J. G. *et al.* (2018) “COSMIC: the Catalogue Of Somatic Mutations In Cancer,” *Nucleic Acids Research*, **47**, pp. 941–947.

Terai, H. *et al.* (2018) “ER stress signaling promotes the survival of cancer ‘Persister Cells’ tolerant to EGFR tyrosine Kinase inhibitors,” *Cancer Research*, **78(4)**, pp. 1044–1057.

das Thakur, M. *et al.* (2013) “Modelling vemurafenib resistance in melanoma reveals a strategy to forestall drug resistance,” *Nature*, **494(7436)**, pp. 251–255.

Thomas, S. M. and Brugge, J. S. (1997) “Cellular Functions Regulated By SRC Family Kinases,” *Annual Review of Cell and Developmental Biology*, **13(1)**, pp. 513–609.

Thress, K. S. *et al.* (2015) “Acquired EGFR C797S mutation mediates resistance to AZD9291 in non–small cell lung cancer harboring EGFR T790M,” *Nature Medicine*, **21(6)**, pp. 560–562.

To, C. *et al.* (2019) “Single and Dual Targeting of Mutant EGFR with an Allosteric Inhibitor,” *Cancer Discovery*, **(9)**, pp. 926–43.

- Tough, I. M. *et al.* (1961) "Cytogenetic Studies In Chronic Myeloid Leukaemia And Acute Leukaemia Associated With Mongolism," *The Lancet*, **277(7174)**, pp. 411–417.
- Tracy, S. *et al.* (2004) "Gefitinib Induces Apoptosis in the EGFR^{L858R} Non–Small-Cell Lung Cancer Cell Line H3255," *Cancer Research*, **64(20)**, pp. 7241–7244.
- Trepel, J. *et al.* (2010) "Targeting the dynamic HSP90 complex in cancer," *Nature Reviews Cancer*, **10(8)**, pp. 537–549.
- Tsoukalas, N. *et al.* (2017) "Epithelial-mesenchymal transition in non small-cell lung cancer," *Anticancer Research*, **37(4)**, pp. 1773–1778.
- Uchibori, K. *et al.* (2017) "Brigatinib combined with anti-EGFR antibody overcomes osimertinib resistance in EGFR-mutated non-small-cell lung cancer," *Nature Communications*, **8**, p. 14768.
- Uitdehaag, J. C. M. *et al.* (2014) "Comparison of the cancer gene targeting and biochemical selectivities of all targeted kinase inhibitors approved for clinical use," *PLoS ONE*, **9(3)**, p. e92146.
- Uitdehaag, J. C. M. and Zaman, G. J. R. (2011) "A theoretical entropy score as a single value to express inhibitor selectivity," *BMC Bioinformatics*, **12**, p. 94.
- Urata, Y. *et al.* (2016) "Randomized Phase III Study Comparing Gefitinib With Erlotinib in Patients With Previously Treated Advanced Lung Adenocarcinoma: WJOG 5108L," *Journal of Clinical Oncology*, **34(27)**, pp. 3248–3257.
- Vanhaesebroeck, B. and Alessi, D. R. (2000) "The PI3K-PKB1 connection: More than just a road to PKB," *Biochemical Journal*, **346(3)**, pp. 561–576.
- Varga, A. *et al.* (2015) "3009 Activity of rociletinib in EGFR mutant NSCLC patients with a history of CNS involvement," *European Journal of Cancer*, **51**, p. S598.
- Vengoji, R. *et al.* (2019) "Afinitinib and Temozolomide combination inhibits tumorigenesis by targeting EGFRvIII-cMet signaling in glioblastoma cells," *Journal of Experimental and Clinical Cancer Research*, **38(1)**, p. 266.
- Vivanco, I. *et al.* (2012) "Differential sensitivity of glioma- versus lung cancer-specific EGFR mutations to EGFR kinase inhibitors.," *Cancer discovery*, **2(5)**, pp. 458–71.
- Vivanco, I. and Sawyers, C. L. (2002) "The phosphatidylinositol 3-kinase-AKT pathway in humancancer," *Nature Reviews Cancer*, **2(7)**, pp. 489–501.
- Vogelstein, B. *et al.* (2013) "Cancer Genome Landscapes," *Science*, **339(6127)**, pp. 1546–1558.

- Voon, P. J. *et al.* (2013) "Letter to Editor: EGFR Exon 20 Insertion A763-Y764insFQEA and response to Erlotinib.," *Molecular Cancer Therapeutics*, **12(November)**, pp. 20–25.
- Vyse, S. and Huang, P. H. (2019) "Targeting EGFR exon 20 insertion mutations in non-small cell lung cancer," *Signal Transduction and Targeted Therapy*, **4(1)**, p. 5.
- Wakeling, A. E. *et al.* (2002) "ZD1839 (Iressa)," *Cancer Research*, **62(20)**, pp. 5749–5754.
- Walter, A. O. *et al.* (2013) "Discovery of a mutant-selective covalent inhibitor of EGFR that overcomes T790M mediated resistance in NSCLC," *Cancer Discovery*, **3(12)**, pp. 1404–1415.
- Ward, C. W. *et al.* (2007) "The insulin and EGF receptor structures: new insights into ligand-induced receptor activation," *Trends in Biochemical Sciences*, **32(3)**, pp. 129–137.
- Ward, C. W., Hoyne, P. A. and Flegg, R. H. (1995) "Insulin and epidermal growth factor receptors contain the cysteine repeat motif found in the tumor necrosis factor receptor," *Proteins: Structure, Function, and Genetics*, **22(2)**, pp. 141–153.
- Ware, K. E. *et al.* (2013a) "A mechanism of resistance to gefitinib mediated by cellular reprogramming and the acquisition of an FGF2-FGFR1 autocrine growth loop," *Oncogenesis*, **2(3)**, p. e39.
- Ware, K. E. *et al.* (2013b) "A mechanism of resistance to gefitinib mediated by cellular reprogramming and the acquisition of an FGF2-FGFR1 autocrine growth loop," *Oncogenesis*, **2(3)**, p. e39.
- Watanabe, S. *et al.* (2014) "Effectiveness of gefitinib against non-small-cell lung cancer with the uncommon EGFR mutations G719X and L861Q.," *Journal of thoracic oncology : official publication of the International Association for the Study of Lung Cancer*, **9(2)**, pp. 189–94.
- Watanabe, S. *et al.* (2017) "T790M-Selective EGFR-TKI Combined with Dasatinib as an Optimal Strategy for Overcoming EGFR-TKI Resistance in T790M-Positive Non-Small Cell Lung Cancer," *Molecular Cancer Therapeutics*, **16(11)**, pp. 2563–2571.
- Weenink, B. *et al.* (2020) "Immunotherapy in glioblastoma: Current shortcomings and future perspectives," *Cancers*, **12(3)**, p. 751.
- Weernink, P. A. O. and Rijksen, G. (1995) "Activation and translocation of c-Src to the cytoskeleton by both platelet-derived growth factor and epidermal growth factor," *Journal of Biological Chemistry*, **270(5)**, pp. 2264–2267.

- Wehrman, T. *et al.* (2007) “Structural and Mechanistic Insights into Nerve Growth Factor Interactions with the TrkA and p75 Receptors,” *Neuron*, **53(1)**, pp. 25–38.
- Wei, Y. *et al.* (2016) “A platinum-based hybrid drug design approach to circumvent acquired resistance to molecular targeted tyrosine kinase inhibitors,” *Scientific Reports*, **6**, p. 25363.
- Weiner, G. J. (2010) “Rituximab: Mechanism of action,” *Seminars in Hematology*, **47(2)**, pp. 115–123.
- Weng, C. H. *et al.* (2019) “Epithelial-mesenchymal transition (EMT) beyond EGFR mutations per se is a common mechanism for acquired resistance to EGFR TKI,” *Oncogene*, **38(4)**, pp. 455–468.
- Westover, D. *et al.* (2018) “Mechanisms of acquired resistance to first- and second-generation EGFR tyrosine kinase inhibitors,” *Annals of Oncology*, **29(suppl_1)**, pp. i10–i19.
- Whitesell, L. *et al.* (2014) “HSP90 empowers evolution of resistance to hormonal therapy in human breast cancer models,” *Proceedings of the National Academy of Sciences of the United States of America*. 2014/12/10, **111(51)**, pp. 18297–18302.
- Whitmarsh, A. J. *et al.* (1995) “Integration of MAP kinase signal transduction pathways at the serum response element,” *Science*, **269(5222)**, p. 403.
- Wlesmann, C. *et al.* (1999) “Crystal structure of nerve growth factor in complex with the ligand- binding domain of the TrkA receptor,” *Nature*, **401(6749)**, pp. 184–188.
- Wong, A. J. *et al.* (1992) “Structural alterations of the epidermal growth factor receptor gene in human gliomas,” *Proceedings of the National Academy of Sciences of the United States of America*, **89(7)**, pp. 2965–2969.
- Wong, J. P. *et al.* (2016) “Dual Targeting of PDGFR α and FGFR1 Displays Synergistic Efficacy in Malignant Rhabdoid Tumors.,” *Cell reports*, **17(5)**, pp. 1265–1275.
- Wu, J.-Y. *et al.* (2011) “Effectiveness of Tyrosine Kinase Inhibitors on ‘Uncommon’ Epidermal Growth Factor Receptor Mutations of Unknown Clinical Significance in Non-Small Cell Lung Cancer,” *Clinical Cancer Research*, **17(11)**, pp. 3812–3821.
- Wu, J.-Y. and Shih, J.-Y. (2016) “Effectiveness of tyrosine kinase inhibitors on uncommon E709X epidermal growth factor receptor mutations in non-small-cell lung cancer.,” *OncoTargets and therapy*, **9**, pp. 6137–6145.

- Wu, R. *et al.* (2000) "Somatic mutations of fibroblast growth factor receptor 3 (FGFR3) are uncommon in carcinomas of the uterine cervix," *Oncogene*, **19(48)**, pp. 5543–5546.
- Wu, X. *et al.* (1996) "Involvement of p27KIP1 in G1 arrest mediated by an anti-epidermal growth factor receptor monoclonal antibody.," *Oncogene*, **12(7)**, pp. 1397–403.
- Wu, Y. L. *et al.* (2014) "Afatinib versus cisplatin plus gemcitabine for first-line treatment of Asian patients with advanced non-small-cell lung cancer harbouring EGFR mutations (LUX-Lung 6): An open-label, randomised phase 3 trial," *The Lancet Oncology*, **15(2)**, pp. 213–222.
- Wu, Y. L. *et al.* (2017) "Dacomitinib versus gefitinib as first-line treatment for patients with EGFR-mutation-positive non-small-cell lung cancer (ARCHER 1050): a randomised, open-label, phase 3 trial," *The Lancet Oncology*, **18(11)**, pp. 1454–1466.
- Xu, J. *et al.* (2016) "EGFR tyrosine kinase inhibitor (TKI) in patients with advanced non-small cell lung cancer (NSCLC) harboring uncommon EGFR mutations: A real-world study in China," *Lung Cancer*, **96**, pp. 87–92.
- Xu, L. *et al.* (2010) "Epidermal growth factor receptor regulates MET levels and invasiveness through hypoxia-inducible factor-1 α in non-small cell lung cancer cells," *Oncogene*, **29(18)**, pp. 2616–2627.
- Xu, L. *et al.* (2012) "Combined EGFR/MET or EGFR/HSP90 inhibition is effective in the treatment of lung cancers codriven by mutant EGFR containing T790M and MET," *Cancer Research*. 2012/05/04, **72(13)**, pp. 3302–3311.
- Xu, W. *et al.* (2007) "Sensitivity of epidermal growth factor receptor and ErbB2 exon 20 insertion mutants to Hsp90 inhibition," *British Journal of Cancer*, **97(6)**, pp. 741–744.
- Yamada, T. *et al.* (2019) "Retrospective efficacy analysis of immune checkpoint inhibitors in patients with EGFR-mutated non-small cell lung cancer," *Cancer Medicine*, **8(4)**, pp. 1521–1529.
- Yamaguchi, H. and Hendrickson, W. A. (1996) "Structural basis for activation of human lymphocyte kinase Lck upon tyrosine phosphorylation," *Nature*, **384(6608)**, p. 484.
- Yamaguchi, N. *et al.* (2014) "Dual ALK and EGFR inhibition targets a mechanism of acquired resistance to the tyrosine kinase inhibitor crizotinib in ALK rearranged lung cancer.," *Lung Cancer*, **83(1)**, pp. 37–43.

- Yamamoto, H. *et al.* (2014) “Novel germline mutation in the transmembrane domain of HER2 in familial lung adenocarcinomas,” *Journal of the National Cancer Institute*, **106(1)**, pp. djt338–djt338.
- Yang, J. C. H. *et al.* (2012) “Afatinib for patients with lung adenocarcinoma and epidermal growth factor receptor mutations (LUX-Lung 2): A phase 2 trial,” *The Lancet Oncology*, **13(5)**, pp. 539–548.
- Yang, J. C. H. *et al.* (2015a) “Clinical activity of afatinib in patients with advanced non-small-cell lung cancer harbouring uncommon EGFR mutations: A combined post-hoc analysis of LUX-Lung 2, LUX-Lung 3, and LUX-Lung 6,” *The Lancet Oncology*, **16(7)**, pp. 830–838.
- Yang, J. C.-H. *et al.* (2015b) “Afatinib versus cisplatin-based chemotherapy for EGFR mutation-positive lung adenocarcinoma (LUX-Lung 3 and LUX-Lung 6): analysis of overall survival data from two randomised, phase 3 trials,” *The Lancet Oncology*, **16(2)**, pp. 141–151.
- Yang, J. C.-H. *et al.* (2015c) “Clinical activity of afatinib in patients with advanced non-small-cell lung cancer harbouring uncommon EGFR mutations: a combined post-hoc analysis of LUX-Lung 2, LUX-Lung 3, and LUX-Lung 6,” *The Lancet Oncology*, **16(7)**, pp. 830–838.
- Yang, J. C.-H. *et al.* (2017a) “Osimertinib in Pretreated T790M-Positive Advanced Non-Small-Cell Lung Cancer: AURA Study Phase II Extension Component.,” *Journal of clinical oncology : official journal of the American Society of Clinical Oncology*, **35(12)**, pp. 1288–1296.
- Yang, J. J. *et al.* (2017b) “A phase III randomised controlled trial of erlotinib vs gefitinib in advanced non-small cell lung cancer with EGFR mutations,” *British Journal of Cancer*, **116(5)**, pp. 568–574.
- Yang, M. *et al.* (2016) “NSCLC harboring EGFR exon-20 insertions after the regulatory C-helix of kinase domain responds poorly to known EGFR inhibitors,” *International Journal of Cancer*, **139(1)**, pp. 171–176.
- Yano, S. *et al.* (2011) “Hepatocyte growth factor expression in EGFR mutant lung cancer with intrinsic and acquired resistance to tyrosine kinase inhibitors in a Japanese cohort,” *Journal of Thoracic Oncology*, **6(12)**, pp. 2011–2017.
- Yap, A. S., Brieher, W. M. and Gumbiner, B. M. (1997) “Molecular and functional analysis of cadherin-based adherens junctions,” *Annual Review of Cell and Developmental Biology*, **13**, pp. 119–146.
- Yap, T. A. *et al.* (2010) “Phase I trial of the irreversible EGFR and HER2 kinase inhibitor BIBW 2992 in patients with advanced solid tumors.,” *Journal of Clinical Oncology*, **28(25)**, pp. 3965–72.

- Yarden, Y. and Sliwkowski, M. X. (2001) "Untangling the ErbB signalling network," *Nature Reviews Molecular Cell Biology*, **2(2)**, pp. 127–137.
- Yasuda, H. *et al.* (2013) "Structural, biochemical, and clinical characterization of epidermal growth factor receptor (EGFR) exon 20 insertion mutations in lung cancer," *Science Translational Medicine*, **5(216)**, p. 216ra177.
- Yaziji, H. *et al.* (2004) "HER-2 Testing in Breast Cancer Using Parallel Tissue-Based Methods," *Journal of the American Medical Association*, **291(16)**, pp. 1972–1977.
- Yeatman, T. J. (2004) "A Renaissance For SRC," *Nature Reviews Cancer*, **4**, pp. 470–80.
- Ymer, S. I. *et al.* (2011) "Glioma Specific Extracellular Missense Mutations in the First Cysteine Rich Region of Epidermal Growth Factor Receptor (EGFR) Initiate Ligand Independent Activation," *Cancers*, **3(2)**, pp. 2032–2049.
- Yoda, S. *et al.* (2018) "Sequential ALK inhibitors can select for lorlatinib-resistant compound ALK mutations in ALK-positive lung cancer," *Cancer Discovery*, **8(6)**, pp. 714–729.
- Yoh, K. *et al.* (2017) "Vandetanib in patients with previously treated *RET*-rearranged advanced non-small-cell lung cancer (LURET): an open-label, multicentre phase 2 trial," *The Lancet Respiratory Medicine*, **5(1)**, pp. 42–50.
- York, E. R. *et al.* (2017) "Tolerable and Effective Combination of Full-Dose Crizotinib and Osimertinib Targeting MET Amplification Sequentially Emerging after T790M Positivity in EGFR-Mutant Non-Small Cell Lung Cancer," *Journal of Thoracic Oncology*, **12(7)**, pp. e85–e88.
- Yosaatmadja, Y. *et al.* (2015) "Binding mode of the breakthrough inhibitor AZD9291 to epidermal growth factor receptor revealed," *Journal of Structural Biology*, **192(3)**, pp. 539–544.
- Yoshida, H. *et al.* (2018) "Nivolumab in non-small-cell lung cancer with EGFR mutation," *Annals of Oncology*, **29(3)**, pp. 777–778.
- Yoshida, T. *et al.* (2014) "Tyrosine Phosphoproteomics Identifies Both Codrivers and Cotargeting Strategies for T790M-Related EGFR-TKI Resistance in Non-Small Cell Lung Cancer," *Clinical Cancer Research*, **20(15)**, pp. 4059 LP – 4074.
- Yu, H. A. *et al.* (2013) "Analysis of Tumor Specimens at the Time of Acquired Resistance to EGFR-TKI Therapy in 155 Patients with EGFR-Mutant Lung Cancers," *Clinical Cancer Research*, **19(8)**, pp. 2240–2246.

- Yu, H. A. and Riely, G. J. (2013) "Second-generation epidermal growth factor receptor tyrosine kinase inhibitors in lung cancers.," *Journal of the National Comprehensive Cancer Network: JNCCN*, **11(2)**, pp. 161–9.
- Yun, C.-H. *et al.* (2007) "Structures of lung cancer-derived EGFR mutants and inhibitor complexes: Mechanism of activation and insights into differential inhibitor sensitivity," *Cancer Cell*, **11(3)**, pp. 217–227.
- Yun, C.-H. *et al.* (2008) "The T790M mutation in EGFR kinase causes drug resistance by increasing the affinity for ATP.," *Proceedings of the National Academy of Sciences of the United States of America*, **105(6)**, pp. 2070–5.
- Zandi, R. *et al.* (2007) "Mechanisms for oncogenic activation of the epidermal growth factor receptor," *Cellular Signalling*, **19(10)**, pp. 2013–2023.
- von Zastrow, M. and Sorkin, A. (2007) "Signaling on the endocytic pathway," *Current Opinion in Cell Biology*, pp. 436–445.
- Zeng, L., Yang, N. and Zhang, Y. (2018) "GOPC-ROS1 Rearrangement as an Acquired Resistance Mechanism to Osimertinib and Responding to Crizotinib Combined Treatments in Lung Adenocarcinoma," *Journal of Thoracic Oncology*, pp. e114–e116.
- Zhang, B. *et al.* (2018) "Complex epidermal growth factor receptor mutations and their responses to tyrosine kinase inhibitors in previously untreated advanced lung adenocarcinomas," *Cancer*, **124(11)**, pp. 2399–2406.
- Zhang, J. *et al.* (2006a) "Activation of STAT3 by EGFR variant III: Tyrosine residue 1068 is the primary STAT3 docking site on EGFR," *Cancer Research*, **66(8 Supplement)**.
- Zhang, J. *et al.* (2007) "SRC-family kinases are activated in non-small cell lung cancer and promote the survival of epidermal growth factor receptor-dependent cell lines.," *The American Journal of Pathology*, **170(1)**, pp. 366–376.
- Zhang, X. *et al.* (2006b) "An Allosteric Mechanism for Activation of the Kinase Domain of Epidermal Growth Factor Receptor," *Cell*, **125(6)**, pp. 1137–1149.
- Zhang, X. H. F. *et al.* (2009) "Latent Bone Metastasis in Breast Cancer Tied to Src-Dependent Survival Signals," *Cancer Cell*, **16(1)**, pp. 67–78.
- Zhang, Y. *et al.* (2000) "Activation of Stat3 in v-Src-transformed fibroblasts requires cooperation of Jak1 kinase activity," *Journal of Biological Chemistry*, **275(32)**, pp. 24935–24944.
- Zhao, J. *et al.* (2018) "Effective treatment of pulmonary adenocarcinoma harboring triple EGFR mutations of L858R,T790M, and cis-C797S by osimertinib,

bevacizumab, and brigatinib combination therapy: A case report,” *OncoTargets and Therapy*, **11**, pp. 5545–5550.

Zheng, D. *et al.* (2017) “EGFR G796D mutation mediates resistance to osimertinib,” *Oncotarget*, **8(30)**, pp. 49671–49679.

Zhou, B. P. *et al.* (2001) “HER-2/neu induces p53 ubiquitination via Akt-mediated MDM2 phosphorylation,” *Nature Cell Biology*, **3(11)**, pp. 973–982.

Zhou, C. *et al.* (2011) “Erlotinib versus chemotherapy as first-line treatment for patients with advanced EGFR mutation-positive non-small-cell lung cancer (OPTIMAL, CTONG-0802): a multicentre, open-label, randomised, phase 3 study,” *The Lancet Oncology*, **12(8)**, pp. 735–742.

Zhou, W. *et al.* (2009) “Novel mutant-selective EGFR kinase inhibitors against EGFR T790M,” *Nature*, **462(7276)**, pp. 1070–1074.

Zhu, H. *et al.* (2009) “Oncogenic EGFR signaling cooperates with loss of tumor suppressor gene functions in gliomagenesis,” *Proceedings of the National Academy of Sciences of the United States of America*, **106(8)**, pp. 2712–2716.

Zinzani, P. L. and Broccoli, A. (2017) “Possible novel agents in marginal zone lymphoma,” *Best Practice and Research: Clinical Haematology*, pp. 149–157.

Zou, J. X. *et al.* (2002) “Activated Src oncogene phosphorylates R-Ras and suppresses integrin activity,” *Journal of Biological Chemistry*, **277(3)**, pp. 1824–1827.

Zwang, Y. and Yarden, Y. (2009) “Systems biology of growth factor-induced receptor endocytosis,” *Traffic*, **10(4)**, pp. 349–363.